

AD-A192 146

NONLINEAR FLYING QUALITY PARAMETERS BASED ON DYNAMIC
INVERSION(U) HONEYWELL SYSTEMS AND RESEARCH CENTER
MINNEAPOLIS MN B G MORTON ET AL 30 OCT 87 F8231-FR

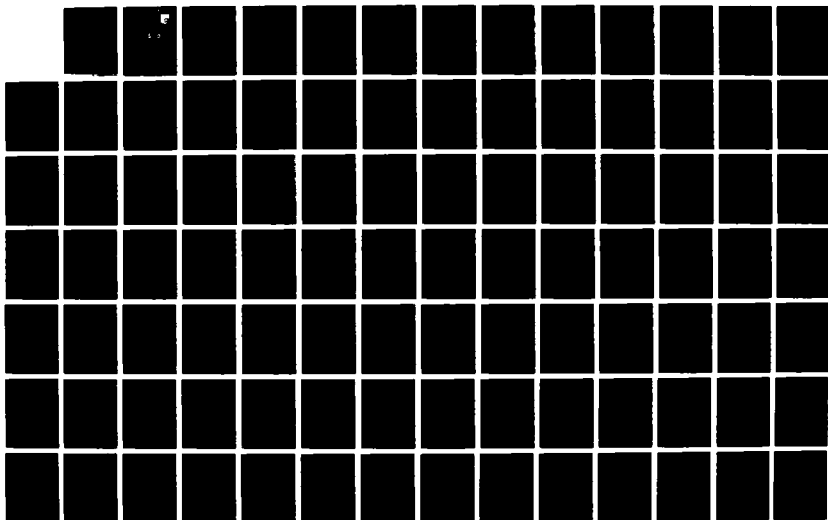
1/2

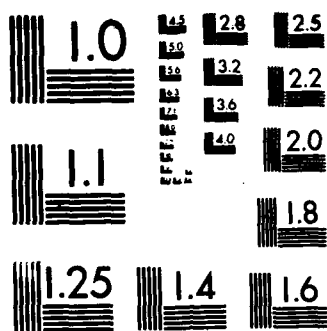
UNCLASSIFIED

AFWAL-TR-87-3079 F33615-86-C-3612

F/G 1/1

NL





MICROCOPY RESOLUTION TEST CHART
NATIONAL BUREAU OF STANDARDS-1963-A

DTIC FILE COPY

2

AD-A192 146

AFWAL-TR-87-3079



**NONLINEAR FLYING QUALITY PARAMETERS
BASED ON DYNAMIC INVERSION**

**Honeywell
Systems and Research Center
3660 Technology Drive
Minneapolis, Minnesota 55418**

**DTIC
ELECTE
MAR 23 1988**

October 1987

FINAL REPORT FOR PERIOD JUNE 1986 - JUNE 1987

Approved for public release; distribution unlimited.

**FLIGHT DYNAMICS LABORATORY
AIR FORCE WRIGHT AERONAUTICAL LABORATORIES
AIR FORCE SYSTEMS COMMAND
WRIGHT-PATTERSON AIR FORCE BASE, OHIO 45433-6553**

88 3 14 07 3

NOTICE

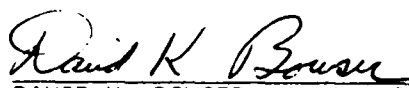
When Government drawings, specifications, or other data are used for any purpose other than in connection with a definitely related Government procurement operation, the United States Government thereby incurs no responsibility nor any obligation whatsoever; and the fact that the government may have formulated, furnished, or in any way supplied the said drawings, specifications, or other data, is not to be regarded by implication or otherwise as in any manner licensing the holder or any other person or corporation, or conveying any rights or permission to manufacture use, or sell any patented invention that may in any way be related thereto.

This report has been reviewed by the Office of Public Affairs (ASD/PA) and is releasable to the National Technical Information Service (NTIS). At NTIS, it will be available to the general public, including foreign nations.

This technical report has been reviewed and is approved for publication.



CHARLES F. SUCHOMEL
Project Engineer
Control Dynamics Branch
Flight Control Division



DAVID K. BOWSER, Acting Chief
Control Dynamics Branch
Flight Control Division

FOR THE COMMANDER



H. MAX DAVIS, Assistant for
Research and Technology
Flight Control Division
Flight Dynamics Laboratory

If your address has changed, if you wish to be removed from our mailing list, or if the addressee is no longer employed by your organization please notify AFWAL/FIGCB, W-PAFB, OH 45433 to help us maintain a current mailing list.

Copies of this report should not be returned unless return is required by security considerations, contractual obligations, or notice on a specific document.

UNCLASSIFIED

SECURITY CLASSIFICATION OF THIS PAGE

REPORT DOCUMENTATION PAGE

1a REPORT SECURITY CLASSIFICATION UNCLASSIFIED		1b RESTRICTIVE MARKINGS N/A	
2a SECURITY CLASSIFICATION AUTHORITY N/A		3 DISTRIBUTION/AVAILABILITY OF REPORT Approved for public release; distribution is unlimited.	
2b DECLASSIFICATION/DOWNGRADING SCHEDULE N/A			
4 PERFORMING ORGANIZATION REPORT NUMBER(S) Honeywell SRC Report F0231-FR		5 MONITORING ORGANIZATION REPORT NUMBER(S) AFWAL-TR-87-3079	
6a NAME OF PERFORMING ORGANIZATION Honeywell Systems and Research Center	6b OFFICE SYMBOL (If applicable) SCT	7a NAME OF MONITORING ORGANIZATION Flight Dynamics Laboratory (AFWAL/FIGCB) AF Wright Aeronautical Lab	
6c ADDRESS (City, State, and ZIP Code) 3660 Technology Drive Minneapolis, MN 55418		7c ADDRESS (City, State, and ZIP Code) Wright-Patterson AFB, OH 45433-6553	
8a NAME OF FUNDING/SPONSORING ORGANIZATION Air Force Wright Aeronautical Laboratories	8b OFFICE SYMBOL (If applicable) FIGCB	9 PROCUREMENT INSTRUMENT IDENTIFICATION NUMBER F33615-86-C-3612	
8c ADDRESS (City, State, and ZIP Code) Wright-Patterson AFB, OH 45433-6553		10 SOURCE OF FUNDING NUMBERS	
		PROGRAM ELEMENT NO 62201F	PROJECT NO. 2403
11 LE (Include Security Classification) Nonlinear Flying Quality Parameters Based on Dynamic Inversion			
12 PERSONAL AUTHOR(S) B.G. Morton, M.R. Elgersma, C.A. Harvey, G. Hines			
13a TYPE OF REPORT Final	13b COVERED FROM June 86 TO June 87	14 DATE OF REPORT (Year, Month, Day) 1987 October 30	15 PAGE COUNT 162
16 SUPPLEMENTARY NOTATION			
17 COSATI CODES		18 SUBJECT TERMS (Continue on reverse if necessary and identify by block number)	
FIELD	GROUP	SUB-GROUP	
		Dynamic Inversion/ Nonlinear Inversion / Nonlinear Flying Qualities, Equilibrium Manifold/ Lift/Drag Ratio / Highly Dynamic Maneuvers	
19 ABSTRACT (Continue on reverse if necessary and identify by block number) <p>This report documents the results of efforts to develop tools that can be used for the computation of nonlinear flying quality parameters. A variety of candidate nonlinear flying quality parameters and candidate specifications for them were developed. These parameters are genuinely different from expressions derived from linearized models. They depend on the nonlinear aerodynamic functions themselves and not their derivatives, and these parameters can be computed directly from preliminary nonlinear aircraft models. <i>Keywords:</i></p>			
20 DISTRIBUTION/AVAILABILITY OF ABSTRACT <input checked="" type="checkbox"/> UNCLASSIFIED/UNLIMITED <input type="checkbox"/> SAME AS RPT <input type="checkbox"/> DTIC USERS		21 ABSTRACT SECURITY CLASSIFICATION UNCLASSIFIED	
22a NAME OF RESPONSIBLE INDIVIDUAL Charles F. Suchomel		22b TELEPHONE (Include Area Code) (513) 255-8496	22c OFFICE SYMBOL AFWAL/FIGCB

FOREWORD

This report describes results of research performed under Contract No. F33615-86-C-3612 entitled "Nonlinear Flying Qualities," prepared for the Flying Qualities Group of the Control Dynamics Branch (FIGCB) of the Air Force Wright Aeronautical Laboratories (AFWAL). The general objective of the program was to develop and evaluate analytical methods which can be used to calculate Nonlinear Flying Quality Parameters (NLFQP's). The specific objective was to provide interactive computer-aided analysis tools (based on the nonlinear inversion concept) for evaluating nonlinear flying qualities of current airplanes and guiding the development of future airplanes with improved flying qualities.

The research was performed at the Honeywell Systems and Research Center between 30 June 1986 and 30 June 1987. At Honeywell, the research was conducted by Drs. C.A. Harvey and B.G. Morton, Principal Investigators; Mr. M.R. Elgersma and Ms. G. Hines, Associate Investigators; and Dr. M.F. Barrett, Program Manager. Dr. G.R. Sell, a professor in the School of Mathematics of the University of Minnesota, served as a consultant. The AFWAL/FIGCB technical administration was performed by Mr. C.F. Suchomel, Project Engineer.

Accession For	
NTIS GRA&I	<input checked="" type="checkbox"/>
DTIC TAB	<input type="checkbox"/>
Unannounced	<input type="checkbox"/>
Justification	
By	
Distribution	
Availability Codes	
Dist	Avail. and/or Special
A-1	



TABLE OF CONTENTS

Section	Page
1 INTRODUCTION	1
2 OVERVIEW AND SUMMARY OF REPORT	3
3 NONLINEAR MODELS	6
3.1 Notation	6
3.2 Introduction to the Equations of Motion	10
3.3 Equations of Motion	12
4 EQUILIBRIUM MANIFOLD	18
4.1 Introduction	18
4.2 Class of Systems	19
4.3 Equations of the Form $F(x,u) = f(x) + g(x) h(x,u)$	22
4.4 Introduction to Aircraft Equilibrium	27
4.5 Calculation of Aircraft Equilibrium	29
5 ANALYSIS OF AIRCRAFT DYNAMICS	40
5.1 Partial Dynamic Inversion	40
5.2 Theory of Complementary Dynamics	46
5.3 Aircraft Complementary Dynamics	50
5.4 Canonical Forms for the Complementary Dynamic Equations	61
5.5 The Liapunov Functions	67
6 NONLINEAR FLYING QUALITIES	73
6.1 Commanded Dynamic Parameters	74
6.2 Complementary Dynamic Parameters	78
6.3 Lift-to-Drag Ratios of Aircraft with Smooth Lift Curves	81
6.4 Highly Dynamic Phenomena	87
6.5 Dynamic Flying Quality Metrics	90
6.6 Stability and Controllability of Rotational Energy, Angular Momentum, Angular Rate	93
7. THE MANEUVERS	96
7.1 Roll Reversal	97
7.2 BARRELROLL	127
7.3 DIVINGTURN	136
REFERENCES	145
APPENDIX A	147
APPENDIX B	149

LIST OF ILLUSTRATIONS

Figure		Page
3.1	Equations of Motion in Mixed Coordinate System	10
3.2	Equations of Motion in Wind Axis-Euler Angle Coordinate System	11
4.1	Schematic Representation of Typical System	20
6.1	Drag and Lift Data for the F4, F14, and F15	84
6.2	Axial and Normal Force Data for the F4, F14, and F15	85
6.3	Axial Force Data for the F4, F14, and F15	86
7.1	States During UNLOADEDREVERSAL	99
7.2	Altitude, Crossrange, Theta and Psi During UNLOADEDREVERSAL	101
7.3	Commands and Command Responses During UNLOADEDREVERSAL	102
7.4	Accelerations, Aero Forces, Alpha, Beta and Speed During UNLOADEDREVERSAL	103
7.5	Control Activity During UNLOADEDREVERSAL	104
7.6	A-Parameters During UNLOADEDREVERSAL	106
7.7	B-Parameters During UNLOADEDREVERSAL	107
7.8	Eigenvalues and ψ , V^2 Comparisons During UNLOADEDREVERSAL	108
7.9	States During LOADEDREVERSAL	109
7.10	Altitude, Crossrange, Theta and Psi During LOADEDREVERSAL	110
7.11	Commands and Command Responsibility During LOADEDREVERSAL	111
7.12	Accelerations, Aero Forces, Alpha, Beta and Speed During LOADEDREVERSAL	114
7.13	Control Activity During LOADEDREVERSAL	115
7.14	A-Parameters During LOADEDREVERSAL	116
7.15	B-Parameters During LOADEDREVERSAL	117

LIST OF ILLUSTRATIONS (Continued)

Figure		Page
7.16	Eigenvalues and ψ , V^2 Comparisons During LOADEDREVERSAL	118
7.17	States During LOADED2REVERSAL	119
7.18	Altitude, Crossrange, Theta and Psi During LOADED2REVERSAL	120
7.19	Commands and Commands Responses During LOADED2REVERSAL	121
7.20	Accelerations, Aero Forces, Alpha, Beta and Speed During LOADED2REVERSAL	122
7.21	Control Activity During LOADED2REVERSAL	123
7.22	A-Parameters During LOADED2REVERSAL	124
7.23	B-Parameters During LOADED2REVERSAL	125
7.24	Eigenvalues and ψ , V^2 Comparisons During LOADED2REVERSAL	126
7.25	States During BARRELROLL	128
7.26	Altitude, Crossrange, Theta and Psi During BARRELROLL	129
7.27	Command and Command Responses During BARRELROLL	130
7.28	Control Activity During BARRELROLL	131
7.29	Accelerations, Aero Forces, Alpha, Beta and Speed During BARRELROLL	132
7.30	A-Parameters During BARRELROLL	133
7.31	B-Parameters During BARRELROLL	134
7.32	Eigenvalues and ψ , V^2 Comparisons During BARRELROLL	135
7.33	Groundtrace of Turn During DIVINGTURN	137
7.34	Change in Altitude During DIVINGTURN	138
7.35	States during DIVINGTURN	139

LIST OF ILLUSTRATIONS (Concluded)

Figure		Page
7.36	Accelerations, Aero Forces, Alpha, Beta and Speed During DIVINGTURN	140
7.37	Command and Command Responses During DIVINGTURN	141
7.38	Control Activity During DIVINGTURN	142

SECTION 1: INTRODUCTION

The usefulness of current flying qualities parameters is limited by their almost complete dependence on linear analysis. This dependence is based on mathematical tractability and analysis of a class of small amplitude maneuvers about trim conditions. The limitations of existing flying quality parameters leave expensive and extensive flight testing as the only accurate means of assessing flying quality during highly dynamic maneuvers. Inadequacies found during flight test can lead to extremely costly modifications and redesigns. This motivated our program aimed at the development of flying quality parameters which take into account the nonlinearities encountered during current and future combat maneuvers.

We took a novel approach to provide interactive and computer-aided analysis tools which can be used in developing and evaluating nonlinear flying quality parameters (NLFQPs). This approach is based on a technology called dynamic inversion which we used to generate maneuvers and analyze flying qualities. To enhance our analytical developments and to expose the issues concerning NLFQPs to the academic community, Professor George R. Sell served as a consultant.

Our technical program consisted of: a review of existing techniques, problem formulation, technical development, validation and illustration. In the problem formulation, the analytical structure of models was defined along with preliminary definitions of sets of maneuvers and potential NLFQPs to be examined. The technical approach consisted of analytic, algorithmic, and software development. Maneuvers were flown in simulation during the validation and illustration to demonstrate the utility of the technical development.

The concept of dynamic inversion is quite simple. Suppose the aircraft model is defined by:

$$\dot{x} = f(x) + \delta$$

where f represents the uncontrolled aircraft dynamics and δ is the commanded actuator signal.

For a desired aircraft response:

$$\dot{x} = L(x) + (\text{pilot command})$$

dynamic inversion is a control structure which forces the aircraft to respond as desired. Dynamic inversion is done as follows:

- 1) Measure the state x
- 2) Compute $f(x) - L(x)$
- 3) Generate the actuator command signal: $\delta = L(x) - f(x) + (\text{pilot command})$

For details, see section 5.1 .

SECTION 2: OVERVIEW AND SUMMARY OF REPORT

This report documents the results of our efforts to develop tools that can be used for the computation of nonlinear flying quality parameters. We have developed many new ideas for approaching this problem. In the course of our activities, we have found a variety of candidate nonlinear flying quality parameters and candidate specifications for them. These parameters are genuinely different from expressions derived from linearized models: we work with the nonlinear aerodynamic functions themselves and not their derivatives. We believe the candidate specifications we have outlined in this report could be applied to current and future Air Force vehicles to improve their flying qualities. The parameters we have defined here can be computed directly from preliminary nonlinear aircraft models.

First we give a brief outline of the sections to come, and then follow with a more detailed outline. Section 3 shows the nonlinear aircraft models we used. Sections 4 and 5 present the theoretical techniques we used while working with the nonlinear models. Most of these techniques were developed during the course of the program to help us identify and compute the parameters discussed in section 6. Anyone interested in getting to the flying qualities right away can go straight to section 6 and look through sections 3, 4, and 5 as needed. Section 7 contains the simulation results. Section 7 is followed by the reference list, and by the appendices treating trajectories and dynamical properties of maneuvers.

Section 3 is a complete description of these models in the form used. These are the standard equations of motion in a form which is not completely general, but general enough to capture most of the important features of the models commonly in use. Our techniques will apply to fully general models, but only at the expense of increased analytical complexity. A description of the application of dynamic inversion to the general models can be found in section 3.4 of the technical proposal for this contract (in response to PRDA 86-1 PMRN).

The one special assumption made is that the effect of the m control inputs to the aircraft can be represented by a 6-by- m matrix function of the state that multiplies an m dimensional vector function of the state and the control input signals. This is the situation that arises when, for example, the controls are described by aerodynamic derivatives such as $C_{m\delta}$ that are functions of the state.

Section 4 discusses a novel approach to the computation of trim conditions for the models discussed in section 3. Here we exploit the special form of the equations to reduce the computations to an algorithm that is simple enough to allow analytic computations. Sections 4.1 and 4.2 explain the basic ideas behind this approach and present the class of models to which they can be applied. Section 4.3 makes the algorithm explicit for a family of systems that includes those presented in section 3. Section 4.4 explains the two different ways that we have implemented these ideas for the solution of aircraft equilibria. Section 4.5 gives the details of the computations for the aircraft models, using both approaches discussed in section 4.4. Included in section 4.5 is a special treatment for aircraft exhibiting left/right symmetry and other special features that are often assumed and which simplify the results.

Section 5 is our analysis of nonlinear aircraft dynamics using partial dynamic inversion. Section 5.1 is a short summary of the method of partial dynamic inversion and five examples of inversion approaches that we investigated on this program. Section 5.2 introduces the theory of complementary dynamics in a general setting, then section 5.3 shows the algorithm for computing the complementary dynamics for the nonlinear airplane models. The dimensionless coordinates are introduced here to make it possible to fit the equations into a reasonable amount of space and to reduce the number of independent parameters appearing in the equations of motion. Then, for the special cases mentioned before, the special form of the complementary dynamic parameters is derived explicitly. It is shown then that for typical models in this form, the $\alpha, \beta, \Theta, \Phi$ complementary dynamic equations are stable and have unique equilibria. Even if the uncontrolled aircraft is unstable, the nonlinear inverter stabilizes the aircraft. Section 5.4 then shows how to transform the general $\alpha, \beta, \Theta, \Phi$ complementary dynamic equations into canonical forms, so that Liapunov functions can be applied. Section 5.5 then demonstrates how the Liapunov functions are constructed, and explains the significance of the result to aircraft stability.

The theory developed in sections 3, 4, and 5 is central to the discussion of nonlinear flying qualities in section 6, but it is not a prerequisite. The reader is warned that the parameters developed in section 6 are represented in terms of the dimensionless coordinates developed in section 5.3, and that conversions to account for units in the final answers might be necessary before meaningful comparisons can be made between different aircraft.

In section 6.1 we introduce the notion of commanded dynamics, then present a list of the sections from the MIL-F-8785C document that we believe are specifications for commanded

dynamics. Then we present some parameters that we call commanded dynamic parameters, derived from the form of the nonlinear models. These include the basic \dot{Q} command effectiveness parameter, the dynamic pitch-control ratio, the minimum lateral-directional command effectiveness parameter, and the dynamic lateral-directional control ratio vector. In section 6.2 we introduce the notion of complementary dynamics, then present a list of the sections from the MIL-F-8785C document that we believe are specifications for complementary dynamics. Then we discuss our complementary parameters that were developed in complete detail in section 5. Specific comparisons are indicated between our complementary dynamic parameters and the specifications in sections 3.2.1.1 (longitudinal static stability), 3.4.1 (dangerous flight conditions) and 3.4.2 (flight at high angle of attack) of MIL-F-8785C. The discussions at the end of cases 1 and 2 of section 5.5 should be read in conjunction with section 6.2. Section 6.3 is a short but very interesting discussion of lift-to-drag ratios, what they look like for the F-4, the F-14, and the F-15 aircraft for all angles of attack, and why that has a bearing on flying quality. Section 6.4 contains some criteria for coordinated flight at high angle of attack and for sustained high-angle-of-attack maneuvering. In section 6.5 we present an approach towards defining dynamic flying quality metrics using the coordinated-flight U,P,Q,R dynamic-inversion controller discussed in section 6.4 (A prototype of this controller is demonstrated in the simulations of sections 7.2 and 7.3). In section 6.6, some parameters for measuring the influence of the dynamic aerodynamic coefficients on flying qualities are given.

Section 7 presents some maneuvers generated by the batch simulation using nonlinear, partial dynamic inversion controllers. Section 7.1 contains some examples of a roll reversal, section 7.2 is a barrel roll, and section 7.3 is a highly-dynamic diving turn. We list the main developments that arose from analysis of the simulations in the summary section 7.4

There is a list of references, and then the two appendices. The first appendix discusses the trajectories of vehicles at equilibrium. The second appendix was written by George Sell. In it, he proves a fundamental lemma for the general theory of dynamic inversion.

SECTION 3 : NONLINEAR MODELS

In this section we describe the aircraft equations of motion. For more details on the notation and derivation of the aircraft equations of motion, see [E3].

3.1 Notation

Coordinates:

$$\begin{bmatrix} U \\ V \\ W \end{bmatrix} = \text{velocity vector of the c.g. in body-axis coordinates}$$

$$\begin{bmatrix} V \\ \beta \\ \alpha \end{bmatrix} = \text{velocity vector of the c.g. in wind-axis coordinates} \\ = (\text{speed, sideslip angle, angle of attack})$$

$$M = \text{Mach number} = \frac{\text{speed}}{\text{speed of sound}}$$

$$\begin{bmatrix} P \\ Q \\ R \end{bmatrix} = \text{angular velocity vector in body-axis coordinates}$$

Ψ, Θ, Φ = Euler angles for heading, elevation, and bank angle (yaw, pitch, roll sequence)

$$\begin{bmatrix} T \\ \delta_a \\ \delta_e \\ \delta_r \end{bmatrix} = \begin{bmatrix} \text{engine thrust} \\ \text{total aileron angle} \\ \text{total elevator angle} \\ \text{total rudder angle} \end{bmatrix}$$

Tabular aero data (from wind tunnel testing):

In general these are nonlinear tabular functions of many variables, e.g. the aero force in the x direction is given by $N_x(M, V, \alpha, \beta, \dot{\alpha}, \dot{\beta}, P, Q, R, T, \delta_a, \delta_e, \delta_r, \dots)$. In this report, we have only kept the $M, V, \alpha, \beta, P, Q, R, T, \delta_a, \delta_e, \delta_r$ dependence. Furthermore, we have expanded the functions in a Taylor series with respect to $P, Q, R, T, \delta_a, \delta_e, \delta_r$ and kept only the two lowest order terms in the Taylor series. For example,

$$\begin{aligned} N_x(M, V, \alpha, \beta, P, Q, R, T, \delta_a, \delta_e, \delta_r) = \\ \frac{1}{2} \rho V^2 S [C_x(M, \alpha, \beta) + C_{x_p}(M, \alpha, \beta) P + C_{x_q}(M, \alpha, \beta) Q + C_{x_r}(M, \alpha, \beta) R] + \\ C_{x_T}(M, \alpha, \beta) T + \frac{1}{2} \rho V^2 S [C_{x_{\delta_a}}(M, \alpha, \beta) \delta_a + C_{x_{\delta_e}}(M, \alpha, \beta) \delta_e + C_{x_{\delta_r}}(M, \alpha, \beta) \delta_r] + \\ \text{higher order terms.} \end{aligned}$$

When linear analysis is done, the above types of expressions are expanded further in a Taylor series with respect to the velocity components too (e.g. M, α, β or U, V, W) and only the two lowest order terms kept. In this report, we will be working directly with the nonlinear functions of M, α , and β instead of expanding them in a Taylor series in M, α, β .

$$\begin{bmatrix} C_x(M, \alpha, \beta) \\ C_y(M, \alpha, \beta) \\ C_z(M, \alpha, \beta) \end{bmatrix} = \text{static nonlinear aero force functions in body-axis coordinates.}$$

$$\begin{bmatrix} C_l(M, \alpha, \beta) \\ C_m(M, \alpha, \beta) \\ C_n(M, \alpha, \beta) \end{bmatrix} = \text{static nonlinear aero moment functions in body axes}$$

Note: the above nonlinear functions of M, α , and β are the coefficients on the zeroeth order terms in the Taylor expansion with respect to $P, Q, R, T, \delta_a, \delta_e, \delta_r$

$$\begin{bmatrix} C_{x_p}(M, \alpha, \beta) & C_{x_q}(M, \alpha, \beta) & C_{x_r}(M, \alpha, \beta) \\ C_{y_p}(M, \alpha, \beta) & C_{y_q}(M, \alpha, \beta) & C_{y_r}(M, \alpha, \beta) \\ C_{z_p}(M, \alpha, \beta) & C_{z_q}(M, \alpha, \beta) & C_{z_r}(M, \alpha, \beta) \end{bmatrix} = \text{dynamic nonlinear aero force functions in body}$$

axes

$$\begin{bmatrix} C_{l_p}(M, \alpha, \beta) & C_{l_q}(M, \alpha, \beta) & C_{l_r}(M, \alpha, \beta) \\ C_{m_p}(M, \alpha, \beta) & C_{m_q}(M, \alpha, \beta) & C_{m_r}(M, \alpha, \beta) \\ C_{n_p}(M, \alpha, \beta) & C_{n_q}(M, \alpha, \beta) & C_{n_r}(M, \alpha, \beta) \end{bmatrix} = \text{dynamic nonlinear aero moment functions in body}$$

axes

$$\begin{bmatrix} C_{x_r}(M, \alpha, \beta) & C_{x_{\delta_a}}(M, \alpha, \beta) & C_{x_{\delta_e}}(M, \alpha, \beta) & C_{x_{\delta_r}}(M, \alpha, \beta) \\ C_{y_r}(M, \alpha, \beta) & C_{y_{\delta_a}}(M, \alpha, \beta) & C_{y_{\delta_e}}(M, \alpha, \beta) & C_{y_{\delta_r}}(M, \alpha, \beta) \\ C_{z_r}(M, \alpha, \beta) & C_{z_{\delta_a}}(M, \alpha, \beta) & C_{z_{\delta_e}}(M, \alpha, \beta) & C_{z_{\delta_r}}(M, \alpha, \beta) \end{bmatrix} =$$

nonlinear aero coefficients describing forces due to the controls in body axes

$$\begin{bmatrix} C_{l_r}(M, \alpha, \beta) & C_{l_{\delta_a}}(M, \alpha, \beta) & C_{l_{\delta_e}}(M, \alpha, \beta) & C_{l_{\delta_r}}(M, \alpha, \beta) \\ C_{m_r}(M, \alpha, \beta) & C_{m_{\delta_a}}(M, \alpha, \beta) & C_{m_{\delta_e}}(M, \alpha, \beta) & C_{m_{\delta_r}}(M, \alpha, \beta) \\ C_{n_r}(M, \alpha, \beta) & C_{n_{\delta_a}}(M, \alpha, \beta) & C_{n_{\delta_e}}(M, \alpha, \beta) & C_{n_{\delta_r}}(M, \alpha, \beta) \end{bmatrix} =$$

nonlinear aero coefficients describing moments due to the controls in body axes

Note: the above nonlinear functions of M , α , and β are the coefficients on the first order terms in the Taylor expansion with respect to $P, Q, R, T, \delta_a, \delta_e, \delta_r$

Physical parameters:

ρ = air density

g = gravity

Physical parameters for the aircraft:

m, c, b, S = mass, mean aerodynamic chord, wing span, wing area

$$\begin{bmatrix} I_{xx} & -I_{xy} & -I_{xz} \\ -I_{xy} & I_{yy} & -I_{yz} \\ -I_{xz} & -I_{yz} & I_{zz} \end{bmatrix} = \text{moment of inertia matrix in body axes}$$

3.2 Introduction to the Equations of Motion

Consider a 6DOF nonlinear aircraft model having four control inputs. The equations of motion are often given in a mixed system of coordinates. There are eight states that the forces and moments depend on. The rigid-body mechanics are most easily expressed in the body-axis velocity (U, V, W) and angular rate (P, Q, R) coordinates, and two of the Euler angles: bank angle and elevation (Φ, Θ). The forces and moments do not depend on the heading angle, Ψ , so it is not included as a state. The result of not including Ψ as a state is that the equilibria will generally consist of vertical helices instead of just straight lines in inertial space (see appendix A). The aerodynamics are more easily expressed in terms of wind-axis velocity (V, β, α) in place of (U, V, W). In order to fit the aircraft model into the framework presented earlier, a single system of eight states will be used, and the angular rates will be expressed as derivatives of the Euler angles ($\dot{\Phi}, \dot{\Theta}, \dot{\Psi}$) in place of (P, Q, R). In this mixed coordinate system, the equations of motion of an aircraft are of the form shown in Figure 3.1.

Mixed Coordinate
Aircraft
Integrator Chains

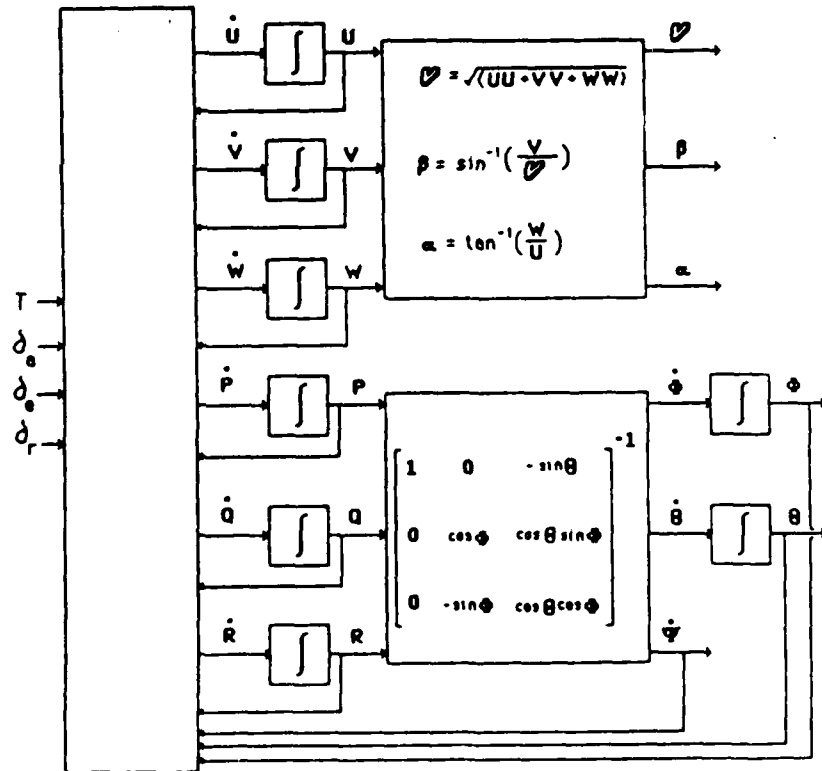


Figure 3.1 Equations of Motion in Mixed Coordinate System

In the wind-axis and Euler angle coordinates, the state vector is $x = (V, \beta, \alpha, \dot{\Phi}, \dot{\Theta}, \dot{\Psi}, \Phi, \Theta)$. The form of the equations of motion in this case are shown in Figure 3.2

Wind-Axis, Euler-Angle Aircraft Integrator Chains

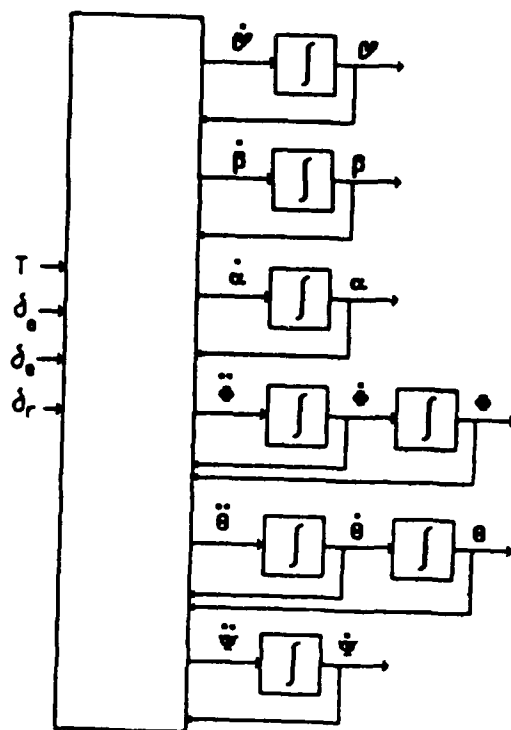


Figure 3.2 Equations of Motion in Wind-Axis and Euler Angle Coordinate System

3.3 Equations of Motion

The aircraft equations of motion [E3] may be written in the form

$$0 = f(\dot{x}, x) + g(x) h(x, u) \quad (3.3.1)$$

where

$$x \text{ is } (V, \beta, \alpha, \dot{\Phi}, \dot{\Theta}, \dot{\Psi}, \Phi, \Theta)^T, \quad u \text{ is } \begin{bmatrix} T \\ \delta_a \\ \delta_e \\ \delta_r \end{bmatrix}$$

$f \text{ is } 6 \times 1 \quad g \text{ is } 6 \times 4 \quad \text{and} \quad h \text{ is } 4 \times 1$

All the tabular aero functions which are denoted by capital C's with subscripts, like C_x , C_{x_p} , C_{l_δ} , etc. are nonlinear functions of (M, α, β) . M is a function of V and air temperature.

The top three rows of (3.3.1) are the rigid-body force equations, while the bottom three rows of (3.3.1) are the rigid-body moment equations. The quantity $f(\dot{x}, x) + g(x) h(x, u)$ contains the expressions $\begin{bmatrix} P \\ Q \\ R \end{bmatrix}$ and $\begin{bmatrix} U \\ V \\ W \end{bmatrix}$ which are given in terms of the state x by

$$\begin{bmatrix} P \\ Q \\ R \end{bmatrix} = \begin{bmatrix} 1 & 0 & -\sin(\Theta) \\ 0 & \cos(\Phi) & \cos(\Theta)\sin(\Phi) \\ 0 & -\sin(\Phi) & \cos(\Theta)\cos(\Phi) \end{bmatrix} \begin{bmatrix} \dot{\Phi} \\ \dot{\Theta} \\ \dot{\Psi} \end{bmatrix} \quad (3.3.2)$$

$$\begin{bmatrix} U \\ V \\ W \end{bmatrix} = V \begin{bmatrix} \cos(\beta)\cos(\alpha) \\ \sin(\beta) \\ \cos(\beta)\sin(\alpha) \end{bmatrix} \quad (3.3.3)$$

The four components of $h(x, u)$ are the forces (divided by mg) produced by the controls $\begin{bmatrix} T \\ \delta_a \\ \delta_e \\ \delta_r \end{bmatrix}$:

$$h(x,u) = \begin{bmatrix} \frac{T}{mg} \\ \frac{\frac{1}{2}\rho V^2 S}{mg} \sin(\delta_a - \frac{Pb}{2V}) \\ \frac{\frac{1}{2}\rho V^2 S}{mg} \sin(\delta_e - \alpha) \\ \frac{\frac{1}{2}\rho V^2 S}{mg} \sin(\delta_r - \beta) \end{bmatrix} \quad (3.3.4)$$

This form for h is an example of the way that h can depend on x and u in a nonlinear way. The sin functions were chosen to account for the fact that surface deflections are bounded even if the surfaces could rotate through a full 2π radians. The shift in the arguments of the sin functions account for the change in airflow at the surfaces caused by the aircraft's rolling motion and angle of attack. The h vector gets premultiplied by the 6 by 4 $g(x)$ matrix, so all four controls can influence all six degrees of freedom.

The derivative in the rotating accelerating frame of the aircraft (sometimes referred to as the covariant derivative) of the linear momentum is

$$\left(\begin{bmatrix} 1 & 0 & 0 \\ 0 & 1 & 0 \\ 0 & 0 & 1 \end{bmatrix} \frac{d}{dt} - \begin{bmatrix} 0 & R & -Q \\ -R & 0 & P \\ Q & -P & 0 \end{bmatrix} \right) \left(m \begin{bmatrix} U \\ V \\ W \end{bmatrix} \right) - mg \begin{bmatrix} -\sin(\Theta) \\ \cos(\Theta)\sin(\Phi) \\ \cos(\Theta)\cos(\Phi) \end{bmatrix}.$$

The aerodynamic forces with zero control input (divided by mg) are:

$$\frac{\frac{1}{2}\rho V^2 S}{mg} \begin{bmatrix} C_x \\ C_y \\ C_z \end{bmatrix} + \frac{1}{2V} \begin{bmatrix} C_{x_p} & C_{x_q} & C_{x_r} \\ C_{y_p} & C_{y_q} & C_{y_r} \\ C_{z_p} & C_{z_q} & C_{z_r} \end{bmatrix} \begin{bmatrix} b & 0 & 0 \\ 0 & c & 0 \\ 0 & 0 & b \end{bmatrix} \begin{bmatrix} p \\ q \\ r \end{bmatrix}.$$

So the top three rows of $f(\dot{x}, x)$ are

$$\frac{-1}{mg} \left[\left(\begin{bmatrix} 1 & 0 & 0 \\ 0 & 1 & 0 \\ 0 & 0 & 1 \end{bmatrix} \frac{d}{dt} - \begin{bmatrix} 0 & R & -Q \\ -R & 0 & P \\ Q & -P & 0 \end{bmatrix} \right) \left(m \begin{bmatrix} U \\ V \\ W \end{bmatrix} \right) - mg \begin{bmatrix} -\sin(\Theta) \\ \cos(\Theta)\sin(\Phi) \\ \cos(\Theta)\cos(\Phi) \end{bmatrix} \right] +$$

$$\frac{1/2\rho V^2 S}{mg} \begin{bmatrix} C_x \\ C_y \\ C_z \end{bmatrix} + \frac{1}{2V} \begin{bmatrix} C_{x_p} & C_{x_q} & C_{x_r} \\ C_{y_p} & C_{y_q} & C_{y_r} \\ C_{z_p} & C_{z_q} & C_{z_r} \end{bmatrix} \begin{bmatrix} b & 0 & 0 \\ 0 & c & 0 \\ 0 & 0 & b \end{bmatrix} \begin{bmatrix} P \\ Q \\ R \end{bmatrix} \quad (3.3.5)$$

Note that no ρ dynamics have been included. However, the controller (introduced in section 5.1) can be assumed to be using a measured (so varying) value of ρ in these equations. This corresponds to treating ρ as a slowly varying parameter, compared to the rapidly varying state. A consequence is that the equilibrium helices (see Appendix A) will vary slowly as altitude is lost.

The forces (divided by mg) produced by the controls give the top three rows of $g(x)$ multiplied by $h(x,u)$:

$$\begin{bmatrix} C_{x_r} & C_{x_b} & C_{x_s} & C_{x_t} \\ C_{y_r} & C_{y_b} & C_{y_s} & C_{y_t} \\ C_{z_r} & C_{z_b} & C_{z_s} & C_{z_t} \end{bmatrix} \begin{bmatrix} \frac{T}{mg} \\ \frac{1/2\rho V^2 S}{mg} \sin(\delta_a - \frac{Pb}{2V}) \\ \frac{1/2\rho V^2 S}{mg} \sin(\delta_e - \alpha) \\ \frac{1/2\rho V^2 S}{mg} \sin(\delta_r - \beta) \end{bmatrix}$$

The resulting linear momentum equations give the top three rows of $0 = f(\dot{x}, x) + g(x) h(x, u)$

$$\begin{bmatrix} 0 \\ 0 \\ 0 \end{bmatrix} = \frac{-1}{mg} \left(\left(\begin{bmatrix} 1 & 0 & 0 \\ 0 & 1 & 0 \\ 0 & 0 & 1 \end{bmatrix} \frac{d}{dt} - \begin{bmatrix} 0 & R & -Q \\ -R & 0 & P \\ Q & -P & 0 \end{bmatrix} \right) \left(m \begin{bmatrix} U \\ V \\ W \end{bmatrix} \right) - mg \begin{bmatrix} -\sin(\Theta) \\ \cos(\Theta)\sin(\Phi) \\ \cos(\Theta)\cos(\Phi) \end{bmatrix} \right) +$$

$$\frac{1/2\rho V^2 S}{mg} \begin{bmatrix} C_x \\ C_y \\ C_z \end{bmatrix} + \frac{1}{2V} \begin{bmatrix} C_{x_p} & C_{x_q} & C_{x_r} \\ C_{y_p} & C_{y_q} & C_{y_r} \\ C_{z_p} & C_{z_q} & C_{z_r} \end{bmatrix} \begin{bmatrix} b & 0 & 0 \\ 0 & c & 0 \\ 0 & 0 & b \end{bmatrix} \begin{bmatrix} P \\ Q \\ R \end{bmatrix} +$$

$$\begin{bmatrix} C_{x_T} & C_{x_\delta} & C_{x_\epsilon} & C_{x_\beta} \\ C_{y_T} & C_{y_\delta} & C_{y_\epsilon} & C_{y_\beta} \\ C_{z_T} & C_{z_\delta} & C_{z_\epsilon} & C_{z_\beta} \end{bmatrix} \begin{bmatrix} \frac{T}{mg} \\ \frac{1}{2}\rho V^2 S \sin(\delta_s - \frac{Pb}{2V}) \\ \frac{1}{2}\rho V^2 S \sin(\delta_e - \alpha) \\ \frac{1}{2}\rho V^2 S \sin(\delta_r - \beta) \end{bmatrix} \quad (3.3.6)$$

The derivative in the rotating accelerating frame of the aircraft (sometimes referred to as the covariant derivative) of the angular momentum is

$$\left(\begin{bmatrix} 1 & 0 & 0 \\ 0 & 1 & 0 \\ 0 & 0 & 1 \end{bmatrix} \frac{d}{dt} - \begin{bmatrix} 0 & R & -Q \\ -R & 0 & P \\ Q & -P & 0 \end{bmatrix} \right) \begin{bmatrix} I_{xx} & -I_{xy} & -I_{xz} \\ -I_{xy} & I_{yy} & -I_{yz} \\ -I_{xz} & -I_{yz} & I_{zz} \end{bmatrix} \begin{bmatrix} P \\ Q \\ R \end{bmatrix}$$

The aerodynamic moments with zero control inputs, multiplied by

$$\frac{1}{mg} \begin{bmatrix} b & 0 & 0 \\ 0 & c & 0 \\ 0 & 0 & b \end{bmatrix}^{-1}$$

are :

$$\frac{1}{2}\rho V^2 S \begin{bmatrix} C_l \\ C_m \\ C_n \end{bmatrix} + \frac{1}{2V} \begin{bmatrix} C_{l_p} & C_{l_q} & C_{l_r} \\ C_{m_p} & C_{m_q} & C_{m_r} \\ C_{n_p} & C_{n_q} & C_{n_r} \end{bmatrix} \begin{bmatrix} b & 0 & 0 \\ 0 & c & 0 \\ 0 & 0 & b \end{bmatrix} \begin{bmatrix} P \\ Q \\ R \end{bmatrix}$$

So the bottom three rows of $f(\dot{x}, x)$ are

$$\frac{-1}{mg} \begin{bmatrix} b & 0 & 0 \\ 0 & c & 0 \\ 0 & 0 & b \end{bmatrix}^{-1} \left(\begin{bmatrix} 1 & 0 & 0 \\ 0 & 1 & 0 \\ 0 & 0 & 1 \end{bmatrix} \frac{d}{dt} - \begin{bmatrix} 0 & R & -Q \\ -R & 0 & P \\ Q & -P & 0 \end{bmatrix} \right) \begin{bmatrix} I_{xx} & -I_{xy} & -I_{xz} \\ -I_{xy} & I_{yy} & -I_{yz} \\ -I_{xz} & -I_{yz} & I_{zz} \end{bmatrix} \begin{bmatrix} P \\ Q \\ R \end{bmatrix} + \quad (3.3.7)$$

$$\frac{1}{2}\rho V^2 S \begin{bmatrix} C_l \\ C_m \\ C_n \end{bmatrix} + \frac{1}{2V} \begin{bmatrix} C_{l_p} & C_{l_q} & C_{l_r} \\ C_{m_p} & C_{m_q} & C_{m_r} \\ C_{n_p} & C_{n_q} & C_{n_r} \end{bmatrix} \begin{bmatrix} b & 0 & 0 \\ 0 & c & 0 \\ 0 & 0 & b \end{bmatrix} \begin{bmatrix} P \\ Q \\ R \end{bmatrix}$$

The moments produced by the controls, multiplied by

$$\frac{1}{mg} \begin{bmatrix} b & 0 & 0 \\ 0 & c & 0 \\ 0 & 0 & b \end{bmatrix}^{-1}$$

give the bottom three rows of $g(x)$ multiplied by $h(x,u)$:

$$\begin{bmatrix} C_{l_r} & C_{l_q} & C_{l_p} & C_{l_s} \\ C_{m_r} & C_{m_q} & C_{m_p} & C_{m_s} \\ C_{n_r} & C_{n_q} & C_{n_p} & C_{n_s} \end{bmatrix} \begin{bmatrix} \frac{T}{mg} \\ \frac{1}{2}\rho V^2 S \frac{\sin(\delta_a - \frac{Pb}{2V})}{mg} \\ \frac{1}{2}\rho V^2 S \frac{\sin(\delta_e - \alpha)}{mg} \\ \frac{1}{2}\rho V^2 S \frac{\sin(\delta_r - \beta)}{mg} \end{bmatrix}$$

So the angular momentum equations, multiplied by

$$\frac{1}{mg} \begin{bmatrix} b & 0 & 0 \\ 0 & c & 0 \\ 0 & 0 & b \end{bmatrix}^{-1}$$

are :

$$\begin{bmatrix} 0 \\ 0 \\ 0 \end{bmatrix} = \frac{-1}{mg} \begin{bmatrix} b & 0 & 0 \\ 0 & c & 0 \\ 0 & 0 & b \end{bmatrix}^{-1} \left(\begin{bmatrix} 1 & 0 & 0 \\ 0 & 1 & 0 \\ 0 & 0 & 1 \end{bmatrix} \frac{d}{dt} - \begin{bmatrix} 0 & R & -Q \\ -R & 0 & P \\ Q & -P & 0 \end{bmatrix} \right) \begin{bmatrix} I_{xx} & -I_{xy} & -I_{xz} \\ -I_{xy} & I_{yy} & -I_{yz} \\ -I_{xz} & -I_{yz} & I_{zz} \end{bmatrix} \begin{bmatrix} P \\ Q \\ R \end{bmatrix} +$$

$$\frac{1}{2}\rho V^2 S \begin{bmatrix} C_l \\ C_m \\ C_n \end{bmatrix} + \frac{1}{2V} \begin{bmatrix} C_{l_p} & C_{l_q} & C_{l_r} \\ C_{m_p} & C_{m_q} & C_{m_r} \\ C_{n_p} & C_{n_q} & C_{n_r} \end{bmatrix} \begin{bmatrix} b & 0 & 0 \\ 0 & c & 0 \\ 0 & 0 & b \end{bmatrix} \begin{bmatrix} P \\ Q \\ R \end{bmatrix} +$$

$$\begin{bmatrix} C_{l_T} & C_{l_{\delta_a}} & C_{l_{\delta_r}} & C_{l_{\delta_s}} \\ C_{m_T} & C_{m_{\delta_a}} & C_{m_{\delta_r}} & C_{m_{\delta_s}} \\ C_{n_T} & C_{n_{\delta_a}} & C_{n_{\delta_r}} & C_{n_{\delta_s}} \end{bmatrix} \begin{bmatrix} \frac{T}{mg} \\ \frac{1}{2}\rho V^2 S}{mg} \sin(\delta_a - \frac{Pb}{2V}) \\ \frac{1}{2}\rho V^2 S}{mg} \sin(\delta_e - \alpha) \\ \frac{1}{2}\rho V^2 S}{mg} \sin(\delta_r - \beta) \end{bmatrix} \quad (3.3.8)$$

So

$$f(\dot{x}, x) = \begin{bmatrix} \text{expression(3.3.5)} \\ \text{expression(3.3.7)} \end{bmatrix} \quad (3.3.9)$$

and

$$g(x) = \begin{bmatrix} C_{x_T} & C_{x_{\delta_a}} & C_{x_{\delta_r}} & C_{x_{\delta_s}} \\ C_{y_T} & C_{y_{\delta_a}} & C_{y_{\delta_r}} & C_{y_{\delta_s}} \\ C_{z_T} & C_{z_{\delta_a}} & C_{z_{\delta_r}} & C_{z_{\delta_s}} \\ C_{l_T} & C_{l_{\delta_a}} & C_{l_{\delta_r}} & C_{l_{\delta_s}} \\ C_{m_T} & C_{m_{\delta_a}} & C_{m_{\delta_r}} & C_{m_{\delta_s}} \\ C_{n_T} & C_{n_{\delta_a}} & C_{n_{\delta_r}} & C_{n_{\delta_s}} \end{bmatrix} \quad (3.3.10)$$

The $0 = f + g h$ equations represent the dynamics while the kinematic equations for the relationship between the Euler angle rates and the body-axis rates are given by (3.3.2) .

SECTION 4 : EQUILIBRIUM MANIFOLD

4.1 Introduction

Systems of ordinary differential equations (ODE) with no control inputs typically have a set of isolated equilibrium points (so that the set of equilibrium points is zero-dimensional) . If a single control parameter is added, then for each fixed value of the control parameter, there will be a corresponding set of isolated equilibrium points. The family of equilibrium points generated in this way forms a one-dimensional set. Similarly, systems with m control parameters will typically have m -dimensional equilibrium sets. When the ODE are not continuous with respect to the controls or other parameters, the equilibrium set can also be discontinuous. However, the equilibrium equations used in this report will still remain valid, they just change value suddenly when the discontinuity is reached. Under fairly general conditions on the ODEs, the equilibrium set will be a smooth mathematical set called an " m -dimensional manifold." Although this m -dimensional manifold is often parameterized by the m control inputs ([R],[YSJ],[MKC],[CM], and [G]) it is sometimes easier to choose a different set of coordinates on this manifold. We could choose, for example, some of the state variables from the ODE, or functions of the state variables. Instead of first fixing the m controls and calculating the associated equilibrium values of the states, we can fix m of the state variables and solve for the equilibrium values of the other states and the controls.

For a given set of state variables, the dependence of the ODE on one subset of the state variables may be more complicated than on the others. For example, the ODE may be transcendental, discontinuous, or even tabular in some of the variables, while only polynomial or even linear in others. Analytic computations will be simplest if we choose as coordinates on the equilibrium manifold the m states on which the ODE has the most complicated dependence. This way, for each value of these coordinates, the equilibrium equations can be solved by relatively simple means. If the equations are algebraic in the remaining variables, we can solve them using standard techniques [BCLA],[PY],[vdW],[W] . In subsection 4.4, we explicitly compute the equilibrium manifold for a six-degree-of-freedom aircraft model.

4.2 Class of Systems

The class of systems described in this section includes the aircraft example shown in Figure 3.2 which has 8 states, 4 controls, and 6 integrator chains of lengths 1, 1, 1, 2, 2, and 1.

Given a system of ordinary differential equations of the form $\dot{x} = \bar{F}(x,u)$, we can rewrite it as $F(\dot{x},x,u) = 0$ by setting $F(\dot{x},x,u) = \bar{F}(x,u) - \dot{x}$. We will consider systems with n states x , k integrator chains (degrees of freedom), and m controls u . The indexed set of ordinary differential equations can be written as (see Figure 4.1)

$$F_i(\dot{x}_{1,c_1}, \dot{x}_{2,c_2}, \dots, \dot{x}_{k,c_k}, x, u) = 0 \quad i = 1, \dots, k \quad (4.2.1)$$

$$x_{i,j+1} = \dot{x}_{i,j} \quad i = 1, \dots, k \quad j = 1, \dots, c_i - 1$$

$$\text{where } c_1 + c_2 + \dots + c_k = n$$

(c_1 through c_k are the lengths of the k integrator chains.)

$$x = \{ x_{i,j} \} \quad i = 1, \dots, k \quad j = 1, \dots, c_i \text{ for each } i$$

where $x_{i,j}$ is the j^{th} integrator output (state) in the i^{th} chain.

$$u = \{ u_i \} \quad i = 1, \dots, m$$

We assume that F has the necessary properties to ensure existence and uniqueness of solutions.

Typically, $F(\dot{x},x,u)$ may be written as $\bar{F}(x,u) - \dot{x}$, and in this case the system may be represented schematically as shown in Figure 4.1.

Integrator Chains

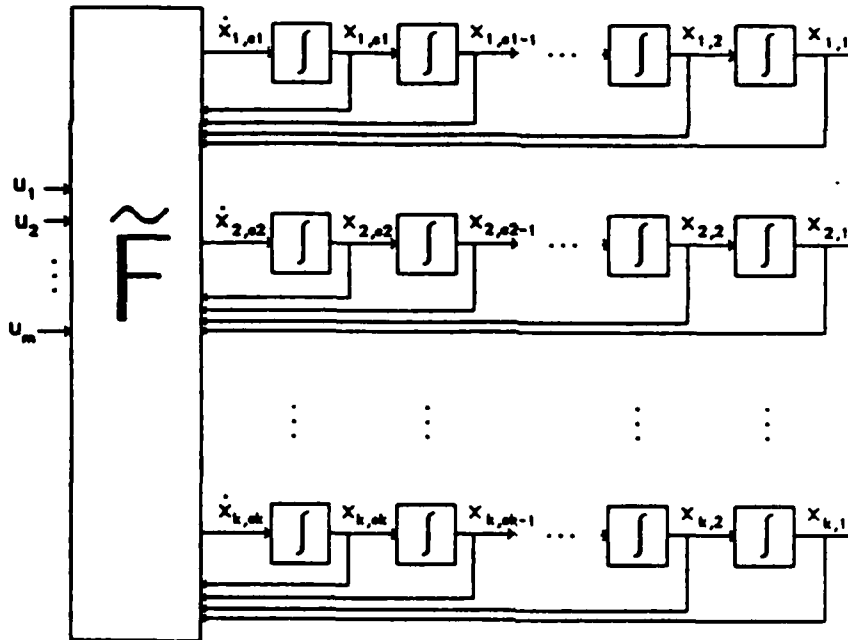


Figure 4.1 Schematic Representation of Typical System

By definition, equilibria are solutions of equation (4.2.1) for which \dot{x} is constant. Consequently the equilibrium set is the set of solutions of the following equations in the (x,u) space.

(4.2.2)

$$F_i(0,0, \dots, 0, x, u) = 0 \quad i = 1, \dots, k$$

$$x_{i,j+1} = 0 \quad i = 1, \dots, k \quad j = 1, \dots, c_i - 1$$

This obviously reduces to k equations in the m entries of u and the k nonzero entries of x , ($x_{i,1}$ $i = 1, \dots, k$). From the Implicit Function Theorem [M], at the regular points, the

equilibrium space is (locally) an m -dimensional manifold.

Sometimes, by changing the coordinates of the system, it is possible to simplify computations. If F is algebraic in k of the elements of (\bar{x}, h) , where $(\bar{x}(x_{i,1}, u), h(x_{i,1}, u))$ is any change of coordinates on the $(x_{i,1}, u)$ space, then parameterize the equilibrium set by the other m entries of $(\bar{x}(x_{i,1}, u), h(x_{i,1}, u))$. For each value of these m parameters, the equilibrium computations reduce to solving k algebraic equations, F , in k unknowns. Solutions can be found by a number of methods, e.g. repeated resultants, Grobner bases, etc. [BCLA], [PY], [vdW], and [W]. If F is algebraic in more than k of the elements of $(\bar{x}(x_{i,1}, u), h(x_{i,1}, u))$, solve the algebraic system for the k algebraic elements of lowest degree. This reduces the number of calculations involved in solving the algebraic system. If the system is linear in some of these k variables, then these can be eliminated by linear algebra, leaving a simpler algebraic system to solve.

The change of coordinates to $(\bar{x}(x_{i,1}, u), h(x_{i,1}, u))$ can be essential in getting the system into algebraic form, and very helpful in reducing the order of the system of algebraic equations. This will be demonstrated in subsection 4.3 .

4.3 Equations of the Form $F(\dot{x},x,u) = f(\dot{x},x) + g(x) h(x,u)$

Dynamics

In the previous section we were using state-space systems defined explicitly by

$$\dot{x} = \tilde{F}(x,u)$$

or, by letting

$$F(\dot{x},x,u) = \tilde{F}(x,u) - \dot{x}$$

the same system was defined implicitly by

$$F(\dot{x},x,u) = 0. \quad (4.3.1)$$

This is a system of k equations. We would like to analytically reduce this to a set of $k-m$ equations in m fewer unknowns. Whether or not we can do this depends on the algebraic structure of the system of equations. In the rest of this subsection we will be considering a case for which this reduction is possible. Note that for the aircraft equations of motion $k = 6$ and $m = 4$, so $k-m = 2$.

Consider the case where $F(\dot{x},x,u)$ has the special form

$$F(\dot{x},x,u) = f(\dot{x},x) + g(x) h(x,u) \quad (4.3.2)$$

Equation 4.3.1 now takes the form

$$0 = f(\dot{x},x) + g(x)h(x,u) \quad (4.3.3)$$

where

f is	$k \times 1$	(column vector)
g is	$k \times m$	(matrix with $k > m$)
h is	$m \times 1$	(column vector)

In this case, the only dependence of F on the m controls, u , enters through the m functions $h(\dot{x}, x, u)$. F depends on h in a linear way, so we can eliminate h using linear algebra. To eliminate h , split the equations into two parts

$$\begin{bmatrix} 0 \\ 0 \end{bmatrix} = \begin{bmatrix} P_1 f(\dot{x}, x) \\ P_2 f(\dot{x}, x) \end{bmatrix} + \begin{bmatrix} P_1 g(x) \\ P_2 g(x) \end{bmatrix} h(x, u) \quad (4.3.4)$$

where

P_1 is any m rows of a k by k identity matrix.

P_2 is the remaining $k-m$ rows of the k by k identity matrix.

If the $g(x)$ matrix is full rank, it has m independent rows. In this case choose P_1 to select out these independent rows so that $P_1 g(x)$ is invertible, then

$$h(\dot{x}, x, u) = - (P_1 g(x))^{-1} P_1 f(\dot{x}, x) \quad (4.3.5)$$

Plug this expression for h into the $0 = P_2 f(\dot{x}, x) + P_2 g(x) h(\dot{x}, x, u)$ equation to get

$$0 = P_2 f(\dot{x}, x) - P_2 g(x) (P_1 g(x))^{-1} P_1 f(\dot{x}, x) \quad (4.3.6)$$

Separating out f gives

$$0 = \left[P_2 - P_2 g(x) (P_1 g(x))^{-1} P_1 \right] f(\dot{x}, x) \quad (4.3.7)$$

or

$$0 = g^\perp(x) f(\dot{x}, x) \quad (4.3.8)$$

where $g^\perp(x)$ is the following $k-m$ by k matrix :

$$g^\perp(x) = \left[P_2 - P_2 g(x) (P_1 g(x))^{-1} P_1 \right] \quad (4.3.9)$$

Note that $[g^\perp(x) g(x)] = 0$, this is the reason for choosing the "perpendicular" superscript on g , ie g^\perp . Equation 4.3.8 can be derived directly from equation 4.3.3 by premultiplying equation 4.3.3 with $g^\perp(x)$.

Equilibrium

At equilibrium $\dot{x} = 0$ and the only nonzero entries of x are $(x_{i,1} \quad i = 1, \dots, k)$. So at equilibrium, equation 4.3.7 represents $k-m$ equations in k unknowns. Therefore the solution set is m -dimensional.

Consider the case where f is polynomial in $k-m$ of the nonzero entries of x , and g does not depend on these $k-m$ variables. Split the nonzero entries of x in to two groups y and z .

Let $y = \{x_{i,1}\}$ where i takes on $k-m$ of the values that correspond to variables in which f is polynomial.

Let $z = \{x_{i,1}\}$ where i takes on the remaining m values.

The function f is polynomial in the entries of y . Let p be the number of monomials in the entries of y on which f depends, e.g. if $f = 1 + 3y_1 + y_2 + y_1^7 y_2$ then $p = 4$.

Let \hat{y} be a column vector containing these p monomials.

In this case

$$f(0,x) = \tilde{f}(z) \hat{y} \quad (4.3.10)$$

where $\tilde{f}(z)$ is a k by p matrix of coefficients. See (4.5.9) through (4.5.11) for an aircraft example.

Since g only depends on z , g^\perp has the form

$$g^\perp(z) = \left[P_2 - P_2 g(z) (P_1 g(z))^{-1} P_1 \right] \quad (4.3.11)$$

and Equation 4.3.8 becomes

$$0 = \left[g^\perp(z) \tilde{f}(z) \right] \hat{y} \quad (4.3.12)$$

Equation 4.3.12 is a set of $k-m$ polynomials in the $k-m$ entries of y , with coefficients that depend on z . For each value of z , this set of polynomials can be solved using repeated resultants or various other methods [BCLA], [PY], [vdW], and [W]. These techniques reduce the system of $k-m$ polynomials in $k-m$ variables into a new system of $k-m$ polynomials of the following form.

$$q_{k-m}(y_1, y_2, \dots, y_{k-m}) = 0$$

$$q_{k-m-1}(y_1, y_2, \dots, y_{k-m-1}) = 0$$

.

.

.

$$q_2(y_1, y_2) = 0$$

$$q_1(y_1) = 0$$

The $q_1(y_1)$ polynomial in one variable can be solved numerically by placing its coefficients into a companion matrix, then finding the eigenvalues of this companion matrix using EISPACK [SBDGIKM]. If the $q_1(y_1)$ polynomial is represented by

$$q_1(y_1) = a_0 + a_1 y_1 + \dots + a_{d-1} y_1^{d-1} + a_d y_1^d \quad (4.3.13)$$

then the companion matrix is of the form

$$\begin{bmatrix} 0 & 1 & 0 & \dots & 0 \\ 0 & 0 & 1 & \dots & 0 \\ 0 & 0 & 0 & \dots & . \\ . & . & . & \dots & . \\ . & . & . & \dots & . \\ . & . & . & \dots & 0 \\ 0 & 0 & 0 & \dots & 1 \\ -\frac{a_0}{a_d} & -\frac{a_1}{a_d} & -\frac{a_2}{a_d} & \dots & -\frac{a_{d-1}}{a_d} \end{bmatrix} \quad (4.3.14)$$

The eigenvalues of this matrix will be the roots of the polynomial q_1 . Each root, y_1 , of this polynomial is then plugged back into the $q_2(y_1, y_2)$ polynomial. Since y_1 is now known, $q_2(y_1, y_2)$ is now a polynomial in only one unknown, y_2 . Put the coefficients of the q_2 polynomial into a companion matrix and solve for y_2 . Continue this process of back substitution until all the values of $(y_1, y_2, \dots, y_{k-m})$ are solved for.

At this point, y has been determined for a given set of values of z . Since the nonzero

components of x consist of the entries of y and z , we now have all the entries in x , so we can solve for the inputs, u , by solving equation 4.3.5

$$h(x,u) = - (P_1 g(x))^{-1} P_1 f(0,x)$$

for u .

All the points in the equilibrium space can be calculated by dividing the m -dimensional set of coordinates, z , into a grid. For each point in this grid, calculate the corresponding y and u . An $(m-1)$ -dimensional family of one-dimensional slices of this equilibrium space can be plotted to visualize the space.

The methods for solving systems of polynomial equations work in principle for any number of polynomials, they are much simpler, however, when the number of polynomials is small. For example, a system of two or three polynomials each of degree two or three can be solved quickly, while a system of four or five polynomials each of degree two or three can take several minutes of computer time to solve.

So far the methods described are quite general. In the next section, we will be considering a concrete example. For the aircraft example, $k = 6$ and $m = 4$, so we are left with 2 equations in 6 unknowns. The equations are polynomial in several of the unknowns. Choose the two $(k-m)$ entries of y from these polynomial type unknowns. Use the remaining four unknowns (z) to parameterize the equilibrium manifold. For each set of values of these four parameters, solve the two polynomial equations for the remaining two unknowns (y).

4.4 Introduction to Aircraft Equilibrium

The kind of equilibrium manifold that we get will depend on what we choose for the states (outputs of integrators). We will not include Ψ as a state since none of the forces or moments depend on Ψ . At equilibrium, $\dot{\Psi}$ can take on any constant value (including zero), so the equilibrium trajectories will be vertical helices (see Appendix A). Note that straight line trajectories are just infinitely fat vertical helices with $\dot{\Psi} = 0$. "Steady" maneuvers such as a 3 g pullup are precluded since the component of gravity is varying greatly during such a maneuver. It would still be possible to trim about a 3 g pull up if we considered time varying ODE and trimmed about some nominal trajectory. When we refer to equilibrium in this report, we will be referring to the vertical helix type of equilibrium.

Equilibrium is attained when the six outputs ($V, \beta, \alpha, \Phi, \Theta, \dot{\Psi}$) all remain constant. If we specify the constant values for four of the outputs then the equilibrium equations will determine the corresponding values for the four inputs and the remaining two outputs.

For several choices of sets of four constant outputs, the equations are algebraic in the remaining variables. This allows us to solve the system of nonlinear equations for the corresponding inputs and the remaining two outputs. Two cases will be considered.

Case 1: The simplest case occurs for low speed flight (say Mach < .6) where the aerodynamic functions are independent of Mach. For instance $C_x(M, \alpha, \beta)$ becomes just $C_x(\alpha, \beta)$. In this case the equations are second-order polynomial in V and $\dot{\Psi}$, so it is easiest to specify constant values for the four outputs ($\beta, \alpha, \Phi, \Theta$) then solve the system of two second-order

polynomials for the remaining two outputs ($V, \dot{\Psi}$) and then solve for the inputs $\begin{bmatrix} T \\ \delta_a \\ \delta_e \\ \delta_r \end{bmatrix}$.

Case 2: For high-speed flight, when the aerodynamic functions depend on Mach number (Mach is a function of V and air temperature) the equations are no longer polynomial in V . However, the equations are still second-order polynomial in $\dot{\Psi}$ and second-order polynomials in trigonometric functions of Φ and Θ . Since trig functions are rational functions of complex exponentials, the equations are rational in $e^{i\Phi}$ and $e^{i\Theta}$. By multiplying the equations through

by the common denominator of these rational functions, the equations become fourth-order polynomial in $e^{i\theta}$ and $e^{i\phi}$. In this case it is easiest to specify constant values for the four outputs (V, β, α, Φ) then solve a system of two polynomials for the remaining two outputs

$(e^{i\theta}, \psi)$ and then solve for the inputs $\begin{bmatrix} T \\ \delta_a \\ \delta_e \\ \delta_r \end{bmatrix}$.

4.5 Calculation of Aircraft Equilibrium

At equilibrium, $x = \text{constant}$; i.e. $(V, \beta, \alpha, \dot{\Phi}, \dot{\Theta}, \dot{\Psi}, \Phi, \Theta) = \text{constant}$. Since Θ, Φ are constant, $\dot{\Theta} = 0$ and $\dot{\Phi} = 0$, so (3.3.2) becomes

$$\begin{bmatrix} P \\ Q \\ R \end{bmatrix} = \begin{bmatrix} 1 & 0 & -\sin(\Theta) \\ 0 & \cos(\Phi) & \cos(\Theta)\sin(\Phi) \\ 0 & -\sin(\Phi) & \cos(\Theta)\cos(\Phi) \end{bmatrix} \begin{bmatrix} \dot{\Phi} \\ \dot{\Theta} \\ \dot{\Psi} \end{bmatrix} = \quad (4.5.1)$$

$$\begin{bmatrix} 1 & 0 & -\sin(\Theta) \\ 0 & \cos(\Phi) & \cos(\Theta)\sin(\Phi) \\ 0 & -\sin(\Phi) & \cos(\Theta)\cos(\Phi) \end{bmatrix} \begin{bmatrix} 0 \\ 0 \\ \dot{\Psi} \end{bmatrix} = \dot{\Psi} \begin{bmatrix} -\sin(\Theta) \\ \cos(\Theta)\sin(\Phi) \\ \cos(\Theta)\cos(\Phi) \end{bmatrix}.$$

This says that $\begin{bmatrix} P \\ Q \\ R \end{bmatrix}$ is constant so the $\frac{d}{dt}$ operator in the covariant derivative of the angular momentum can be eliminated. Similarly, $\begin{bmatrix} V \\ \beta \\ \alpha \end{bmatrix}$ is constant, which implies $\begin{bmatrix} U \\ V \\ W \end{bmatrix}$ is constant so the $\frac{d}{dt}$ operator in the covariant derivative of the linear momentum can be eliminated. Also note that in general (3.3.3) gives us

$$\begin{bmatrix} U \\ V \\ W \end{bmatrix} = V \begin{bmatrix} \cos(\beta)\cos(\alpha) \\ \sin(\beta) \\ \cos(\beta)\sin(\alpha) \end{bmatrix}.$$

Using the expressions for P , Q , and R from equation 4.5.1, the skew symmetric matrix in the covariant derivative expression becomes:

$$\begin{bmatrix} 0 & R & -Q \\ -R & 0 & P \\ Q & -P & 0 \end{bmatrix} = \dot{\Psi} \begin{bmatrix} 0 & \cos(\Theta)\cos(\Phi) & -\cos(\Theta)\sin(\Phi) \\ -\cos(\Theta)\cos(\Phi) & 0 & -\sin(\Theta) \\ \cos(\Theta)\sin(\Phi) & \sin(\Theta) & 0 \end{bmatrix}$$

We will use the following names to keep the notation more compact:

$$E_{\Phi\Theta} = \begin{bmatrix} 0 & \cos(\Theta)\cos(\Phi) & -\cos(\Theta)\sin(\Phi) \\ -\cos(\Theta)\cos(\Phi) & 0 & -\sin(\Theta) \\ \cos(\Theta)\sin(\Phi) & \sin(\Theta) & 0 \end{bmatrix}$$

$$l_{\beta\alpha} = \begin{bmatrix} \cos(\beta)\cos(\alpha) \\ \sin(\beta) \\ \cos(\beta)\sin(\alpha) \end{bmatrix} \quad l_{\Phi\Theta} = \begin{bmatrix} -\sin(\Theta) \\ \cos(\Theta)\sin(\Phi) \\ \cos(\Theta)\cos(\Phi) \end{bmatrix}$$

$$C_{xyz} = \begin{bmatrix} C_x \\ C_y \\ C_z \end{bmatrix}$$

$$C_{lmn} = \begin{bmatrix} C_l \\ C_m \\ C_n \end{bmatrix}$$

$$C_{xyzpqr} = \begin{bmatrix} C_{xp} & C_{xq} & C_{xr} \\ C_{yp} & C_{yq} & C_{yr} \\ C_{zp} & C_{zq} & C_{zr} \end{bmatrix}$$

$$C_{lmnpqr} = \begin{bmatrix} C_{lp} & C_{lq} & C_{lr} \\ C_{mp} & C_{mq} & C_{mr} \\ C_{np} & C_{nq} & C_{nr} \end{bmatrix}$$

$$I_{mo} = \begin{bmatrix} I_{xx} & -I_{xy} & -I_{xz} \\ -I_{xy} & I_{yy} & -I_{yz} \\ -I_{xz} & -I_{yz} & I_{zz} \end{bmatrix}$$

$$BCB = \begin{bmatrix} b & 0 & 0 \\ 0 & c & 0 \\ 0 & 0 & b \end{bmatrix}$$

$$V_{nom}^2 = \frac{mg}{\frac{1}{2}\rho S}$$

Plugging all this into equations (3.3.1), (3.3.5), (3.3.7), (3.3.10), and (3.3.4) gives the equilibrium expressions for f , g , and h in terms of $(V, \beta, \alpha, \dot{\Psi}, \Phi, \Theta)$ and the four controls.

The top three rows of $f(0, x)$ become

$$\begin{aligned} & \frac{V\dot{\Psi}}{g} E_{\Phi\Theta} l_{\beta\alpha} + l_{\Phi\Theta} + \\ & \left(\frac{V}{V_{nom}} \right)^2 \left(C_{xyz} + \frac{\dot{\Psi}}{2V} C_{xyzpqr} BCB l_{\Phi\Theta} \right) \end{aligned} \quad (4.5.2)$$

while the bottom three rows of $f(0, x)$ become

$$\frac{\dot{\Psi}^2}{mg} BCB^{-1} E_{\Theta\Theta} I_{mo} 1_{\Theta\Theta} + \left(\frac{V}{V_{nom}} \right)^2 \left(C_{lmm} + \frac{\dot{\Psi}}{2V} C_{lmm\dot{\Psi}} BCB^{-1} 1_{\Theta\Theta} \right) . \quad (4.5.3)$$

$g(x)$ is left unchanged since each entry only depends on $(M(V), \beta, \alpha)$:

$$g(x) = \begin{bmatrix} C_{x_T} & C_{x_b} & C_{x_s} & C_{x_a} \\ C_{y_T} & C_{y_b} & C_{y_s} & C_{y_a} \\ C_{z_T} & C_{z_b} & C_{z_s} & C_{z_a} \\ C_{l_T} & C_{l_b} & C_{l_s} & C_{l_a} \\ C_{m_T} & C_{m_b} & C_{m_s} & C_{m_a} \\ C_{n_T} & C_{n_b} & C_{n_s} & C_{n_a} \end{bmatrix}$$

and the $h(0, x, u)$ vector becomes

$$h(0, x, u) = \begin{bmatrix} \frac{T}{mg} \\ \frac{V^2}{V_{nom}^2} \sin(\delta_a + \frac{\dot{\Psi} \sin(\Theta) b}{2V}) \\ \frac{V^2}{V_{nom}^2} \sin(\delta_e - \alpha) \\ \frac{V^2}{V_{nom}^2} \sin(\delta_r - \beta) \end{bmatrix} . \quad (4.5.4)$$

The $g^\perp(x)$ matrix described in equation (4.3.9) requires the selection of P_1 and P_2 . The choice given below is motivated by the desire to make $[P_1 g(x)]$ invertible for typical aircraft. Let

$$P_1 = \begin{bmatrix} 1 & 0 & 0 & 0 & 0 & 0 \\ 0 & 0 & 0 & 1 & 0 & 0 \\ 0 & 0 & 0 & 0 & 1 & 0 \\ 0 & 0 & 0 & 0 & 0 & 1 \end{bmatrix} .$$

Let

$$P_2 = \begin{bmatrix} 0 & 1 & 0 & 0 & 0 & 0 \\ 0 & 0 & 1 & 0 & 0 & 0 \end{bmatrix}$$

Using P_1 , P_2 , and $g(x)$ we can form

$$g^\perp(x) = P_2 - P_2 g(x) (P_1 g(x))^{-1} P_1 \quad (4.5.5)$$

Note: For aircraft with left/right symmetry, the elevator and thrust only affect the first, third, and fifth rows of $f(\dot{x}, x) + g(x) h(\dot{x}, x, u)$ while the rudder and aileron only affect the second, fourth, and sixth rows of $f(\dot{x}, x) + g(x) h(\dot{x}, x, u)$. The result is that the $g(x)$ matrix then has the following simplified form:

$$g(x) = \begin{bmatrix} C_{x_T} & 0 & C_{x_{\delta_e}} & 0 \\ 0 & C_{y_{\delta_a}} & 0 & C_{y_{\delta_r}} \\ C_{z_T} & 0 & C_{z_{\delta_e}} & 0 \\ 0 & C_{l_{\delta_a}} & 0 & C_{l_{\delta_r}} \\ C_{m_T} & 0 & C_{m_{\delta_e}} & 0 \\ 0 & C_{n_{\delta_a}} & 0 & C_{n_{\delta_r}} \end{bmatrix} \quad (4.5.6)$$

In this simpler situation, $P_1 g(x)$ can be inverted explicitly so equation (4.5.5) gives $g^\perp(x)$ as :

$$g^\perp(x) = \begin{bmatrix} 0 & 1 & 0 & \frac{C_{y_{\delta_r}} C_{n_{\delta_a}} - C_{y_{\delta_a}} C_{n_{\delta_r}}}{C_{l_{\delta_a}} C_{n_{\delta_r}} - C_{l_{\delta_r}} C_{n_{\delta_a}}} & 0 & \frac{C_{y_{\delta_r}} C_{l_{\delta_a}} - C_{y_{\delta_a}} C_{l_{\delta_r}}}{C_{l_{\delta_a}} C_{n_{\delta_r}} - C_{l_{\delta_r}} C_{n_{\delta_a}}} \\ \frac{C_{z_{\delta_e}} C_{m_T} - C_{z_T} C_{m_{\delta_e}}}{C_{x_T} C_{m_{\delta_e}} - C_{x_{\delta_e}} C_{m_T}} & 0 & 1 & 0 & \frac{C_{x_{\delta_e}} C_{z_T} - C_{x_T} C_{z_{\delta_e}}}{C_{x_T} C_{m_{\delta_e}} - C_{x_{\delta_e}} C_{m_T}} & 0 \end{bmatrix}$$

In the further simplifying situation where the thrust is aligned with the x axis ($C_{z_T} = 0 = C_{m_T}$) and the ailerons only produce a rolling moment ($C_{y_{\delta_a}} = 0 = C_{n_{\delta_a}}$), we get:

$$g^\perp(x) = \begin{bmatrix} 0 & 1 & 0 & 0 & 0 & -\frac{C_{y\delta_1}}{C_{m\delta_1}} \\ 0 & 0 & 1 & 0 & -\frac{C_{z\delta_1}}{C_{m\delta_1}} & 0 \end{bmatrix} \quad (4.5.8)$$

If $C_{y\delta_1}$ and $C_{z\delta_1}$ are also neglected, then $g^\perp = P_2$. In general the $g(x)$ matrix can be a full matrix, and $g^\perp(x)$ can be computed numerically for each value of x used. In the case where $g^\perp(x)$ is computed numerically, it is better to use the singular value decomposition algorithm (e.g. in LINPACK [DMBS]) in place of equation (4.5.5) because the SVD algorithm is numerically more stable and works even when $P_1 g(x)$ is not invertible.

We now have two equations,

$$\begin{bmatrix} 0 \\ 0 \end{bmatrix} = g^\perp(x) f(0, x) \quad (4.5.9)$$

in the six unknowns, $x = (V, \beta, \alpha, \dot{\Psi}, \Theta, \Phi)$.

Case 1 : (same as in subsection 4.4) The case where the aero functions do not depend on Mach.

$$\text{Let } y = (V, \dot{\Psi}), \quad \hat{y} = \begin{bmatrix} 1 \\ V \\ \dot{\Psi} \\ V\dot{\Psi} \end{bmatrix}, \quad \text{and } z = (\beta, \alpha, \Phi, \Theta).$$

In this case $\tilde{f}(z)$ is the following 6 by 4 matrix, where 0_3 is a column of three zeros.

$$\tilde{f}(z) = \begin{bmatrix} 1_{\Phi\Theta} & \frac{C_{xyz}}{V_{nom}^2} & \frac{C_{xyzpqr}}{V_{nom}^2} \frac{BCB}{2} 1_{\Phi\Theta} + \frac{E_{\Phi\Theta}}{g} 1_{\beta\alpha} & 0_3 \\ 0_3 & \frac{C_{lmn}}{V_{nom}^2} & \frac{C_{lmnpqr}}{V_{nom}^2} \frac{BCB}{2} 1_{\Phi\Theta} & \frac{BCB^{-1}}{mg} E_{\Phi\Theta} I_{mo} 1_{\Phi\Theta} \end{bmatrix}$$

so the equilibrium equations become

$$\begin{bmatrix} 0 \\ 0 \end{bmatrix} = g^\perp(\beta, \alpha, \Phi, \Theta) \tilde{f}(\beta, \alpha, \Phi, \Theta) \begin{bmatrix} 1 \\ V \\ V\dot{\Psi} \\ \dot{\Psi}^2 \end{bmatrix} .$$

Choose values for $\beta, \alpha, \Phi, \Theta$ and solve the above set of two equations for $V, \dot{\Psi}$. These equations are second-order polynomials in V and $\dot{\Psi}$, of the following form:

$$0 = p(V, \dot{\Psi}) = p_{00} + p_{20} V^2 + p_{11} V \dot{\Psi} + p_{02} \dot{\Psi}^2 \quad (4.5.10)$$

$$0 = q(V, \dot{\Psi}) = q_{00} + q_{20} V^2 + q_{11} V \dot{\Psi} + q_{02} \dot{\Psi}^2 \quad (4.5.11)$$

where

$$\begin{bmatrix} p_{00} & p_{20} & p_{11} & p_{02} \\ q_{00} & q_{20} & q_{11} & q_{02} \end{bmatrix} = g^\perp(\beta, \alpha, \Phi, \Theta) \tilde{f}(\beta, \alpha, \Phi, \Theta) .$$

The two polynomial equations, (4.5.10) and (4.5.11), can be solved using direct elimination, or by using resultants. Two polynomial equations (whose leading coefficients are nonzero) have a solution if and only if their resultant is zero [vdW]. Given two polynomials poly1 and poly2 in several variables, of degree n1 and n2 respectively in some particular variable (say x), their resultant with respect to x is the determinant of the (n1+n2) by (n1+n2) matrix formed as follows. Take the coefficients on powers of x from poly1 and put them in the top row of the matrix starting on the left side. repeat this row n2 times, shifting to the right by one column for each row. Fill in row n2 + 1 with the coefficient on the powers of x from poly2. Repeat this row n1 times, shifting to the right by one column for each row.

The resultant of polynomials (4.5.10) and (4.5.11) (with respect to $\dot{\Psi}$ with $p_{02}q_{02} \neq 0$) is the determinant of the following matrix whose entries are shifted rows of the coefficients on the $\dot{\Psi}$ terms. ($n1 + n2 = 4$ unless p_{02} or q_{02} is zero).

$$0 = \det \begin{bmatrix} p_{00} + p_{20}V^2 & p_{11}V & p_{02} & 0 \\ 0 & p_{00} + p_{20}V^2 & p_{11}V & p_{02} \\ q_{00} + q_{20}V^2 & q_{11}V & q_{02} & 0 \\ 0 & q_{00} + q_{20}V^2 & q_{11}V & q_{02} \end{bmatrix} = k_4 V^4 + k_2 V^2 + k_0 \quad (4.5.15)$$

$$k_4 = (p_{20}q_{02} - q_{20}p_{02})^2 - (p_{11}q_{02} - q_{11}p_{02})(p_{20}q_{11} - q_{20}p_{11}) \quad (4.5.16)$$

$$k_2 = 2 (p_{00}q_{02} - q_{00}p_{02})(p_{20}q_{02} - q_{20}p_{02}) - (p_{11}q_{02} - q_{11}p_{02})(p_{00}q_{11} - q_{00}p_{11}) \quad (4.5.17)$$

$$k_0 = (p_{00}q_{02} - q_{00}p_{02})^2 \quad (4.5.18)$$

The k 's depend on the p_{ij} 's and q_{ij} 's so they depend on $\beta, \alpha, \Phi, \Theta$. Since no odd order terms in V appear in the polynomial on the right hand side of equation (4.5.15), it is of second-order in V^2 so it can be solved using the quadratic formula:

$$V^2 = \frac{-k_2 \pm \sqrt{(k_2^2 - 4k_4k_0)}}{2k_4} \quad (4.5.19)$$

From (4.5.19) we see that there are at most two positive real solutions for V . From numerical evaluation of several aircraft models, we have seen that typically one solution of (4.5.19) is large and positive while the other is so small that the aerodynamic control surfaces would not have enough authority to hold the aircraft at that equilibrium. The equilibrium associated with the large speed is typically associated with low $\dot{\Psi}$ values and corresponds to reasonable flight regimes, while the low-speed equilibrium is often associated with large $\dot{\Psi}$, spin-type flight.

Use the real positive values of V to find $\dot{\Psi}$ as follows. First, eliminate $\dot{\Psi}^2$ from the two polynomials by forming the expression

$$q_{02} p(V, \dot{\Psi}) - p_{02} q(V, \dot{\Psi})$$

The $\dot{\Psi}^2$ terms cancel in this expression, leaving

$$0 = q_{02}(p_{00} + p_{20}V^2 + p_{11}V\dot{\Psi}) - p_{02}(q_{00} + q_{20}V^2 + q_{11}V\dot{\Psi}) \quad (4.5.20)$$

so

$$\dot{\Psi} = \frac{(q_{02}p_{00} - p_{02}q_{00}) + (q_{02}p_{20} - p_{02}q_{20})V^2}{(p_{02}q_{11} - q_{02}p_{11})V} \quad (4.5.21)$$

(Note: If q_{02} and p_{02} are both zero, then there is no $\dot{\Psi}^2$ term to start with.)

Use these values of V and $\dot{\Psi}$ in f and g to solve for h :

$$h(0, x, u) = -[P_1 g(x)]^{-1} [P_1 f(0, x)]$$

Finally, use this value of h to solve the following equations for

$$\begin{bmatrix} T \\ \delta_a \\ \delta_e \\ \delta_r \end{bmatrix}$$

$$\begin{bmatrix} \frac{T}{mg} \\ \frac{V^2}{V_{nom}^2} \sin(\delta_a + \frac{\dot{\Psi} \sin(\Theta) b}{2V}) \\ \frac{V^2}{V_{nom}^2} \sin(\delta_e - \alpha) \\ \frac{V^2}{V_{nom}^2} \sin(\delta_r - \beta) \end{bmatrix} = h(0, x, u)$$

Case 2 : (See subsection 4.4) When the aero functions depend on Mach number, let $z = (V, \beta, \alpha, \Phi)$, $y = (e^{i\Theta}, \dot{\Psi})$, and \hat{y} is the vector of 7 monomials in $e^{i\Theta}$ and $\dot{\Psi}$ on which f depends:

$$\hat{y} = \text{transpose}((e^{-i\Theta}, 1, e^{i\Theta}), \dot{\Psi}(e^{-i\Theta}, e^{i\Theta}), \dot{\Psi}^2(e^{-i2\Theta}, 1, e^{i2\Theta}))$$

The two equations (4.5.9) are second-order polynomials in $\dot{\Psi}$, $\sin(\Theta)$, and $\cos(\Theta)$. The

only Θ dependence comes from the $1_{\Phi\Theta}$ and $E_{\Phi\Theta}$ in $f(0,x)$ (see equations 4.5.2 and 4.5.3) .
Substitute for $\cos(\Theta)$ and $\sin(\Theta)$ using

$$\sin(\Theta) = \frac{e^{i\Theta} - e^{-i\Theta}}{2i} \quad \cos(\Theta) = \frac{e^{i\Theta} + e^{-i\Theta}}{2}$$

where $i = \sqrt{-1}$.

This lets us write $1_{\Phi\Theta}$ and $E_{\Phi\Theta}$ in terms of $e^{i\Theta}$ and $e^{-i\Theta}$.

$$E_{\Phi\Theta} = E_{\Phi} e^{i\Theta} + \bar{E}_{\Phi} e^{-i\Theta} \quad 1_{\Phi\Theta} = 1_{\Phi} e^{i\Theta} + \bar{1}_{\Phi} e^{-i\Theta}$$

where

$$E_{\Phi} = \begin{bmatrix} 0 & \frac{\cos(\Phi)}{2} & \frac{-\sin(\Phi)}{2} \\ \frac{-\cos(\Phi)}{2} & 0 & \frac{-1}{2i} \\ \frac{\sin(\Phi)}{2} & \frac{1}{2i} & 0 \end{bmatrix} \quad , \quad 1_{\Phi} = \begin{bmatrix} \frac{-1}{2i} \\ \frac{\sin(\Phi)}{2} \\ \frac{\cos(\Phi)}{2} \end{bmatrix} ,$$

and the over-bar signifies complex conjugation.

Plug these expressions for $1_{\Phi\Theta}$ and $E_{\Phi\Theta}$ into (4.5.2) and (4.5.3) . The result is

$$f(0,x) = \tilde{f}(z) \hat{y} = [\tilde{f}_{123}(z) , \tilde{f}_{45}(z) , \tilde{f}_{678}(z)] \begin{bmatrix} \hat{y}_{123} \\ \Psi \hat{y}_{45} \\ \Psi^2 \hat{y}_{678} \end{bmatrix}$$

where

$$\hat{y}_{123} = \begin{bmatrix} e^{-i\Theta} \\ 1 \\ e^{i\Theta} \end{bmatrix} \quad \hat{y}_{45} = \begin{bmatrix} e^{-i\Theta} \\ e^{i\Theta} \end{bmatrix} \quad \hat{y}_{678} = \begin{bmatrix} e^{-i2\Theta} \\ 1 \\ e^{i2\Theta} \end{bmatrix}$$

$$\tilde{f}_{123}(z) = \begin{bmatrix} \bar{I}_\Phi & \frac{V^2}{V_{\text{nom}}^2} C_{xyz} & I_\Phi \\ 0_3 & \frac{V^2}{V_{\text{nom}}^2} C_{lmn} & 0_3 \end{bmatrix}$$

$$\tilde{f}_{45}(z) = \begin{bmatrix} \frac{V}{g} \bar{E}_\Phi I_{\beta\alpha} + \frac{V}{V_{\text{nom}}^2} C_{xyz} \frac{BCB}{2} \bar{I}_\Phi & \frac{V}{g} E_\Phi I_{\beta\alpha} + \frac{V}{V_{\text{nom}}^2} C_{xyz} \frac{BCB}{2} I_\Phi \\ \frac{V}{V_{\text{nom}}^2} C_{lmn} \frac{BCB}{2} \bar{I}_\Phi & \frac{V}{V_{\text{nom}}^2} C_{lmn} \frac{BCB}{2} I_\Phi \end{bmatrix}$$

$$\tilde{f}_{678}(z) = \begin{bmatrix} 0_3 & 0_3 & 0_3 \\ \frac{BCB^{-1}}{mg} \bar{E}_\Phi I_{mo} \bar{I}_\Phi & \frac{BCB^{-1}}{mg} (\bar{E}_\Phi I_{mo} I_\Phi + E_\Phi I_{mo} \bar{I}_\Phi) & \frac{BCB^{-1}}{mg} E_\Phi I_{mo} I_\Phi \end{bmatrix}$$

Multiply both sides of the equations, $0_2 = g^\perp(z) \tilde{f}(z) \hat{y}$, by $e^{i2\Theta}$ to make $\hat{y} e^{i2\Theta}$ polynomial in $e^{i\Theta}$. The resulting two equations are second-order polynomial in $\dot{\Psi}$ and fourth-order polynomial in $e^{i\Theta}$ of the form :

$$0 = p_0(e^{i\Theta}) + p_1(e^{i\Theta})\dot{\Psi} + p_2(e^{i\Theta})\dot{\Psi}^2 \quad (4.5.22)$$

$$0 = q_0(e^{i\Theta}) + q_1(e^{i\Theta})\dot{\Psi} + q_2(e^{i\Theta})\dot{\Psi}^2 \quad (4.5.23)$$

where

$$\begin{bmatrix} p_0(e^{i\Theta}) \\ q_0(e^{i\Theta}) \end{bmatrix} = g^\perp(z) \tilde{f}_{123}(z) [\hat{y}_{123} e^{i2\Theta}]$$

$$\begin{bmatrix} p_1(e^{i\Theta}) \\ q_1(e^{i\Theta}) \end{bmatrix} = g^\perp(z) \tilde{f}_{45}(z) [\hat{y}_{45} e^{i2\Theta}]$$

$$\begin{bmatrix} p_2(e^{i\Theta}) \\ q_2(e^{i\Theta}) \end{bmatrix} = g^\perp(z) \tilde{f}_{678}(z) [\hat{y}_{678} e^{i2\Theta}] \quad .$$

Form the resultant (with respect to $\dot{\Psi}$) again

$$0 = \det \begin{bmatrix} p_0 & p_1 & p_2 & 0 \\ 0 & p_0 & p_1 & p_2 \\ q_0 & q_1 & q_2 & 0 \\ 0 & q_0 & q_1 & q_2 \end{bmatrix} = (p_0 q_2 - p_2 q_0)^2 - (p_1 q_2 - p_2 q_1)(p_0 q_1 - p_1 q_0) \quad .$$

The right hand side will be a 14th-order polynomial in $e^{i\Theta}$ of the form :

$$e^{i8\Theta} \sum_{k=-6}^{k=6} c_k e^{ik\Theta} \quad (4.5.24)$$

where $c_{-k} = \bar{c}_k$ (so we only need to calculate c_0 through c_6). The polynomial in (4.5.24) is of the form $(e^{i2\Theta})$ (12th-order polynomial in $e^{i\Theta}$). Put the coefficients of this 12th-order polynomial into a companion matrix and find the roots using EISPACK [SBDGIKM]. Keep the roots that have magnitude equal to 1 (Θ is real in these cases). Use these roots to solve for $\dot{\Psi}$.

$$\dot{\Psi} = \frac{q_2(e^{i\Theta}) p_0(e^{i\Theta}) - p_2(e^{i\Theta}) q_0(e^{i\Theta})}{p_2(e^{i\Theta}) q_1(e^{i\Theta}) - q_2(e^{i\Theta}) p_1(e^{i\Theta})}$$

$\dot{\Psi}$ will be real since the extra factors of $e^{i\Theta}$ cancel in numerator and denominator.

Finally, solve for the inputs as in case 1.

SECTION 5 : ANALYSIS OF AIRCRAFT DYNAMICS

In this section we analyze the nonlinear aircraft equations using dynamic inversion. Our goal is to show how dynamic inversion can be used to develop flying quality parameters. Some candidate parameters arising from the analysis in this section are presented in section 6: Nonlinear Flying Qualities.

5.1 Partial Dynamic Inversion

The 6 DOF nonlinear aircraft equations of motion are of the form:

$$\dot{x} = f(x) + g(x) h(x,u) \quad (5.1.1)$$

with

- x in an n dimensional state space ($n=8$ for our aircraft model)
- u in an m dimensional control space ($m=4$ for our aircraft model)
- f : an n by 1 vector depending on x
- g : an n by m matrix depending on x
- h : an m by 1 vector depending on x and u

Equation 5.1.1 splits into the following form

$$\begin{bmatrix} \dot{x}_1 \\ \dot{x}_2 \\ \dot{x}_3 \end{bmatrix} = \begin{bmatrix} f_1(x) \\ f_2(x) \\ f_3(x) \end{bmatrix} + \begin{bmatrix} g_1(x) \\ g_2(x) \\ 0 \end{bmatrix} h(x,u) \quad (5.1.2)$$

where the first k equations represent the dynamics ($k=6$ for a 6DOF aircraft):

$$\begin{bmatrix} \dot{x}_1 \\ \dot{x}_2 \end{bmatrix} = \begin{bmatrix} f_1(x) \\ f_2(x) \end{bmatrix} + \begin{bmatrix} g_1(x) \\ g_2(x) \end{bmatrix} h(x,u) \quad (5.1.3)$$

and the last $n-k$ equations represent the kinematics ($n-k=2$ for our 6DOF aircraft model):

$$\dot{x}_3 = f_3(x) \quad (5.1.4)$$

We split the dynamic state in equation 5.1.3 into the x_1 and x_2 parts to distinguish the states x_1 we wish to control directly, from the states x_2 we choose not to control directly. When $m = k$ we can control all k of the degrees of freedom. When $m < k$, we can only control part of the dynamics, because there are fewer independent degrees of control authority than degrees of freedom. In equation 5.1.2 we have :

- x_1 in an m -dimensional space
- x_2 in a $(k-m)$ -dimensional space ($k \geq m$)
- x_3 in an $(n-k)$ -dimensional space ($n \geq k$)
- f_1 : an m by 1 vector depending on x
- f_2 : a $k-m$ by 1 vector depending on x
- f_3 : an $n-k$ by 1 vector depending on x
- g_1 : an m by m matrix depending on x
- g_2 : a $k-m$ by m matrix depending on x

In cases where we cannot invert all of the dynamics, we can still do a partial inverse. The x_1 dynamics can be inverted as follows. Let v be some function of the pilot's commands, then given a set of desired dynamics $\dot{x}_1 = F_1(x,v)$, put

$$h(x,u) = [g_1(x)]^{-1} [\dot{x}_1 - f_1(x)] = [g_1(x)]^{-1} [F_1(x,v) - f_1(x)] \quad (5.1.5)$$

and then solve $h(x,u)$ for u , the signal to the actuators, as a function of x (which we assume can be measured) and the external input v . Equation 5.1.5 involves the inverse of $g_1(x)$ which might only exist in some subset of the state space. In this sense, the analysis is not global.

To determine the uncontrolled x_2 dynamics and the kinematics, substitute the expression for $h(x,u)$ from 5.1.5 into 5.1.2 to obtain

$$\begin{aligned}\dot{x}_1 &= F_1(x,v) \\ \dot{x}_2 &= f_2(x) + g_2(x)[g_1(x)]^{-1}[F_1(x,v) - f_1(x)] \\ \dot{x}_3 &= f_3(x)\end{aligned}$$

This partial inversion process involves several choices. The first choice made (choice of x_1) determines which dynamic states are controlled directly. The second choice made (choice of $F_1(x,v)$) determines the dynamics for those states. Some examples we explored on this program are shown below.

Example 1 : The U,P,Q,R Inverter

$$x_1 = \begin{bmatrix} U \\ P \\ Q \\ R \end{bmatrix} \quad x_2 = \begin{bmatrix} V \\ W \end{bmatrix} \quad x_3 = \begin{bmatrix} \Phi \\ \Theta \end{bmatrix}$$

$$F_1(x,v) = \begin{bmatrix} \lambda_U & 0 & 0 & 0 \\ 0 & \lambda_P & 0 & 0 \\ 0 & 0 & \lambda_Q & 0 \\ 0 & 0 & 0 & \lambda_R \end{bmatrix} \begin{bmatrix} U - U_{cmd} \\ P - P_{cmd} \\ Q - Q_{cmd} \\ R - R_{cmd} \end{bmatrix}$$

where

$$v = \begin{bmatrix} U_{cmd} \\ P_{cmd} \\ Q_{cmd} \\ R_{cmd} \end{bmatrix}$$

Example 2 : The U,β,Φ,Θ Inverter

$$x_1 = \begin{bmatrix} U \\ \beta \\ \Phi \\ \Theta \end{bmatrix} \quad x_2 = \begin{bmatrix} \alpha \\ \Psi \end{bmatrix} \quad x_3 = \begin{bmatrix} \Phi \\ \Theta \end{bmatrix}$$

$$F_1(x,v) = \begin{bmatrix} \lambda_U & 0 & 0 & 0 & 0 & 0 \\ 0 & \lambda_\beta & 0 & 0 & 0 & 0 \\ 0 & 0 & -\zeta_\Phi \omega_\Phi & 0 & -\omega_\Phi^2 & 0 \\ 0 & 0 & 0 & -\zeta_\Theta \omega_\Theta & 0 & -\omega_\Theta^2 \end{bmatrix} \begin{bmatrix} U - U_{cmd} \\ \beta - \beta_{cmd} \\ \Phi \\ \Theta \\ \Phi - \Phi_{cmd} \\ \Theta - \Theta_{cmd} \end{bmatrix}$$

where

$$v = \begin{bmatrix} U_{cmd} \\ \beta_{cmd} \\ \Phi_{cmd} \\ \Theta_{cmd} \end{bmatrix}$$

Example 3 : The β,α,Φ,Θ Inverter

$$x_1 = \begin{bmatrix} \beta \\ \alpha \\ \Phi \\ \Theta \end{bmatrix} \quad x_2 = \begin{bmatrix} \dot{v} \\ \dot{\Psi} \end{bmatrix} \quad x_3 = \begin{bmatrix} \Phi \\ \Theta \end{bmatrix}$$

$$F_1(x,v) = \begin{bmatrix} \lambda_\beta & 0 & 0 & 0 & 0 & 0 \\ 0 & \lambda_\alpha & 0 & 0 & 0 & 0 \\ 0 & 0 & -\zeta_\Phi \omega_\Phi & 0 & -\omega_\Phi^2 & 0 \\ 0 & 0 & 0 & -\zeta_\Theta \omega_\Theta & 0 & -\omega_\Theta^2 \end{bmatrix} \begin{bmatrix} \beta - \beta_{cmd} \\ \alpha - \alpha_{cmd} \\ \Phi \\ \Theta \\ \Phi - \Phi_{cmd} \\ \Theta - \Theta_{cmd} \end{bmatrix}$$

where

$$v = \begin{bmatrix} \beta_{cmd} \\ \alpha_{cmd} \\ \Phi_{cmd} \\ \Theta_{cmd} \end{bmatrix}$$

Example 4 : An alternative $\beta, \alpha, \Phi, \Theta$ controller

Given an external command

$$v = \begin{bmatrix} \beta_{cmd} \\ \alpha_{cmd} \\ \Phi_{cmd} \\ \Theta_{cmd} \end{bmatrix}$$

find the associated equilibrium values of V_{cmd} .

$$(V_{cmd})^2 = \frac{-b \pm \sqrt{b^2 - 4ac}}{2a}$$

where a, b, and c are functions of β_{cmd} , α_{cmd} , Φ_{cmd} , Θ_{cmd} (see equation 4.5.19 in the equilibrium section) .

If there are two positive real equilibrium speeds to choose from, the larger one is chosen. Next U_{cmd} is computed ($U_{cmd} = V_{cmd} \cos(\alpha_{cmd}) \cos(\beta_{cmd})$) . Finally, this U_{cmd} , along with β_{cmd} , Φ_{cmd} , and , Θ_{cmd} are sent to the U, β, Φ, Θ inverter.

Example 5 : A $\beta, \alpha, \gamma, \mu$ controller

Given an external command

$$v = \begin{bmatrix} \beta_{cmd} \\ \alpha_{cmd} \\ \gamma_{cmd} \\ \mu_{cmd} \end{bmatrix}$$

where γ is the velocity pitch angle (flight path angle) and μ is the velocity roll angle (rolling around the velocity vector). The $\beta, \alpha, \gamma, \mu$ controller first performs a change of coordinates from β_{cmd} , α_{cmd} , γ_{cmd} , μ_{cmd} to β_{cmd} , α_{cmd} , Φ_{cmd} , Θ_{cmd} , using the following

transformations:

$$\begin{bmatrix} -\sin(\Theta) \\ \cos(\Theta)\sin(\Phi) \\ \cos(\Theta)\cos(\Phi) \end{bmatrix} = \begin{bmatrix} \cos(\alpha)\cos(\beta) & -\cos(\alpha)\sin(\beta) & -\sin(\alpha) \\ \sin(\beta) & \cos(\beta) & 0 \\ \sin(\alpha)\cos(\beta) & -\sin(\alpha)\sin(\beta) & \cos(\alpha) \end{bmatrix} \begin{bmatrix} -\sin(\gamma) \\ \cos(\gamma)\sin(\mu) \\ \cos(\gamma)\cos(\mu) \end{bmatrix} .$$

The top row of this equation gives us

$$\Theta = \sin^{-1} \left[\cos(\alpha)\cos(\beta)\sin(\gamma) + \cos(\alpha)\sin(\beta)\cos(\gamma)\sin(\mu) + \sin(\alpha)\cos(\gamma)\cos(\mu) \right]$$

while the ratio of the second and third rows gives us

$$\Phi = \tan^{-1} \left[\frac{-\sin(\beta)\sin(\gamma) + \cos(\beta)\cos(\gamma)\sin(\mu) + 0}{-\sin(\alpha)\cos(\beta)\sin(\gamma) + \sin(\alpha)\sin(\beta)\cos(\gamma)\sin(\mu) + \cos(\alpha)\cos(\gamma)\cos(\mu)} \right] .$$

These values of β_{cmd} , α_{cmd} , Φ_{cmd} , Θ_{cmd} are then used to find the associated equilibrium values of V_{cmd} .

$$(V_{cmd})^2 = \frac{-b \pm \sqrt{b^2 - 4ac}}{2a}$$

where a, b, and c are functions of β_{cmd} , α_{cmd} , Φ_{cmd} , Θ_{cmd} (see equation 4.5.19 in the equilibrium section).

If there are two positive real equilibrium speeds to choose from, the larger one is chosen. Next U_{cmd} is computed ($U_{cmd} = V_{cmd} \cos(\beta_{cmd})\cos(\alpha_{cmd})$). Finally, this U_{cmd} , along with β_{cmd} , Φ_{cmd} , and Θ_{cmd} are sent to the U, β, Φ, Θ inverter.

For an introduction to the partial inversion method, and its application to the 3DOF longitudinal axis of an aircraft, see [E1]. A related method of controlling nonlinear systems can be found in [HSM].

When using dynamic inversion, the x_1 vector contains m states which can be controlled exactly by the m control inputs. We have no direct control over x_2 and x_3 , so we have to check that they remain stable. This analysis is done in subsections 5.2 through 5.5.

5.2 Theory of Complementary Dynamics

We will be considering systems with m controls and k chains of integrators (with $k > m$). Note that for conventional 6DOF aircraft models, $k=6$ and $m = 4$. When the m controls are used to control m of the integrator chains, the dynamics of the remaining $k-m$ chains will be completely determined. We will derive the expression for the dynamics of these remaining integrator chains.

We are working with state-space systems defined implicitly by equation 2.1 which contained the relation

$$F(\dot{x}, x, u) = 0. \quad (5.2.1)$$

This is a system of k equations. We would like to analytically reduce this to a set of $k-m$ equations in m fewer unknowns. Whether or not we can do this depends on the algebraic structure of the system of equations. In the rest of this subsection we will be considering a case for which this reduction is possible.

Consider the case where $F(\dot{x}, x, u)$ has the special form

$$F(\dot{x}, x, u) = -e(x)\dot{x} + f(x) + g(x)h(x, u) \quad (5.2.2)$$

Equation 5.2.1 now takes the form

$$e(x)\dot{x} = f(x) + g(x)h(x, u) \quad (5.2.3)$$

where

e is k by k (square matrix)
 f is k by 1 (column vector)
 g is k by m (matrix with $k > m$)
 h is m by 1 (column vector)

In this case, the only dependence of F on the m controls, u , enters through the m functions $h(x, u)$. F depends on h in a linear way, so we can eliminate h using linear algebra. To eliminate h , split the equations into two parts

$$\begin{bmatrix} P_1 & e(x)\dot{x} \\ P_2 & e(x)\dot{x} \end{bmatrix} = \begin{bmatrix} P_1 & f(x) \\ P_2 & f(x) \end{bmatrix} + \begin{bmatrix} P_1 & g(x) \\ P_2 & g(x) \end{bmatrix} h(x,u) \quad (5.2.4)$$

where

P_1 is any m rows of a k by k identity matrix.

P_2 is the remaining $k-m$ rows of the k by k identity matrix.

If the $g(x)$ matrix is full rank, it has m independent rows. In this case choose P_1 so that $P_1 g(x)$ is invertible, then

$$h(x,u) = (P_1 g(x))^{-1} P_1 (e(x)\dot{x} - f(x)) \quad (5.2.5)$$

Plug this expression for h into the $P_2 e(x)\dot{x} = P_2 f(x) + P_2 g(x) h(x,u)$ equation to get

$$P_2 e(x)\dot{x} = P_2 f(x) + P_2 g(x) (P_1 g(x))^{-1} P_1 (f(x) - e(x)\dot{x}) \quad (5.2.6)$$

Separating out e and f gives

$$\left[P_2 - P_2 g(x) (P_1 g(x))^{-1} P_1 \right] e(x)\dot{x} = \left[P_2 - P_2 g(x) (P_1 g(x))^{-1} P_1 \right] f(x) \quad (5.2.7)$$

or

$$g^\perp(x) e(x)\dot{x} = g^\perp(x) f(x) \quad (5.2.8)$$

where g^\perp is the following $k-m$ by k matrix :

$$g^\perp(x) = \left[P_2 - P_2 g(x) (P_1 g(x))^{-1} P_1 \right] \quad (5.2.9)$$

Note that $[g^\perp(x)g(x)] = 0$, so equation 5.2.8 can be derived directly from equation 5.2.3 by premultiplying equation 5.2.3 with $g^\perp(x)$.

\dot{x} is the column vector with elements $\{\dot{x}_{i,ci}\}$ $i = 1, \dots, k$ (see section 4.2).

Split $x = (\{x_{i,j}\} \quad i = 1, \dots, k \quad j = 1, \dots, c_i)$ into two groups y and z .

Let $y = (\{x_{i,j}\} \quad j = 1, \dots, c_i)$ where i takes on the $k-m$ values corresponding to the uncontrolled chains.

Let $z = (\{x_{i,j}\} \quad j = 1, \dots, c_i)$ where i takes on the m values corresponding to the controlled chains.

Using this split of x into y and z , $e(x)\dot{x}$ splits as follows.

$$e(x)\dot{x} = e_1(y,z)\dot{y} + e_2(y,z)\dot{z} \quad (5.2.10)$$

where

$e_1(y,z)$ is a k by $k-m$ matrix

$e_2(y,z)$ is an k by m matrix

Plugging equation 5.2.10 into equation 5.2.8 gives

$$g^\perp(y,z)e_1(y,z)\dot{y} = g^\perp(y,z)(f(y,z) - e_2(y,z)\dot{z}) \quad (5.2.11)$$

If the $k-m$ by $k-m$ matrix $g^\perp(y,z)e_1(y,z)$ is invertible, then from equation 5.2.11 we get

$$\dot{y} = \left[g^\perp(y,z)e_1(y,z) \right]^{-1} g^\perp(y,z)(f(y,z) - e_2(y,z)\dot{z}) \quad (5.2.12)$$

Note: when the $k-m$ by $k-m$ matrix $g^\perp(y,z)e_1(y,z)$ is singular or nearly singular, the nonlinear inverter will produce very large signals which will typically be unacceptable.

If any controller uses the m controls to control the m z -chains to constant values, then $\dot{z} = 0$ and equation 5.2.12 reduces to

$$\dot{y} = \left[g^\perp(y,z)e_1(y,z) \right]^{-1} g^\perp(y,z)f(y,z) \quad (5.2.13)$$

If $f(y,z)$ is polynomial in the entries of y , then let \hat{y} be the column vector containing the p monomials in the entries of y on which f depends. In this case f can be rewritten as

$$f(y,z) = \tilde{f}(z) \hat{y} \quad (5.2.14)$$

where $\tilde{f}(z)$ is a $k-m$ by p matrix of coefficients. Equation 5.2.13 now becomes

$$\dot{y} = \left[g^\perp(y,z)e_1(y,z) \right]^{-1} \left[g^\perp(y,z)\tilde{f}(z) \right] \hat{y} \quad (5.2.15)$$

Now consider the special case where $g^\perp(y,z)$ and $e_1(y,z)$ do not depend on y .

$$\text{Let } R(z) = \left[g^\perp(z)e_1(z) \right]^{-1} \left[g^\perp(z)\tilde{f}(z) \right] \quad (5.2.16)$$

Using R , equation 5.2.15 can be written as

$$\dot{y} = R(z) \hat{y} \quad . \quad (5.2.17)$$

Equation 5.2.17 is a polynomial ODE in y , for each fixed value of z . The equilibria of these ODE are given by the solution of the polynomial equations :

$$0 = \left[g^\perp(z) \bar{f}(z) \right] \hat{y} \quad . \quad (5.2.18)$$

The entries of the $k-m$ by p matrix $R(z)$ are referred to as the stability parameters since they determine the stability of the uncontrolled chains of integrators.

5.3 Aircraft Complementary Dynamics

Introduction

The 6DOF aircraft equations of motion can be written in the form:

$$e(x)\dot{x} = f(x) + g(x)h(x,u) \quad (5.3.1)$$

where $x = (V, \beta, \alpha, \dot{\Phi}, \dot{\Theta}, \dot{\Psi}, \Phi, \Theta)$.

Equation 5.3.1 can then be put in the form

$$e_1(z)\dot{y} + e_2(y,z)\dot{z} = \tilde{f}(z)\hat{y} + g(z)h(y,z,u) \quad (5.3.2)$$

where $y = (V, \dot{\Psi})$, $z = (\beta, \alpha, \dot{\Phi}, \dot{\Theta}, \Phi, \Theta)$, and $\hat{y} = \begin{bmatrix} 1 \\ V \\ \dot{\Psi} \\ V^2 \\ V\dot{\Psi} \\ \dot{\Psi}^2 \end{bmatrix}$.

Equation 5.3.2 is in the form required for the calculation of the complementary dynamics discussed in subsection 5.2.

We will derive the expressions for $e_1(z)$, $e_2(y,z)$, $\tilde{f}(z)$, and $g(z)$. The equations of motion of an aircraft are simplest in body-axis coordinates $(U, V, W, P, Q, R, \Phi, \Theta)$, so we will start with them, then change coordinates to $x = (V, \beta, \alpha, \dot{\Phi}, \dot{\Theta}, \dot{\Psi}, \Phi, \Theta)$. The reason for changing to these new coordinates is that the complementary dynamics are simpler then.

Dimensionless equations of motion in (U,V,W,P,Q,R,Φ,Θ) coordinates

In order to make the equations of motion easier to manipulate, we will take various groups of expressions which appear together and give them a combined name. The most natural way to do this is to form various dimensionless groups of expressions.

(N.B. : to distinguish dimensionless parameters from physical ones, we could have put tildas over each dimensionless variable in the remaining part of the report. We decided not to for notational ease.)

In the following pages, it will be shown how to make the equations of motion presented in section 3.3 take on the following dimensionless form:

Dimensionless force equations (forces divided by mg) :

$$\begin{bmatrix} \dot{U} \\ \dot{V} \\ \dot{W} \end{bmatrix} = \Omega \begin{bmatrix} U \\ V \\ W \end{bmatrix} + 1_{\Phi\Theta} + V^2 C_{xyz} + V C_{xyz\Phi\Theta} \begin{bmatrix} P \\ Q \\ R \end{bmatrix} + g_{xyz} h(x,u) \quad (5.3.3)$$

Dimensionless moment equations (moments divided by {mg d_{nom}}) :

$$I_{mo} \begin{bmatrix} \dot{P} \\ \dot{Q} \\ \dot{R} \end{bmatrix} = \Omega I_{mo} \begin{bmatrix} P \\ Q \\ R \end{bmatrix} + V^2 C_{lmn} + V C_{lmn\Phi\Theta} \begin{bmatrix} P \\ Q \\ R \end{bmatrix} + g_{lmn} h(x,u) \quad (5.3.4)$$

Each term in the above equations is dimensionless. The terms in these two equations will be described in the next page.

In equations 5.3.3 and 5.3.4 , all variables were made dimensionless using the following constants:

$$\text{Let} \quad V_{nom} = \sqrt{\frac{mg}{\frac{1}{2}\rho S}}$$

Then define t_{nom} , d_{nom} , and I_{nom} in terms of V_{nom} , m, and g , the acceleration due to gravity.

$$t_{nom} = \frac{V_{nom}}{g} \quad , \quad d_{nom} = V_{nom} t_{nom} \quad , \quad \text{and} \quad I_{nom} = m(d_{nom})^2 \quad .$$

To make the notation more compact, we will combine the dimensionless chord and wingspan ($b = \frac{\text{wing span}}{d_{\text{nom}}}$, $c = \frac{\text{mean aerodynamic chord}}{d_{\text{nom}}}$) with the associated aero functions as follows:

$$C_{xyz} = \begin{bmatrix} C_x(\alpha, \beta) \\ C_y(\alpha, \beta) \\ C_z(\alpha, \beta) \end{bmatrix} \quad C_{xyzpqr} = \frac{1}{2} \begin{bmatrix} C_{x_p}(\alpha, \beta) & C_{x_q}(\alpha, \beta) & C_{x_r}(\alpha, \beta) \\ C_{y_p}(\alpha, \beta) & C_{y_q}(\alpha, \beta) & C_{y_r}(\alpha, \beta) \\ C_{z_p}(\alpha, \beta) & C_{z_q}(\alpha, \beta) & C_{z_r}(\alpha, \beta) \end{bmatrix} \begin{bmatrix} b & 0 & 0 \\ 0 & c & 0 \\ 0 & 0 & b \end{bmatrix}$$

$$C_{lmn} = \begin{bmatrix} b & 0 & 0 \\ 0 & c & 0 \\ 0 & 0 & b \end{bmatrix} \begin{bmatrix} C_l(\alpha, \beta) \\ C_m(\alpha, \beta) \\ C_n(\alpha, \beta) \end{bmatrix}$$

$$C_{lmnpqr} = \frac{1}{2} \begin{bmatrix} b & 0 & 0 \\ 0 & c & 0 \\ 0 & 0 & b \end{bmatrix} \begin{bmatrix} C_{l_p}(\alpha, \beta) & C_{l_q}(\alpha, \beta) & C_{l_r}(\alpha, \beta) \\ C_{m_p}(\alpha, \beta) & C_{m_q}(\alpha, \beta) & C_{m_r}(\alpha, \beta) \\ C_{n_p}(\alpha, \beta) & C_{n_q}(\alpha, \beta) & C_{n_r}(\alpha, \beta) \end{bmatrix} \begin{bmatrix} b & 0 & 0 \\ 0 & c & 0 \\ 0 & 0 & b \end{bmatrix}$$

Note that b and c are themselves dimensionless now, so the above expressions are still dimensionless.

All speeds are divided by V_{nom} (eg $U = \frac{\text{axial speed}}{V_{\text{nom}}}$) and the derivatives are taken with respect to $t = \frac{\text{time}}{t_{\text{nom}}}$. P, Q, and R are angular rates multiplied by t_{nom} . I_{xx} , I_{yy} , etc. are moments of inertia divided by I_{nom} .

$$\Omega = \begin{bmatrix} 0 & R & -Q \\ -R & 0 & P \\ Q & -P & 0 \end{bmatrix} , \quad l_{\Phi\Theta} = \begin{bmatrix} -\sin(\Theta) \\ \cos(\Theta)\sin(\Phi) \\ \cos(\Theta)\cos(\Phi) \end{bmatrix} , \quad I_{mo} = \begin{bmatrix} I_{xx} & -I_{xy} & -I_{xz} \\ -I_{xy} & I_{yy} & -I_{yz} \\ -I_{xz} & -I_{yz} & I_{zz} \end{bmatrix} ,$$

$$g_{xyz} = \begin{bmatrix} C_{x_T} & C_{x_\delta} & C_{x_\delta} & C_{x_\delta} \\ C_{y_T} & C_{y_\delta} & C_{y_\delta} & C_{y_\delta} \\ C_{z_T} & C_{z_\delta} & C_{z_\delta} & C_{z_\delta} \end{bmatrix} , \quad \text{and} \quad g_{lmn} = \begin{bmatrix} b & 0 & 0 \\ 0 & c & 0 \\ 0 & 0 & b \end{bmatrix} \begin{bmatrix} C_{l_T} & C_{l_\delta} & C_{l_\delta} & C_{l_\delta} \\ C_{m_T} & C_{m_\delta} & C_{m_\delta} & C_{m_\delta} \\ C_{n_T} & C_{n_\delta} & C_{n_\delta} & C_{n_\delta} \end{bmatrix} .$$

Dimensionless equations of motion in $(V, \beta, \alpha, \dot{\Phi}, \dot{\Theta}, \dot{\Psi}, \Phi, \Theta)$ coordinates

Change coordinates from (U, V, W) to (V, β, α) using the following formula :

$$\begin{bmatrix} U \\ V \\ W \end{bmatrix} = V \begin{bmatrix} 1 \\ \beta \\ \alpha \end{bmatrix} \quad \text{where} \quad \begin{bmatrix} 1 \\ \beta \\ \alpha \end{bmatrix} = \begin{bmatrix} \cos(\alpha)\cos(\beta) \\ \sin(\beta) \\ \sin(\alpha)\cos(\beta) \end{bmatrix} . \quad (5.3.5)$$

Differentiating gives

$$\begin{bmatrix} \dot{U} \\ \dot{V} \\ \dot{W} \end{bmatrix} = L_1 L_0 \begin{bmatrix} \dot{V} \\ \dot{\beta} \\ \dot{\alpha} \end{bmatrix}$$

where

$$L_1 = \begin{bmatrix} \cos(\alpha)\cos(\beta) & -\cos(\alpha)\sin(\beta) & -\sin(\alpha) \\ \sin(\beta) & \cos(\beta) & 0 \\ \sin(\alpha)\cos(\beta) & -\sin(\alpha)\sin(\beta) & \cos(\alpha) \end{bmatrix} \quad \text{and} \quad L_0 = \begin{bmatrix} 1 & 0 & 0 \\ 0 & V & 0 \\ 0 & 0 & V\cos(\beta) \end{bmatrix} .$$

Change coordinates from (P, Q, R, Φ, Θ) to $(\dot{\Phi}, \dot{\Theta}, \dot{\Psi}, \Phi, \Theta)$ using the following formula :

$$\begin{bmatrix} P \\ Q \\ R \end{bmatrix} = L_2 \begin{bmatrix} \dot{\Phi} \\ \dot{\Theta} \\ \dot{\Psi} \end{bmatrix} \quad (5.3.6)$$

where

$$L_2 = \begin{bmatrix} 1 & 0 & -\sin(\Theta) \\ 0 & \cos(\Phi) & \cos(\Theta)\sin(\Phi) \\ 0 & -\sin(\Phi) & \cos(\Theta)\cos(\Phi) \end{bmatrix} .$$

Differentiating gives

$$\begin{bmatrix} \dot{P} \\ \dot{Q} \\ \dot{R} \end{bmatrix} = \dot{L}_2 \begin{bmatrix} \dot{\Phi} \\ \dot{\Theta} \\ \dot{\Psi} \end{bmatrix} + L_2 \begin{bmatrix} \ddot{\Phi} \\ \ddot{\Theta} \\ \ddot{\Psi} \end{bmatrix}$$

where

$$\dot{L}_2 = \begin{bmatrix} 0 & 0 & 0 \\ 0 & -\sin(\Phi) & \cos(\Theta)\cos(\Phi) \\ 0 & -\cos(\Phi) & -\cos(\Theta)\sin(\Phi) \end{bmatrix} \dot{\Phi} + \begin{bmatrix} 0 & 0 & -\cos(\Theta) \\ 0 & 0 & -\sin(\Theta)\sin(\Phi) \\ 0 & 0 & -\sin(\Theta)\cos(\Phi) \end{bmatrix} \dot{\Theta} \quad (5.3.7)$$

The expressions for P, Q, and R can also be put into Ω to give

$$\Omega = \Omega_1 \dot{\Phi} + \Omega_2 \dot{\Theta} + \Omega_3 \dot{\Psi}$$

where

$$\Omega_1 = \begin{bmatrix} 0 & 0 & 0 \\ 0 & 0 & 1 \\ 0 & -1 & 0 \end{bmatrix}, \quad \Omega_2 = \begin{bmatrix} 0 & -\sin(\Phi) & -\cos(\Phi) \\ \sin(\Phi) & 0 & 0 \\ \cos(\Phi) & 0 & 0 \end{bmatrix},$$

and

$$\Omega_3 = \begin{bmatrix} 0 & \cos(\Theta)\cos(\Phi) & -\cos(\Theta)\sin(\Phi) \\ -\cos(\Theta)\cos(\Phi) & 0 & -\sin(\Theta) \\ \cos(\Theta)\sin(\Phi) & \sin(\Theta) & 0 \end{bmatrix}.$$

Substituting all this into equations 5.3.3 and 5.3.4 gives the equations of motion in $(V, \beta, \alpha, \dot{\Phi}, \dot{\Theta}, \dot{\Psi}, \Phi, \Theta)$ coordinates.

Force equations :

$$L_1 L_0 \begin{bmatrix} \dot{V} \\ \dot{\beta} \\ \dot{\alpha} \end{bmatrix} = \Omega V \begin{bmatrix} 1_{\beta\alpha} \\ 1_{\Phi\Theta} \\ V^2 C_{xyz} + V C_{xyzpqr} \end{bmatrix} L_2 \begin{bmatrix} \dot{\Phi} \\ \dot{\Theta} \\ \dot{\Psi} \end{bmatrix} + g_{xyz} h(x, u) \quad (5.3.8)$$

Moment equations :

$$I_{mo} \left(\dot{L}_2 \begin{bmatrix} \dot{\Phi} \\ \dot{\Theta} \\ \dot{\Psi} \end{bmatrix} + L_2 \begin{bmatrix} \ddot{\Phi} \\ \ddot{\Theta} \\ \ddot{\Psi} \end{bmatrix} \right) = \Omega I_{mo} L_2 \begin{bmatrix} \dot{\Phi} \\ \dot{\Theta} \\ \dot{\Psi} \end{bmatrix} + V^2 C_{lmn} + V C_{lmnpqr} L_2 \begin{bmatrix} \dot{\Phi} \\ \dot{\Theta} \\ \dot{\Psi} \end{bmatrix} + g_{lmn} h(x, u) \quad (5.3.9)$$

Expressions for $e_1(z)$, $e_2(y,z)$, and $\tilde{f}(z)$

Equations 5.3.8 and 5.3.9 can be rewritten as

$$\begin{bmatrix} L_1 L_0 & 0_{3 \times 3} \\ 0_{3 \times 3} & I_{mo} L_2 \end{bmatrix} \begin{bmatrix} \dot{V} \\ \dot{\beta} \\ \dot{\alpha} \\ \dot{\Phi} \\ \dot{\Theta} \\ \dot{\Psi} \end{bmatrix} = \tilde{f}(\beta, \alpha, \dot{\Phi}, \dot{\Theta}, \Phi, \Theta) \begin{bmatrix} 1 \\ V \\ \dot{\Psi} \\ V^2 \\ V\dot{\Psi} \\ \dot{\Psi}^2 \end{bmatrix} + g(z)h(y,z,u) \quad (5.3.10)$$

To fit $\tilde{f}(z)$ into the space on the page, split it into its first three columns and its last three columns.

$$\text{Let } \tilde{f}(z) = \begin{bmatrix} \tilde{f}_{123}(z) & \tilde{f}_{456}(z) \end{bmatrix}$$

In the expression for $\tilde{f}_{123}(z)$, use the following notation

Let

$$\Omega_4 = \Omega_1 \dot{\Phi} + \Omega_2 \dot{\Theta}, \quad L_5 = L_2 \begin{bmatrix} \dot{\Phi} \\ \dot{\Theta} \\ 0 \end{bmatrix}, \quad L_6 = \dot{L}_2 \begin{bmatrix} \dot{\Phi} \\ \dot{\Theta} \\ 0 \end{bmatrix}, \quad L_7 = \dot{L}_2 \begin{bmatrix} 0 \\ 0 \\ 1 \end{bmatrix}$$

so

$$\Omega = \Omega_4 + \Omega_3 \dot{\Psi}, \quad L_2 \begin{bmatrix} \dot{\Phi} \\ \dot{\Theta} \\ \dot{\Psi} \end{bmatrix} = L_5 + l_{\Phi\Theta} \dot{\Psi}, \quad \text{and} \quad \dot{L}_2 \begin{bmatrix} \dot{\Phi} \\ \dot{\Theta} \\ \dot{\Psi} \end{bmatrix} = L_6 + L_7 \dot{\Psi}. \quad (5.3.10b)$$

Substituting equation 5.3.10b into equations 5.3.8 and 5.3.9 gives

$$\tilde{f}_{123}(z) = \begin{bmatrix} l_{\Phi\Theta} & \Omega_4 l_{\beta\alpha} + C_{xyzpq\alpha} L_5 & 0_3 \\ -I_{mo} L_6 + \Omega_4 I_{mo} L_5 & C_{lmnpq\alpha} L_5 & \Omega_4 I_{mo} l_{\Phi\Theta} + \Omega_3 I_{mo} L_5 - I_{mo} L_7 \end{bmatrix} \quad (5.3.11)$$

and

$$\tilde{f}_{456}(z) = \begin{bmatrix} C_{xyz} & \Omega_3 l_{\beta\alpha} + C_{xyzpq\alpha} l_{\Phi\Theta} & 0_3 \\ C_{lmn} & C_{lmnpq\alpha} l_{\Phi\Theta} & \Omega_3 I_{mo} l_{\Phi\Theta} \end{bmatrix} \quad (5.3.12)$$

In equation 5.3.10 , $g(z)$ is given by

$$g(z) = \begin{bmatrix} g_{xyz}(\beta, \alpha) \\ g_{lmn}(\beta, \alpha) \end{bmatrix}$$

and an example of what $h(y,z,u)$ can be is given by

$$h(y,z,u) = \begin{bmatrix} \frac{\text{Thrust}}{mg} \\ V^2 \sin(\delta_a - \frac{Pb}{2V}) \\ V^2 \sin(\delta_e - \alpha) \\ V^2 \sin(\delta_r - \beta) \end{bmatrix}$$

Equation 5.3.10 can be rewritten as

$$\begin{bmatrix} 1_{\beta\alpha} & 0_3 \\ 0_3 & I_{mo} 1_{\Phi\Theta} \end{bmatrix} \begin{bmatrix} \dot{V} \\ \dot{\Psi} \end{bmatrix} + \begin{bmatrix} VL_3 & 0_{3 \times 2} \\ 0_{3 \times 2} & I_{mo} L_4 \end{bmatrix} \begin{bmatrix} \dot{\beta} \\ \dot{\alpha} \\ \dot{\Phi} \\ \dot{\Theta} \end{bmatrix} = \tilde{f}(z) \begin{bmatrix} 1 \\ \dot{V} \\ \dot{\Psi} \\ V^2 \\ V\dot{\Psi} \\ \dot{\Psi}^2 \end{bmatrix} + g(z)h(y,z,u) \quad (5.3.13)$$

where

$$L_3 = \begin{bmatrix} -\cos(\alpha)\sin(\beta) & -\sin(\alpha)\cos(\beta) \\ \cos(\beta) & 0 \\ -\sin(\alpha)\cos(\beta) & \cos(\alpha)\cos(\beta) \end{bmatrix} \quad \text{and} \quad L_4 = \begin{bmatrix} 1 & 0 \\ 0 & \cos(\Phi) \\ 0 & -\sin(\Phi) \end{bmatrix}$$

so

$$e_1(z) = \begin{bmatrix} 1_{\beta\alpha} & 0_3 \\ 0_3 & I_{mo} 1_{\Phi\Theta} \end{bmatrix} \quad \text{and} \quad e_2(y,z) = \begin{bmatrix} VL_3 & 0_{3 \times 2} \\ 0_{3 \times 2} & I_{mo} L_4 \end{bmatrix}$$

This is now in the form of equation 5.3.2 so we can apply the results of subsection 5.2 .

First multiply equation 5.3.2 by $g^\perp(z)$

(where $g^\perp(z)$ is a 2 by 6 matrix which satisfies $g^\perp(z) g(z) = 0$, see section 4.3).

$$g^\perp(z)e_1(z)\dot{y} + g^\perp(z)e_2(z)\dot{z} = g^\perp(z)\tilde{f}(z)\hat{y} \quad (5.3.14)$$

so

$$\dot{y} = \left[g^\perp(z) e_1(z) \right]^{-1} g^\perp(z) (\tilde{f}(z) \hat{y} - e_2(y, z) \dot{z}) \quad (5.3.15)$$

Equation 5.3.15 holds in general. When $\dot{z} = 0$, equation 5.3.15 reduces to

$$\dot{y} = \left[g^\perp(z) e_1(z) \right]^{-1} g^\perp(z) \tilde{f}(z) \hat{y} \quad (5.3.16)$$

and the second and third columns of $\tilde{f}(z)$ go to zero, leaving only columns 1, 4, 5, and 6 so equation 5.3.16 reduces to

$$\begin{bmatrix} \dot{V} \\ \dot{\Psi} \end{bmatrix} = \left[g^\perp(z) e_1(z) \right]^{-1} g^\perp(z) \begin{bmatrix} \tilde{f}_1(z) & \tilde{f}_4(z) & \tilde{f}_5(z) & \tilde{f}_6(z) \end{bmatrix} \begin{bmatrix} 1 \\ V^2 \\ V\dot{\Psi} \\ \dot{\Psi}^2 \end{bmatrix} \quad (5.3.17)$$

Equation 5.3.17 represents the complementary dynamics. It is a system of 2 quadratic O.D.E.'s with the following coefficients (where subscripts represent the powers of V and $\dot{\Psi}$ respectively) :

$$\begin{bmatrix} a_{00} & a_{20} & a_{11} & a_{02} \\ b_{00} & b_{20} & b_{11} & b_{02} \end{bmatrix} = \left[g^\perp(z) e_1(z) \right]^{-1} g^\perp(z) \begin{bmatrix} \tilde{f}_1(z) & \tilde{f}_4(z) & \tilde{f}_5(z) & \tilde{f}_6(z) \end{bmatrix} \quad (5.3.18)$$

The inverse of $g^\perp(z) e_1(z)$ needed in equation 5.3.18 can be computed as follows. Start by partitioning the 2 by 6 $g^\perp(z)$ matrix into four parts.

$$g^\perp(z) = \begin{bmatrix} g_a & g_b \\ g_c & g_d \end{bmatrix} \quad (5.3.19)$$

where g_a , g_b , g_c , and g_d are each size 1 by 3. Using this notation,

$$g^\perp(z) e_1(z) = \begin{bmatrix} g_a^1 \beta_\alpha & g_b^1 I_{mo}^1 \Phi \Theta \\ g_c^1 \beta_\alpha & g_d^1 I_{mo}^1 \Phi \Theta \end{bmatrix} \quad (5.3.20)$$

Since $g^\perp(z) e_1(z)$ is a 2 by 2 matrix, it is trivial to invert.

Explicit formulas for special cases

For aircraft whose controls have left/right symmetry, the elevator and thrust only affect the first, third, and fifth rows of (5.3.1) while the rudder and aileron only affect the second, forth, and sixth rows of (5.3.1) . The result is that the $g(x)$ matrix then has the following simplified form:

$$g(z) = \begin{bmatrix} C_{x_T} & 0 & C_{x_{\delta_e}} & 0 \\ 0 & C_{y_{\delta_a}} & 0 & C_{y_{\delta_r}} \\ C_{z_T} & 0 & C_{z_{\delta_e}} & 0 \\ 0 & bC_{l_{\delta_a}} & 0 & bC_{l_{\delta_r}} \\ cC_{m_T} & 0 & cC_{m_{\delta_e}} & 0 \\ 0 & bC_{n_{\delta_a}} & 0 & bC_{n_{\delta_r}} \end{bmatrix} \quad (5.3.21)$$

In this simpler situation, the transpose of (4.5.8) becomes :

$$\text{transpose} \left[g^\perp(z) \right] = \begin{bmatrix} 0 & \frac{C_{z_{\delta_e}} C_{m_T} - C_{z_T} C_{m_{\delta_e}}}{C_{x_T} C_{m_{\delta_e}} - C_{x_{\delta_e}} C_{m_T}} \\ 1 & 0 \\ 0 & 1 \\ \frac{1}{b} \frac{C_{y_{\delta_e}} C_{n_{\delta_r}} - C_{y_{\delta_r}} C_{n_{\delta_e}}}{C_{l_{\delta_e}} C_{n_{\delta_r}} - C_{l_{\delta_r}} C_{n_{\delta_e}}} & 0 \\ 0 & \frac{1}{c} \frac{C_{x_{\delta_e}} C_{z_T} - C_{x_T} C_{z_{\delta_e}}}{C_{x_T} C_{m_{\delta_e}} - C_{x_{\delta_e}} C_{m_T}} \\ \frac{1}{b} \frac{C_{y_{\delta_e}} C_{l_{\delta_r}} - C_{y_{\delta_r}} C_{l_{\delta_e}}}{C_{l_{\delta_e}} C_{n_{\delta_r}} - C_{l_{\delta_r}} C_{n_{\delta_e}}} & 0 \end{bmatrix} \quad (5.3.22)$$

or, in case the denominators in 5.3.22 are zero, use

$$\text{transpose } \left[g^\perp(z) \right] = \begin{bmatrix} 0 & c(C_{Z_\delta} C_{m_T} - C_{Z_T} C_{m_\delta}) \\ b(C_{l_\delta} C_{n_\delta} - C_{l_\delta} C_{n_\delta}) & 0 \\ 0 & c(C_{X_T} C_{m_\delta} - C_{X_\delta} C_{m_T}) \\ C_{y_\delta} C_{n_\delta} - C_{y_\delta} C_{n_\delta} & 0 \\ 0 & C_{X_\delta} C_{Z_T} - C_{X_T} C_{Z_\delta} \\ C_{y_\delta} C_{l_\delta} - C_{y_\delta} C_{l_\delta} & 0 \end{bmatrix}$$

In the further simplifying situation where the thrust is along the x axis ($C_{Z_T} = 0 = C_{m_T}$) and the ailerons only produce a rolling moment ($C_{y_\delta} = 0 = C_{n_\delta}$), Equation 5.3.22 reduces to :

$$g^\perp(z) = \begin{bmatrix} 0 & 1 & 0 & 0 & 0 & -\frac{C_{y_\delta}}{bC_{n_\delta}} \\ 0 & 0 & 1 & 0 & -\frac{C_{Z_\delta}}{cC_{m_\delta}} & 0 \end{bmatrix} \quad (5.3.23)$$

Using this $g^\perp(z)$ along with a symmetric aircraft,

$$(I_{xy} = 0 = I_{yz} \text{ , } C_y(\alpha, 0) = C_l(\alpha, 0) = C_n(\alpha, 0) = 0 \text{)}$$

with no dynamic aero coefficients,

$$(C_{xyz_{PQR}} = 0 = C_{lmnp_{PQR}})$$

and flying with no sideslip and wings level

$$(\beta = 0 = \Phi)$$

reduces equation 5.3.18 to the following simple form:

$$\begin{bmatrix} a_{00} & a_{20} & a_{11} & a_{02} \\ b_{00} & b_{20} & b_{11} & b_{02} \end{bmatrix} = \left[g^\perp(z) e_1(z) \right]^{-1} g^\perp(z) \begin{bmatrix} \tilde{f}_1(z) & \tilde{f}_4(z) & \tilde{f}_5(z) & \tilde{f}_6(z) \end{bmatrix} = \quad (5.3.24)$$

$$\begin{bmatrix} \frac{\cos(\Theta)}{\sin(\alpha)} & \frac{C_z - C_m \frac{C_{z\delta_0}}{C_{m\delta_0}}}{\sin(\alpha)} & 0 & \frac{C_{z\delta_0}}{c C_{m\delta_0}} \frac{[\cos(\Theta) \ 0 \ \sin(\Theta)] I_{m0} 1_{\Phi\Theta}}{\sin(\alpha)} \\ 0 & 0 & \frac{\cos(\gamma) \frac{b C_{n\delta_0}}{C_{y\delta_0}}}{\cos(\Theta) I_{zz} + \sin(\Theta) I_{xz}} & 0 \end{bmatrix}$$

where $\gamma = \Theta - \alpha$ when $\Phi = 0 = \beta$. The eight parameters in the above system typically have the following signs.

$$\begin{bmatrix} a_{00} & a_{20} & a_{11} & a_{02} \\ b_{00} & b_{20} & b_{11} & b_{02} \end{bmatrix} = \begin{bmatrix} + & - & 0 & + \\ 0 & 0 & - & 0 \end{bmatrix}$$

which results in a globally stable phase portrait in the physical ($V > 0$) half of the ($V, \dot{\Psi}$) phase space.

5.4 Canonical Forms for the Complementary Dynamic Equations

We have seen that the complementary dynamic equations are of the form:

$$\begin{bmatrix} \dot{V} \\ \ddot{\Psi} \end{bmatrix} = \begin{bmatrix} a_{00} + a_{20}V^2 + a_{11}V\dot{\Psi} + a_{02}\dot{\Psi}^2 \\ b_{00} + b_{20}V^2 + b_{11}V\dot{\Psi} + b_{02}\dot{\Psi}^2 \end{bmatrix}. \quad (5.4.1)$$

These equations describe the dynamical behavior of the aircraft when the control inputs are used to keep the direction of the velocity vector (α, β) and the attitude (Φ, Θ) constant. Stable equilibrium solutions represent steady-state flight conditions - we are therefore interested in determining when equations 5.4.1 admit stable equilibria. Furthermore, we would like to characterize the dynamical behavior of the solutions away from equilibria to describe the aircraft's transient behavior. The transient behavior of the model should reflect some of the flying qualities of the aircraft during precision pointing or tracking tasks. We will show in the next section how to compute parameters that quantify the transient behavior in terms suitable for flying quality evaluation. Specifically, we will construct Liapunov functions that describe the stability of the equilibria and provide a bound on the settling time to equilibrium from a non-equilibrium condition.

Before constructing the Liapunov functions, we will transform the physical $(V, \dot{\Psi})$ coordinates into a new set of coordinates (x, y) that describe the system more economically. The new coordinates will be related to the original $(V, \dot{\Psi})$ coordinates by an invertible linear transformation. In the new coordinates, the Liapunov functions have an especially simple form that renders the flow in the phase space easy to visualize.

The coordinate transformation is developed through a computational algorithm based on manipulation of quadratic forms. Note that equations (5.4.1) can be written:

$$\dot{V} = \begin{bmatrix} 1 & V & \dot{\Psi} \end{bmatrix} \begin{bmatrix} a_{00} & 0 & 0 \\ 0 & a_{20} & \frac{a_{11}}{2} \\ 0 & \frac{a_{11}}{2} & a_{02} \end{bmatrix} \begin{bmatrix} 1 \\ V \\ \dot{\Psi} \end{bmatrix}, \quad \ddot{\Psi} = \begin{bmatrix} 1 & V & \dot{\Psi} \end{bmatrix} \begin{bmatrix} b_{00} & 0 & 0 \\ 0 & b_{20} & \frac{b_{11}}{2} \\ 0 & \frac{b_{11}}{2} & b_{02} \end{bmatrix} \begin{bmatrix} 1 \\ V \\ \dot{\Psi} \end{bmatrix}. \quad (5.4.2)$$

In this way the complementary dynamics are defined in terms of the quadratic forms A

and B represented by the 3x3 matrices above whose entries are simple functions of the coefficients a_{ij} and b_{ij} . For convenience of notation, we write the above equations:

$$\dot{\mathbf{V}} = \mathbf{A}(\mathbf{V}, \dot{\mathbf{\Psi}}), \quad \ddot{\mathbf{\Psi}} = \mathbf{B}(\mathbf{V}, \dot{\mathbf{\Psi}}). \quad (5.4.2')$$

We need to know how the equations above transform when the coordinates of the phase space undergo a linear transformation. Choose coordinates (x, y) related to the $(\mathbf{V}, \dot{\mathbf{\Psi}})$ coordinates by an invertible transformation F:

$$\begin{bmatrix} f_{11} & f_{12} \\ f_{12} & f_{22} \end{bmatrix} \begin{bmatrix} x \\ y \end{bmatrix} = \begin{bmatrix} \mathbf{V} \\ \dot{\mathbf{\Psi}} \end{bmatrix}, \quad (5.4.3)$$

then

$$\dot{\mathbf{V}} = \begin{bmatrix} 1 & x & y \end{bmatrix} \bar{\mathbf{A}} \begin{bmatrix} 1 \\ x \\ y \end{bmatrix}, \quad \ddot{\mathbf{\Psi}} = \begin{bmatrix} 1 & x & y \end{bmatrix} \bar{\mathbf{B}} \begin{bmatrix} 1 \\ x \\ y \end{bmatrix} \quad (5.4.4)$$

where

$$\bar{\mathbf{A}} = \begin{bmatrix} 1 & 0 \\ 0 & \mathbf{F} \end{bmatrix}^T \mathbf{A} \begin{bmatrix} 1 & 0 \\ 0 & \mathbf{F} \end{bmatrix}, \quad \bar{\mathbf{B}} = \begin{bmatrix} 1 & 0 \\ 0 & \mathbf{F} \end{bmatrix}^T \mathbf{B} \begin{bmatrix} 1 & 0 \\ 0 & \mathbf{F} \end{bmatrix}. \quad (5.4.5)$$

In the convenient notation, $\dot{\mathbf{V}} = \bar{\mathbf{A}}(x, y)$, $\ddot{\mathbf{\Psi}} = \bar{\mathbf{B}}(x, y)$. To eliminate $\dot{\mathbf{V}}$ and $\ddot{\mathbf{\Psi}}$, use $\mathbf{G} = \mathbf{F}^{-1}$

$$\begin{bmatrix} \dot{x} \\ \dot{y} \end{bmatrix} = \begin{bmatrix} g_{11} & g_{12} \\ g_{12} & g_{22} \end{bmatrix} \begin{bmatrix} \dot{\mathbf{V}} \\ \ddot{\mathbf{\Psi}} \end{bmatrix}. \quad (5.4.6)$$

to find

$$\begin{pmatrix} \dot{x} \\ \dot{y} \end{pmatrix} = \begin{bmatrix} g_{11} & g_{12} \\ g_{12} & g_{22} \end{bmatrix} \begin{pmatrix} \bar{A}(x,y) \\ \bar{B}(x,y) \end{pmatrix}. \quad (5.4.7)$$

The formula in equation 5.4.7 describes the complementary dynamics in the new set of coordinates (x,y) . Any property of the system 5.4.7 that remains valid under linear transformations is also a property of the original system 5.4.1, and vice-versa. In particular, the stability of either of these two systems implies the stability of the other.

The reason for introducing new coordinates is to represent the dynamic equations using quadratic forms that are as simple as possible. We think of the change of variables as a transformation $(A,B) \rightarrow (\bar{A},\bar{B})$ used to reduce the number of independent variables required to represent the quadratic forms. There is another transformation useful for the same purpose; we discuss it next.

Suppose a system is represented, as in 5.4.7, by equations of the form:

$$\begin{pmatrix} \dot{x} \\ \dot{y} \end{pmatrix} = H \begin{pmatrix} A(x,y) \\ B(x,y) \end{pmatrix} \quad (5.4.8)$$

for some constant 2×2 matrix H . Pick a nonsingular 2×2 matrix K , and define $\bar{A} = k_{11}A + k_{12}B$, $\bar{B} = k_{21}A + k_{22}B$. The same equation can then be written

$$\begin{pmatrix} \dot{x} \\ \dot{y} \end{pmatrix} = HK^{-1} \begin{pmatrix} \bar{A}(x,y) \\ \bar{B}(x,y) \end{pmatrix}. \quad (5.4.9)$$

Transformations of this type, which do not involve a change of coordinates, may also be used.

We use both types of transformation in deriving canonical forms for the complementary dynamic equations.

Theorem 5.4-1: Suppose the complementary dynamic equations 5.4.1 admit some real equilibrium points and are nondegenerate (nondegenerate means that at least one of the two matrices A and B is rank three, and that any nontrivial linear combination of them is rank at least two - this is a generic condition). Then there is a set of coordinates (x,y) , related to (V, Ψ) by a linear transformation, for which the complementary dynamic equations are in one of the two forms:

$$\begin{pmatrix} \dot{x} \\ \dot{y} \end{pmatrix} = H \begin{pmatrix} 1 - x^2 + y^2 \\ -2xy \end{pmatrix}. \quad (5.4.10)$$

$$\begin{pmatrix} \dot{x} \\ \dot{y} \end{pmatrix} = H \begin{pmatrix} 1 - x^2 - y^2 \\ -2xy \end{pmatrix}. \quad (5.4.11)$$

Proof: Start with A and B represented as in 5.4.2, assume that A is rank three (if A is rank two, interchange A and B). Consider the matrix S defined by

$$S = b_{00}A - a_{00}B = \begin{bmatrix} 0 & 0 & 0 \\ 0 & s_{11} & s_{12} \\ 0 & s_{12} & s_{22} \end{bmatrix}. \quad (5.4.12)$$

The matrix S is symmetric and, because the equations are nonsingular, rank 2. We have assumed that some real equilibria do exist, so the nonzero eigenvalues of S have opposite signs. Therefore, for any real c, there is a 3x3 matrix F_c

$$F_c = \begin{bmatrix} 1 & 0 & 0 \\ 0 & f_{c11} & f_{c21} \\ 0 & f_{c12} & f_{c22} \end{bmatrix} \quad (5.4.13)$$

such that

$$F_c^T S F_c = \begin{bmatrix} 0 & 0 & 0 \\ 0 & 0 & c \\ 0 & c & 0 \end{bmatrix}. \quad (5.4.14)$$

Call the matrix on the righthand side of 5.4.14 B_1 . Because of the assumed nondegeneracy of the equations, F_c can be chosen so that

$$A' = F_c^T A F_c = \begin{bmatrix} a'_{00} & 0 & 0 \\ 0 & a'_{20} & \frac{a'_{11}}{2} \\ 0 & \frac{a'_{11}}{2} & a'_{02} \end{bmatrix}. \quad (5.4.14')$$

has the property that none of the diagonal entries are 0.

From the matrix A' defined in 5.4.14' subtract $\frac{a'_{11}}{2c} B_1$ to obtain

$$A_1 = \begin{bmatrix} a'_{00} & 0 & 0 \\ 0 & a'_{20} & 0 \\ 0 & 0 & a'_{02} \end{bmatrix}. \quad (5.4.15)$$

Now by scaling x and y independently, and by proper choice of c , A_1 and B_1 can be transformed simultaneously to

$$\bar{A} = a_{00} \begin{bmatrix} 1 & 0 & 0 \\ 0 & e & 0 \\ 0 & 0 & f \end{bmatrix}, \quad \bar{B} = \begin{bmatrix} 0 & 0 & 0 \\ 0 & 0 & -1 \\ 0 & -1 & 0 \end{bmatrix}$$

where e and f are either 1 or -1. Because we have assumed real equilibria, $e=-1$ or $f=-1$. The expression is symmetric in x and y , so only two distinct cases arise. These are realized by choosing $e=-1$, and taking $f=1$ or $f=-1$.

In the first case, where $f=1$, the dynamic equations are reduced to the form of 5.4.10. This is the case where there are two real equilibrium points: those corresponding to $(1,0)$ and $(-1,0)$ in the (x,y) coordinates. In the second case, where $f=-1$, the dynamic equations are reduced to the form of 5.4.11. This is the case where there are four real equilibria: those corresponding to $(1,0), (0,1), (-1,0)$, and $(0,-1)$ in the (x,y) coordinates. The proof is complete.

In the original $(V, \dot{\Psi})$ coordinates the complementary dynamic equations were parametrized by 8 independent variables a_{ij}, b_{ij} . By the transformations shown above, the number of independent parameters in the equations can be reduced to the 4 entries of a constant matrix H . The H matrix, and the matrix transformation from the $(V, \dot{\Psi})$ coordinates to the (x,y) coordinates, are all that is required for a complete analysis of the complementary dynamic equations. Expressions for these matrices can be computed from the construction given in the proof of Theorem 5.4-1.

In the next section we construct Liapunov functions for the two canonical forms of Theorem 5.4-1.

5.5 The Liapunov Functions

In the last section we showed how the complementary dynamic equations could be transformed to new coordinates in which fewer parameters are required to specify the system. One advantage of these new coordinates is that they make it easy to write down Liapunov functions for the stable equilibria (when stable equilibria exist). In this section we show how these Liapunov functions are constructed and explain what they can tell us about flying qualities. In one of the cases discussed below, a Liapunov function is used to show global stability of the model in the $V, \dot{\Psi}$ phase plane. Some of the quantities associated with the construction could be used to measure flying quality.

We have seen that the complementary dynamic equations in the coordinates (x, y) look like

$$\begin{bmatrix} \dot{x} \\ \dot{y} \end{bmatrix} = \begin{bmatrix} h_{11} & h_{12} \\ h_{21} & h_{22} \end{bmatrix} \begin{bmatrix} 1 + ey^2 - x^2 \\ -2xy \end{bmatrix} \quad (5.5.1)$$

where the components $h_{11}, h_{12}, h_{21}, h_{22}$ of the matrix H are, for each set of values $\alpha, \beta, \Theta, \Phi$, a set of constants determined by the nonlinear aircraft model. In the case where there are four real equilibria in the $V, \dot{\Psi}$ plane the parameter e takes the value -1 , while in the case of two real equilibria e takes the value $+1$. This representation only applies when there do exist real equilibria. We do not consider the case where there are no real equilibria.

The first step in constructing the Liapunov functions is to take the inner-product of the above equation with the vector $(1 + ey^2 - x^2, -2xy)$ to find

$$(1 + ey^2 - x^2)\dot{x} - 2xy\dot{y} = [(1 + ey^2 - x^2), -2xy] \begin{bmatrix} h_{11} & h_{12} \\ h_{21} & h_{22} \end{bmatrix} \begin{bmatrix} 1 + ey^2 - x^2 \\ -2xy \end{bmatrix}. \quad (5.5.2)$$

The resulting expression on the righthand side of the equation will have a definite sign (except at equilibria) whenever the symmetric matrix $S = \frac{1}{2}(H + H^T)$ is positive or negative definite. Let us suppose for the moment that S is positive definite. The lefthand side of equation 5.5.2 is in each case an expression easy to represent by the derivative of a simple function. The level sets of such a function are transverse to the flow and can be used to characterize the stability of the equilibria.

Of course, there are matrices H for which the quadratic form above is indefinite. When S is indefinite, it may be difficult to determine much of value from the functions constructed below. Still, our experience in working with the F-14 model suggests that, for a wide variety of flight conditions, the H matrix is definite, so that the analysis below is relevant.

CASE 1: $e=+1$

In this case there are two real equilibria: one at $(1,0)$ and the other at $(-1,0)$. For this configuration there are three possibilities for the stability of the equilibria:

case 1 - $(1,0)$ stable and $(-1,0)$ unstable

case 2 - $(1,0)$ unstable and $(-1,0)$ stable

case 3 - $(1,0)$ and $(-1,0)$ saddles.

Our construction will provide a Liapunov function in the first two cases where one of the equilibria is stable.

Define the complex number $z = x + iy$, and think of the transformed V, \dot{V} plane as the complex z plane. The function

$$F(z) = \frac{|1 - z|^2}{|1 + z|^2} \quad (5.5.3)$$

is the one we want to analyze. Except for the values $0, 1, \infty$ the level sets of this function are circles in the plane whose centers lie on the real axis. The value ∞ is realized only at the point $z = -1$ and 0 is realized only at $z = +1$. The 1 -level set is the imaginary axis $x = 0$.

From the geometry of the level sets of the function F , it is clear that the point $z = +1$ is a global attractor for the entire z -plane whenever it can be shown that the function F restricted to the solution curves of the system is decreasing. Then F is a Liapunov function for the flow. There is an easy condition on S to check that will tell us if F is decreasing:

Lemma 5.5-1: If the matrix S is positive definite, then the function F is a Liapunov function for the system 5.5.1.

Proof: In terms of x and y ,

$$F(x + iy) = \frac{(1 - x)^2 + y^2}{(1 + x)^2 + y^2} \quad (5.5.4)$$

and so

$$\frac{d}{dt}F(x + iy) = \frac{-4}{((1 + x)^2 + y^2)^2}((1 + y^2 - x^2)\dot{x} - 2xy\dot{y}) . \quad (5.5.5)$$

At every point other than $z = -1$ the sign of this expression is opposite to that of the quantities in equation 5.5.2. But if S is positive definite, the sign of the quantities in 5.5.2 is positive (except at $z = +1$ where the expressions vanish). It follows that at every point other than an equilibrium value, the trajectories of the solutions to the differential equations are such that F is decreasing along them. Then $(1,0)$ is a globally stable equilibrium, while $(-1,0)$ is a source. The proof is complete.

Observe that the open half-plane $x > 0$ coincides with the set of values (x,y) for which $|F| < 1$. In the case where H is positive definite, we can compute a bound on the rate at which the trajectories starting in this half-plane converge to the equilibrium.

Lemma 5.5-2: Suppose S is positive-definite, and that F_0 , the value of F at a state (x_0, y_0) at time $t=0$, is smaller than 1. Let $\lambda_{\min}(S)$ denote the smaller eigenvalue of S . Then for $(x(t), y(t))$ along the solution trajectory:

$$F(t) < F_0 e^{-4\lambda_{\min}(S)t} \quad (5.5.6)$$

Proof: By the hypothesis on S

$$\begin{aligned} \frac{d}{dt}F &< \frac{-4\lambda_{\min}(S)(1 + x^2 + y^2)^2}{((1 + x)^2 + y^2)^2} \\ &< -4\lambda_{\min}(S)F \end{aligned} \quad (5.5.7)$$

because, for all (x,y) ,

$$F = \frac{(1-x)^2 + y^2}{(1+x)^2 + y^2} \quad (5.5.8)$$

$$< \frac{(1+x^2+y^2)^2}{((1+x)^2+y^2)^2}$$

It follows that F is approaching 0, its value at the equilibrium point $(1,0)$, at least as fast as the solution to the bounding equation

$$\frac{d}{dt}\bar{F} = -4\lambda_{\min}(S)\bar{F} \quad (5.5.9)$$

But the solution for this equation in \bar{F} satisfying the initial condition $\bar{F}(0) = F_0$ is exactly the righthand side of 5.5.6. The proof is complete.

In the case where S is negative definite, the same function F is used to show that $(-1,0)$ is globally stable, while $(1,0)$ is the source. In either case, the eigenvalue λ_{\min} of S having the smaller magnitude gives some quantitative estimate of how stable the stable equilibrium is. If $|\lambda_{\min}|$ is close to zero, for example, the system will be slower to converge than if it is large. Also, it is more likely when $|\lambda_{\min}|$ is small that a small perturbation to one or more of the aircraft model parameters could produce instability in a nominally-stable case. In general, when that smallest magnitude eigenvalue of S is close to 0, the pilot will have to wait for a while before the aircraft settles into a steady-state condition when he commands a constant turn at a fixed $\Theta-\Phi$ attitude. This parameter should also affect the quality of the ride during more dynamic maneuvers.

When the unique physical ($V > 0$) equilibrium is stable, the analysis of this case has a simple interpretation. To reach a desired trim condition, the pilot need only get the angles $\alpha, \beta, \Theta, \Phi$ to the correct values and wait. If his speed is too slow, his speed will increase to the proper value. If too fast, it will slow down. Likewise, the heading rate $\dot{\Psi}$ will find its equilibrium value and stay there. The stability of the unique equilibrium insures that, if the angles are right, the vehicle will naturally take care of the rest.

CASE 2: $c=-1$

In this case there are four real equilibria: $(1,0), (0,1), (-1,0), (0,-1)$. By a general result of Kukles and Casanova (see [KC] or theorem 7 of [Cop]) two of these are saddles, one is a

sink, and the last one is a source. The sink and source must be opposite each other (i.e. negatives of each other) so there are four distinct possibilities: any one of these four points could be the unique attractor. We consider only the case where (1,0) is the attractor, so that (-1,0) is the source and the points (0,1) and (0,-1) are saddles. The other three cases can be converted into this one by a suitable linear transformation, so there is no need to analyze the other cases separately.

The function we consider for this situation is the polynomial

$$F(x,y) = x(1 - y^2 - \frac{1}{3}x^2) . \quad (5.5.10)$$

Lemma 5.5-2: If the matrix S is positive definite, then the function F is a Liapunov function for the system 5.5.1.

Proof: It is easy to see that

$$\frac{d}{dt}F(x,y) = (1 - x^2 - y^2)\dot{x} - 2xy\dot{y} . \quad (5.5.11)$$

Comparing the righthand side of this expression with the quantities in equation 5.5.2, we find that it is positive (except at the equilibria) whenever S is positive definite. So F is an increasing function along the solution curves for 5.5.1. The proof is complete.

To see what this means, consider the 0-level set for the function F . The 0-level set is the union of the y -axis ($x=0$) and the ellipse C defined by $1 - y^2 - \frac{1}{3}x^2 = 0$. The two saddles (0,1) and (0,-1) lie in this set (they are in fact the points of intersection of the line and the ellipse), while the two other equilibria are contained in the region bounded by the ellipse. The point (1,0) is a local maximum for the function F , and the point (-1,0) is a local minimum.

If the matrix S is positive definite, then the function F increases along the solution curves of the differential equation. Therefore, any point inside the region bounded by the y -axis and the right half of the ellipse C will be moved along a trajectory that stays inside that region and approaches the point (1,0). The region bounded by the y -axis and the right half of C is a domain of attraction for the point (1,0). The mirror image region in the left half-plane is a

region of repulsion for unstable point $(-1,0)$.

The saddles at $(0,1)$ and $(0,-1)$ make the global properties of the flow unstable. If the aircraft state gets into the unstable flow region of one of these saddles, however, the pilot will have to change his aircraft's $\alpha, \beta, \Theta, \Phi$ values or fall into an unstable spin or speed condition. The $\alpha, \beta, \Theta, \Phi$ values that give rise to these saddles represent potentially hazardous conditions, while the region bounded by the 0-level set in the right half-plane defines the region where it is safe to fly.

There are two physical equilibria in this case, at most one of them is stable. Even if there is a stable one, the simple strategy of setting the angles $\alpha, \beta, \Theta, \Phi$ to the proper values and waiting will not always work. If the pilot has just completed a maneuver that has left his V and $\dot{\Psi}$ states in a bad spot (too near the unstable equilibrium) and then attempts to keep the angles fixed at the correct values for the stable equilibrium, he could find himself in a divergent speed condition or an unstable spin. If his initial V and $\dot{\Psi}$ are in a good spot (near enough to the stable equilibrium), on the other hand, he will be fine. Trying to end maneuvers at equilibria like these could be a hazardous undertaking.

SECTION 6: NONLINEAR FLYING QUALITIES

In previous sections we discussed nonlinear models of aircraft, the trim set, and the technique of dynamic inversion. These three topics are basic to our understanding of nonlinear flying qualities, which we discuss in this section.

We begin with a discussion of two idealized types of parameters: commanded-dynamic parameters and complementary-dynamic parameters. Both sets of functions are computed directly from the nonlinear aircraft models and they quantify important physical properties of the vehicle's behavior during flight. The commanded-dynamic parameters measure the maneuverability and controllability of the aircraft in the three angle-rate degrees of freedom (P,Q,R). The commanded-dynamic parameters are discussed in subsection 6.1 below.

Subsection 6.2 covers the complementary-dynamic parameters. Complementary-dynamic parameters can be used to construct Liapunov functions for stability analysis of dynamic inversion controllers. The best results we have so far are for the $\alpha, \beta, \Theta, \Phi$ inversion, for which we have derived explicit time and space bounds for the nonlinear dynamic trajectory of the vehicle moving towards a trim condition.

Besides these two types of idealized parameters, we have found several criteria for supermaneuverable vehicles flying along trajectories where aerodynamic forces and inertial terms simultaneously play an important role. We have two main results here

- 1) a simple aerodynamic criterion for smoothness of the aerodynamic loading during rapid α variation
- 2) control design criteria for coordinated flight during highly-dynamic, simultaneous roll-pitch-yaw maneuvers.

These two results are discussed in subsections 6.3 and 6.4

The last two topics of this section are two ideas that were under development at the end of our program. The first is a flying-quality metric for nonlinear aircraft models that could be

evaluated using the coordinated-flight U,P,Q,R dynamic-inversion controller discussed in section 6.4. The second concerns the stability and controllability of the aircraft during maneuvers involving extreme angular rates. The parameters defined in this section quantify the effect of the dynamic derivatives on the rotational energy and angular momentum of the vehicle.

Many of the ideas below were inspired by analysis of maneuvers like those described in section 7, which follows this one. The maneuvers we have looked at were generated by the batch version of our flight simulation program using various dynamic inversion strategies.

6.1 Commanded Dynamic Parameters

Commanded dynamic parameters quantify the pilot's direct command authority over the state of the aircraft by use of controls. Examples of parameters from the MIL-F-8785C specifications of this sort are (by section number):

- 3.2.2.1 Short-period response
- 3.2.2.2 Control feel and stability in maneuvering flight at constant speed
- 3.2.3.3.1 Longitudinal control in catapult takeoff
- 3.2.3.4 Longitudinal control in landing
- 3.3.2.6 Turn coordination
- 3.3.4.(all) Roll control effectiveness
- 3.3.5 Directional control characteristics
- 3.3.7 Lateral-directional control in crosswinds
- 3.3.8 Lateral-directional control in dives
- 3.3.9 Lateral-directional control with asymmetric thrust
- 3.4.2.1.3 Stall prevention and recovery

All these criteria concern command response -- the response of the vehicle in degrees of freedom that the pilot is intentionally changing through direct control. In contrast, there are criteria concerning the response of the aircraft in degrees of freedom that the pilot is not trying to change during the course of a maneuver (e.g. 3.2.1.1.2 Pitch control force variations during rapid speed changes).

In an effort to identify useful new flying quality parameters, we defined some functions of the aircraft state and the nonlinear aircraft model that quantify fundamental limitations on dynamic-maneuver command responses. These functions quantify the command authority available to the pilot to control vehicle dynamics during maneuvers. Below are some examples of these functions applied to the (P,Q,R) command-response. Dimensionless coordinates are used throughout this section (see section 5.3 for the conventions).

Pitch-rate Control

The primary pitch-rate effector in a basic aircraft is the elevator. In dimensionless coordinates (assuming symmetric aircraft, no dynamic derivatives, and a simplified elevator model):

$$I_{yy}\dot{Q} = (R^2 - P^2)I_{xz} + RP(I_{zz} - I_{xx}) + V^2C_m + V^2C_{m_{\delta_e}}\sin(\delta_e - \alpha) \quad (6.1.1)$$

The derivative of Q has an inertial term, an aerodynamic term, and a control term depending on the elevator. A parameter which measures the basic \dot{Q} command effectiveness is

$$\eta_{\dot{Q}_e} = \frac{V^2C_{m_{\delta_e}}}{I_{yy}} \quad (6.1.2)$$

This parameter must be sufficiently large at low speed to assure adequate control of the pitch axis for take-off, landing, and near-stall maneuvers.

Another potentially useful function is the dynamic pitch-control ratio, defined as:

$$v_{\dot{Q}_e} = \left| \frac{(R^2 - P^2)I_{xz} + RP(I_{zz} - I_{xx}) + V^2C_m}{V^2C_{m_{\delta_e}}} \right| \quad (6.1.3)$$

This function measures the ratio of the uncommanded portion of \dot{Q} to the magnitude of the elevator authority. In a region of the state space where this ratio is too large, the pilot will have trouble maintaining attitude control. For example, if the ratio is bigger than 1, the pilot cannot even control the sign of \dot{Q} . Some degradation of pitch control during high- α or rolling maneuvers is expected, $v_{\dot{Q}_e}$ quantifies the extent of degradation.

If R and P are 0, $v_{\dot{Q}_e}$ reduces to the ratio of C_m to $C_{m_{\delta_e}}$. In this case, the parameter is a

function of α alone (assuming coordinated flight) -- it could be used to determine if the vehicle has adequate elevator authority for a desired pullup maneuver.

Roll-rate and Yaw-rate Control

For a symmetric aircraft, the P and R degrees of freedom are most naturally analyzed together. The basic nonlinear equations look like:

$$\begin{bmatrix} I_{xx} & -I_{xz} \\ -I_{xz} & I_{zz} \end{bmatrix} \begin{bmatrix} \dot{P} \\ \dot{R} \end{bmatrix} = \begin{bmatrix} 0 & R & -Q \\ Q & -P & 0 \end{bmatrix} \begin{bmatrix} I_{xx} & 0 & -I_{xz} \\ 0 & I_{yy} & 0 \\ -I_{xz} & 0 & I_{zz} \end{bmatrix} \begin{bmatrix} P \\ Q \\ R \end{bmatrix} + V^2 \begin{bmatrix} C_l \\ C_n \end{bmatrix} + \begin{bmatrix} C_{l\delta_a} & C_{l\delta_r} \\ C_{n\delta_a} & C_{n\delta_r} \end{bmatrix} \begin{bmatrix} V^2 \sin(\delta_a - \frac{Pb}{2V}) \\ V^2 \sin(\delta_r - \beta) \end{bmatrix}$$

In coordinated flight ($\beta = 0$), symmetry causes the aerodynamic functions C_l and C_n to vanish, resulting in a simplification of the righthand side. When the angular velocity vector (P,Q,R) is small, roll/yaw command authority is approximated by the matrix:

$$\eta_{\dot{P}\dot{R}_{ar}} = V^2 \begin{bmatrix} I_{xx} & -I_{xz} \\ -I_{xz} & I_{zz} \end{bmatrix}^{-1} \begin{bmatrix} C_{l\delta_r} & C_{l\delta_a} \\ C_{n\delta_r} & C_{n\delta_a} \end{bmatrix} \quad (6.1.5)$$

The size of the minimum singular value $\sigma_{\min}(\eta_{\dot{P}\dot{R}_{ar}})$ is a bound on the angular-rate authority available in some direction in this two-degree-of-freedom subspace. The singular vectors (input and output) associated with this singular value should be considered as well. The function $\sigma_{\min}(\eta_{\dot{P}\dot{R}_{ar}})$ depends on the speed, α and β , and the vehicle model. The larger it is, the better the pilot can control P and R independently. It can be thought of as a lateral-directional version of the parameter $\eta_{\dot{Q}\dot{e}}$ defined earlier.

For more dynamic but still coordinated maneuvers, the ratio $v_{\dot{P}\dot{R}_{ar}}$ is defined to be the vector:

$$v_{\dot{P}\dot{R}_{ar}} = \frac{1}{V^2} \begin{bmatrix} C_{l_{\delta_a}} & C_{l_{\delta_r}} \\ C_{n_{\delta_a}} & C_{n_{\delta_r}} \end{bmatrix}^{-1} \begin{bmatrix} 0 & R & -Q \\ Q & -P & 0 \end{bmatrix} \begin{bmatrix} I_{xx} & 0 & -I_{xz} \\ 0 & I_{yy} & 0 \\ -I_{xz} & 0 & I_{zz} \end{bmatrix} \begin{bmatrix} P \\ Q \\ R \end{bmatrix} \quad (6.1.6)$$

The two entries in this vector represent the size of the aileron and rudder settings required to match the inertial l and n components of the torque. At states where these values are large, the pilot must use large rudder and aileron commands to maintain or reduce the sizes of P and R. Where these values are too large, the spin condition might be beyond the pilot's control.

The parameters $\eta_{\dot{P}\dot{R}_{ar}}$ and $v_{\dot{P}\dot{R}_{ar}}$ can be defined for uncoordinated flight as well. All that is required is to include the aerodynamic terms in $v_{\dot{P}\dot{R}_{ar}}$.

6.2 Complementary Dynamic Parameters

We define complementary dynamics to be those dynamics of the vehicle associated with states which the pilot is not controlling directly. Depending on the pilot's task, the states associated with the complementary dynamics may vary. We consider the following MIL-F-8785C specifications (listed by their MIL-F-8785C section numbers) to be associated with complementary dynamic phenomena:

- 3.2.1.(all) Longitudinal static stability
- 3.2.2.1.3 Residual oscillations
- 3.2.2.2 Control feel and stability in maneuvering flight at constant speed
- 3.3.1.(all) Lateral-directional mode characteristics
- 3.3.2.1 Lateral-directional response to atmospheric disturbances
- 3.3.5.1 Directional control with speed change
- 3.3.9.3 Transient effects
- 3.4.2.1.2 Stall characteristics
- 3.4.2.2 Post-stall gyrations and spins
- 3.4.2.2.1 Departure from controlled flight
- 3.4.3 Cross-axis coupling in roll maneuvers
- 3.4.4 Control harmony
- 3.4.5 Buffet
- 3.4.11 Direct force controls
- 3.5.5.1 Failure transients
- 3.6.3 Transients and trim changes

All these specifications concern the response of the aircraft to effects other than those directly commanded by the pilot. Included are transient response (in degrees of freedom other than those commanded), disturbance and failure response, dynamic cross-coupling, and stability and damping of dynamical modes.

We have identified some parameters based on the nonlinear models that describe one type of complementary dynamic behavior, we call them complementary dynamic parameters. Our approach makes use of the nonlinear inversion method discussed in section 5.

In the basic example where the pilot has four control inputs to work with, he will be able to command independently only four degrees of freedom, leaving two degrees of freedom constrained by their relation to the others. The motion of the aircraft in those two remaining degrees of freedom is determined by the equations of motion and the pilot's command inputs, but the control the pilot has in those two dimensions is indirect - a side-effect of the direct control exerted in the other four dimensions. The dynamic behavior of the aircraft in the four dimensions where the pilot has control is (within the limits of control effectiveness and neglecting disturbances) determined by the control inputs, so the pilot can directly influence dynamics there. Once the pilot's choice is made, the dynamics in the other two dimensions are completely determined by the aerodynamic and physical properties of the aircraft. These residual or indirectly controlled dynamics will vary from one aircraft to another in a way that can be computed from the nonlinear models. From these dynamics, flying quality parameters can be computed.

To compute these parameters, we make assumptions about the strategy chosen by the pilot to control the aircraft. For illustration, suppose the pilot uses his four controls to keep the direction of his velocity vector (α and β) and the direction of the gravity vector (θ and ϕ) fixed. This strategy might be used by the pilot to execute a steady turn. As was shown in section 5.3, the complementary dynamics for V and $\dot{\Psi}$ are given by the equations:

$$\dot{V} = a_{00} + a_{20}V^2 + a_{11}V\dot{\Psi} + a_{02}\dot{\Psi}^2 \quad (6.2.1)$$

$$\ddot{\Psi} = b_{00} + b_{20}V^2 + b_{11}V\dot{\Psi} + b_{02}\dot{\Psi}^2$$

The stability of these complementary dynamic equations should be highly correlated with the ride quality during the steady turn. If the system is very stable, the ride should feel very steady (good flying qualities for tracking purposes, for example), but if it is only marginally stable the ride quality may feel unsteady or even oscillatory. In the worst case, if the system is unstable, the aircraft might experience a divergent speed condition (compare with MIL-F-8785C section 3.2.1.1) or an unstable spin condition (compare with MIL-F-8785C sections 3.4.1 and 3.4.2). Analysis of the stability of this system was performed in subsection 5.5 of the previous section. We derived Liapunov functions to describe the transient dynamics for V and $\dot{\Psi}$, and we computed a bound on the settling time from a non-equilibrium condition. In one of the two cases analyzed in that subsection (corresponding, perhaps, to a very extreme turn or a turn at high α), we found that the stability of the turn might depend on the values of

V and $\dot{\Psi}$ as the turn is started. The functions and parameters of that section, and other parameters computed in a similar fashion, seem very important in assessing how well aircraft enter and execute turns.

By fixing other combinations of states (or some four-dimensional subspace of the state space), other sets of analytic equations can be obtained. From these equations, other complementary dynamic parameters can be computed.

6.3 : Lift to Drag Ratios of Aircraft with Smooth Lift Curves

Many books on aerodynamics give estimates for the lift and drag of a wing (or aircraft with zero control deflection). These estimates are typically of the form

$$C_L = f_1(AR, \alpha) \quad (6.3.1)$$

$$C_D - C_{D_0} = \frac{(C_L)^2}{f_2(AR)} \quad (6.3.2)$$

where AR is the aspect ratio of the wing (or aircraft) .

Taking the ratio of the equations 6.3.1 and 6.3.2 gives

$$\frac{C_D - C_{D_0}}{C_L} = \frac{f_1(AR, \alpha)}{f_2(AR)} \quad (6.3.3)$$

If the lift were linear in α , then we would get

$$C_L = f_1(AR, \alpha) = C_{L_{\alpha}}(\alpha - \alpha_0) \quad (6.3.4)$$

and equation 6.3.3 would be linear in α

$$\frac{f_1(AR, \alpha)}{f_2(AR)} = \frac{C_{L_{\alpha}}(\alpha - \alpha_0)}{f_2(AR)} \quad (6.3.5)$$

For lift curves that are not linear in α , we would still expect equation 6.3.3 to be fairly linear in α for small α .

For several aircraft with smooth lift curves (no stall discontinuities) such as the F-4, F-14 and F-15, we have examined the low speed lift and drag curves measured during wind tunnel tests and found that the expression on the left-hand side of equation 6.3.3 was very nearly determined by the following simple and interesting form :

$$\frac{C_D - C_{D_0}}{C_L} = \tan(\alpha - \alpha_0) \quad \left(0 \leq \alpha \leq \frac{\pi}{2} \text{ radians} \right) \quad (6.3.6)$$

This formula appears in "USAF Datcom Methods Handbook for Double Delta Wings". The point of giving it here is to show how well it fits the F-4, F-14, and F-15 data for angles of attack ranging from 0 to beyond 90 degrees.

In (6.3.6), α_0 is defined to be the angle of attack at which the drag is minimum. Note that $\tan(\alpha - \alpha_0)$ is nearly linear in $\alpha - \alpha_0$, over a fairly large range of $\alpha - \alpha_0$.

For the F-4 and F-15, AR is approximately 2.9, while on the F-14 (which had wing sweep set at 22°) AR was approximately 7.3; yet equation 6.3.6 still holds. This indicates that even though the numerator and denominator in equation 6.3.3 may each depend on AR, their ratio does not depend on AR for these aircraft.

An interesting interpretation of equation 6.3.6 can be made when a change of coordinates is made from wind axes to body axes.

Let $\tilde{\alpha} = \alpha - \alpha_0$, then

$$\begin{bmatrix} C_X \\ C_Z \end{bmatrix} = - \begin{bmatrix} \cos(\tilde{\alpha}) & -\sin(\tilde{\alpha}) \\ \sin(\tilde{\alpha}) & \cos(\tilde{\alpha}) \end{bmatrix} \begin{bmatrix} C_D \\ C_L \end{bmatrix} \quad (6.3.7)$$

so

$$C_X = -\cos(\tilde{\alpha})C_D + \sin(\tilde{\alpha})C_L = -\cos(\tilde{\alpha})(C_D - C_{D_0}) + \sin(\tilde{\alpha})C_L - \cos(\tilde{\alpha})C_{D_0} \quad (6.3.8)$$

Plugging 6.3.6 into 6.3.8 gives

$$C_X = -C_{D_0} \cos(\tilde{\alpha}) \quad (6.3.9)$$

If equation 6.3.6 were exact then

$$|C_X| \leq C_{D_0} \quad \left(0 \leq \alpha \leq \frac{\pi}{2} \text{ radians} \right) \quad (6.3.10)$$

For the F-4, F-14, and F-15 data shown in figures 6.1, 6.2, and 6.3 at the end of this subsection, C_{D_0} is around .02 and

$$|C_X| \leq 3 C_{D_0} \quad \left(0 \leq \alpha \leq \frac{\pi}{2} \text{ radians} \right) \quad (6.3.11)$$

Since C_{D_0} is so small, the error in the C_D and C_L data from which C_X was calculated may account for much of the discrepancy between (6.3.10) and (6.3.11).

Equation 6.3.11 shows us that at low speed there is much less aerodynamic force in the x direction than in the z direction ($V^2 C_x$ is small at any angle of attack). Consequently, the only significant force the pilot feels in the x direction is due to the throttle. This is true no matter how rapidly α is varying. Therefore, it would seem that aircraft with small magnitude C_x have better flying qualities during rapid α maneuvers than those with C_x of large variation. Note also from the plots that C_z decreases (it is negative) almost monotonically with α , for $0 \leq \alpha \leq \frac{\pi}{2}$ radians. This may be of some use in using n_z at the percussion point to "measure" α (using a lookup table for C_z).

The F-15 data (at 0 sideslip) came from the tests conducted on a 13-percent scale model of the F-15 S/MTD configuration in the NASA-Langley 30x60 ft low-speed wind tunnel, Test No. 489, run 216, no canard, configuration 85.000, between 10 July and 27 July 1985.

The F-4 data (at 0 sideslip) and the F-14 data (at 22° wing sweep, sideslip = 0° and 20°) were taken from [MMTJ].

This report cited reference [Ang] for wind tunnel data for the F-4 and several references containing selected data for the F-14 from wind tunnel tests conducted during 15 March - 16 April, 1971, in the NASA Ames Research Center 12 ft pressure tunnel and during August, 1971, in the NASA Langley Research Center 30x60 ft (full scale) tunnel.

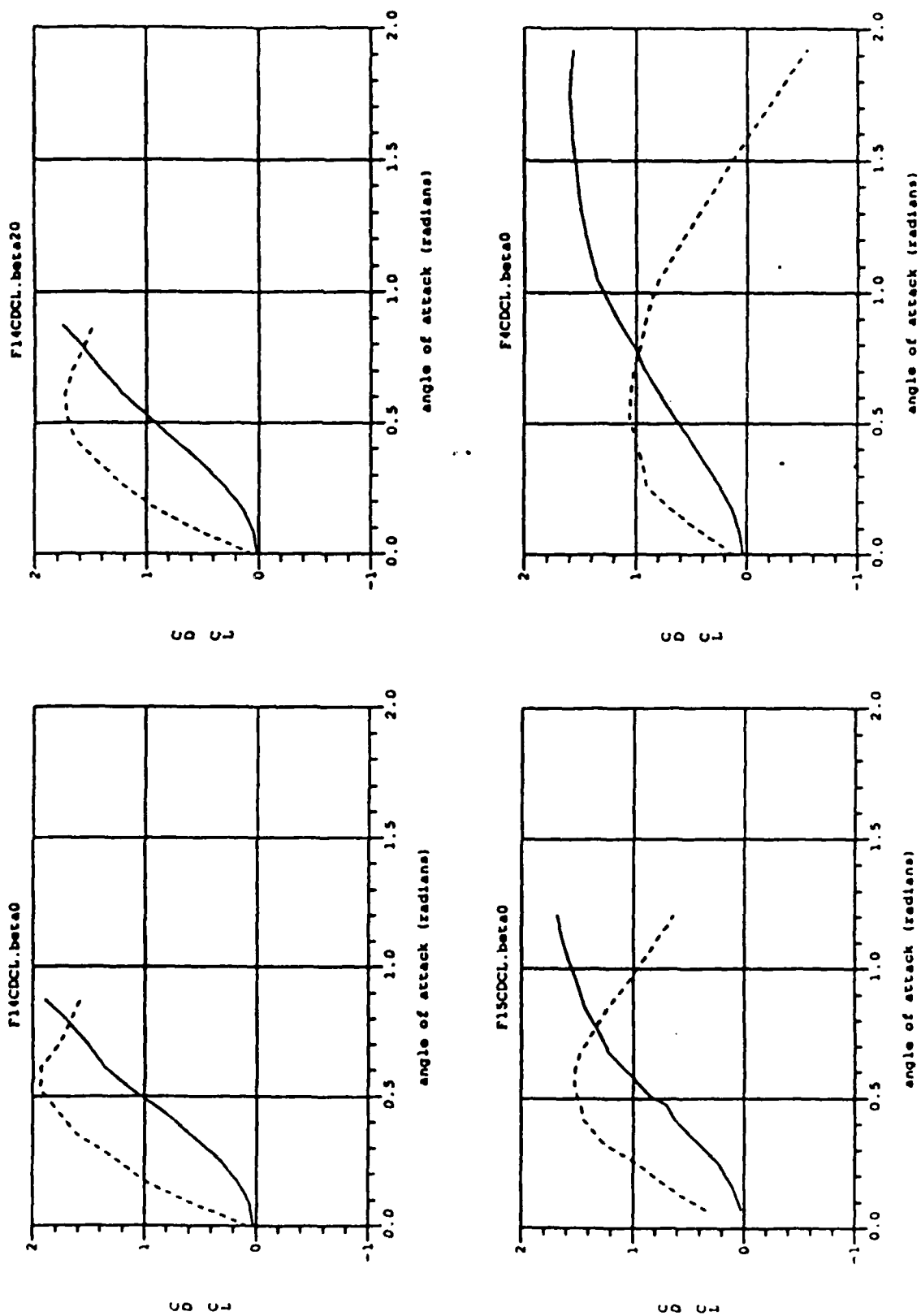


Figure 6.1 Drag and Lift Data for the F4, F14, and F15

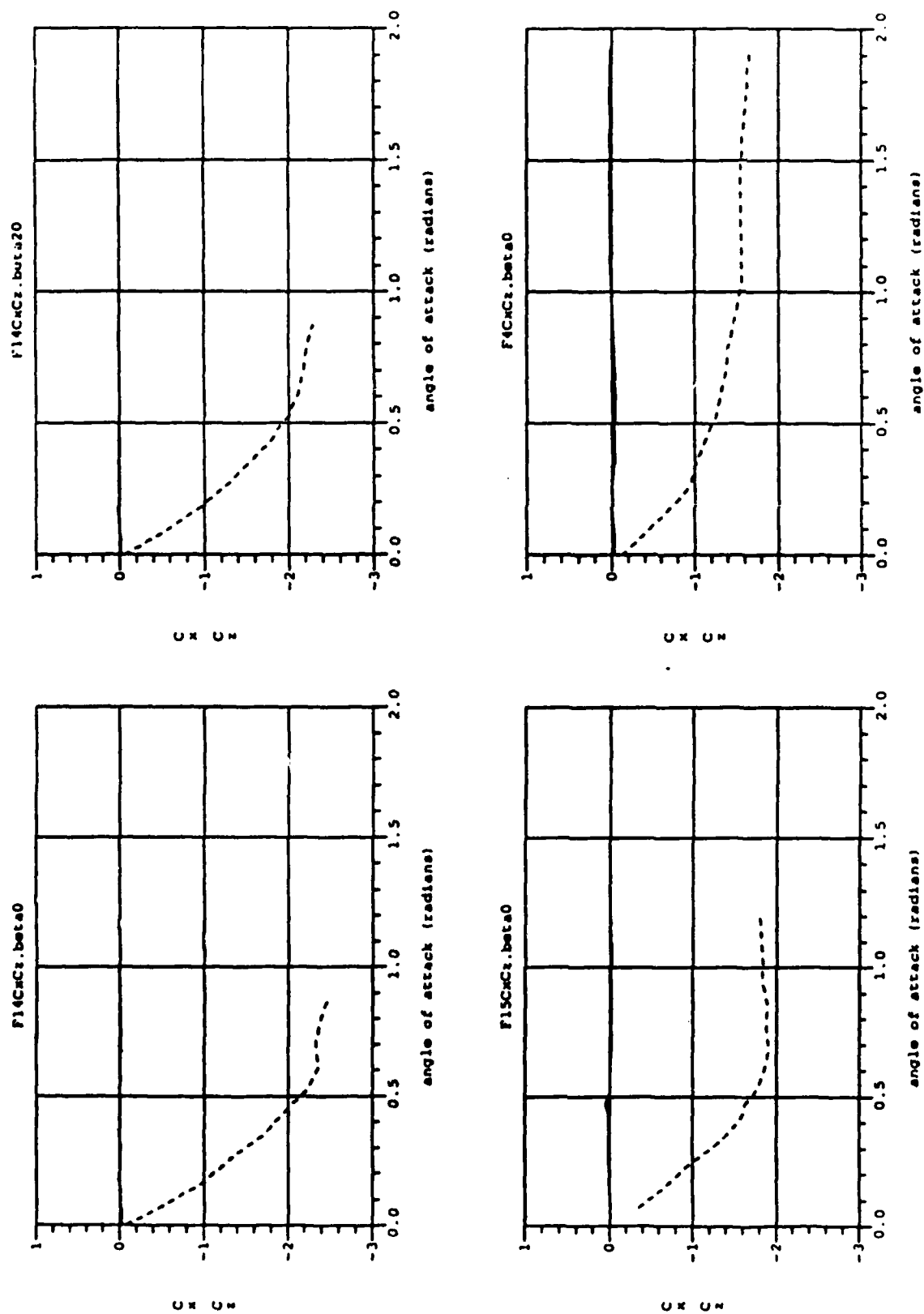


Figure 6.2 Axial and Normal Force Data for the F4, F14, and F15

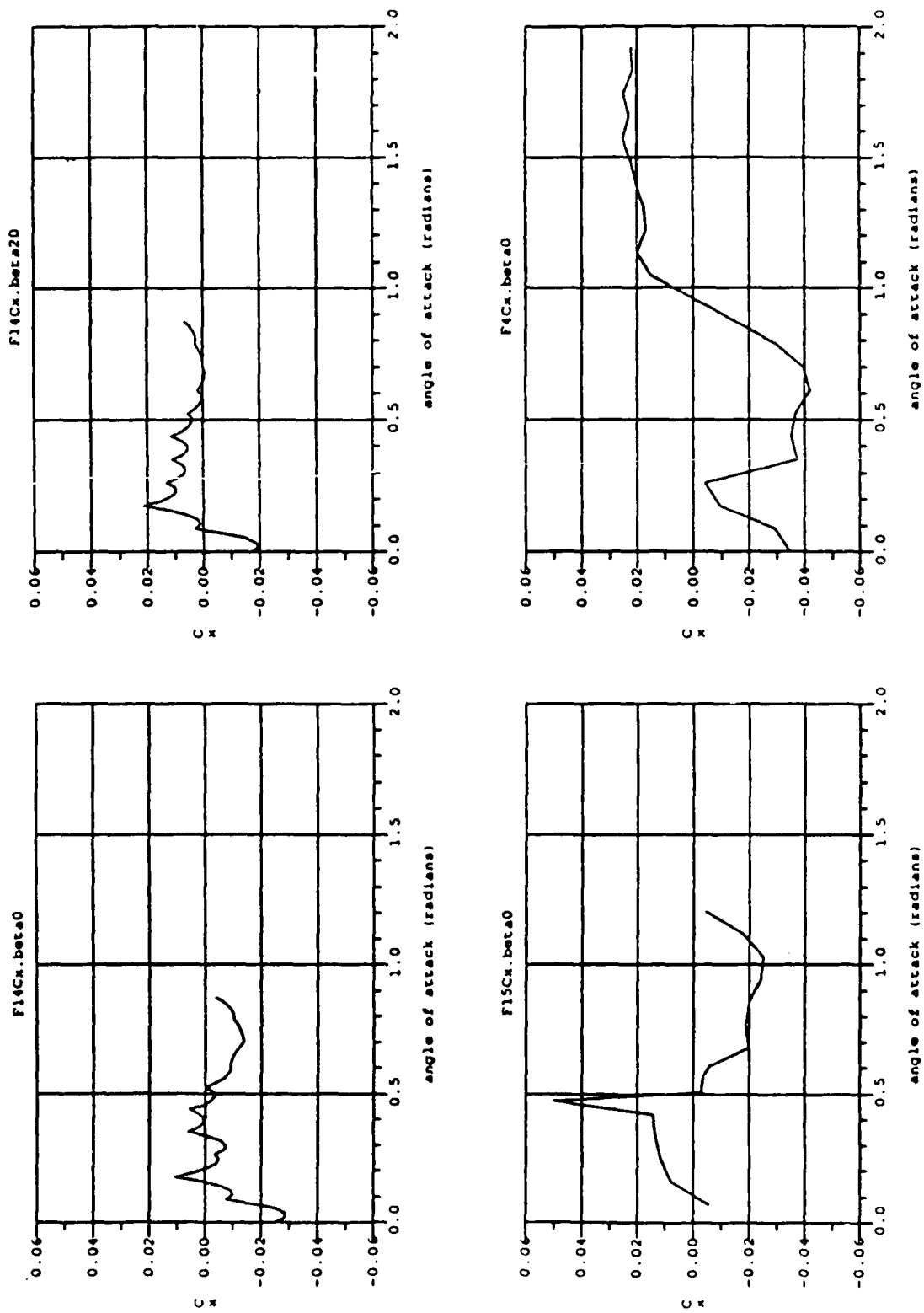


Figure 6.3 Axial Force Data for the F4, F14, F15

6.4 Highly Dynamic Phenomena

For a conventionally configured aircraft at medium to high speed, the largest forces that can act are aerodynamic. Even the most powerful aircraft have thrust-to-weight ratios only slightly greater than 1, while maneuvers reaching levels close to 10 g for short periods of time are not uncommon. For coordinated flight, these high-g maneuvers are achieved by entering high-angle-of-attack regions where the aerodynamic lift and drag forces are strongest. One example of this type of maneuver is the diving-turn maneuver shown later in section 7.3.

The largest force during this diving-turn maneuver is the 8-g normal acceleration encountered during the start of the dive. In less than 3 seconds, α rises from close to zero to nearly 1.1 radians. The vehicle decelerates rapidly, despite the fact that it is diving at full throttle, because the drag term is so large. The elevator is saturated at 1 radian deflection (our assumed saturation value) to maximize the pitch-rate during this period - the high pitch-rate begins while the roll-rate is still large from the initial banking phase. The large pitch-rate increases α rapidly while the airspeed is still near 500 ft/second, large lift and larger drag forces are the result.

An important feature of this high-g diving maneuver is the dominance of the quadratic inertial terms in the nonlinear state equations. That is, the angular rates P, Q, and R become so large in magnitude that the state derivatives are heavily influenced by the product terms PQ, QR, PW, etc. A primary effect of these large angular rates can be seen in the basic lateral velocity equation:

$$\dot{V} = -RU + PW + \cos(\theta)\sin(\phi) + V^2 C_y(\alpha, \beta) + \text{direct rudder acceleration} \quad (6.4.1)$$

This simple model (no dynamic derivatives, only rudder direct forces) illustrates the point. If a maneuver involves turn-coordination at high roll rate, the magnitudes of the terms $-RU$ and PW become comparable with the gravity term, and much greater than the direct rudder force. In our sample maneuver, the roll rate P reaches a value greater than two radians/second and the pitch rate exceeds 1 radian/second in the early part of the maneuver. The maneuver begins at a speed of roughly 500 ft/second (size 2 in the dimensionless units of equation 6.4.1) and at an altitude of about 5000 ft (near sea level, but at least 2700 ft). The inertial acceleration N_y experienced by the pilot is the negative of the sum $[V^2 C_y(\alpha, \beta) + \text{direct rudder force}]$, and this is a small term because the turn is coordinated. The gravity term never gets any larger

than 1, while each of the terms $-RU$ and PW get bigger than 1.

To keep β small, the yaw-rate R must vary in such a way as to keep \dot{V} small. The controller used to generate the diving turn allowed arbitrary commanded P , and chose R to satisfy:

$$R = [PW + \cos(\theta)\sin(\phi) + V^2 C_y(\alpha, \beta) + \text{direct rudder acceleration}]/U \quad (6.4.2)$$

The control strategy based on the dynamic inversion for U, P, Q, R with R chosen to keep β small is called coordinated-flight U, P, Q, R inversion. This controller was used to execute the diving-turn maneuver of section 7.3, it seems a very promising approach for supermaneuverable vehicle control. If the lateral-directional control authority is adequate to generate the necessary P and R values independently, it should work for very extreme combined roll-pitch-yaw maneuvers.

For this control approach to work in practice, the allowed bandwidth of the roll-rate commands must be limited to a region where the rudder is able to generate enough \dot{R} to track the right-hand side of equation 6.4.2. As a part of this restriction, consideration must be given to α because P is multiplied by $\frac{W}{U} = \tan(\alpha)$. The factor $\tan(\alpha)$ implies that at large angles of attack the ratio $\frac{\omega_p(\alpha)}{\omega_R(\alpha)}$ of the bandwidths must be smaller than at low α for coordinated rolls. Equation 6.4.2 can be used to quantify that requirement: for acceptable high-alpha roll-rate response, the bandwidths $\omega_R(\alpha)$ and $\omega_p(\alpha)$ should be related by an inequality of the type:

$$\omega_R(\alpha) > K\omega_p(\alpha)\tan(\alpha) \quad (6.4.3)$$

for some constant K which is (presumably) larger than 1. This inequality can be viewed as a design requirement for acceptable flying qualities at high α (better flying qualities being associated with larger values of K), or it can be taken as a rule for determining the maximum allowable bandwidth of P as a function of α and the bandwidth of R . Alternatively, it can be viewed as a requirement on rudder size needed to provide coordinated flight at high α . The parameter v_{PRAR} defined in section 6.1 must also be considered to determine the achievable performance for this control approach.

NO-A192 146

NONLINEAR FLYING QUALITY PARAMETERS BASED ON DYNAMIC
INVERSION(U) HONEYWELL SYSTEMS AND RESEARCH CENTER
MINNEAPOLIS MN B G MORTON ET AL. 30 OCT 87 F0231-FR

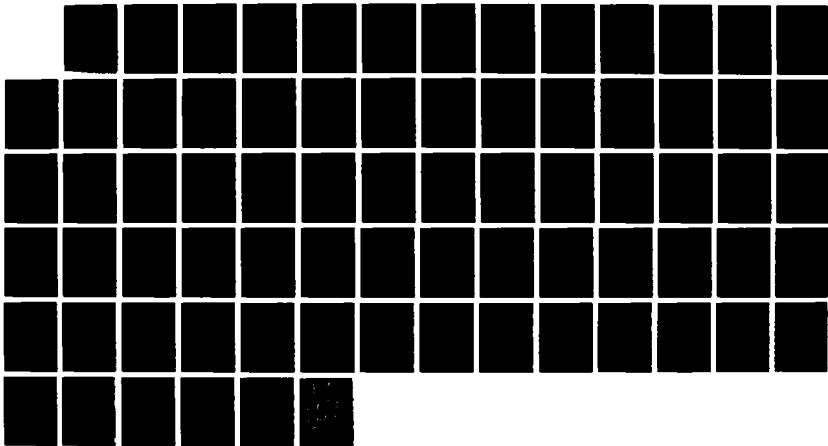
242

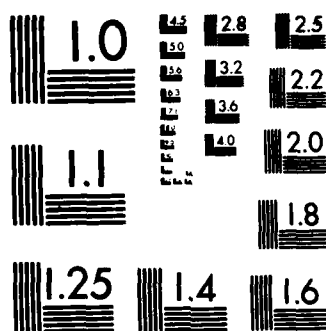
UNCLASSIFIED

AFMIL-TR-87-3079 F33615-86-C-3612

FBI
F/G 1/1

NL





MICROCOPY RESOLUTION TEST CHART
NATIONAL BUREAU OF STANDARDS-1963-A

Along the same lines, it is possible to derive criteria for dynamic control of α in terms of Q control. During coordinated flight, P and R do not contribute directly to $\dot{\alpha}$, but Q does. Assuming $V = 0$:

$$\dot{\alpha} = Q + [U\cos(\theta)\cos(\phi) + W\sin(\theta) - UN_z + WN_x]/V^2 \quad (6.4.4)$$

Consider a maneuver that requires keeping α large for an extended period of time. From 6.1.1, it is clear that if P and R are kept small, the sign of \dot{Q} is determined by the sign of C_m at values of α where $|C_m| > |C_{m_0}|$. If C_m is negative with a large magnitude in the desired α range, then Q will be decreasing rapidly so long as α is kept large. Once Q becomes sufficiently small, the sign of $\dot{\alpha}$ in equation 6.4.4 becomes negative and the desired large α condition is lost. From this analysis, we can see one of the advantages of a thrust-vectoring capability. When the factor C_m dominates C_{m_0} for values of α in a desired range, thrust vectoring can maintain Q so long as V^2 is small enough. In such a situation, it is possible to maintain a large α condition for extended periods of time without generating P and R (i.e., turning) to keep Q in a compatible range.

6.5 Dynamic Flying Quality Metrics

One approach to evaluating flying qualities, given a nonlinear aircraft model, is to use a metric on the space of maneuvers. This idea has been proposed by others, we have chosen not to develop such an approach during this contract. A metric approach could be carried out based on ideas developed during this contract; one way to do this is described briefly below.

Begin by choosing a (small) number of equilibrium conditions for the aircraft model. Dynamic maneuvers begin at various equilibrium conditions; the equilibrium points chosen should be representative of flight conditions where dynamic maneuvers usually start. We could describe the set of points chosen by their equilibrium values of α, β, Θ , and Φ (these coordinates are the easiest to use with our equilibrium computing program). For each point we then compute the fixed values of $V, \dot{\Psi}$, and the actuator inputs. To reduce the number of cases considered, we could start with coordinated conditions where $\beta = 0$.

Next, for each flight condition, pick a set of dynamic command profiles for U, P , and Q as a function of time. Many different sets of profiles can be specified here - the idea is to define a representative sampling of dynamic responses for as many different maneuvers as possible. The aircraft model will be evaluated with respect to this set of candidate maneuvers, so it would be a good idea to include profiles that are characteristic of maneuvers actually used during flight.

Each U, P, Q profile chosen will then be used as input to the U, P, Q, R dynamic inverter. The R command needed by the controller will be generated internally to provide coordinated flight while the simulation tries to fly the trajectory defined by the specified U, P, Q functions. For each maneuver, the model will be evaluated according to a collection of norms chosen to reflect the quality of the response.

For example, for each command profile, we would find the average error in the commanded U, P , and Q responses along the trajectory; as well as the maximum error for each of these variables. Also important is the determination of the extent of control saturation (both position and rate limits) during the flight. These measures of U, P , and Q errors for each maneuver would form a criterion for evaluation of the attitude-rate response, a quantity

important in dynamic tracking or pursuit tasks. By taking the average value of these errors over a representative sample of maneuvers, the evaluator finds an overall sense of the quality of response.

The physical factors about the vehicle reflected by the attitude-rate response errors are things like the mass and moment properties, span and chord, aerodynamic moment coefficients C_l, C_m, C_n , and the actuator position and rate limitations. The aerodynamic force terms C_x, C_y, C_z will probably not be very important for this criterion. It might work out better to fix the throttle setting at a predetermined value for the entire maneuver so that power cycling uncharacteristic of actual maneuvers will not occur. In that case, only the profiles for P and Q need to be specified for each run. It is probably a good idea to classify the responses according to whether or not some saturation occurred during the simulation, and to quantify the tendency to saturate in an average sense. Some evaluation should also be made of the severity of the effects of saturation (i.e. whether instability results).

Another factor to consider is the attitude response during the maneuver, as well as the final equilibrium position and time to settle at the end of the maneuver. For simplicity, we might suppose that the commanded values of P and Q go to 0 at the end. Some (presumably) short time thereafter the vehicle should show some tendency to settle at a new equilibrium, which can be considered the starting point of a subsequent maneuver not yet determined. The length of the path through the attitude space, and the location of and time to settle at the final equilibrium point are all quantities that can be measured and averaged over the maneuver space. The time to settle at the end of a maneuver is a quantity similar in nature to our complementary-dynamic parameters that we developed during this program.

Finally, we would look at the inertial accelerations during the maneuver to assess the environmental stress experienced by the pilot during the maneuver. The values of N_x, N_y, N_z would be computed along each trajectory and compared with acceptable ranges. In the basic nonlinear model, the formulas for these inertial accelerations felt by the pilot are:

$$N_x = -(V^2 C_x(\alpha, \beta) + \text{throttle acceleration}) \quad (6.5.1)$$

$$N_y = -(V^2 C_y(\alpha, \beta) + \text{rudder acceleration})$$

$$N_z = -(V^2 C_z(\alpha, \beta) + \text{elevator acceleration})$$

It would also be worthwhile to compute the acceleration time derivatives, or jerk components, during each maneuver. The jerk components quantify the smoothness of the ride in a way that allows comparison among various models. The jerk components can be computed using implicit differentiation along the trajectory: for example, the x-component of the jerk J_x is:

$$J_x = \frac{dN_x}{dt} = -(2V\dot{V}C_x(\alpha,\beta) + V^2(\frac{\partial C_x}{\partial \alpha}\dot{\alpha} + \frac{\partial C_x}{\partial \beta}\dot{\beta}) + \frac{d(\text{throttle acceleration})}{dt}) \quad (6.5.2)$$

with similar expressions for J_y and J_z . Some overall average of the expression $J_x^2 + J_y^2 + J_z^2$ for the different command profiles might provide a criterion for smoothness of ride during dynamic maneuvers. Note that the jerk components depend explicitly on the partial derivatives of the aerodynamic force functions - these derivatives could be estimated numerically from interpolated table data.

6.6 Stability and Controllability of Rotational Energy, Angular Momentum, Angular Rate

One idea that arose near the end of the program was to identify quantities based on nonlinear aircraft models that characterize the stability and controllability of the rotational energy, angular momentum, and rotation rate of the vehicle during flight. In this section we show how such quantities can be derived and show some examples. As a corollary of this analysis we derive formulas, defined in terms of aerodynamic functions and the moment tensor, which quantify the stability of the rotational dynamics for bounded speed.

Using the nonlinear equations that include dynamic derivatives, we have:

$$\dot{\mathbf{V}} = \mathbf{1}_{\beta\alpha}^T [1_{\phi\theta} + V^2 C_{xyz} + V C_{xyzPQR} \begin{bmatrix} P \\ Q \\ R \end{bmatrix} + g_{xyz} h(x,u)] \quad (6.6.1)$$

$$\begin{bmatrix} \dot{P} \\ \dot{Q} \\ \dot{R} \end{bmatrix} = \mathbf{I}_{mo}^{-1} \left\{ \Omega \mathbf{I}_{mo} \begin{bmatrix} P \\ Q \\ R \end{bmatrix} + V^2 C_{lmn} + V C_{lmnPQR} \begin{bmatrix} P \\ Q \\ R \end{bmatrix} + g_{lmn} h(x,u) \right\}. \quad (6.6.2)$$

These analytic expressions for the derivatives of V , P , Q , and R involve coefficients that depend in a complicated way on the states $\alpha, \beta, \theta, \phi$; but their dependence on V , P , Q , and R is only quadratic. There are V^2 terms in the control input ($g \dots h(x,u)$) expressions associated with the surface effectors, if we identified this dependence explicitly in the equations the form would remain quadratic. From physical considerations the V^2 terms in equation 6.6.1 represent drag effects that dominate $\dot{\mathbf{V}}$ whenever V is large (relative to P , Q , and R). These equations are similar to the ones we encountered in the analysis of the complementary dynamic parameters, only in this case there are no assumptions made about any of the states being kept fixed. We expect they can be analyzed thoroughly to obtain a global stability result, but for now we do not attempt a complete analysis.

Let us suppose that the speed V is bounded, and consider equation 6.6.2. First, observe that the dot product of the vector $[2P, 2Q, 2R]$ with both sides of equation 6.6.2 provides an expression for the time derivative of $P^2 + Q^2 + R^2$, the square of the rate of the angular

speed. The right-hand side is then a cubic function of the variables P, Q, and R with coefficients depending on the speed V, the states $\alpha, \beta, \theta, \phi$, and the control inputs. We have not worked much with this expression because the other functions below seemed more tractable. Still, it might be worth looking at to determine the effectiveness of the control inputs to control the angular speed directly.

Simpler to analyze and (perhaps) more useful is control of the rotational energy about the center of mass. The time derivative of the rotational energy is obtained by taking the dot product of both sides of equation 6.6.2 with the vector [P,Q,R] after first multiplying by the inertia matrix I_{mo} . The resulting expression on the righthand side is now simply a quadratic expression because [P,Q,R] $\Omega = 0$. The equation becomes:

$$\begin{aligned} \frac{d}{dt} [\text{Rotational Energy}] &= \frac{d}{dt} \left[\frac{1}{2} [P, Q, R] I_{mo} \begin{bmatrix} P \\ Q \\ R \end{bmatrix} \right] \\ &= [P, Q, R] \left[V C_{lmnPQR} \begin{bmatrix} P \\ Q \\ R \end{bmatrix} + V^2 C_{lmn} + g_{lmn} h(x, u) \right] . \end{aligned} \quad (6.6.3)$$

The expression we want to consider is the quadratic term $[P, Q, R] C_{lmnPQR} \begin{bmatrix} P \\ Q \\ R \end{bmatrix}$ that appears on the righthand side. For bounded V, this quadratic term will dominate the rotational energy derivative when the angular rate vector [P,Q,R] is large. If the 3x3 matrix $S_{lmnPQR} = \frac{1}{2} (C_{lmnPQR} + C_{lmnPQR}^T)$ is negative definite for all values α and β , the rotational rate must stay bounded. Physically, this matrix represents an angular drag term - its dominant effect on the rotational energy at high angular rate conditions suggests it may be highly correlated with flying qualities for extremely dynamic maneuvers. The sizes of the eigenvalues and the directions of the corresponding eigenvectors in the P,Q,R space are reasonable candidate flying quality parameters.

The total angular momentum squared is another function of the angular velocity vector that can be analyzed to quantify angular stability and control authority during flight. Proceeding as before, we compute

$$\frac{d}{dt}[\text{Angular Momentum}]^2 = \frac{d}{dt} \left[\frac{1}{2} [P, Q, R] I_{mo}^2 \begin{bmatrix} P \\ Q \\ R \end{bmatrix} \right] \quad (6.6.4)$$

$$= [P, Q, R] [V I_{mo} C_{lmnPQR} \begin{bmatrix} P \\ Q \\ R \end{bmatrix} + V^2 I_{mo} C_{lmn} + I_{mo} g_{lmn} h(x, u)] .$$

In this case, the cubic P,Q,R term vanishes because the matrix $I_{mo} \Omega I_{mo}$ is antisymmetric. Now it is the matrix

$$A_{lmnPQR} = \frac{1}{2} (I_{mo} C_{lmnPQR} + C_{lmnPQR}^T I_{mo}^T) \quad (6.6.5)$$

that must be negative-definite to insure stability. The eigenvalues of this matrix and the corresponding eigenvectors, computed as a function of α and β , might also be correlated with flying qualities.

We do not know which function of the angular velocity, if any, is the most important to a pilot during highly dynamic maneuvers. The relation between the sizes of the matrices S_{lmnPQR} and A_{lmnPQR} and the sizes of the different torque-generation control effectors could have a large impact on the vehicle's flyability in terms of the angular rate controllability. Parameters based on all three functions discussed above have a clear physical significance and could be relevant to flying qualities. Also, there may be a correspondence between these parameters and the onset of uncontrolled spin conditions that are sometimes associated with high-angle-of-attack maneuvers.

We must use caution when interpreting the results of this subsection. We do not know how large the rotational rates must be for the dynamic derivative terms to dominate. The maximum rotational rates predicted by the bound on rotational energy from the above equations may exceed the realm where our basic nonlinear model is valid. We have assumed a flat earth, constant air density, and very simple expressions for the aerodynamic functions. We do know, however, that nonlinear models like these are used in practice, and that they give reasonable results when applied to specific regions of flight. Within the realm where these equations accurately model the aircraft dynamics, we expect the parameters above will be worth looking at. If we have a better model, the three angular velocity functions discussed here still have a fundamental physical significance that might be correlated with flying qualities.

SECTION 7: THE MANEUVERS

In this section we present some simulated maneuvers using a subset of the F-14 model found in [MMTJ]. These simulations motivated some of the mathematical expressions that we associated with candidate flying quality parameters in earlier sections. More importantly, they provide a detailed account of the model behavior under carefully controlled conditions. We can, in general, investigate and demonstrate dynamic flight characteristics associated with various levels of flying quality through simulations like these.

Our approach has been based on analysis of the nonlinear aircraft equations, to characterize the dynamic behavior of aircraft during flight. At the start, we began with an idea (dynamic inversion) about how aircraft could be made to fly; we tried out the idea by using it to command simulated maneuvers. By analyzing the results of the simulations, we were able to identify features of the nonlinear equations that could have a significant influence on an aircraft's dynamic behavior during flight. Some of the things we learned are mentioned in the presentation below, others we have already discussed in our earlier section on the candidate parameters.

Our analysis of the maneuvers given here is not so complete as we would like - there remain several questions about the results that should be investigated further. We will point out the unsettled questions as we go.

The three different types of maneuvers discussed here were generated by our batch version of the nonlinear simulation. The first type is a roll reversal - where the aircraft banks first to the right, stabilizes bank angle, then banks back to the left. The second type is a barrel roll. The third type is a highly-dynamic diving turn chosen because of its extreme dynamic behavior.

7.1 Roll Reversal

Three versions of the roll reversal maneuver are presented. All three were generated by a dynamic inversion controller tracking open-loop command profiles for $\alpha, \beta, \gamma, \mu$. The structure of this controller is described in example 5 of subsection 5.1. The primary goal was to fly the maneuver while keeping the flight-path angle γ fixed at zero. The three different versions involved three different criteria for the normal acceleration N_z .

The easiest way to fly the maneuver is to pick a desired μ trajectory and then command $\gamma = 0$, $\beta = 0$, and α to be what it has to be in order to keep the speed nearly constant. The plots in Figure 7.1 through Figure 7.8 show the results for this maneuver. We call this maneuver UNLOADEDREVERSAL. To generate UNLOADEDREVERSAL, we chose a desired μ command profile:

For $0 < t < 5$ seconds commanded $\mu = 0.0$

For $5 < t < 6$ seconds commanded $\mu = \frac{\pi}{3} \sin^2(\pi(t - 5.0)/2.0)$

For $6 < t < 8$ seconds commanded $\mu = \frac{\pi}{3}$

For $8 < t < 10$ seconds commanded $\mu = \frac{\pi}{3} (1 - 2\sin^2(\pi(t - 8.0)/4.0))$

For $10 < t < 12$ seconds commanded $\mu = -\frac{\pi}{3}$

The commanded values for β and γ were fixed at 0 throughout. To derive the command profile for α , we used the approximation (good when γ is constant at 0 and the direct control-surface force terms are small):

$$\dot{\gamma} = V^2 C_L \cos(\mu) - 1 \quad (7.1.1)$$

Note that variables in the dimensionless units of section 5.3 are used here.

We wanted to keep γ constant at 0, and we chose to keep V near a nominal dimensionless speed of 2.2 (roughly 560 feet per second) throughout, so we needed to find an α

command profile (note that β is assumed 0) to solve:

$$C_L(\alpha) = 1/((2.2)^2 \cos(\text{commanded } \mu)) \quad (7.1.2)$$

For small α , the lift coefficient is closely approximated by the relation:

$$C_L(\alpha) = 5.9\alpha + 0.09 \quad (7.1.3)$$

Therefore, we defined the commanded α according to:

$$\text{commanded } \alpha = (-0.09 + 1/((2.2)^2 \cos(\text{commanded } \mu)))/5.9 \quad (7.1.4)$$

It was not essential that we could approximate the lift curve by a linear function of α , any invertible nonlinear function would have worked just as well. If a wider range of α were involved in the maneuver, we would have used a more accurate, nonlinear approximation. Plots of the commanded α and μ profiles, with the simulated responses, can be found in Figure 7.3.

First consider the four plots in Figure 7.1. Each plot shows the graphs of three of the states as functions of time during the maneuver. The name of the maneuver and the states plotted appears at the top of each plot. The way to read these charts having more than one state function plotted on a single graph is as follows: the first-named variable at the top of the graph is represented by the continuous line, the second-named variable is represented by the short-dashed line, and the third-named variable is represented by the long-dashed line. In some cases, one of the three variables plotted remains much smaller in magnitude than the others, so that it appears that only two graphs have been drawn. For example, in the plot for U, V, and W in Figure 7.1 the graph of V is so small that it is difficult to tell that it is there. Some care is required to read these plots correctly. In some of these plots there are rapid transients during the first 2 seconds - they are associated with mismatches of initial conditions at the start of the simulation and should be ignored.

There are few features worth noting in Figure 7.1. The components U and V remain nearly constant during the maneuver while W, though small, increases by a factor of 2 or 3

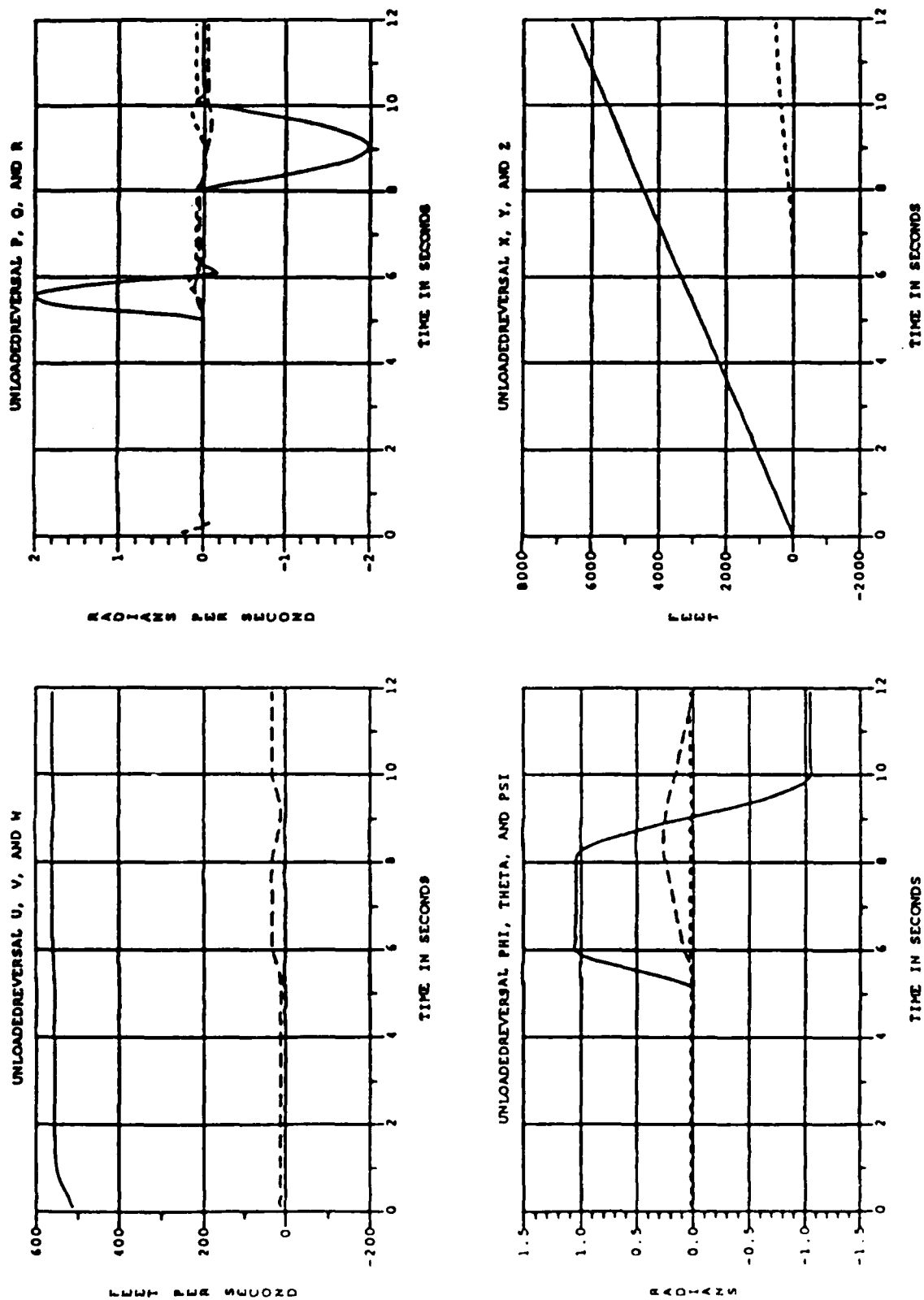


Figure 7.1 States During UNLOADED ROLL REVERSAL

from beginning to end. The behavior of W is driven by the α response, which can be seen in Figure 7.3. The P, Q, R plot shows that a 2-radian/second peak in P and very little Q and R are required to produce the 60 degree bank in one second. The stabilization into the banked-turn requires roughly $\frac{1}{2}$ second. The Φ response is crisp, with little overshoot, and Θ stays nearly fixed. Ψ moves from 0 to roughly 15 degrees with the bank to the right, then back to 0 again after the reverse back to the left. In inertial position coordinates, the path of the vehicle moves to the right about 500 feet during the maneuver from $t=5$ seconds to $t=12$ seconds, and is about to start heading back again when the simulation ends.

Figure 7.2 shows plots of the changes in the inertial position coordinates Y and Z , and of the Euler-angle coordinates Θ and Ψ drawn to appropriate scale. Worth special note is the CHANGE IN ALTITUDE plot, where it is shown that the altitude varies by less than 2 feet during the entire time. Keeping in mind that the maneuver did not begin until $t=5$ seconds (the initial condition transient was a factor at the start), we can see that the altitude was held very nearly constant while the maneuver was performed.

Figure 7.3 shows the comparisons between the open-loop command profiles for $\alpha, \beta, \gamma, \mu$ and the values of these functions during the simulation. After the initial condition transients, all four simulated responses stay within a milliradian of their commanded values. This was a very successful maneuver.

Figure 7.4 shows the simulated values of the inertial accelerations, the aerodynamic force functions, α and β , and the speed. N_y remains very close to 0, N_x changes by about $\frac{1}{2}$ g, and N_z follows a benign path between 1 and 2 g. The speed changes by less than 2 percent.

Figure 7.5 shows the control input behavior during the maneuver. Disregarding the initial transients, these profiles seem fairly reasonable. The aileron does most of the work in a pair of doublets (peak aileron deflection of 50 degrees) during the two rolling periods (we have assumed 1-radian ranges for each of the surfaces - we would have assumed more effective surfaces and performed the same maneuvers with smaller size commands if we had less surface position range. We will deal with saturation phenomena soon, but not for the aileron). The elevator and rudder commands move only slightly, about 5 degrees. The surface command rates look reasonable, there probably should be a plot of (approximate) surface rate activity in a more detailed version of this simulation. The throttle moves up to a setting of

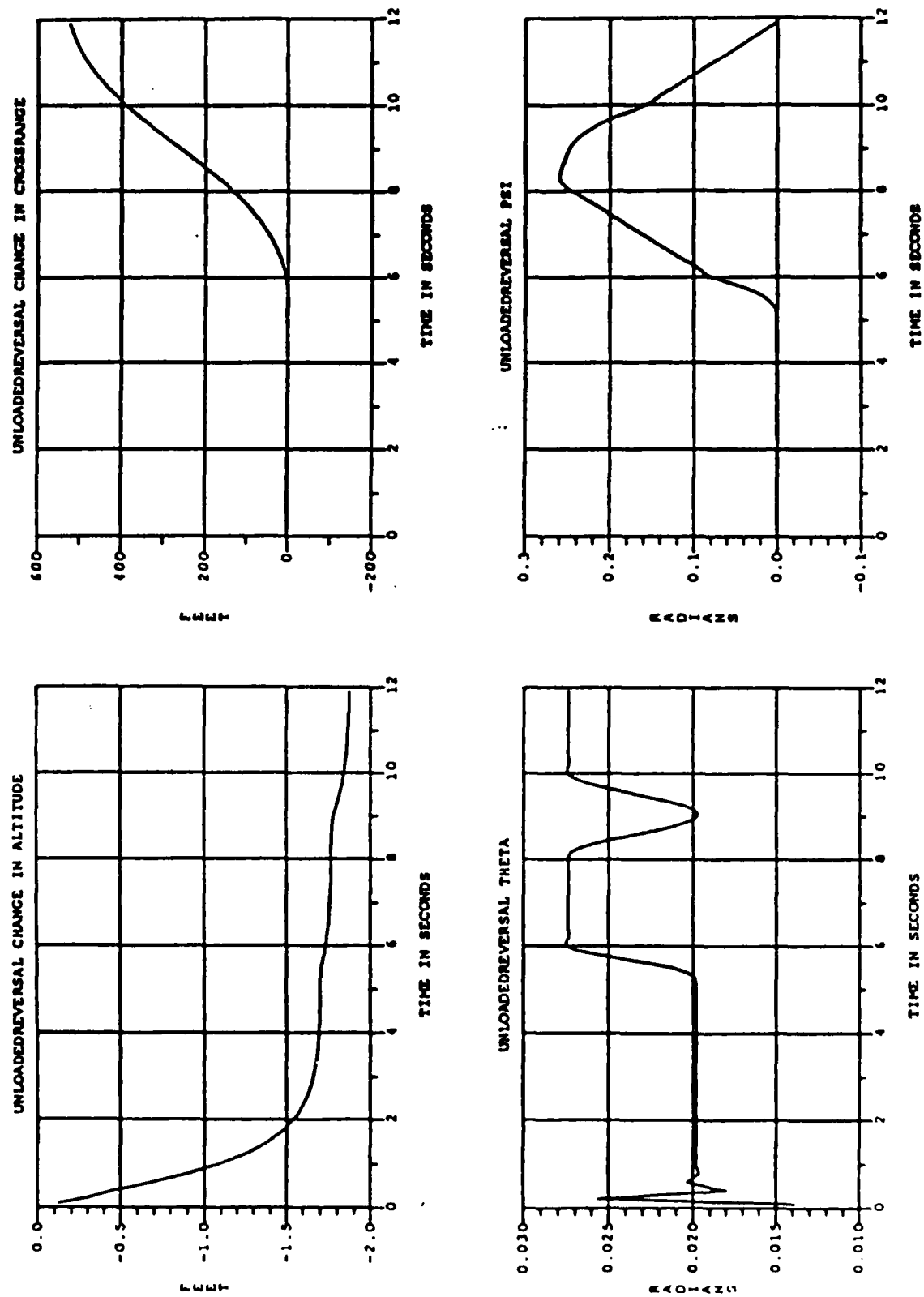


Figure 7.2 Altitude, Crossrange, Theta and Psi During UNLOADED ROLL REVERSAL

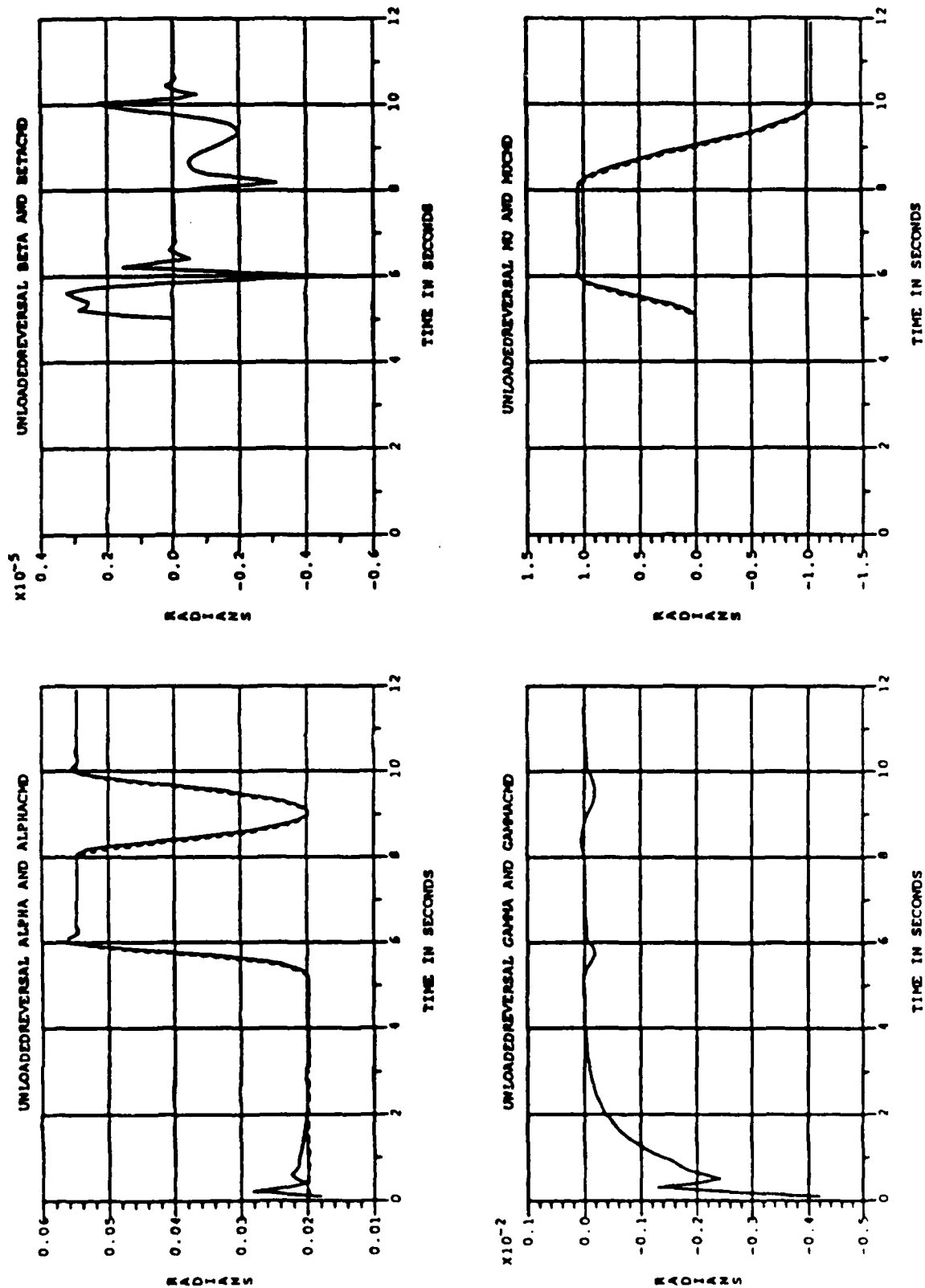


Figure 7.3 Commands and Command Responses During UNLOADED ROLL REVERSAL

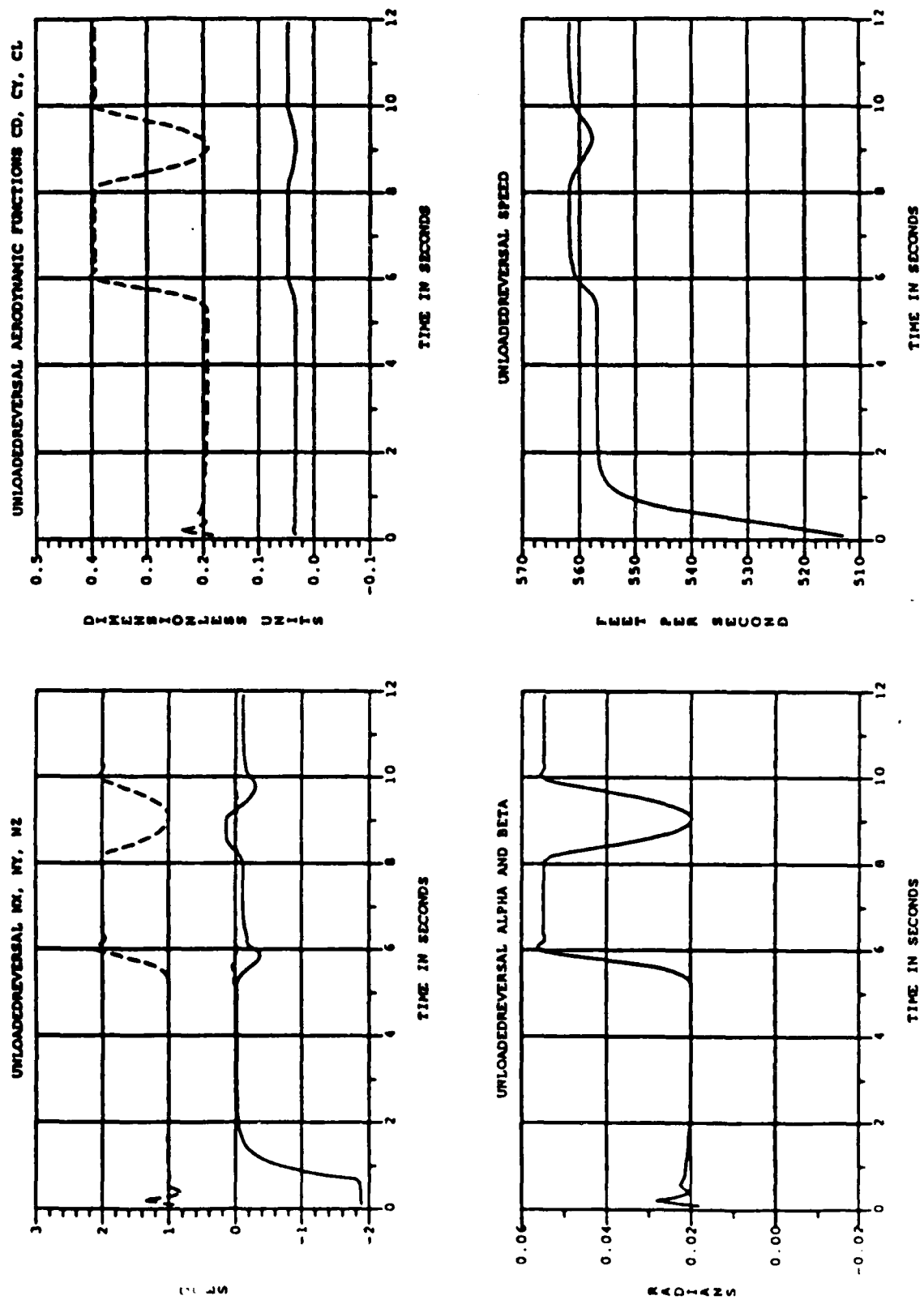


Figure 7.4 Accelerations, Aero Forces, Alpha, Beta and Speed During UNLOADED ROLL REVERSAL

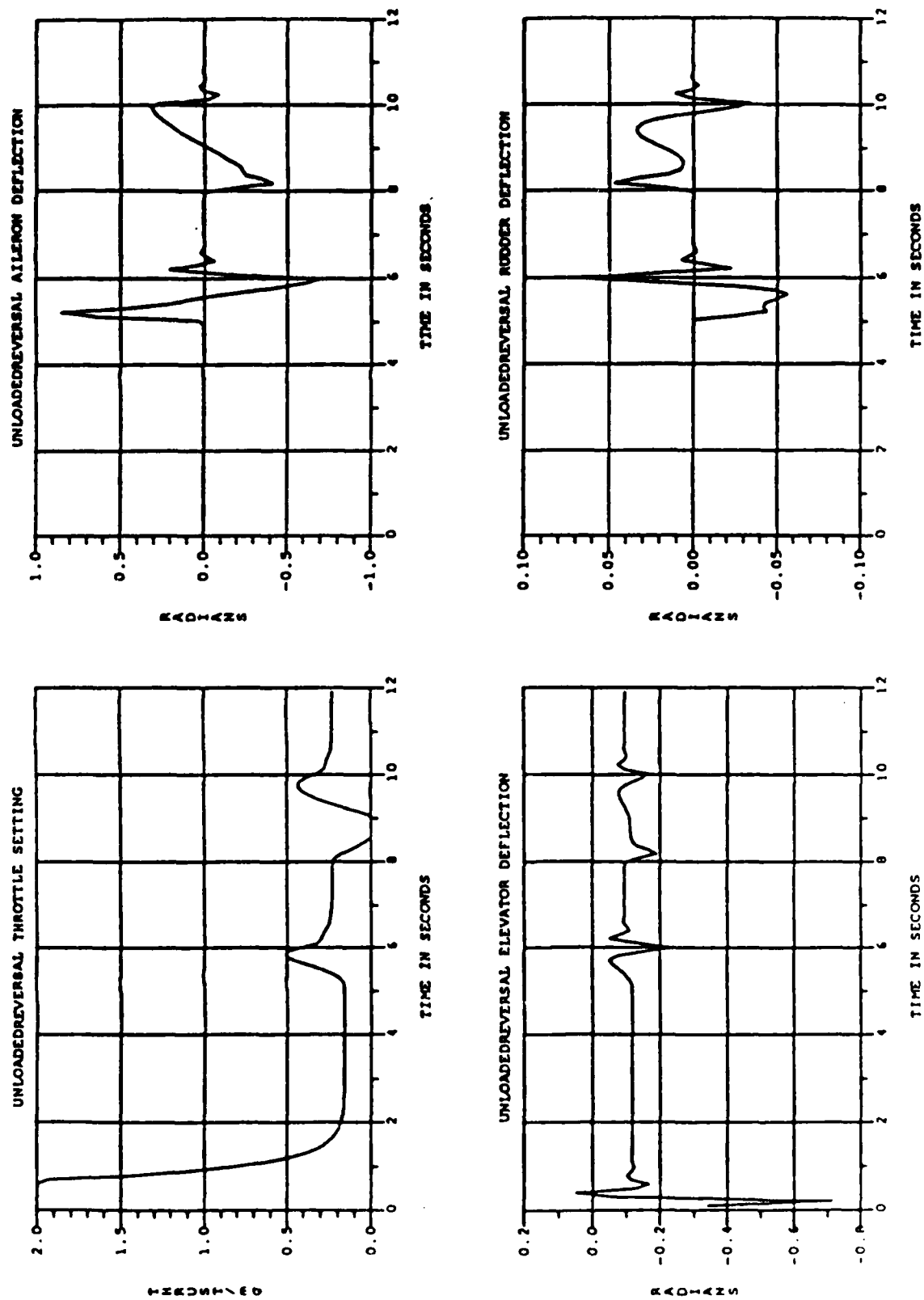


Figure 7.5 Control Activity During UNLOADED ROLL REVERSAL

0.5 g during the initial loading, then moves back to a slower setting when the banked turn is established. During the reversal it moves down to 0.0, then back to 0.4 g during the loading in the opposite direction. The variation of α during the maneuver changes the drag (see Figure 7.4), so some thrust activity is required if speed is to be kept nearly constant. Also, the thrust command was varied by the controller to generate small corrections to the speed necessary because of the direct force contributions of the surfaces, which we neglected when we generated the command profile for α . The controller also had to compensate for the fact that the α -command profile was generated by an approximation to the lift curve. The magnitude and rate of the throttle activity during this maneuver might be considered too large - if so, a different command profile for $\alpha, \beta, \gamma, \mu$ could be chosen or a different inverter used for controlling the aircraft. The throttle was simply doing what it had to do to allow tracking of the $\alpha, \beta, \gamma, \mu$ command profiles in Figure 7.3.

Figures 7.6 and 7.7 depict the eight parameters a_{ij}, b_{ij} associated with the complementary dynamics. From them, we computed that at each time during the maneuver there was a unique physical equilibrium value in the complementary $V, \dot{\Psi}$ phase-plane. Two of the plots in Figure 7.8 show the two eigenvalues at that equilibrium (both are always real for this maneuver - note that the equilibrium is always stable), and the other two plots compare the simulated values of $\dot{\Psi}$ and V^2 with the equilibrium values. The eigenvalues could be used, as discussed in section 5.5, to compute a settling time for the $V, \dot{\Psi}$ functions to their equilibrium values once the states $\alpha, \beta, \Theta, \Phi$ have stabilized. We have not performed this computation yet, but it would not be difficult (we have not coded-up the algorithm on the computer yet). During the transients $\dot{\Psi}$ moves away from the equilibrium values by a significant factor (about 100 percent error), but then moves back to equilibrium very quickly when rolling stops. V^2 , on the other hand, tracks the equilibrium value very closely (after the initial transient).

For this first maneuver, the $\alpha, \beta, \gamma, \mu$ dynamic inverter looks remarkably good.

The second maneuver differed from the first only in the goals for the normal acceleration during the reversal. We called it LOADEDREVERSAL. The objective was to keep $N_z \geq 2$ after the first 60 degree bank. Again, we chose to use the $\alpha, \beta, \gamma, \mu$ controller. The command profiles for β and μ remained the same as in the unloaded case, we changed the command profiles for α and γ . Our new α command profile was the same as the old one until $t=8$ seconds, when the reversal began. To keep N_z above 2 g during the reversal, we chose to keep the α command constant at $(-0.09 + 2/((2.2)^2))/5.9$ (compare with Figure 7.4) after $t=8$

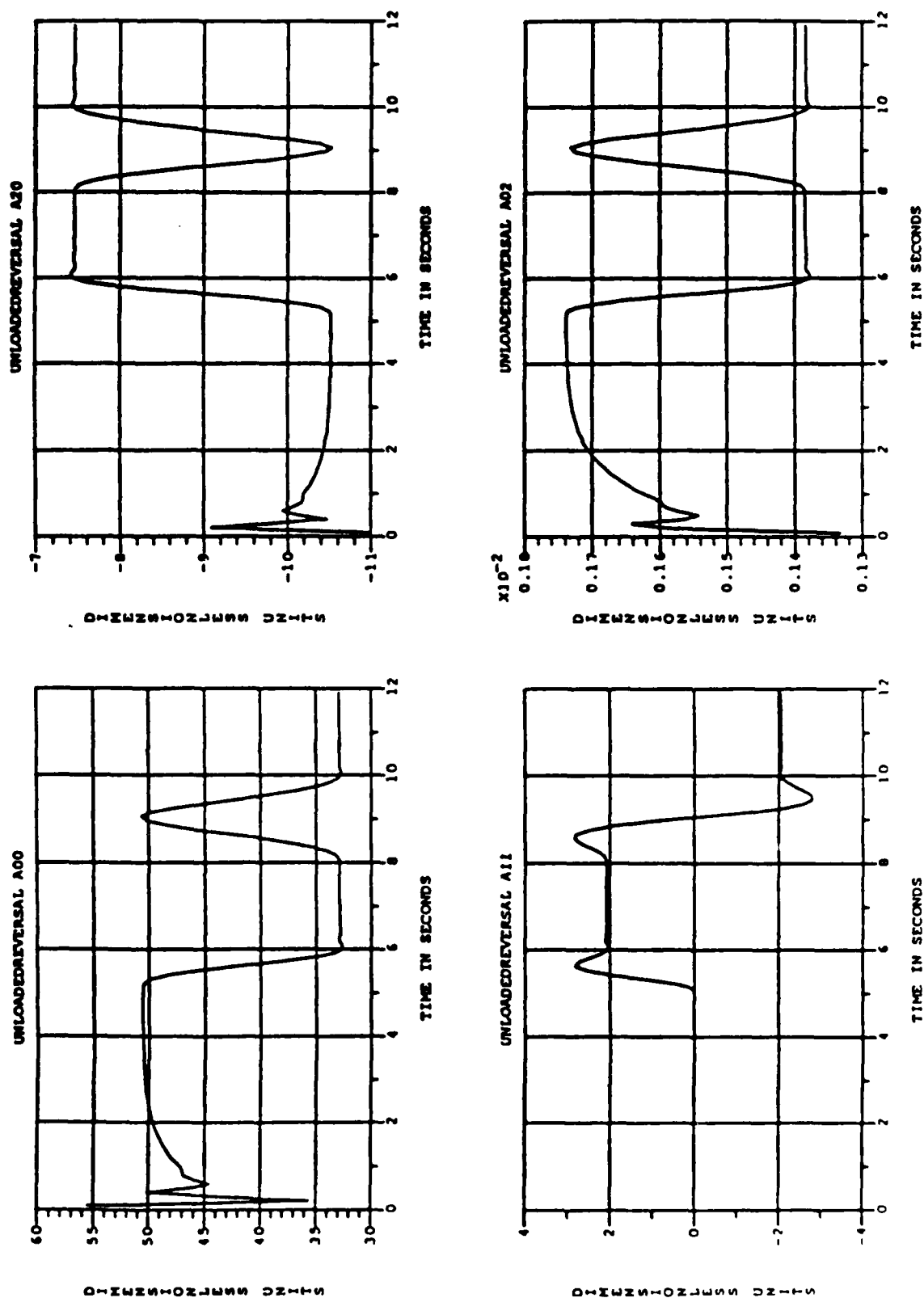


Figure 7.6 A-Parameters During UNLOADEDROLLREVERSAL

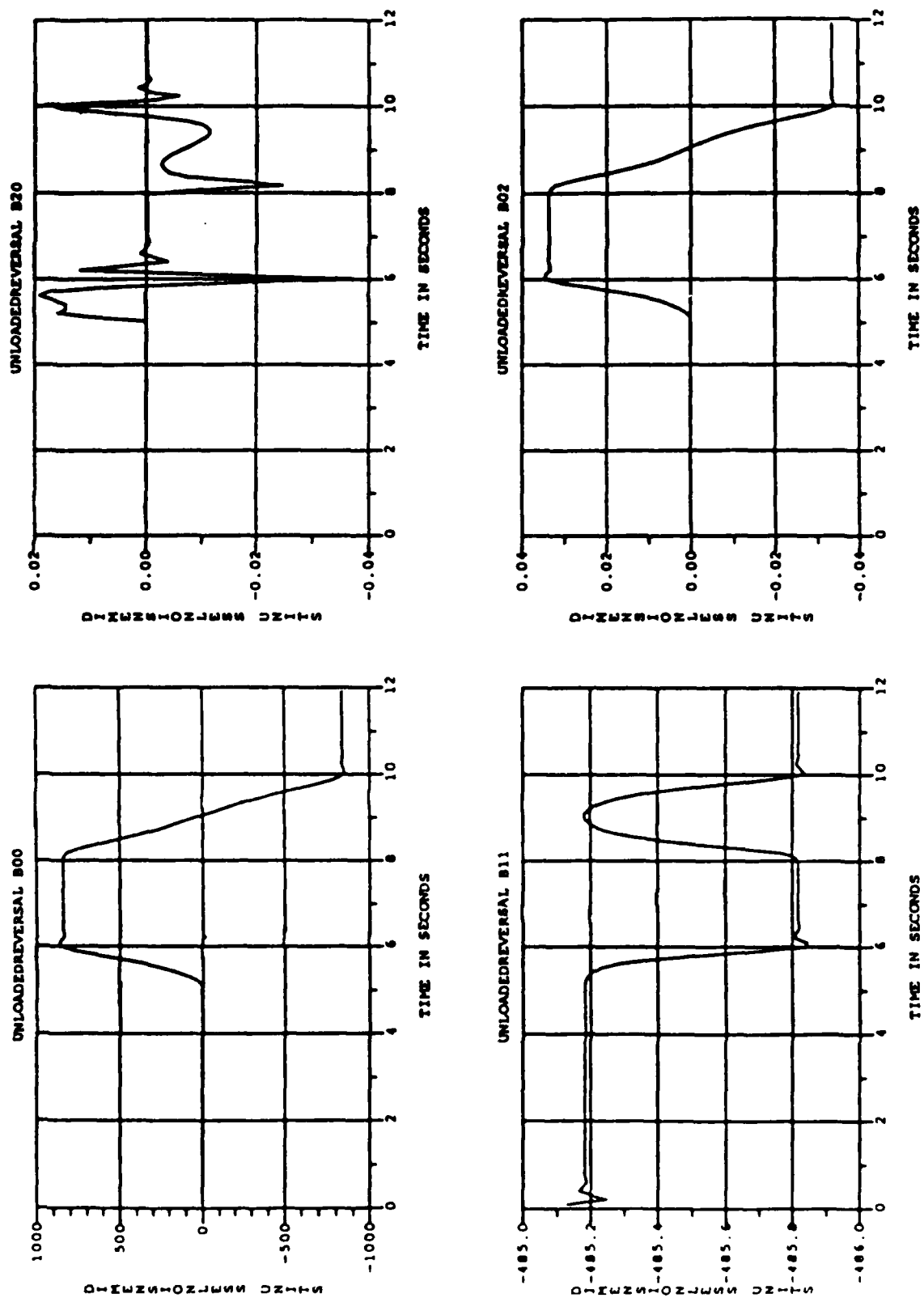


Figure 7.7 B-Parameters During UNLOADED ROLL REVERSAL

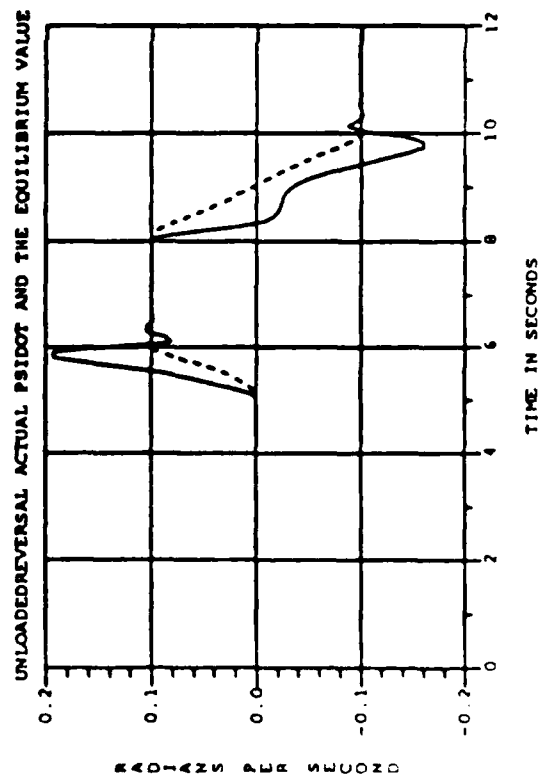
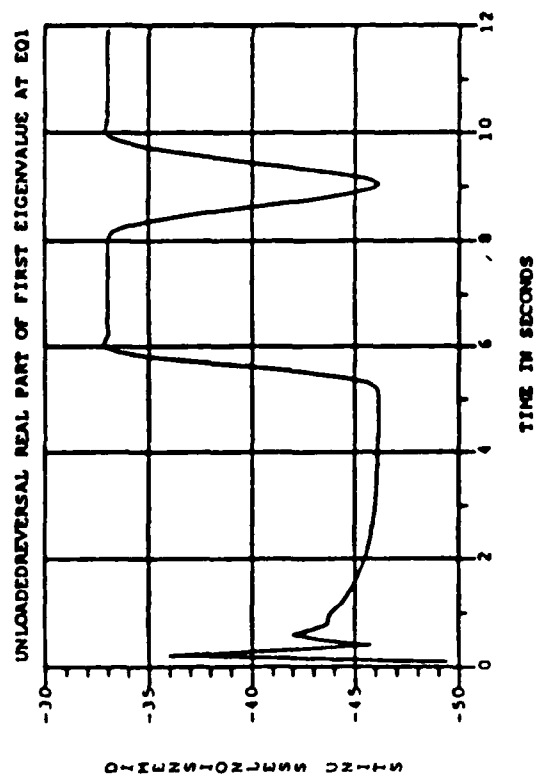
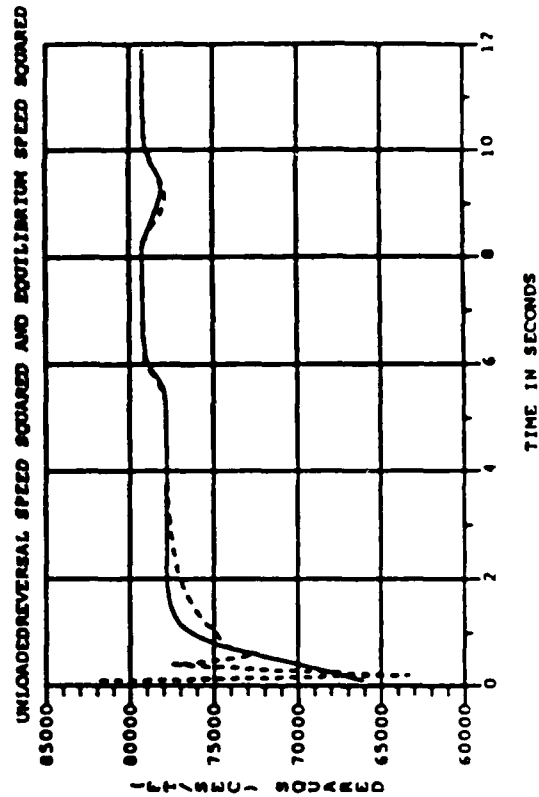
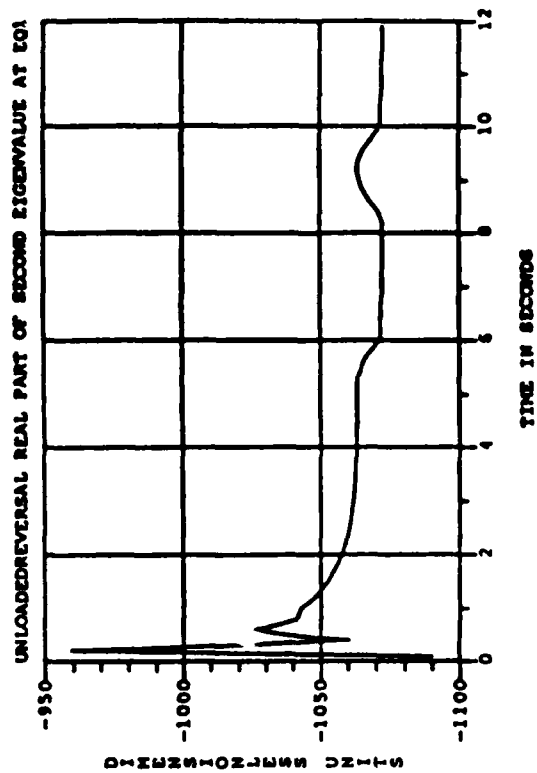


Figure 7.8 Eigenvalues and $\dot{\psi}$, V^2 Comparisons During UNLOADED ROLL REVERSAL

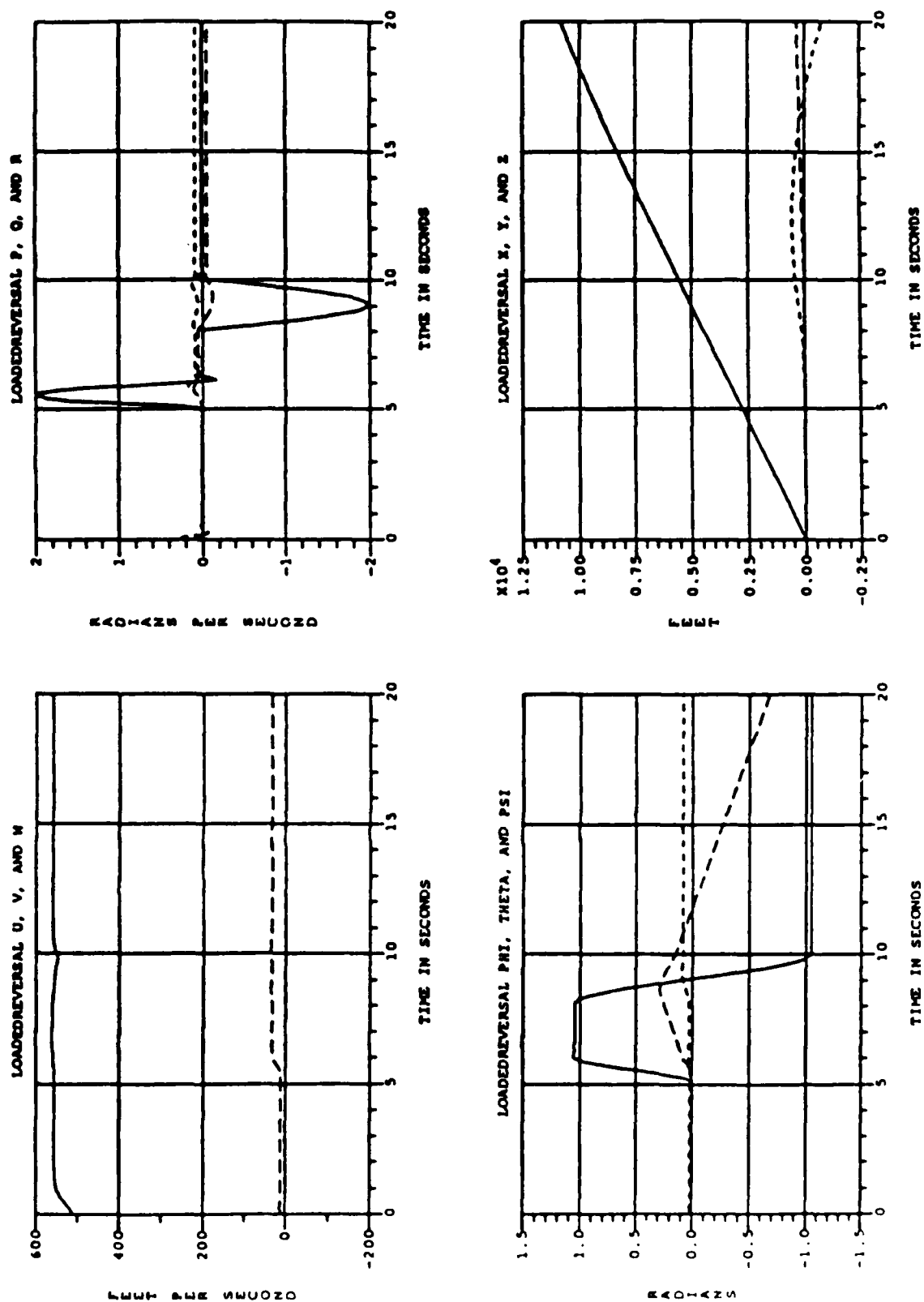


Figure 7.9 States During LOADED REVERSAL

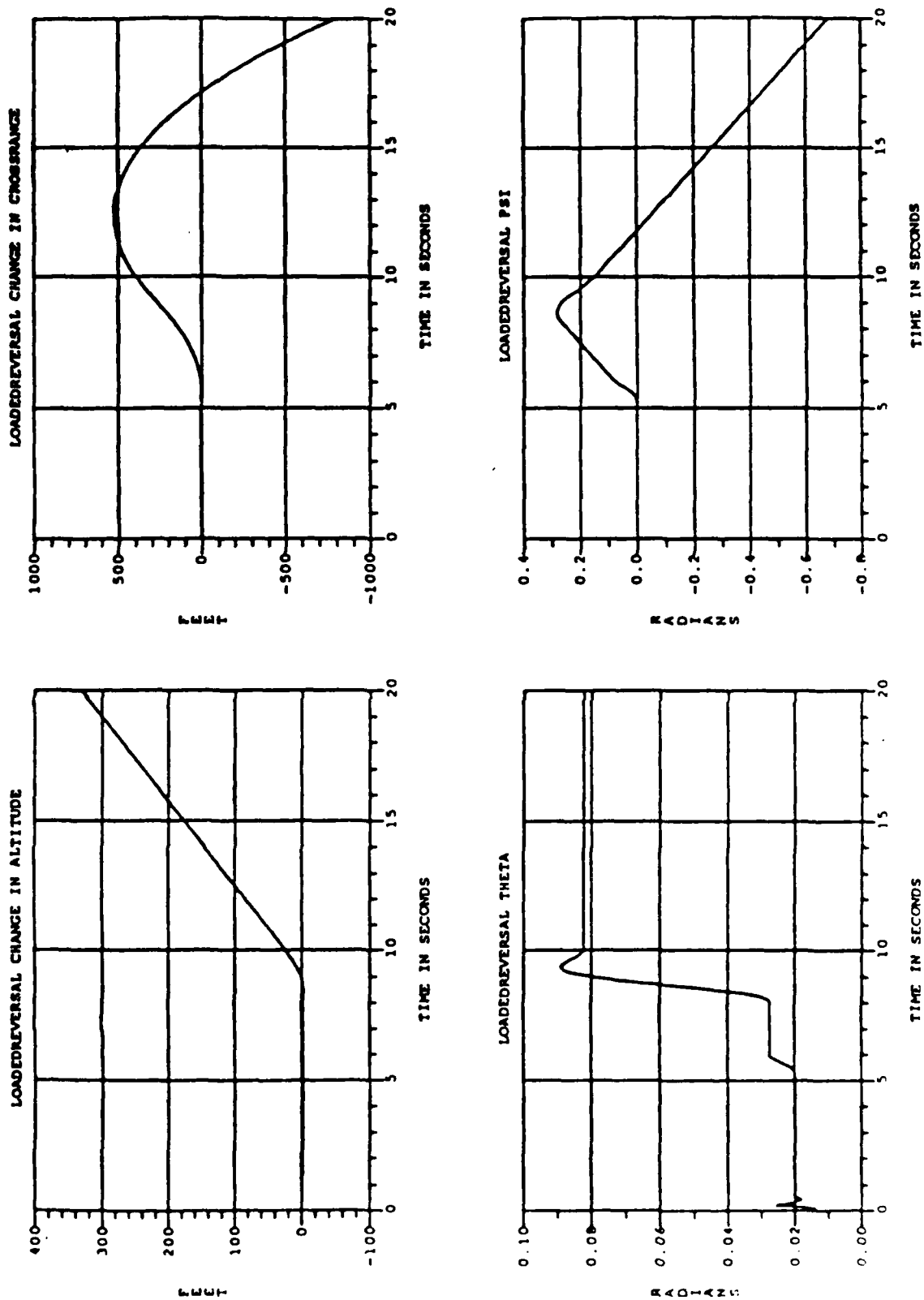


Figure 7.10 Altitude, Crossrange, Theta and Psi During LOADED REVERSAL

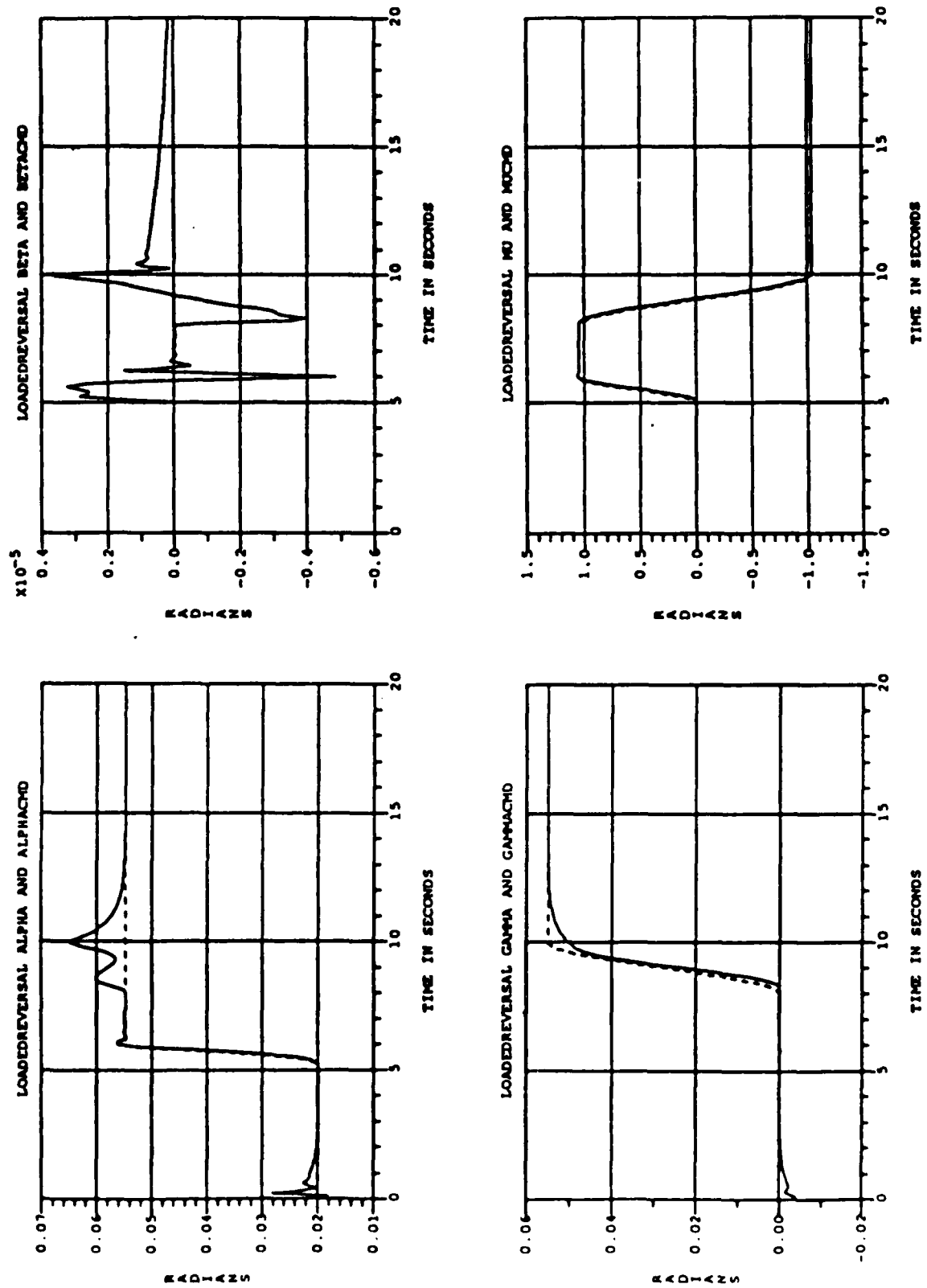


Figure 7.11 Commands and Command Responses During LOADEDREVERSAL

until the end of the simulation. The γ command was not easy to choose: we would have liked to keep $\gamma = 0$ throughout, but it is not physically possible to keep both β and γ at 0 while requiring that N_z be at least 2 g during the reversal. So, we decided to ask for a small amount of γ increase throughout the reversal, the plot for the command profile is shown in Figure 7.11.

The plots for U,V,W and P,Q,R for LOADEDREVERSAL are similar to those for UNLOADEDREVERSAL, except for the value of W during the reversal (note: they are plotted on different timescales). The Euler-angle plots and inertial position plots are notably different, however. As is shown in Figure 7.10, the LOADEDREVERSAL involves an increase in altitude at a rate of about 30 feet/second (as compared with 0 in Figure 7.2) and a final value of θ that is 4 times as large. Figure 7.11 shows that α was the main problem for this maneuver (all the other variables tracked their commands fairly well). The plots in Figure 7.12 show that N_z did remain at least 2 g after the initial bank - the interesting plot is the speed change.

The cause of the ramp deceleration can be seen in Figure 7.13, where it is shown that the throttle turned off while the reversal was in progress. The reason for the throttle shut down is revealed in Figure 7.16. Note the plot showing the actual speed squared as compared with the equilibrium speed squared at the corresponding $\alpha, \beta, \theta, \phi$ points along the trajectory. The problem here is that the $\alpha, \beta, \theta, \phi$ states are very difficult to control independently near $\alpha = 0$. The throttle saturated trying to make the vehicle slow to its equilibrium speed, but there was not nearly enough command authority to reduce the speed.

We conclude that the $\alpha, \beta, \gamma, \mu$ controller was not a good choice for commanding LOADEDREVERSAL -- the failure was not due to the vehicle or its flying qualities. It is worth pointing out that the $\alpha, \beta, \theta, \phi$ controller was stable at every point along the maneuver, as is shown by the plots of the eigenvalues (always negative) in Figure 7.16. This is a case where there is a unique physical equilibrium at every time, but control saturation prevented the inversion from working as it should.

One might wonder if we tried to bring γ back down to 0 after the reversal was completed. The answer is that we did try - the results are shown in Figures 7.17 through 7.24. Note the extreme droop in N_z as soon as the command for γ decreased. We did try to accommodate a decrease in γ by increasing Φ , as can be seen in the plot for μ and MUCMD in

Figure 7.19 but it did not work. The controller was simply not conditioned well enough for this kind of maneuver.

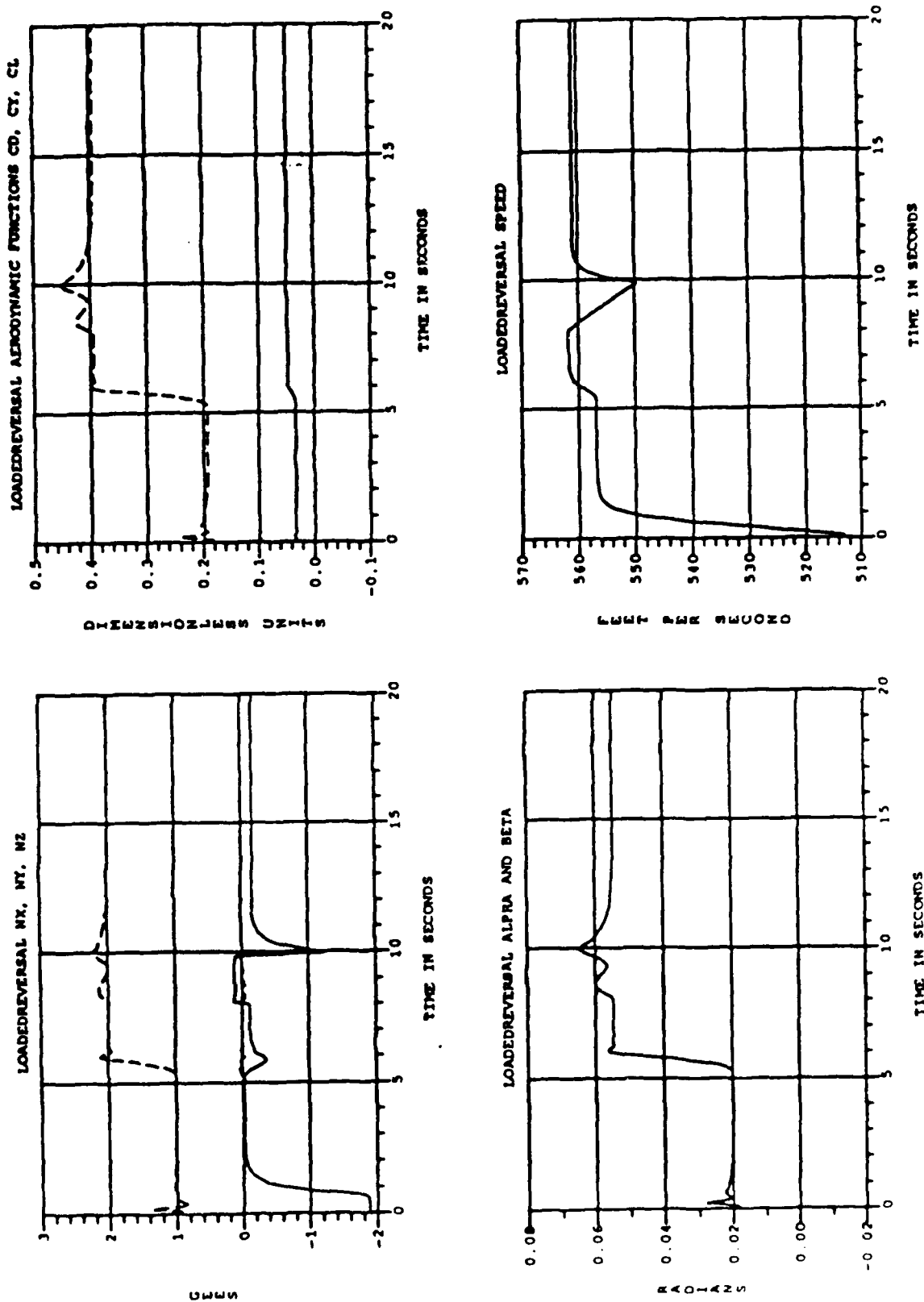


Figure 7.12 Accelerations, Aero Forces, Alpha, Beta and Speed During LOADED REVERSAL

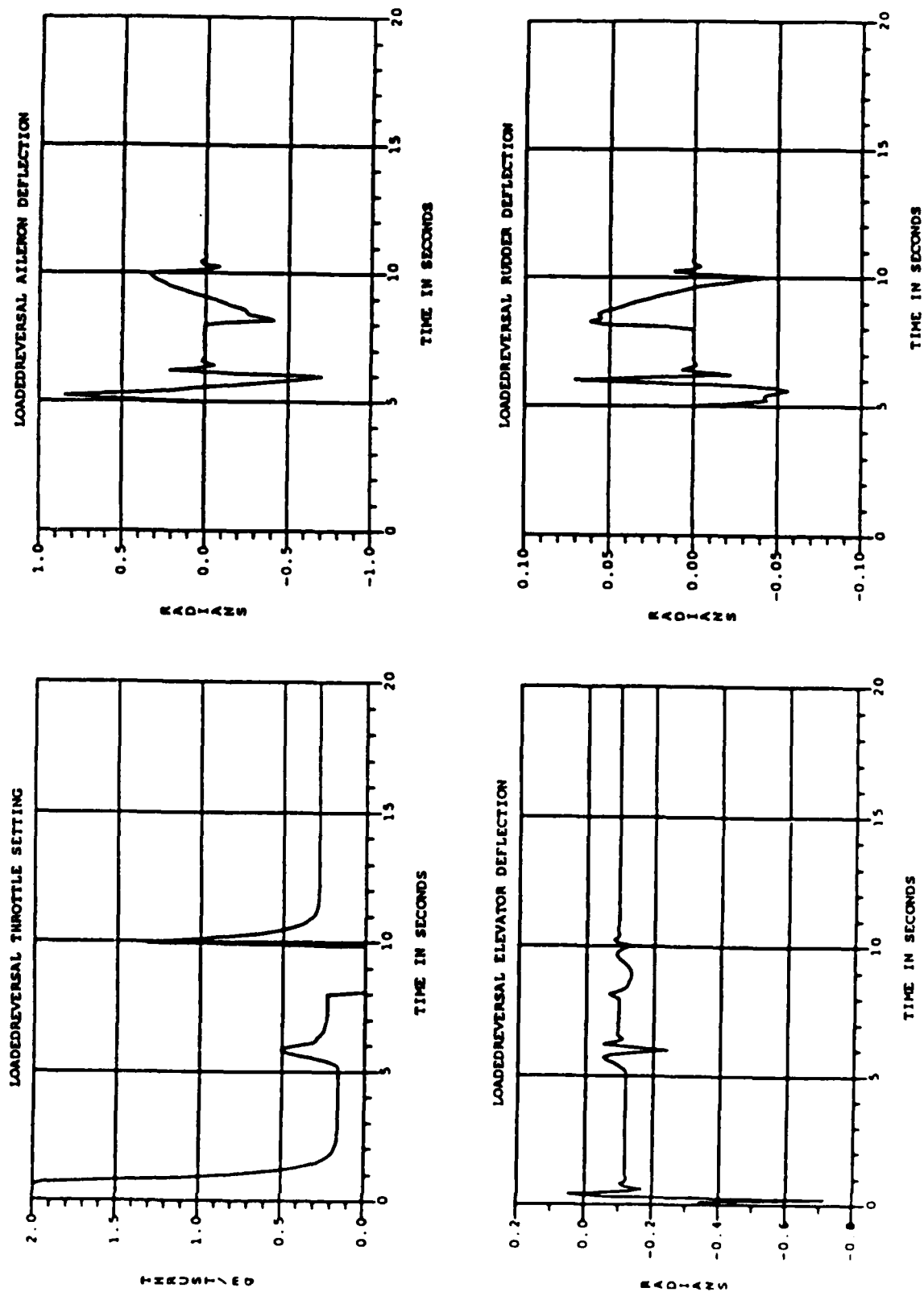


Figure 7.13 Control Activity During LOADED REVERSAL

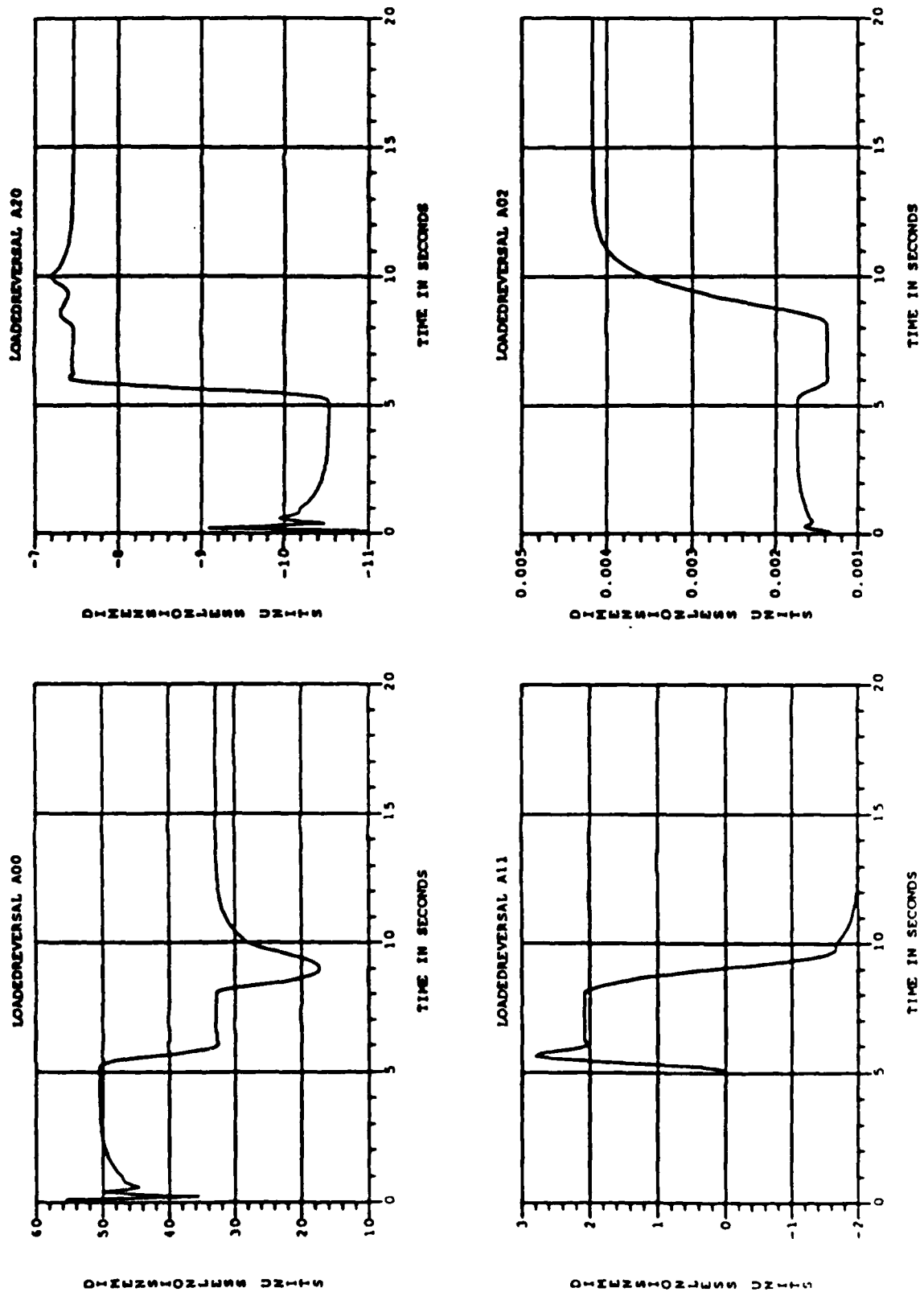


Figure 7.14 A-Parameters During LOADEDREVERSAL

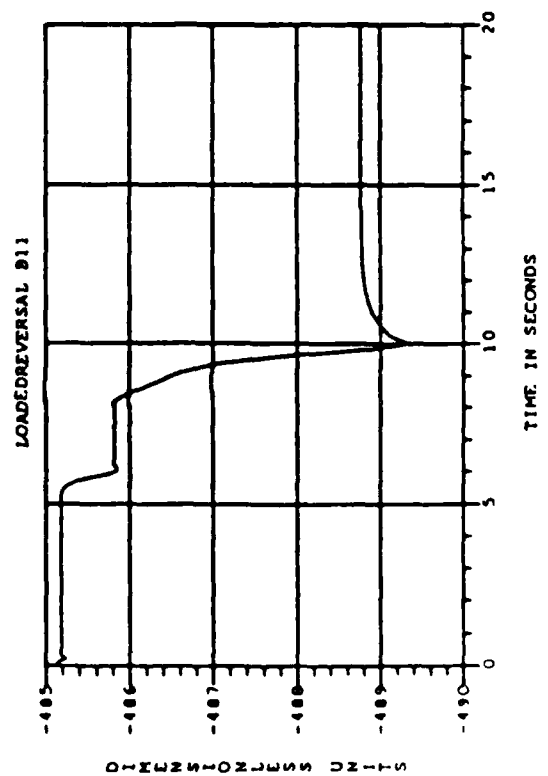
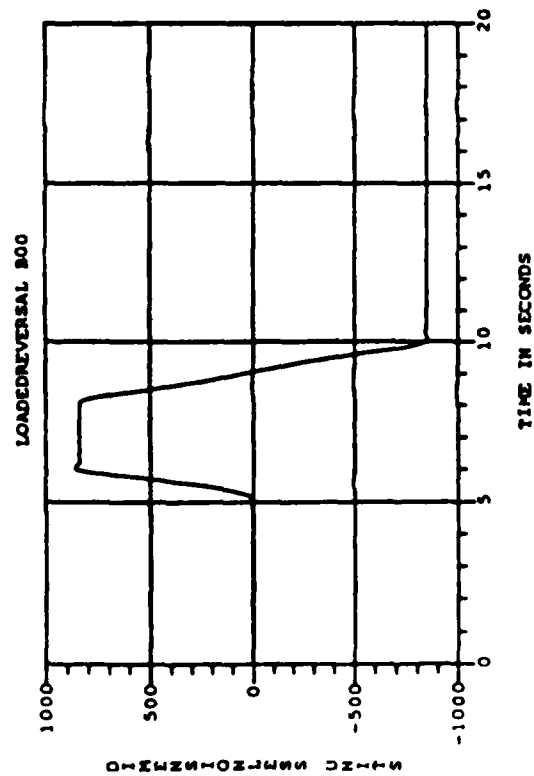
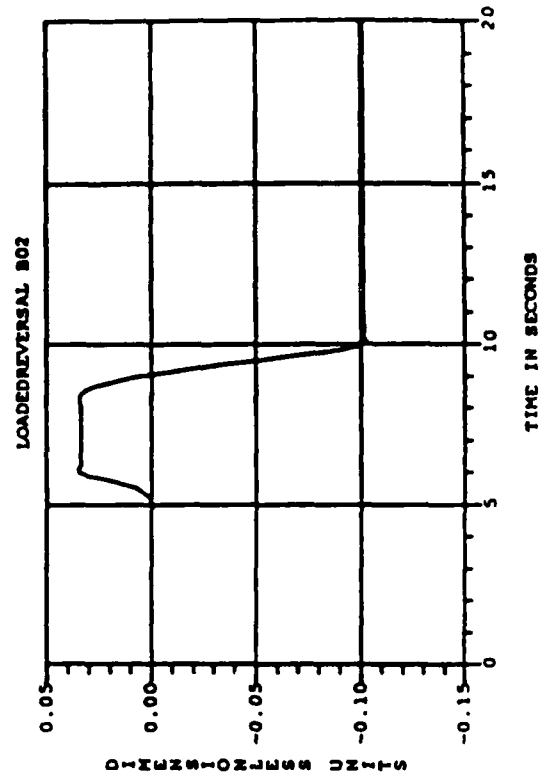
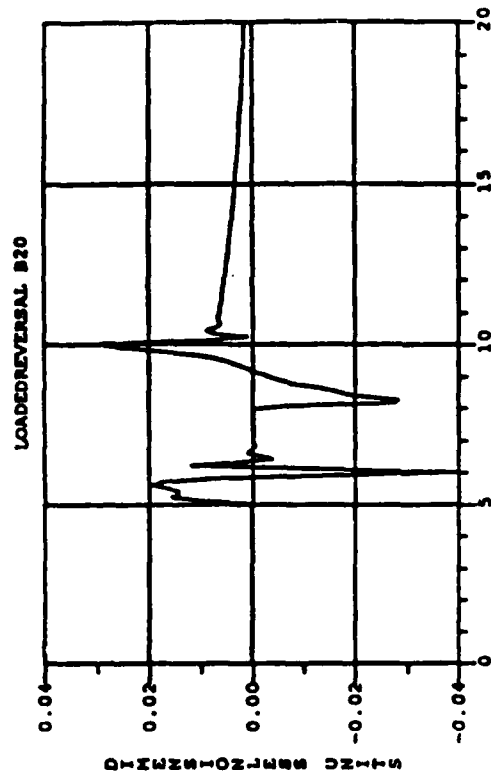


Figure 7.15 B-Parameters During LOADEDREVERSAL

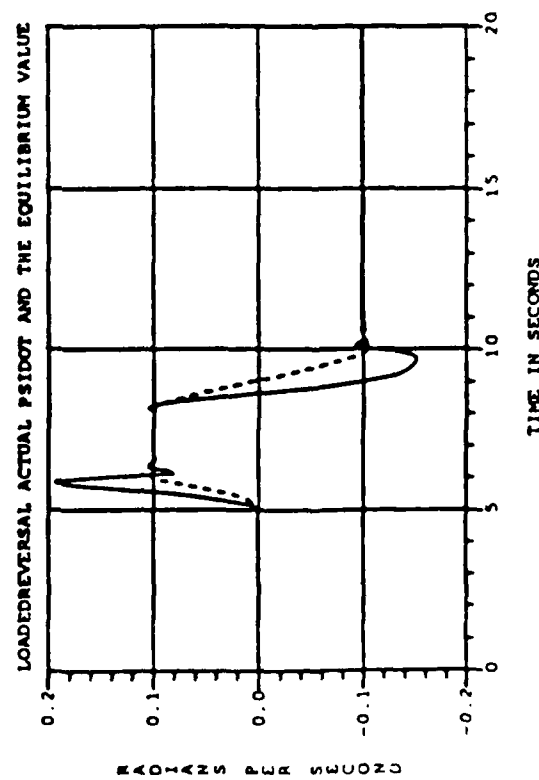
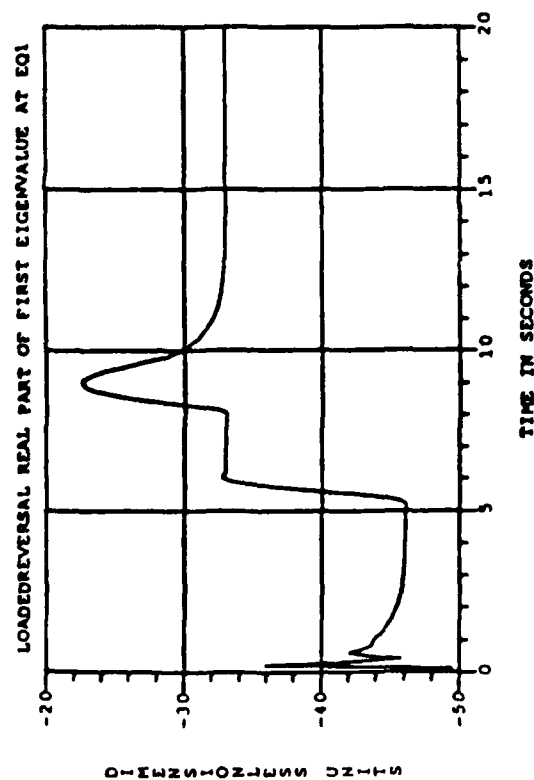
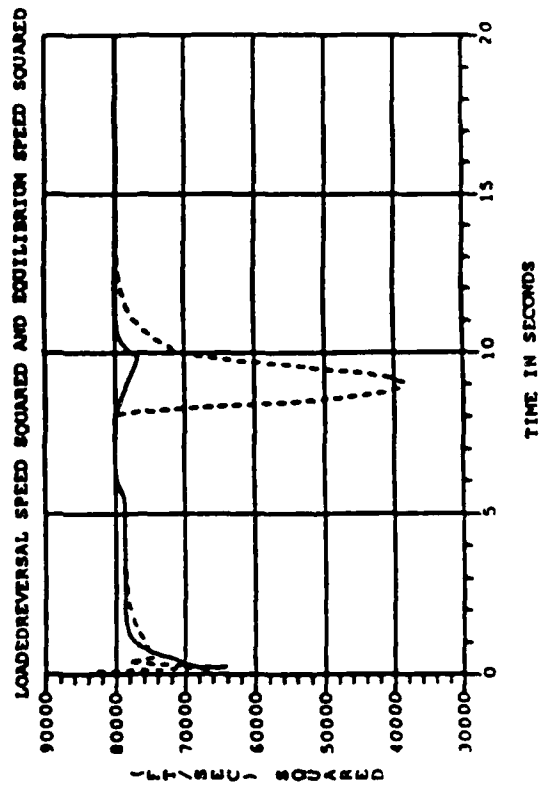
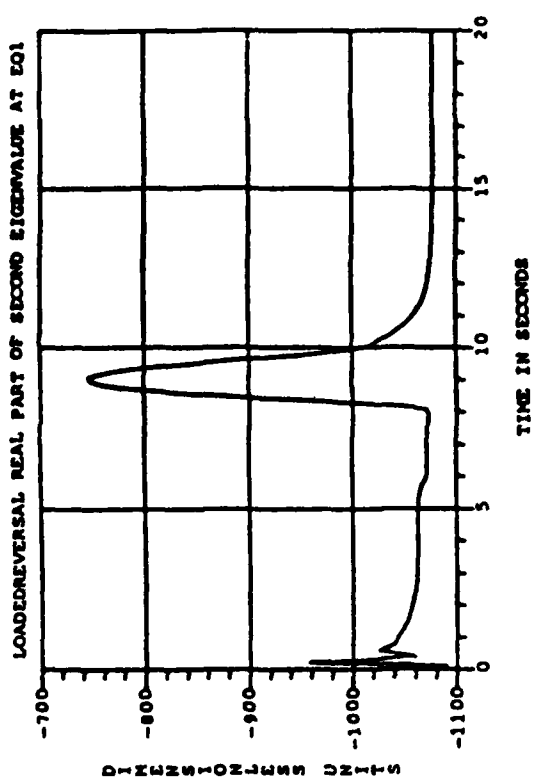


Figure 7.16 Eigenvalues and $\dot{\Psi}$, V^2 Comparisons During LOADEDREVERSAL

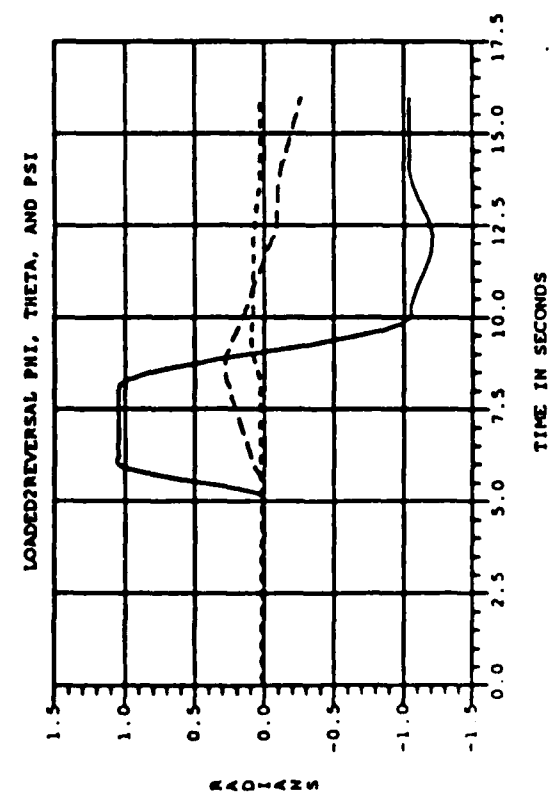
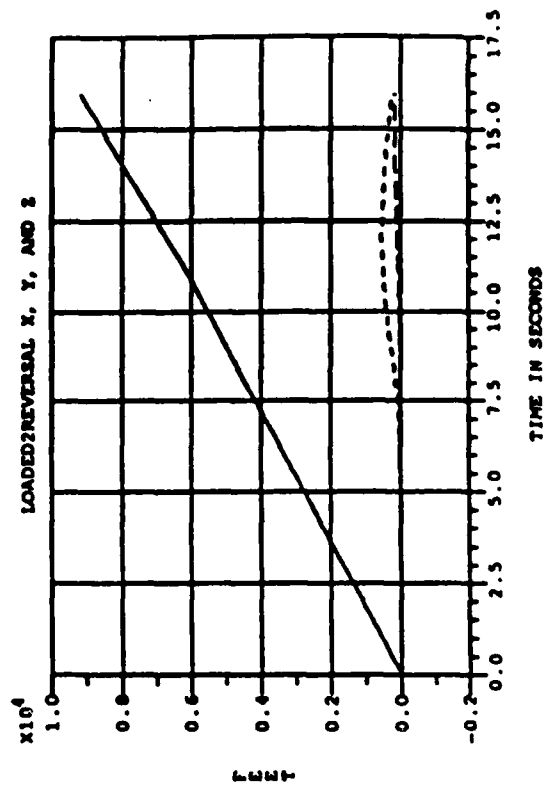
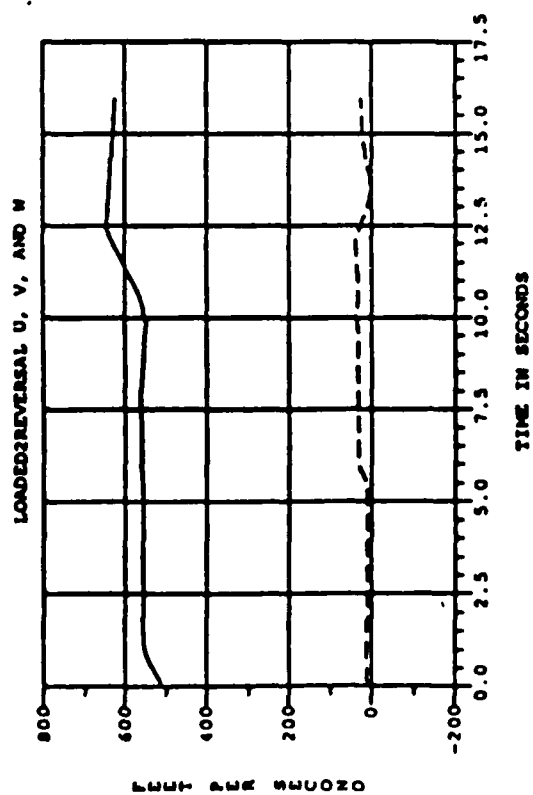
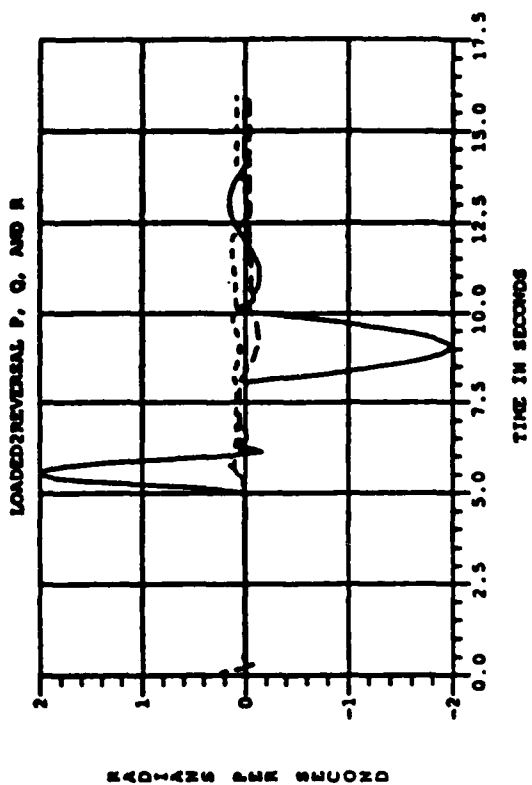


Figure 7.17 States During LOADED2REVERSAL

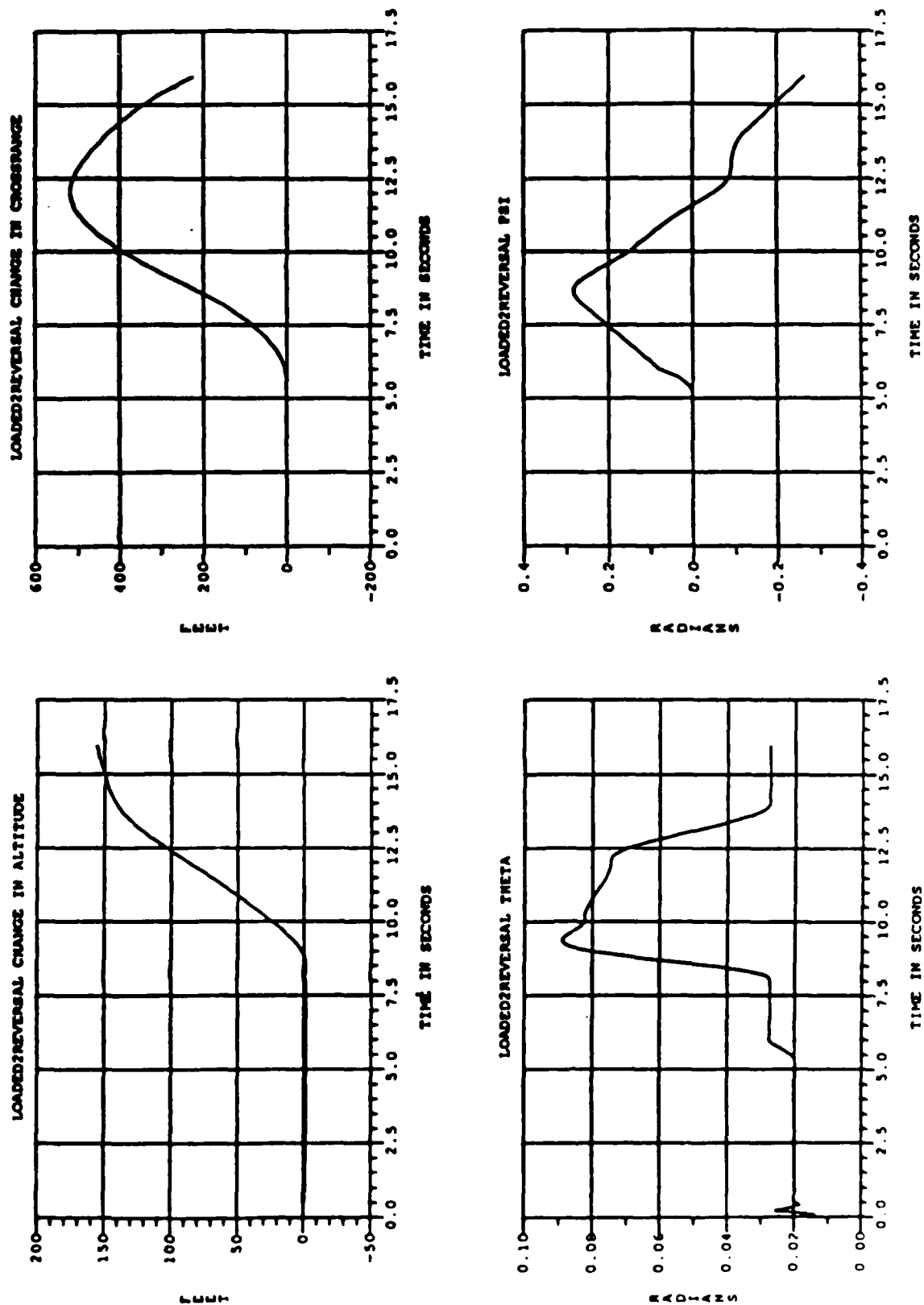


Figure 7.18 Altitude, Crossrange, Theta and Psi During LOADED2REVERSAL

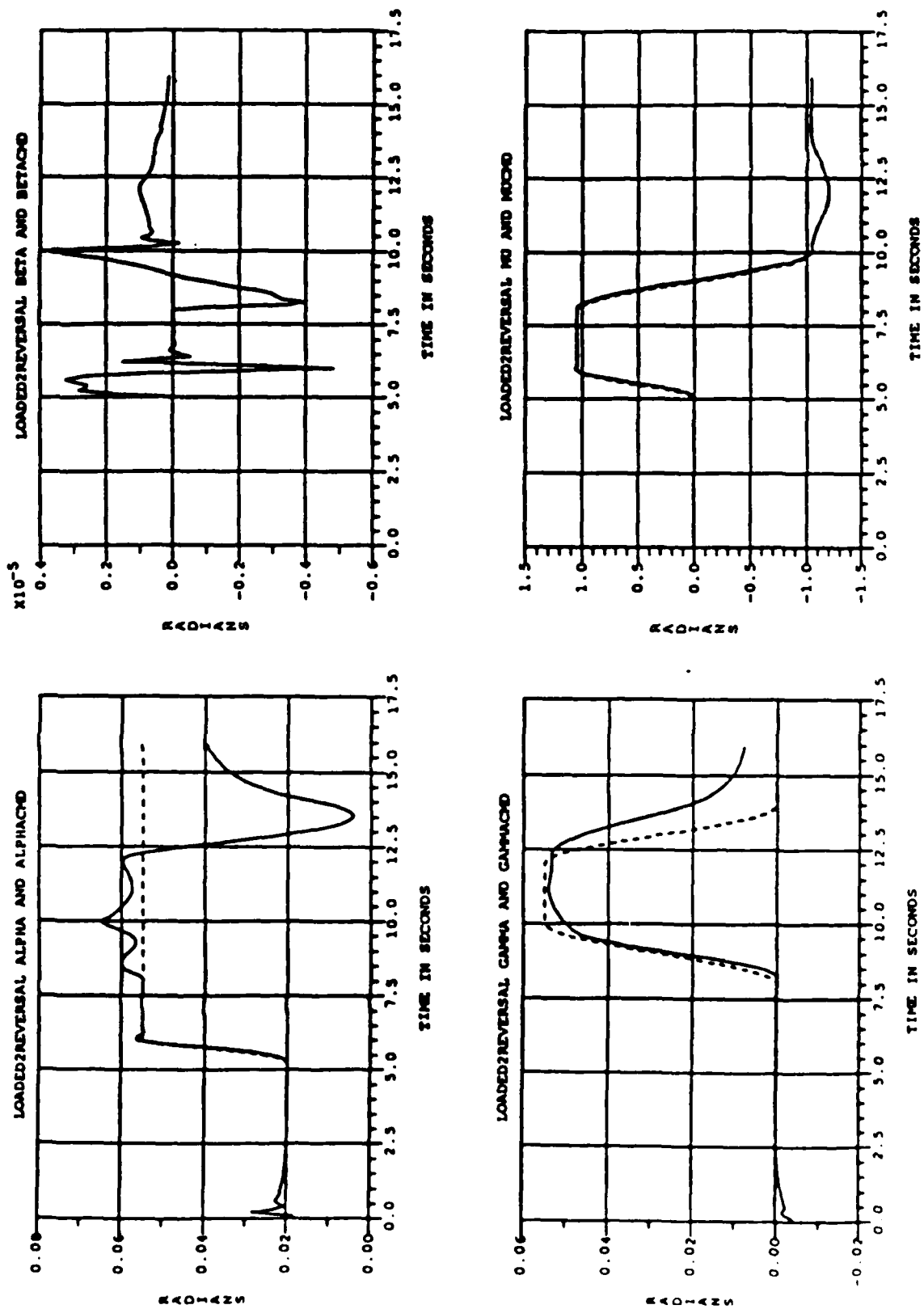


Figure 7.19 Commands and Command Responses During LOADED2REVERSAL

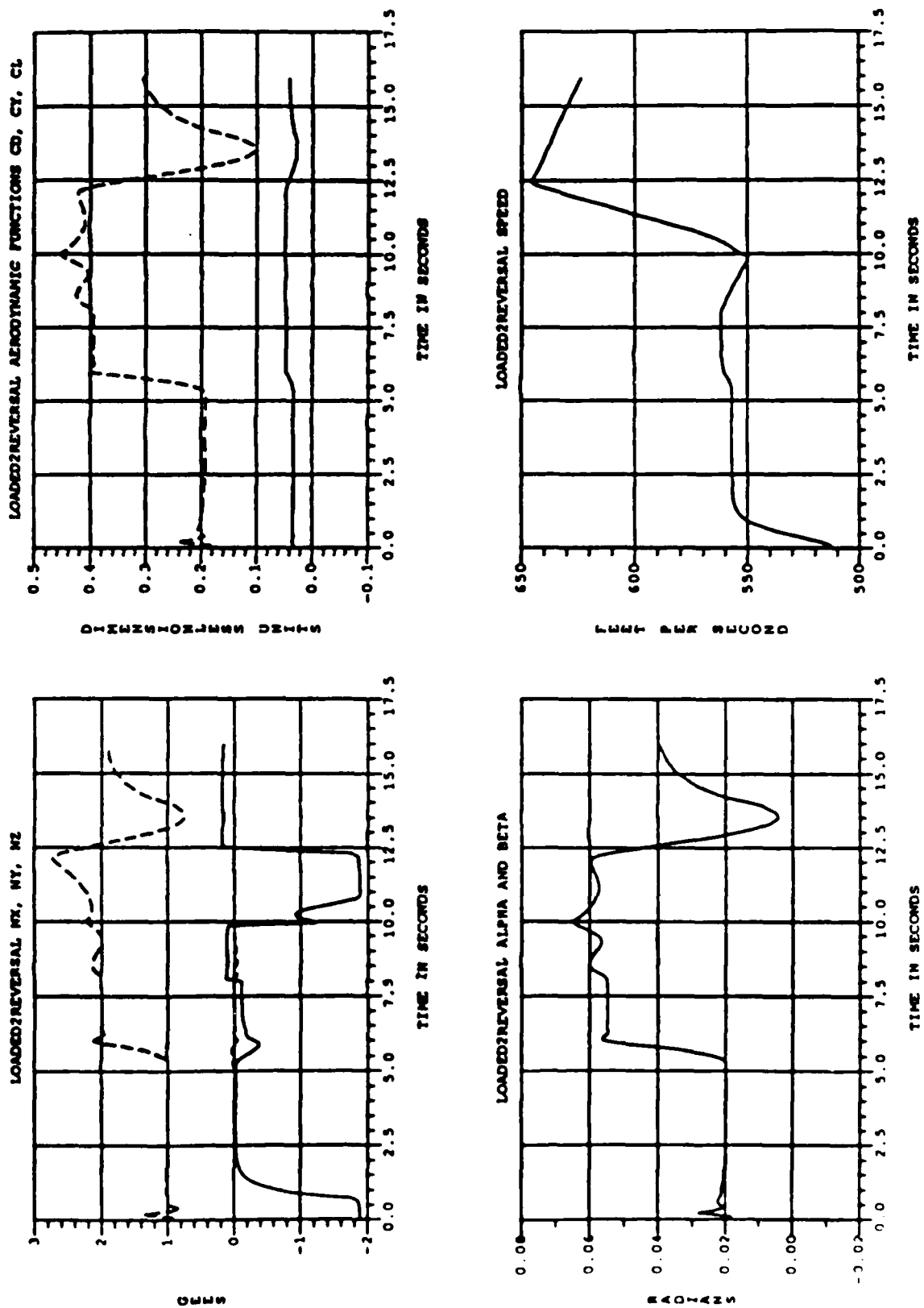


Figure 7.20 Accelerations, Aero Forces, Alpha, Beta and Speed During LOADED 2 REVERSAL

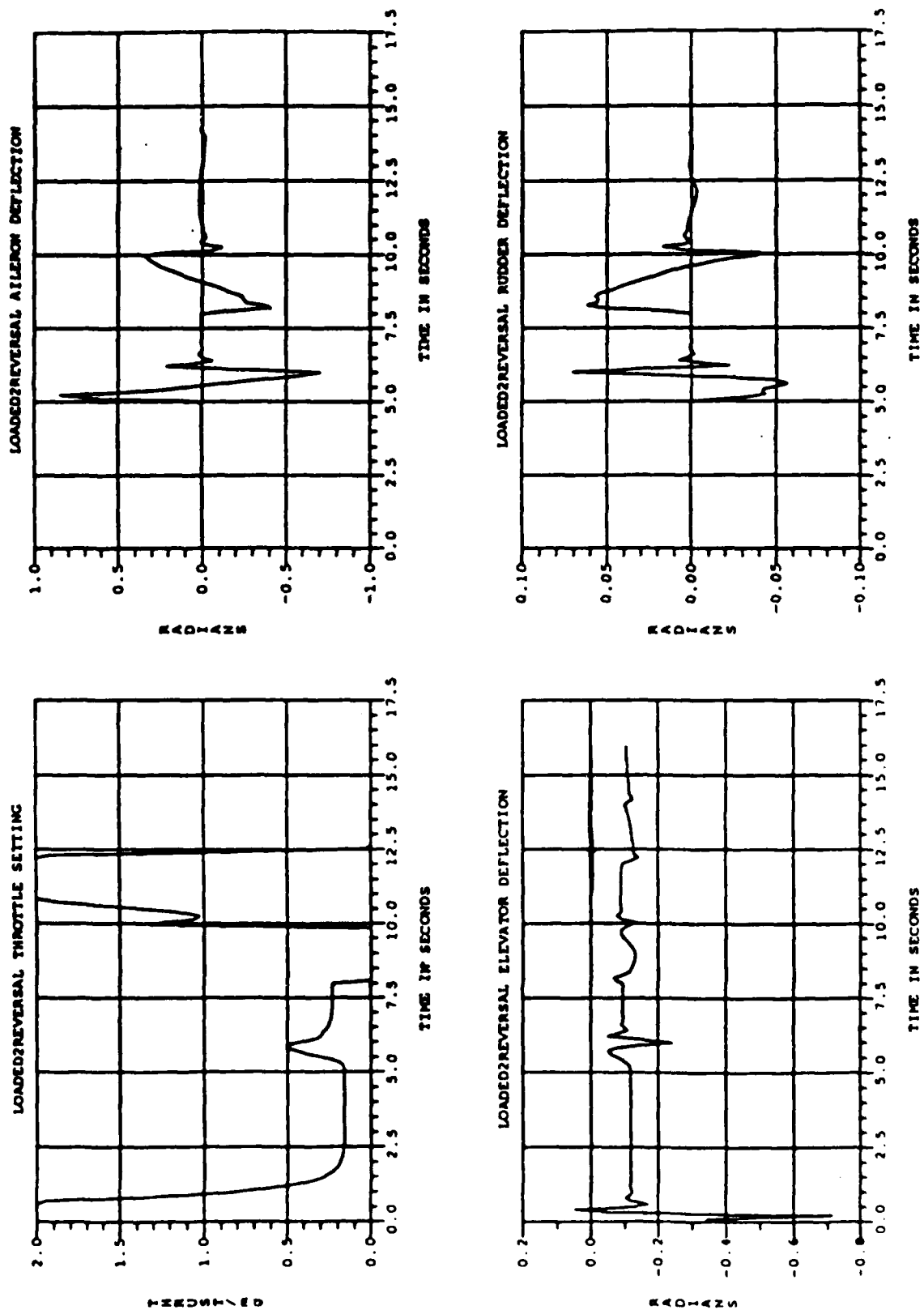


Figure 7.21 Control Activity During LOADED2REVERSAL

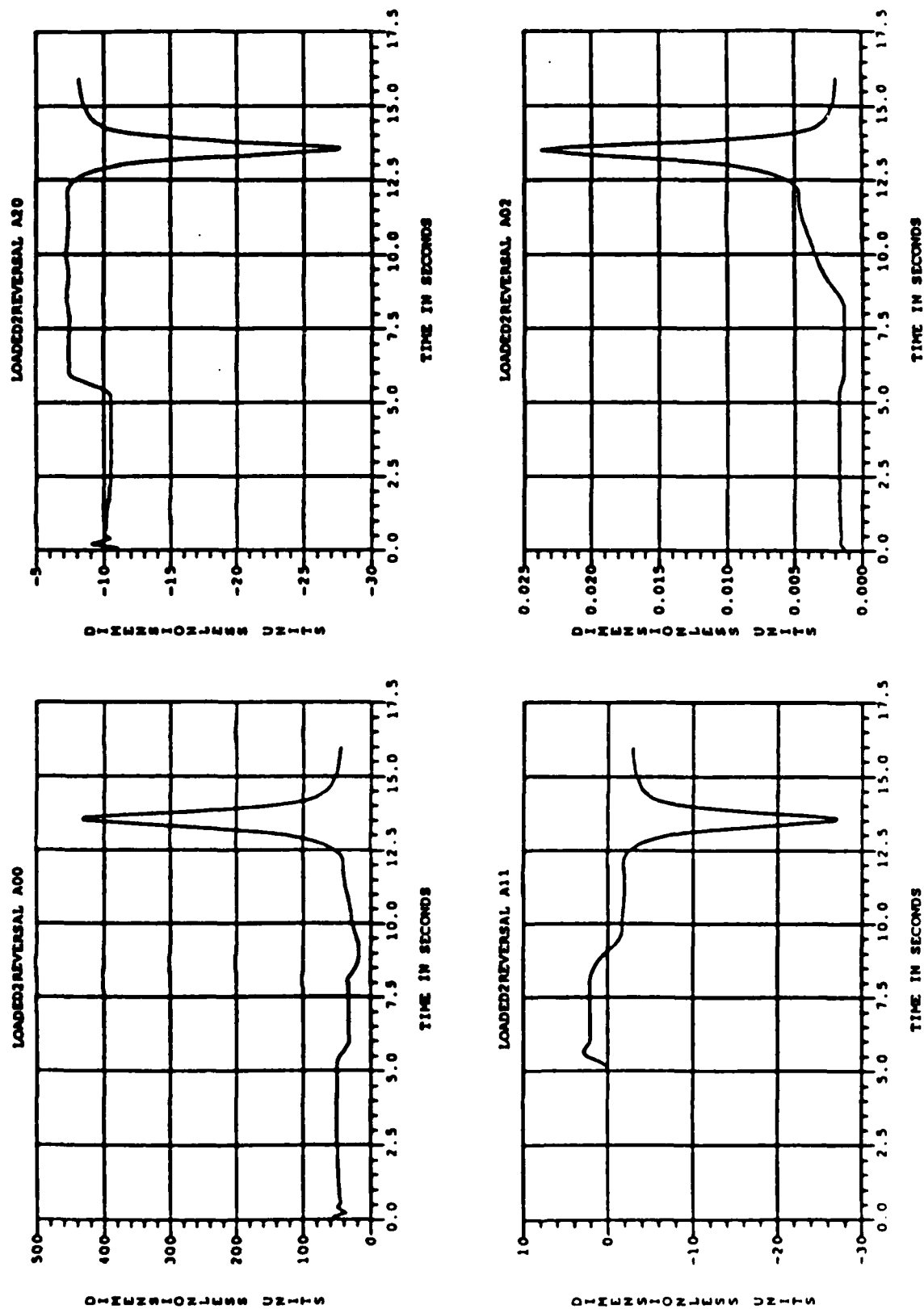


Figure 7.22 A-Parameters During LOADED2REVERSAL

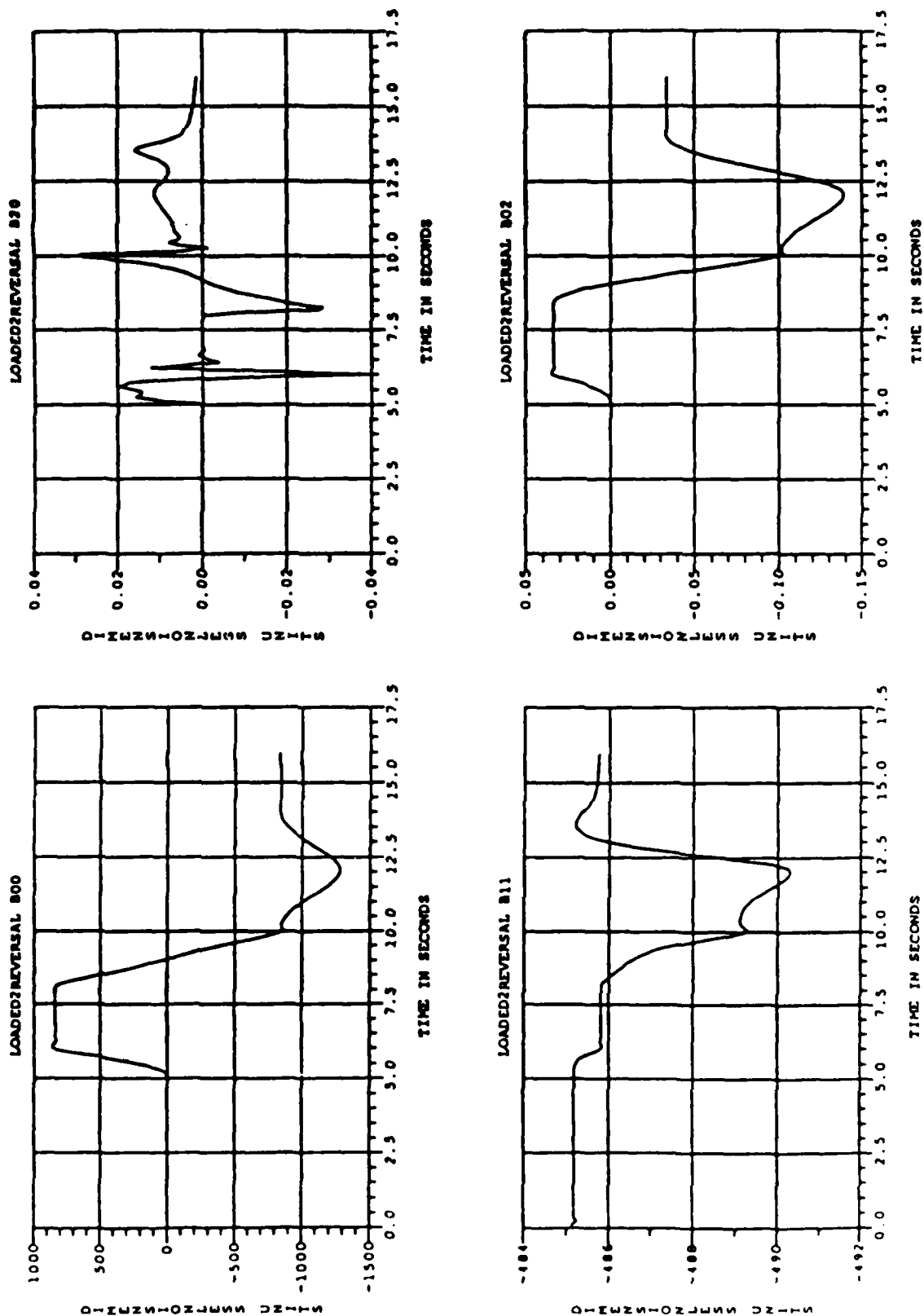


Figure 7.23 B-Parameters During LOADED2REVERSAL

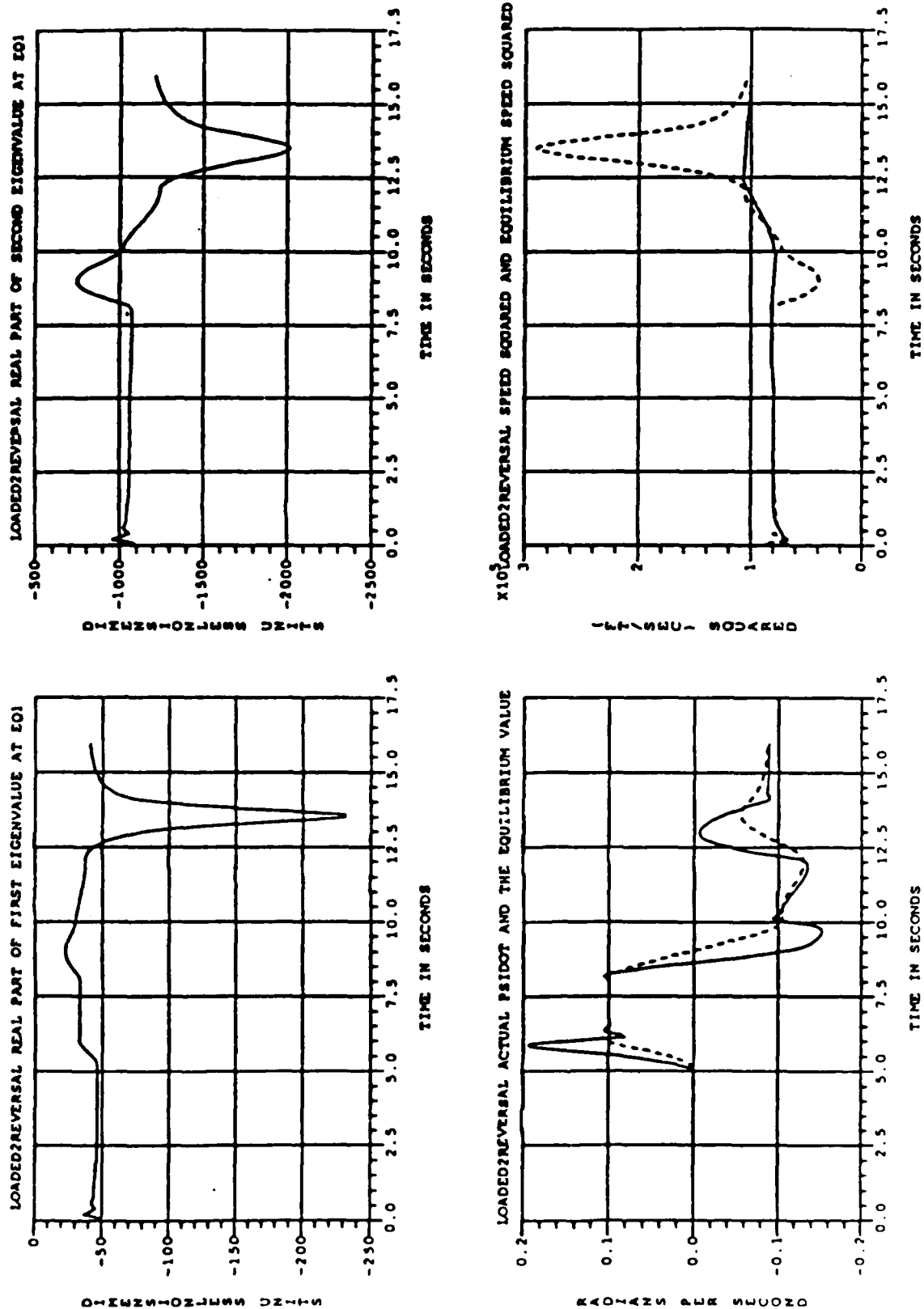


Figure 7.24 Eigenvalues and $\dot{\psi}$, V^2 Comparisons During LOADED2REVERSAL

7.2 BARRELROLL

The maneuver BARRELROLL was the first trajectory generated by the coordinated-flight U,P,Q,R inversion controller described in section 6. The simulation data for this maneuver are shown in Figures 7.25 through 7.32. We chose the command profiles for U, P, and Q shown in Figure 7.27. The strange shapes of the command profiles for P and Q after $t=12$ seconds is a consequence of the strategy used to finish the maneuver: at that time the P and Q commands were used to drive Φ to 360 degrees and Θ back to its equilibrium value at $t=3$ seconds. The commanded R was computed using feedback, approximately by the formula in equation 6.4.2; the term associated with the direct side force due to rudder was neglected. The bandwidth chosen for R was only one-tenth the bandwidth chosen for P in this maneuver. In fact, this was the maneuver which led to the bandwidth parameters discussed in section 6.4.

The simulated responses for U,V,W,P,Q,R, Φ , Θ , Ψ ,x,y,z are shown in Figure 7.25. Note the visible V component that arises during the roll in the U,V,W plot. The other components of the speed are as we would expect. Outside of the (small) overshoots in the angle-variables, the other plots in Figure 7.25 are what a barrelroll should look like.

The plots in Figure 7.26 show the change in altitude, the change in crossrange, Θ , and Ψ as a function of time. The other relevant data in Figure 7.29 show that the speed remained nearly constant (as it was supposed to do), and that the accelerations were all tolerable. The rather large β that arose did cause a transient N_y of about 0.1 g in magnitude. That could have been avoided by asking for a higher bandwidth R control (relative to P).

For this type of maneuver, we would like to investigate the theoretical implications of equation 6.4.2 more thoroughly in the future.

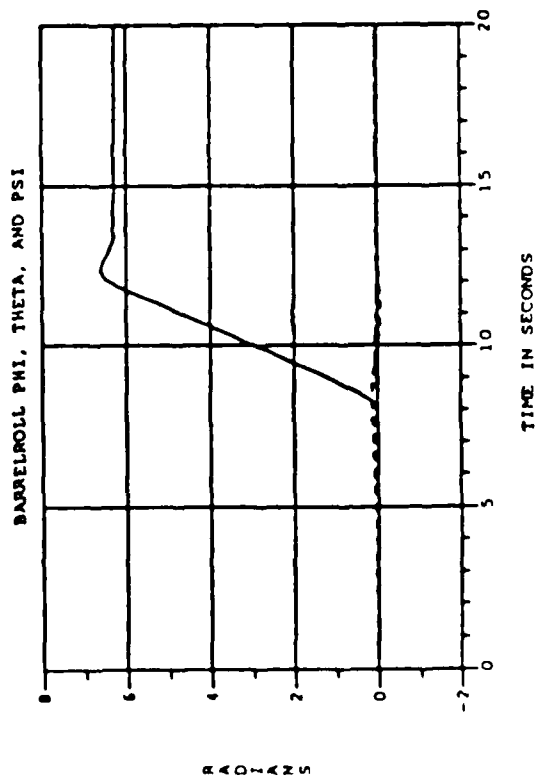
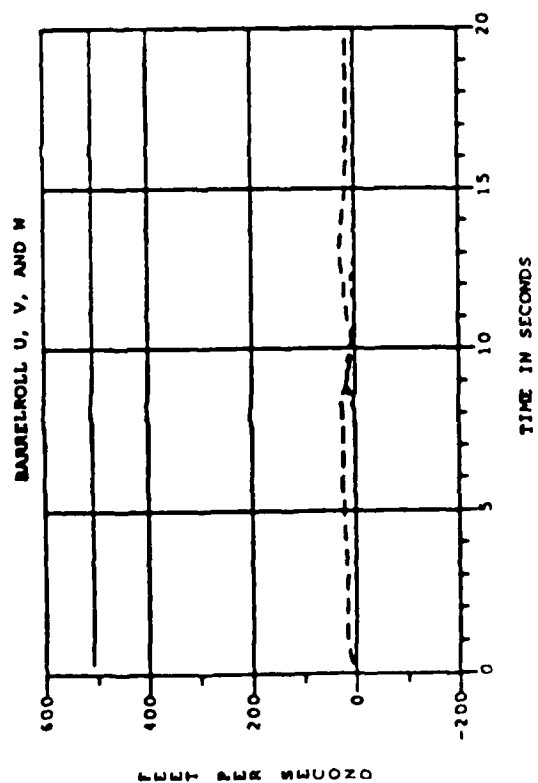
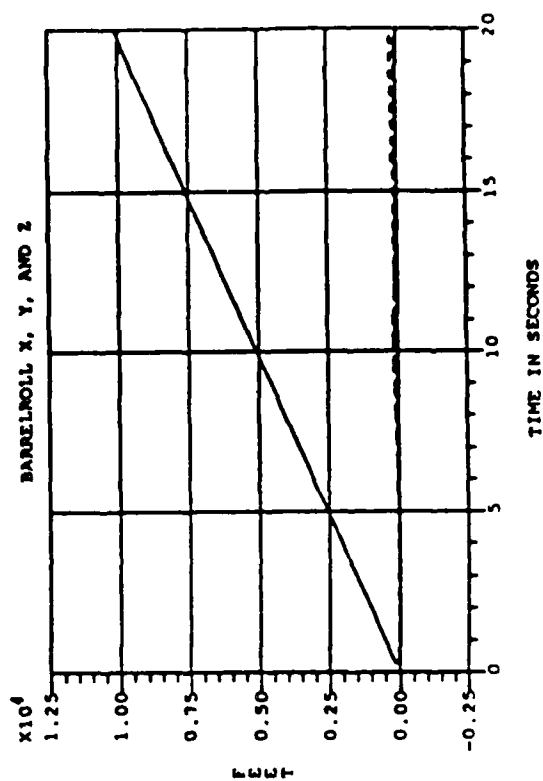
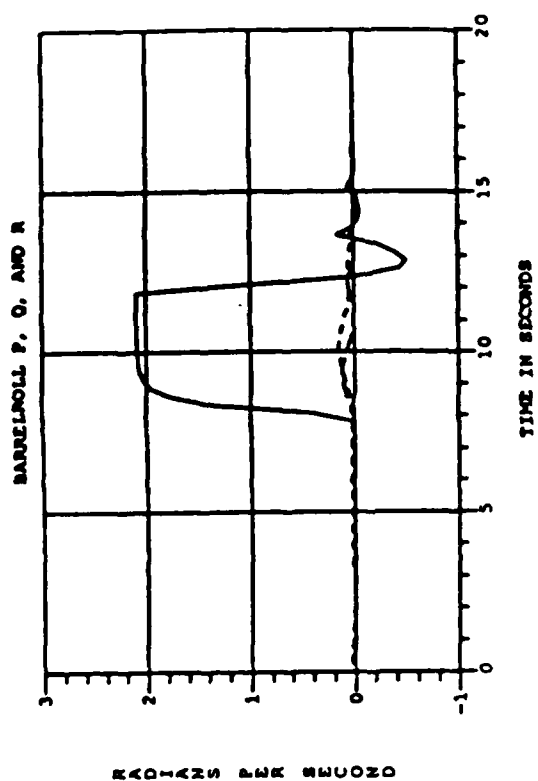


Figure 7.25 States During BARRELROLL

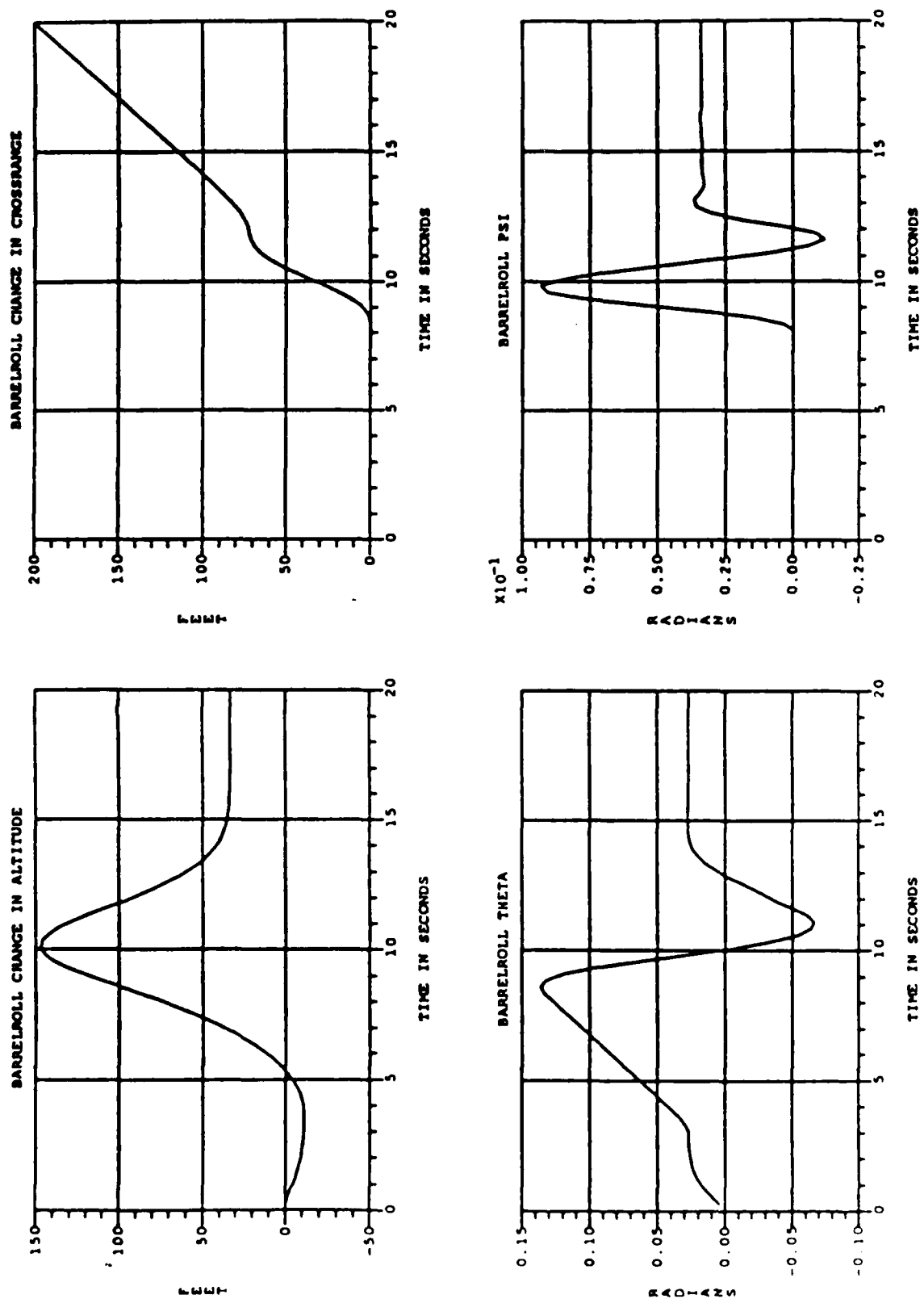


Figure 7.26 Altitude, Crossrange, Theta and Psi During BARRELROLL

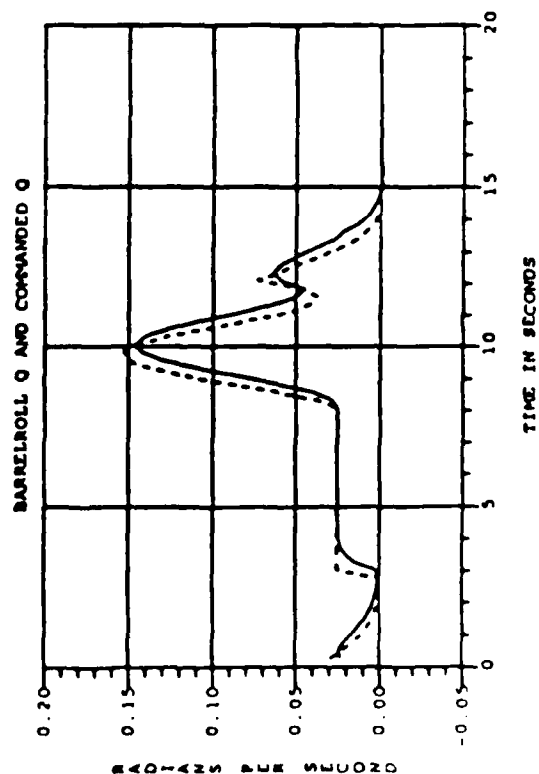
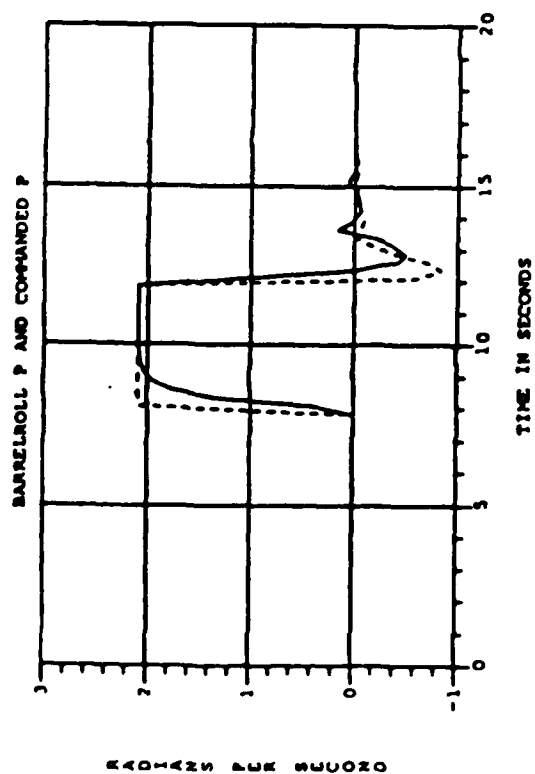
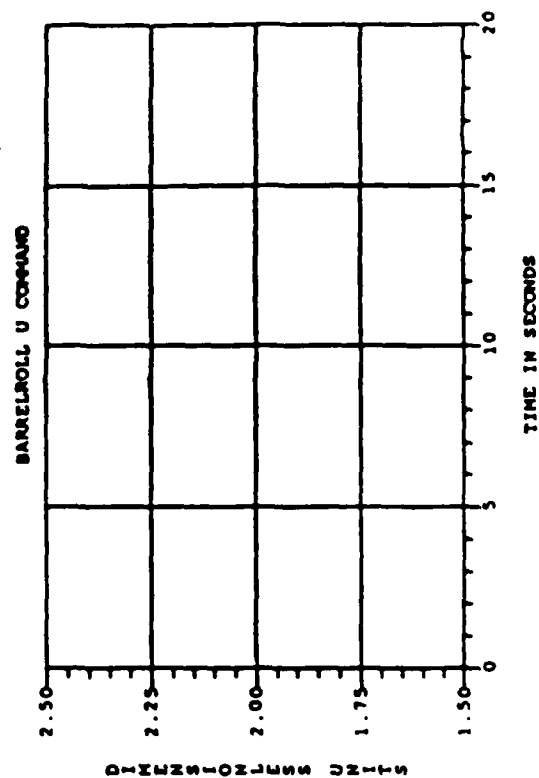
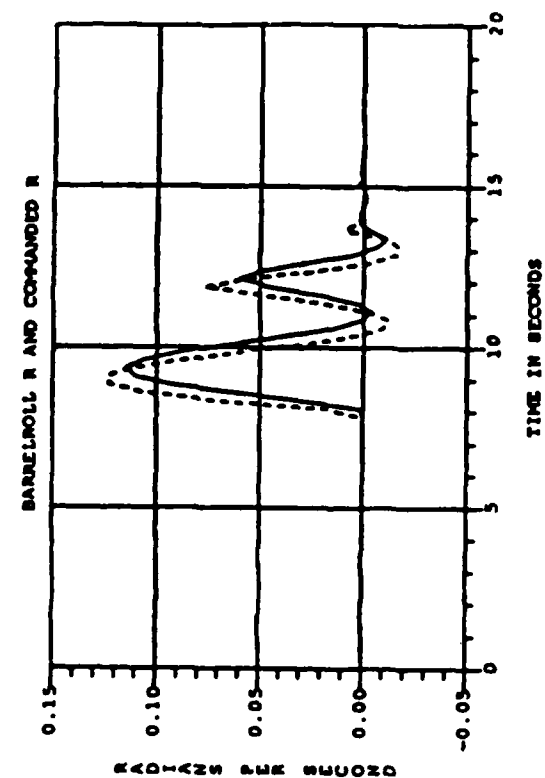


Figure 7.27 Commands and Command Responses During BARRELROLL

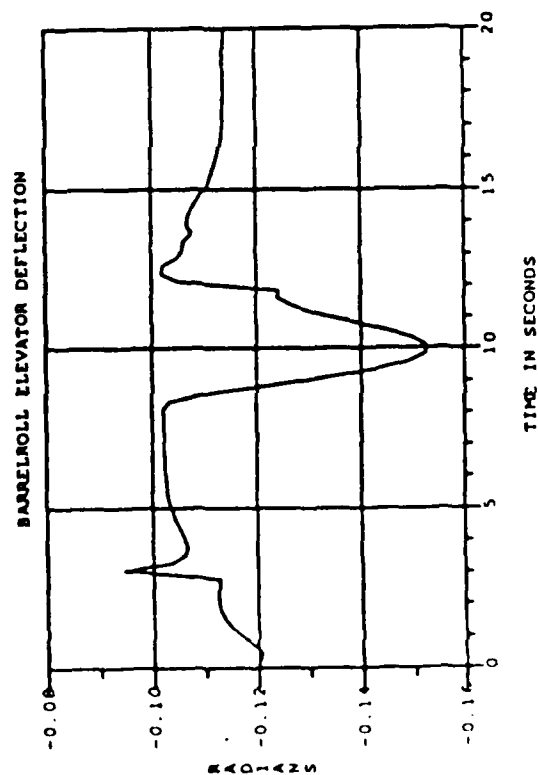
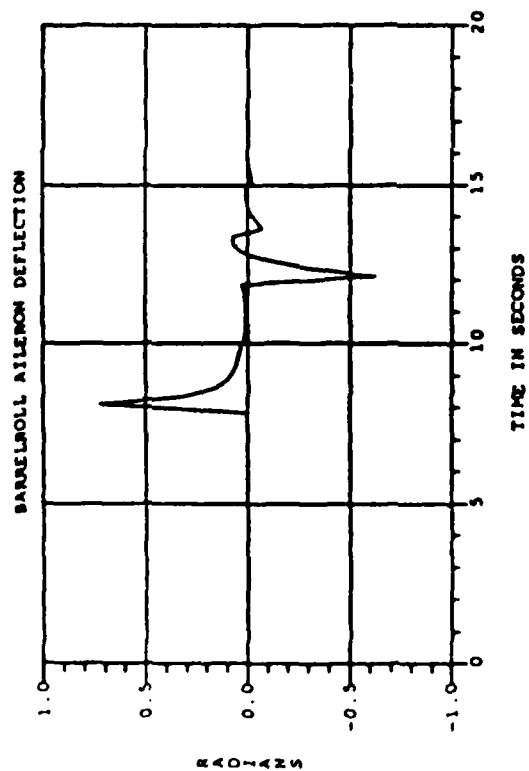
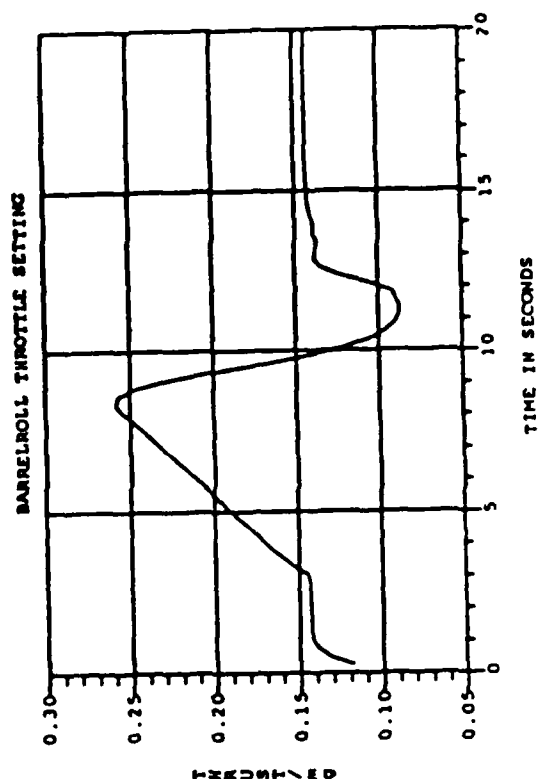
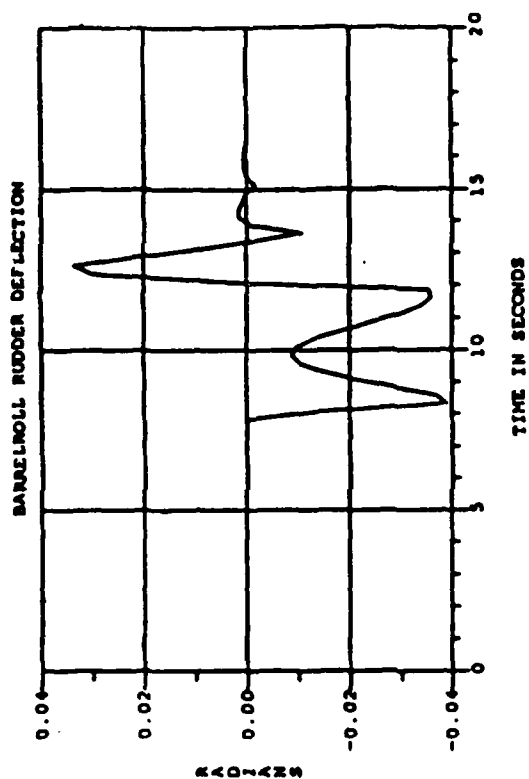


Figure 7.28 Control Activity During BARRELROLL

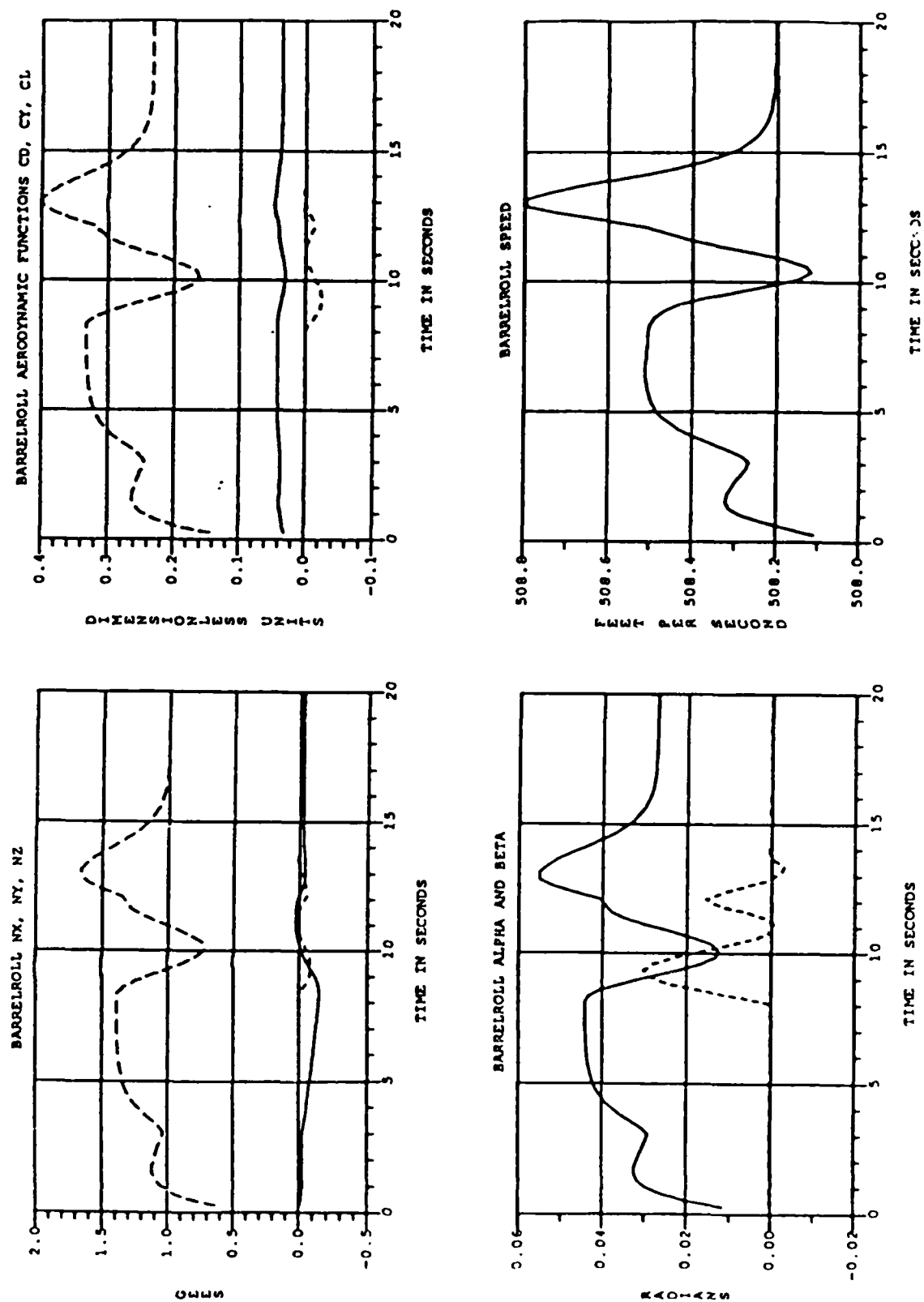


Figure 7.29 Accelerations, Aero Forces, Alpha, Beta and Speed During BARRELROLL

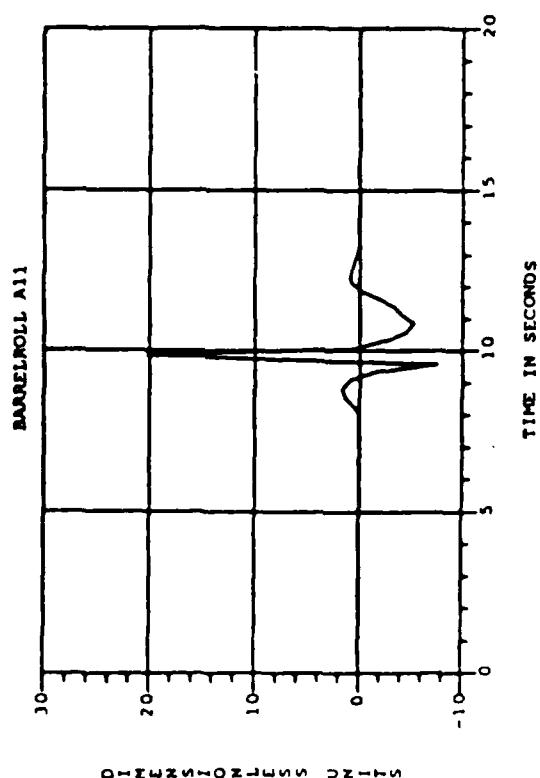
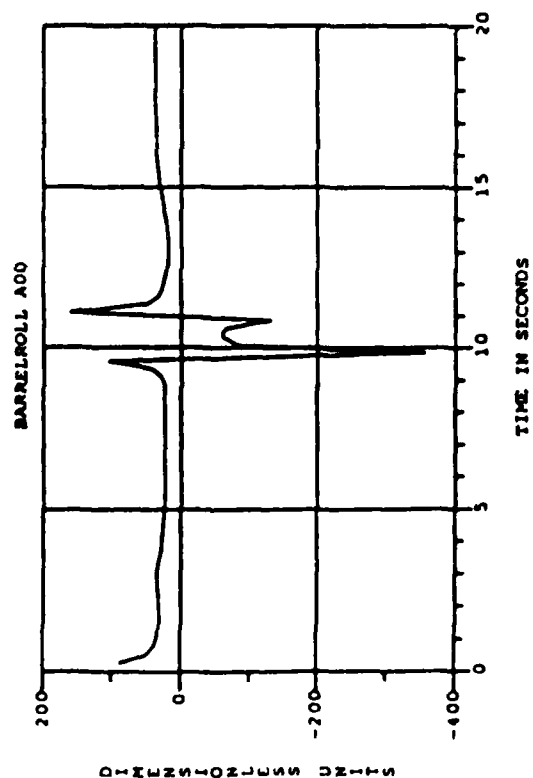
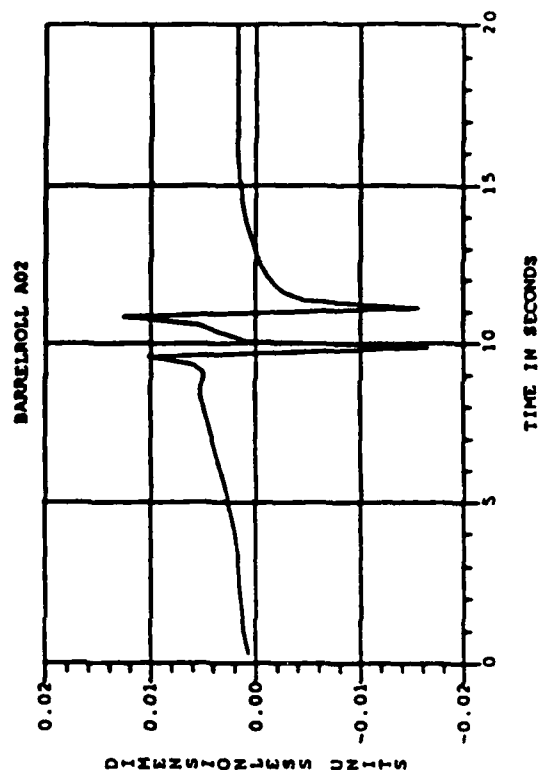
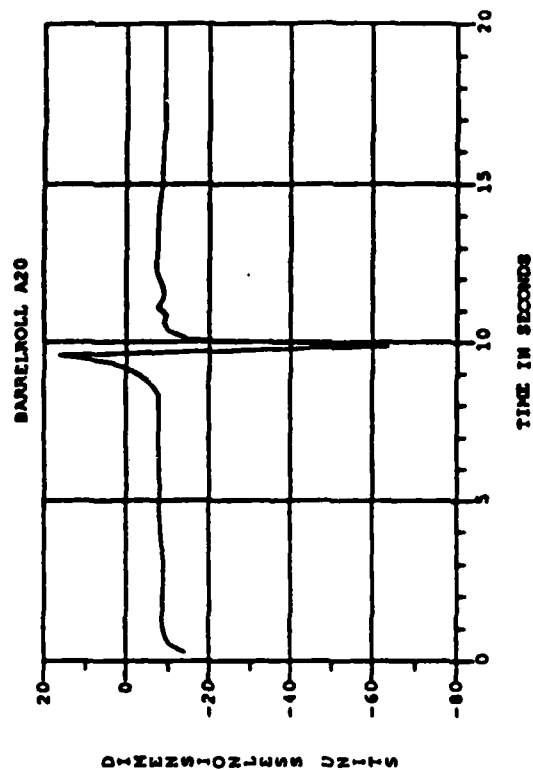


Figure 7.30 A-Parameters During BARRELLROLL

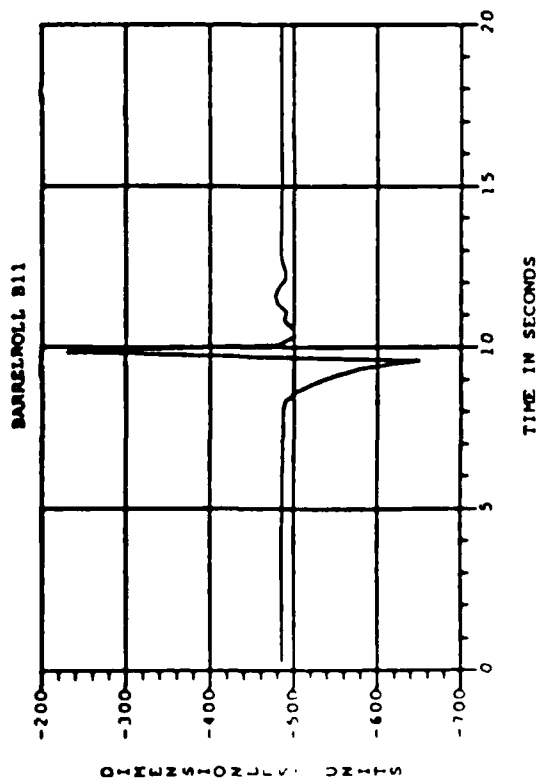
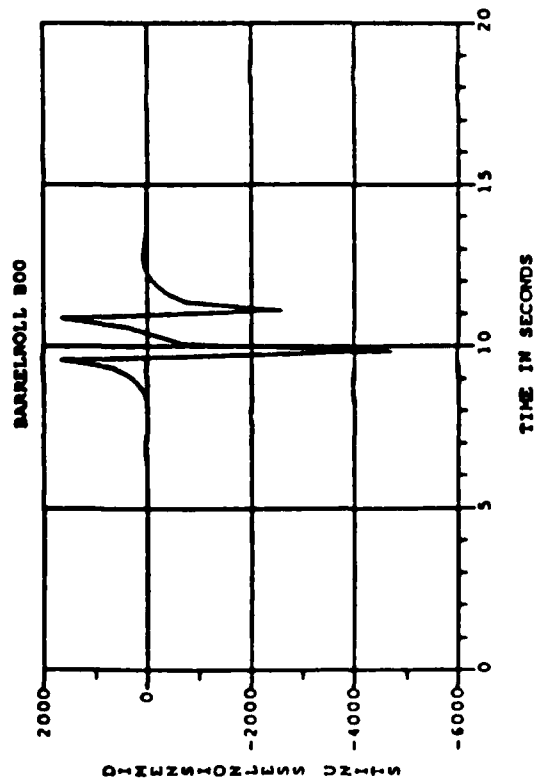
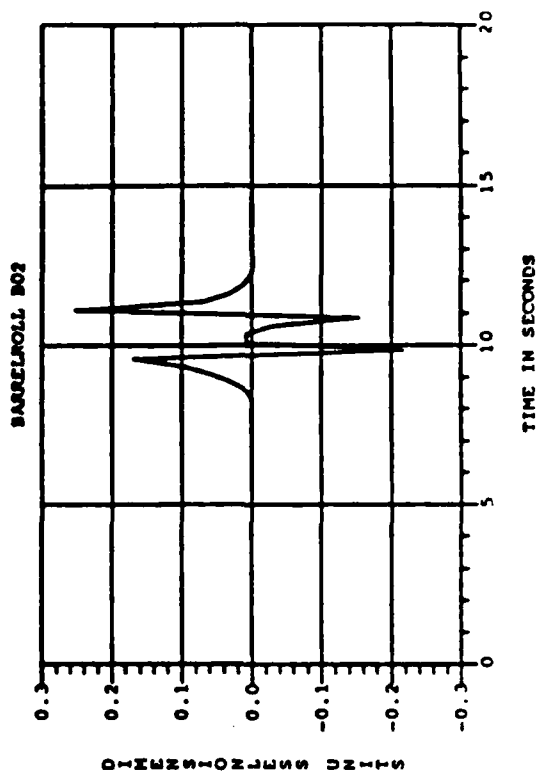
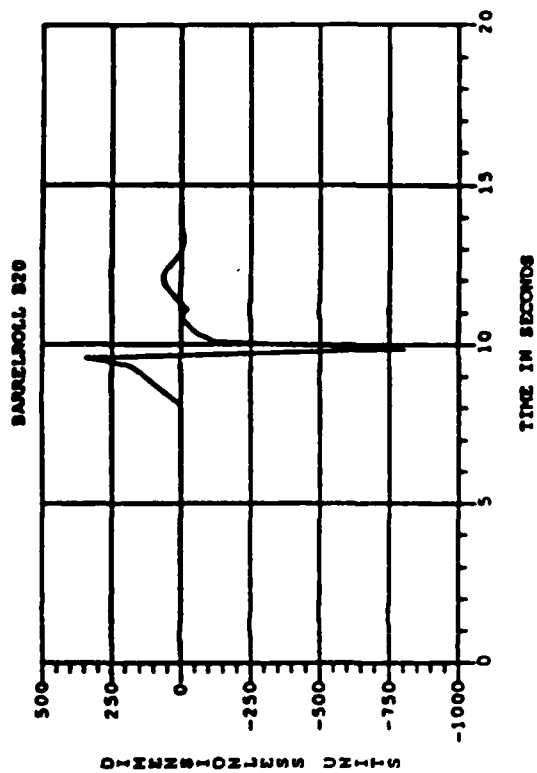


Figure 7.31 B-Parameters During BARRELLROLL

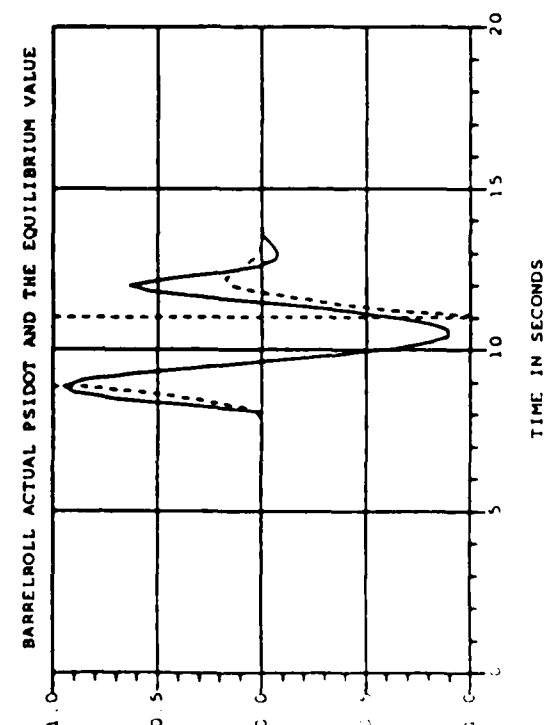
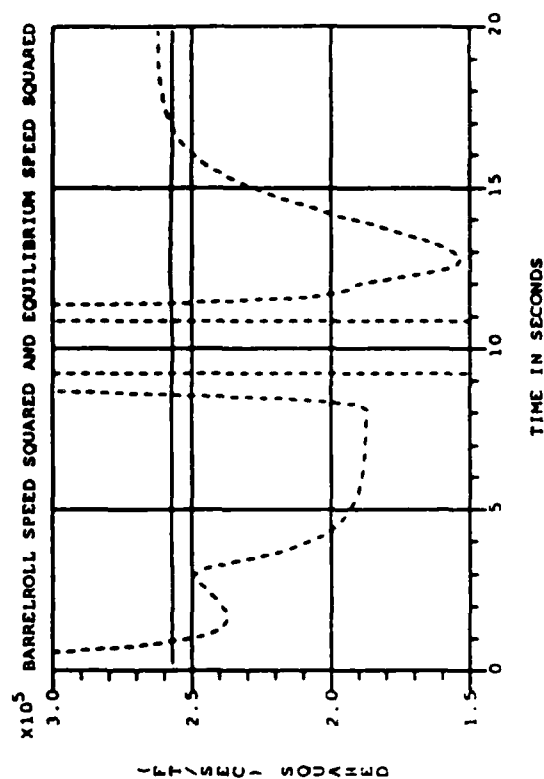
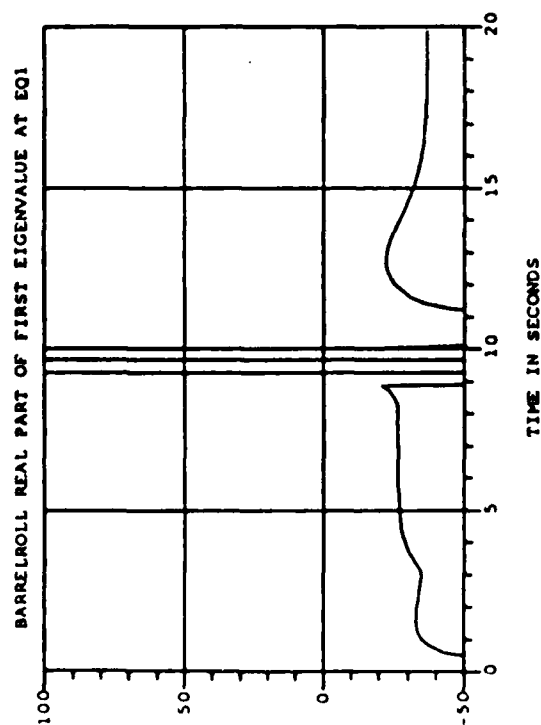
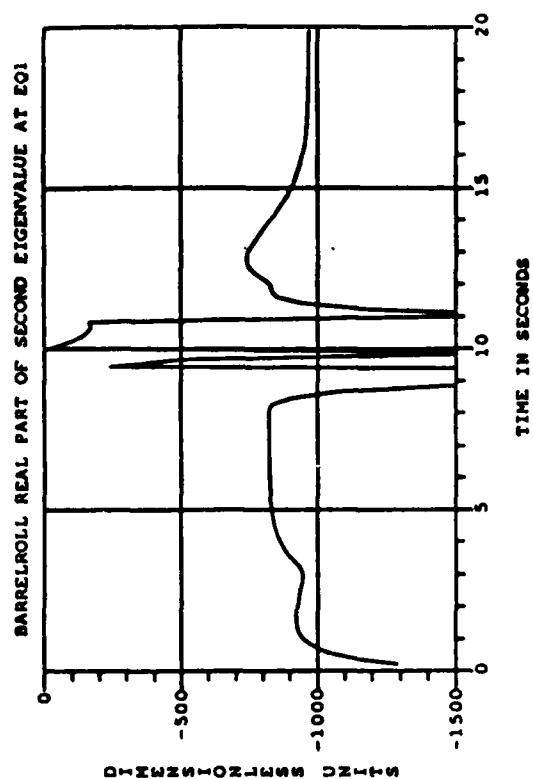


Figure 7.32 Eigenvalues and $\dot{\Psi}$, V^2 Comparisons During BARRELROLL

7.3 DIVINGTURN

Figures 7.33 through 7.38 depict the maneuver DIVINGTURN, which we chose because of its dynamic complexity. A groundtrace of the maneuver in inertial x-y coordinates is shown in Figure 7.33; it is a right-turn (positive y is to the right) that starts at roughly $x=2000$ feet, $y=0$; moves out along the positive x axis and then turns back and heads into the negative x halfspace. The change in altitude is shown in Figure 7.34.

The plots of the vehicle states are shown in Figure 7.35. Note that U drops rapidly between $t=4$ seconds and $t=7$ seconds -- a change of more than 300 feet per second in 3 seconds. At first, we might suspect that the pilot experiences some very unpleasant accelerations in the longitudinal axis, but a glance at the N_x plot in Figure 7.36 shows that N_x is almost ruler flat at -1.2 g during the turn, except for a small bump between 6 and 8 seconds. Our sign convention is chosen so that negative N_x represents a force pushing the pilot back into his seat. That is much better than being pulled out of the seat at 3 g, the situation easiest to imagine when the average value of \dot{U} is -3 g. It was this maneuver that alerted us to the result discussed in section 6.3, that the aerodynamic data for the F-14 has the property that the aerodynamic force vector is almost exactly aligned with the z-direction of the aircraft at large α . The value of N_x shown on the plot is almost constant at -1.2 g because the throttle is saturated at full power, $+1.2$ g, throughout the turn. In fact, the bump between $t=6$ seconds and $t=8$ seconds arose because α exceeded the largest recorded datapoint at 50 degrees during that time, and we were using the table values for $\alpha = 50$ degrees.

A description of the maneuver is as follows: the pilot begins by banking the aircraft a little over 90 degrees, then (while still rolling) he pulls back hard on the stick. All the while the throttle is set at full power. The elevator saturates at its maximum value for three seconds, but Q quickly turns negative because the inertial terms dominate (see the software user's manual, a separate document prepared under this contract). As Q drops, α decreases as well (note: P is 0 during the time when Q drops off, see equation 6.4.4, and the discussion after) until P once again is commanded to be nonzero, generating (with R) some extra \dot{Q} to make Q increase again starting at $t=8$ seconds. The pitch angle, however, decreases steadily to approximately -60 degrees until time $t=12$ seconds. Then the new Q command and the reverse bank command at time $t=12$ seconds brings the nose of aircraft back up and the wings

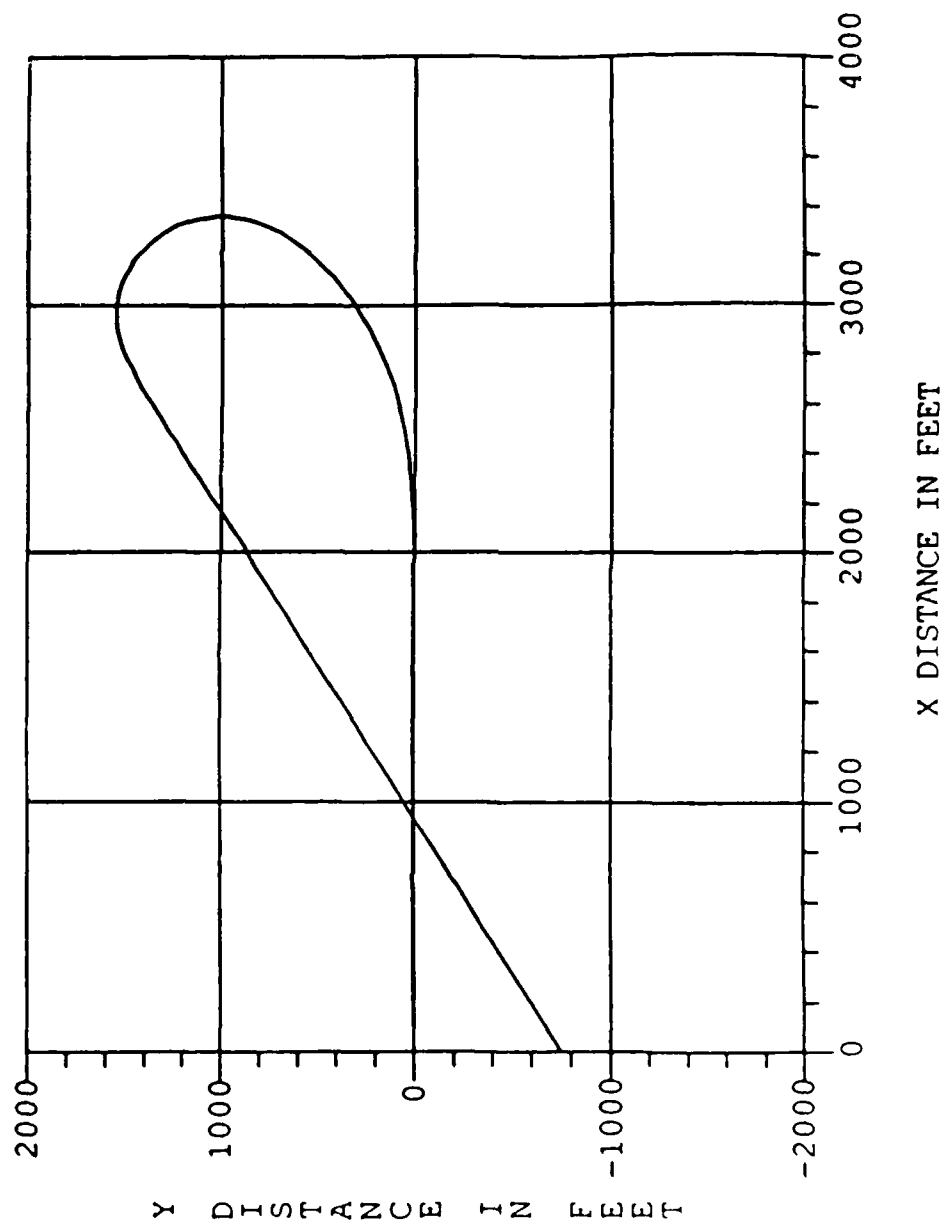


Figure 7.33 Groundtrace of Turn During DIVINGTURN

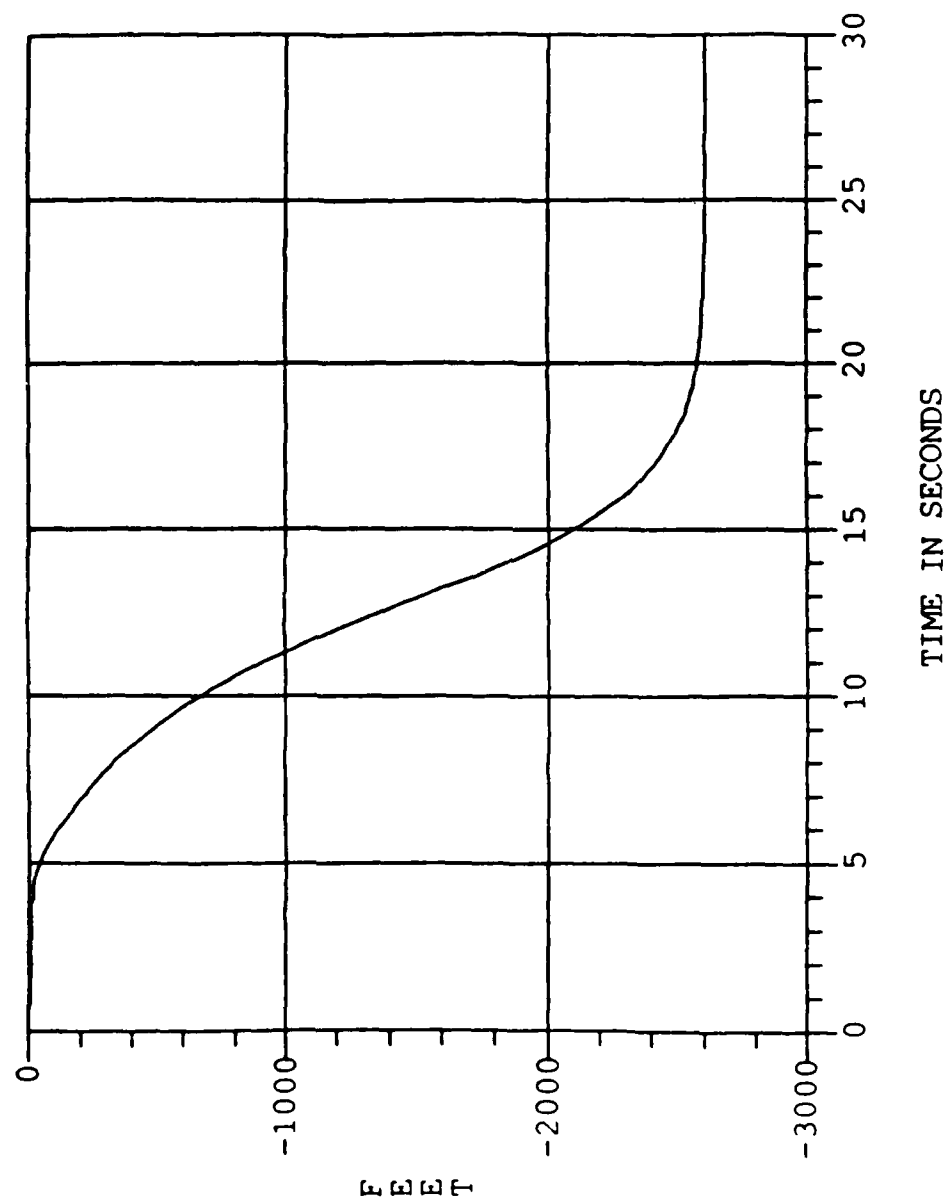


Figure 7.34 Change in Altitude During Diving Turn

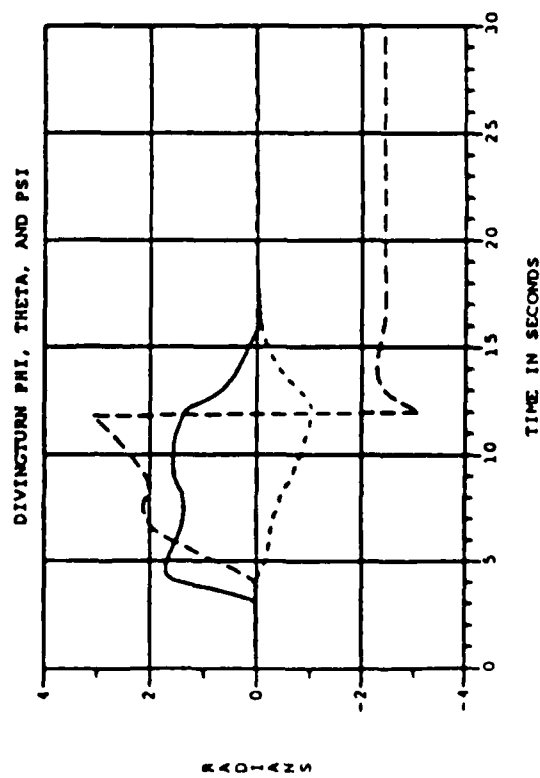
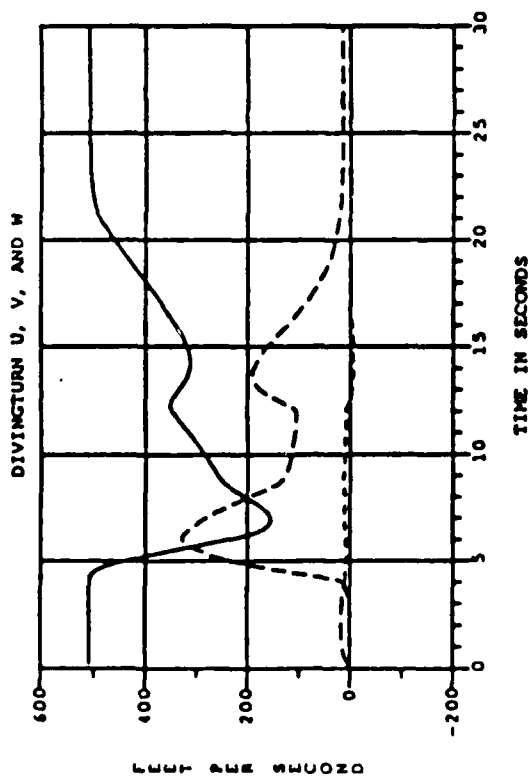
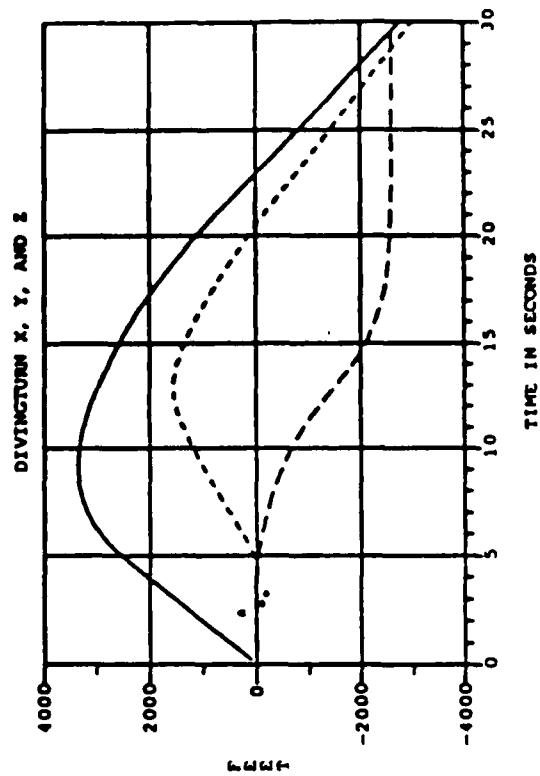
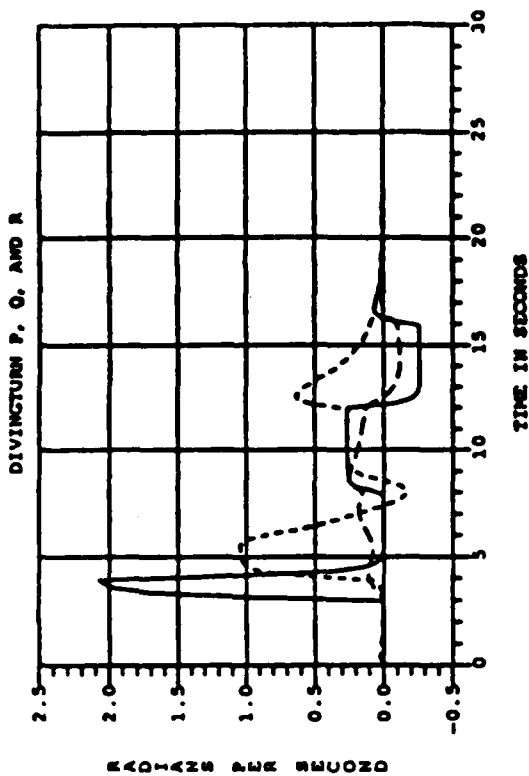


Figure 7.35 States During DIVINGTURN

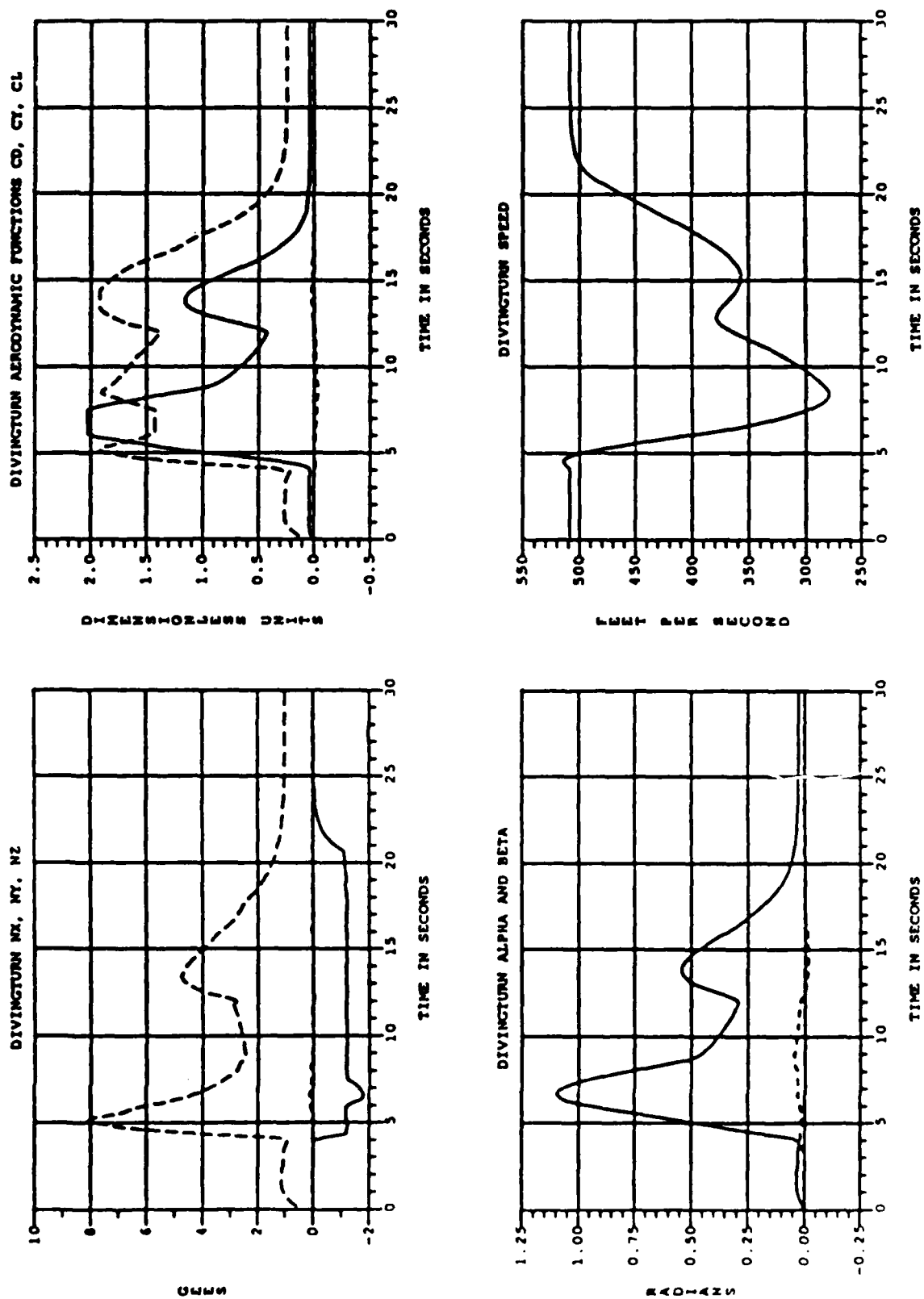


Figure 7.36 Accelerations, Aero Forces, Alpha, Beta and Speed During DIVINGTURN

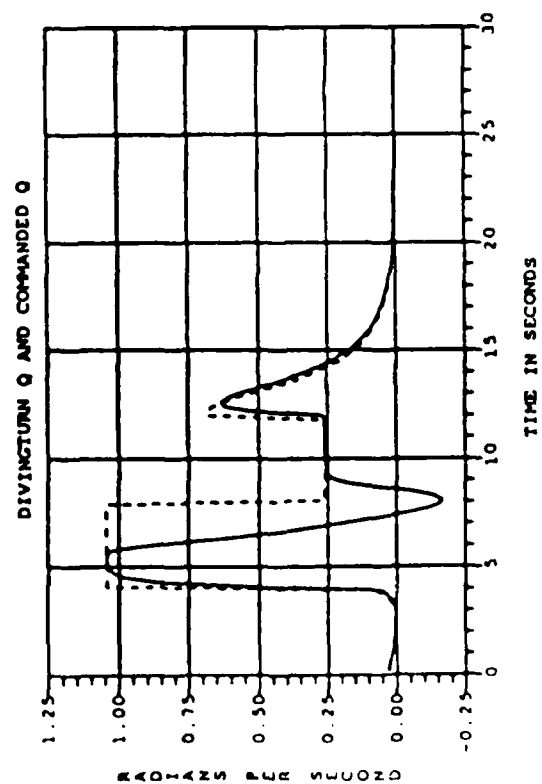
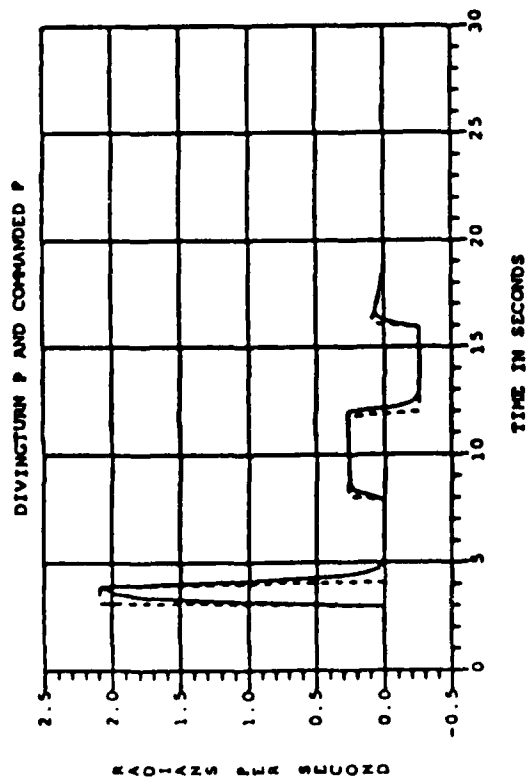
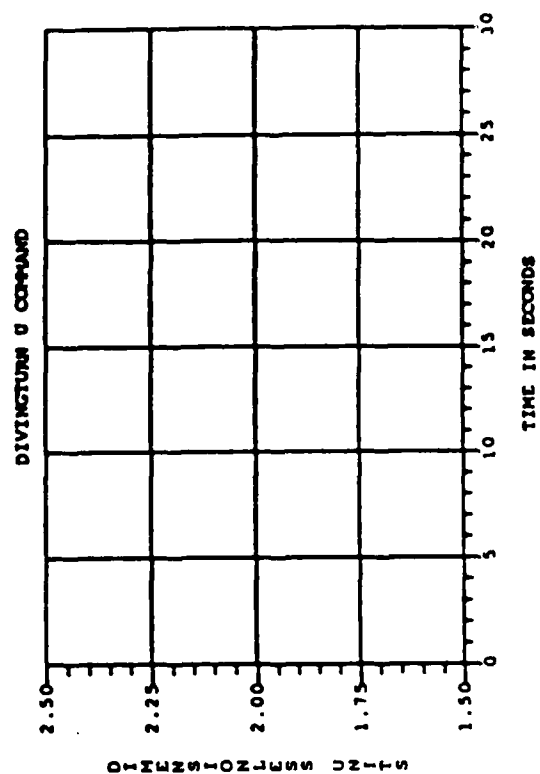
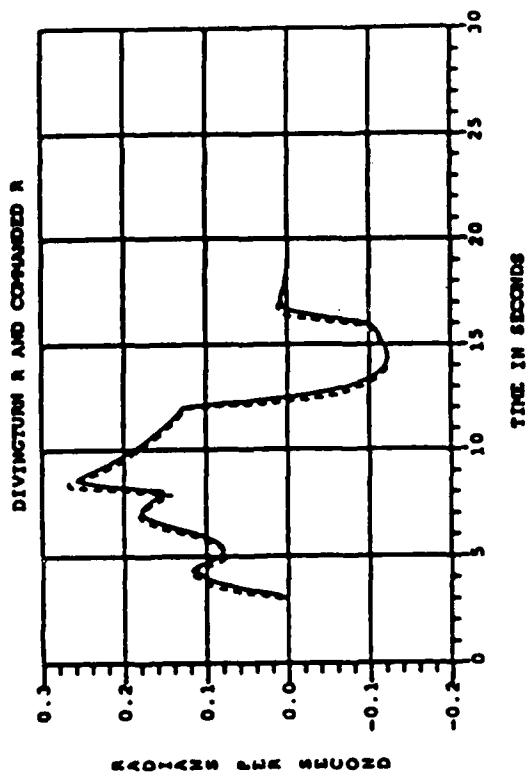


Figure 7.37 Commands and Command Responses During DIVINGTURN

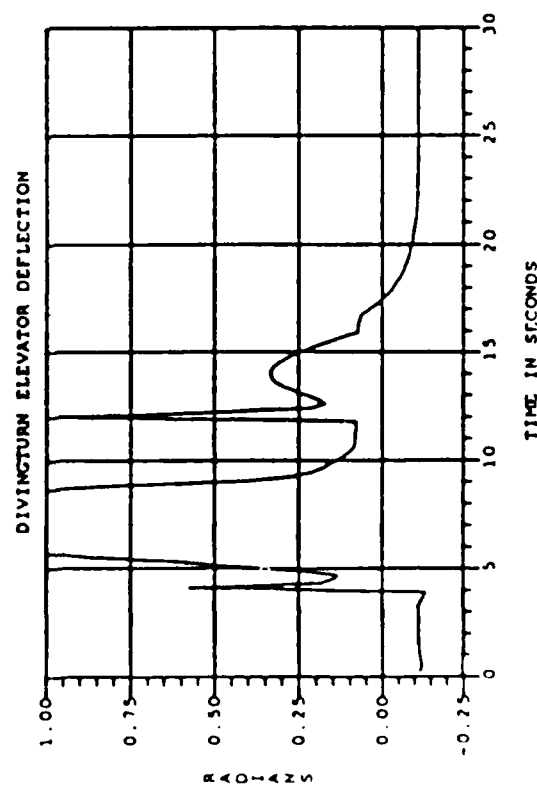
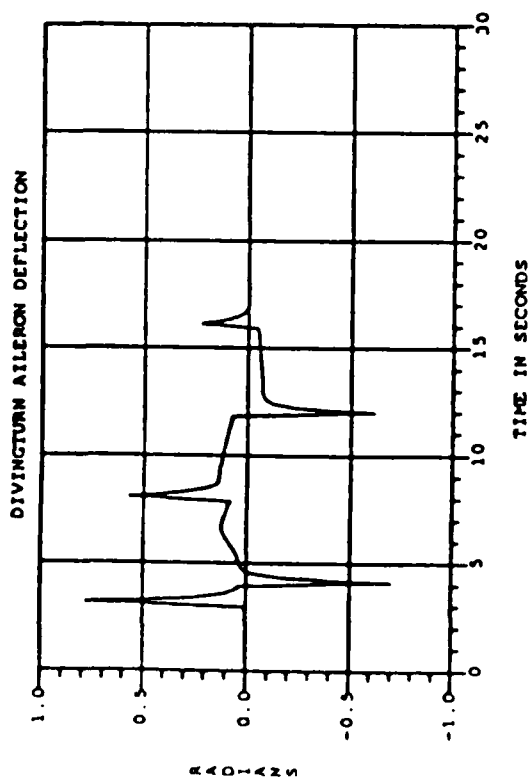
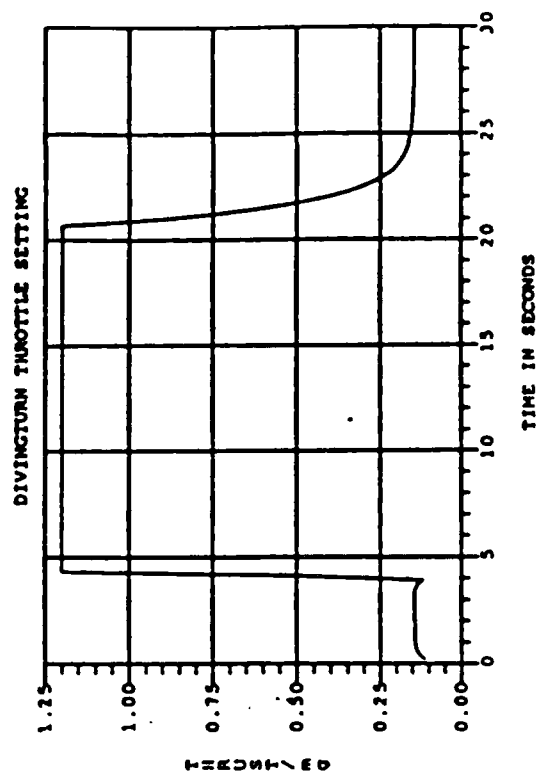
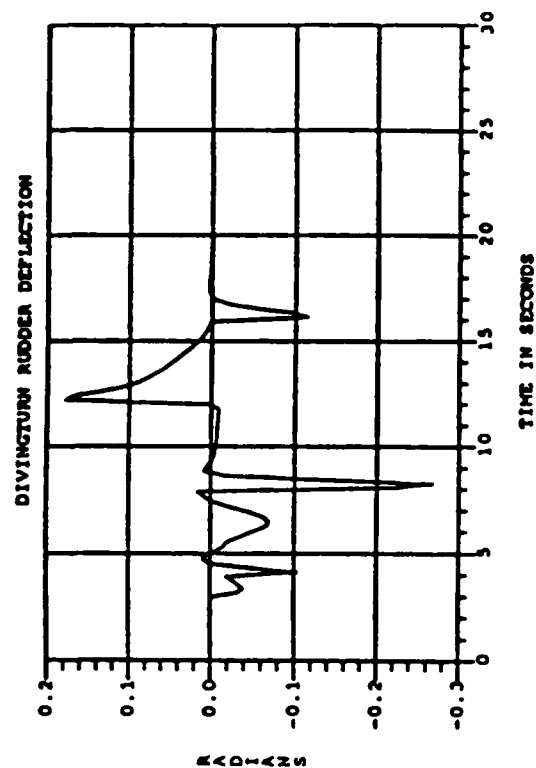


Figure 7.38 Control Activity During DIVINGTURN

back to level. Finally, by about $t=20$ seconds, the aircraft is level again and moving at the desired speed.

Conclusions

From the three types of maneuvers flown in simulation using the dynamic inversion method, we were led to several of the candidate nonlinear flying quality parameters discussed in section 6, and we were forced to a new and improved dynamic inversion concept. One parameter provided an analytic relationship between the bandwidths of the dynamic P and R responses with α restrictions on coordinated flight, another allowed us to understand the effect of the aerodynamic force vector on the accelerations experienced by the pilot. The first maneuver told us little about the aircraft, but it did point out the need for the development of the controller that we used to discover the two important relations just mentioned. Other ideas discussed in section 6 for nonlinear flying qualities also came out of analysis of these simulated maneuvers. We believe the dynamic inversion method and the simulated maneuvers are a very useful tool for developing flying quality parameters.

References

[Ang] E. L. Anglin, "Static Force Tests of a Model of a Twin-Jet Fighter Airplane for Angles of Attack from -10° to 110° and Sideslip Angles from -40° to 40° ," NASA TN D-6425, Aug. 1971.

[BCLA] B. Buchberger, G. E. Collins, R. Loos, R. Albrecht, "Computer Algebra Symbolic and Algebraic Computation," Springer-Verlag, 1983.

[Cop] W. A. Coppel, "A Survey of Quadratic Systems," Journal of Differential Equations 2, 293-304, 1966.

[KC] I. S. Kukles and M. Casanova, "On the Distribution of Critical Points of the First and Second Group (R).," Izv. Vyss. Ucebn. Zaved. Mathematica, No. 6, 88-97, 1964.

[CM] J. V. Carrol, R. K. Mehra, "Bifurcation Analysis of Nonlinear Aircraft Dynamics," Journal of Guidance, Control, and Dynamics, vol. 5, no. 5, Sept.-Oct. , 1982.

[DMBS] J. Dongarra, C. Moler, J. Bunch, and G. Stewart, "LINPACK Users' Guide," SIAM, Philadelphia, 1979.

[E1] M. R. Elgersma "Nonlinear Control, with Application to High Angle of Attack and VSTOL Flight," Masters Thesis, University of Minnesota, 1986.

[E2] M. R. Elgersma, "Control of Nonlinear Systems," Ph. D. Thesis , University of Minnesota, in preparation.

[E3] B. Etkin, "Dynamics of Atmospheric Flight," New York: Wiley, 1972.

[G] R. Gilmore, "Catastrophe Theory for Scientists and Engineers," John Wiley and Sons, 1981.

[HSM] L. R. Hunt, R. Su, and G. Meyer, "Design for Multi-Input Nonlinear Systems," Differential Geometric Control Theory, edited by R. Brockett, R. S. Millman, and H. J.

Sussmann, Birkhauser 1983 .

[M] J. E. Marsden, "Elementary Classical Analysis," San Francisco:Freeman, 1974.

[MKC] R. K. Mehra, W. C. Kessel, J. V. Carrol, "Global Stability and Control Analysis of Aircraft at High Angles of Attack," Cambridge:Scientific Systems, 1977.

[MMTJ] D. Mitchell, T. Meyers, G. Teper and D. Johnston, "Investigations of High-Angle-of-Attack Maneuver-Limiting Factors, Part 3: Appendices - Aerodynamic Models," Technical Report AFWAL-TR-80-3141, Part 3, Systems Technology, Inc., December 1980.

[PY] M. Pohst, D. Y. Y. Yun, "On Solving Systems of Algebraic Equations via Ideal Bases and Elimination Theory," Proceedings of the 1981 ACM Symposium on Symbolic and Algebraic Computation.

[R] A. J. Ross, "A Comparison of Analytical Techniques for Predicting Stability Boundaries for Some Types of Aerodynamic or Cross-Coupling Non-Linearities," article 17, AGAARD CP-333, 1982.

[SBDGIKM] B. T. Smith, J. M. Boyle, J. J. Dongarra, B. S. Garbow, Y. Ikebe, V. C. Klema, C. B. Moler, "Matrix Eigensystem Routines - EISPACK Guide," New York:Springer Verlag, 1976.

[vdW] B. L. van der Waerden, "Algebra," Frederick Ungar Publishing Co. , 1970.

[W] R. J. Walker, "Algebraic Curves," Springer-Verlag , 1978.

[YSJ] J. W. Young, A. A. Schy, and K. G. Johnson, "Pseudosteady-State Analysis of Non-linear Aircraft Maneuvers," NASA Technical Paper 1758, December 1980.

APPENDIX A

TRAJECTORIES IN INERTIAL SPACE

The equilibrium velocities will give trajectories in inertial space which are vertical helices. One way to show this is as follows.

The state is $x = (V, \beta, \alpha, \dot{\Phi}, \dot{\Theta}, \dot{\Psi}, \Phi, \Theta)$. At equilibrium, the state is constant so two of the Euler angles, Φ and Θ , are constant while the third Euler angle, Ψ , is given by

$$\Psi(t) = \Psi(0) + \dot{\Psi} t.$$

The transformation matrix between body axis coordinates and earth fixed coordinates is given by the orthogonal matrix $L_{\Psi\Theta\Phi} = L_{\Psi} L_{\Theta} L_{\Phi}$ where:

$$L_{\Psi} = \begin{bmatrix} \cos(\Psi(t)) & -\sin(\Psi(t)) & 0 \\ \sin(\Psi(t)) & \cos(\Psi(t)) & 0 \\ 0 & 0 & 1 \end{bmatrix}$$

$$L_{\Theta} = \begin{bmatrix} \cos(\Theta) & 0 & \sin(\Theta) \\ 0 & 1 & 0 \\ -\sin(\Theta) & 0 & \cos(\Theta) \end{bmatrix}$$

$$L_{\Phi} = \begin{bmatrix} 1 & 0 & 0 \\ 0 & \cos(\Phi) & -\sin(\Phi) \\ 0 & \sin(\Phi) & \cos(\Phi) \end{bmatrix}$$

The velocity vector is given by $\begin{bmatrix} U \\ V \\ W \end{bmatrix}$ in body axis coordinates, and $\begin{bmatrix} U \\ V \\ W \end{bmatrix} = V \mathbf{1}_{\beta\alpha}$

where $\mathbf{1}_{\beta\alpha}$ is the following unit vector

$$\mathbf{1}_{\beta\alpha} = \begin{bmatrix} \cos(\beta)\cos(\alpha) \\ \sin(\beta) \\ \cos(\beta)\sin(\alpha) \end{bmatrix}.$$

So in earth fixed coordinates, the equilibrium value of the velocity vector is given by

$$L_{\Psi\Theta\Phi} \begin{bmatrix} V \\ 1 \\ \beta_\alpha \end{bmatrix} = V \begin{bmatrix} a \cos(\Psi(t)) - b \sin(\Psi(t)) \\ a \sin(\Psi(t)) + b \cos(\Psi(t)) \\ c \end{bmatrix} \quad (A.1)$$

where

$$\begin{bmatrix} a \\ b \\ c \end{bmatrix} = L_\Theta L_\Phi 1_{\beta_\alpha} \quad .$$

The right-hand side of equation A.1 is usually written as

$$V \begin{bmatrix} \cos(\gamma) \cos(\Psi(t) - \Psi_{vb}) \\ \cos(\gamma) \sin(\Psi(t) - \Psi_{vb}) \\ -\sin(\gamma) \end{bmatrix} \quad (A.2)$$

where the flight path angle, γ , is given by

$$\gamma = -\sin^{-1}(c) = \cos^{-1} \left[\frac{a}{\sqrt{a^2 + b^2}} \right]$$

and

$$\Psi_{vb} = \sin^{-1} \left[\frac{-b}{\sqrt{a^2 + b^2}} \right] \quad .$$

Note: Ψ_{vb} = aircraft heading - velocity vector heading.

Integrating (A.2) gives the trajectory in the earth reference frame.

$$\begin{bmatrix} X_e(t) \\ Y_e(t) \\ Z_e(t) \end{bmatrix} - \begin{bmatrix} X_e(0) \\ Y_e(0) \\ Z_e(0) \end{bmatrix} = \frac{V \cos(\gamma)}{\dot{\Psi}} \left[\begin{bmatrix} \sin(\Psi(t) - \Psi_{vb}) \\ -\cos(\Psi(t) - \Psi_{vb}) \\ -\tan(\gamma) \dot{\Psi} t \end{bmatrix} - \begin{bmatrix} \sin(\Psi(0) - \Psi_{vb}) \\ -\cos(\Psi(0) - \Psi_{vb}) \\ 0 \end{bmatrix} \right] \quad (A.3)$$

This defines a vertical helix of radius $\frac{V}{\dot{\Psi}} \cos(\gamma)$.

DYNAMICAL PROPERTIES OF FLIGHT MANUEVERS

GEORGE R. SELL*

0. Introduction. In this report we show that the study of the dynamical properties of flight maneuvers is governed by the theory of time-varying differential equations. The stability properties of the solutions of these equations are determined by the corresponding properties of the *limiting equations*, see Sell (1967b) and Sacker and Sell (1977). For most flight maneuvers these limiting equations are either autonomous, or periodic in time. In these cases, there is a rich literature for describing the stability properties. A brief outline of the basic theory of limiting equations is included

One of the first objectives is to study the dynamical properties of flight maneuvers in the vicinity of the equilibrium manifold. The Stable Manuever Theorem, which we present here, addresses this issue. This theorem states that if one begins a flight maneuver near a strongly stable equilibrium point, and if the maneuver input is *close to* a nominal input, then the aircraft remains near the equilibrium manifold.

The report contains six sections: 1. Dynamic Inversion, 2. The Equilibrium Manifold, 3. Flight Maneuvers, 4. Limiting Equations, 5. Applications to Flight Maneuvers, and 6. Open Problems.

1. Dynamic Inversion. Many of the dynamical properties of flight maneuvers can be understood by studying a model of the dynamics in terms of an ordinary differential equation with a control parameter. Typically one has a control-theoretic problem of the form

$$(1) \quad w' = W(w, u)$$

where $u \in R^n$ and $w \in R^{n+m}$. We assume that u is restricted to lie in a fixed open bounded set Ω in R^n . Our objective is to describe a control strategy whereby (1) takes on a desired form, say

$$w' = D(w),$$

where $D(w)$ is a desired vector field on R^{n+m} . In order to accomplish this we need to solve

$$(2) \quad W(w, u) = D(w)$$

for u . If the Jacobian matrix $D_u W(w, u)$ is nonsingular and if $D(w)$ assumes values in the range $W(w, \Omega) = \{W(w, u) : u \in \Omega\}$, then one can find a continuous solution $u = u(w)$ of (2).

*Institute for Mathematics and its Applications, University of Minnesota, Minneapolis, Minnesota 55455

Since the state variable w has higher dimension than the control parameter u , the above strategy can only be successful if some restrictions are imposed on the desired function $D(w)$. This means that some of the variables of (1) are controllable while others are not. In order to better understand this, let us look at a special, but rather important, case.

Let us write $w = (x, y)^T$ where $x \in R^n$ and $y \in R^m$.¹ Then (1) takes on the form

$$(3) \quad \begin{cases} \dot{x} = f(x, y, u) \\ \dot{y} = g(x, y, u). \end{cases}$$

for some functions f and g . The strategy is to seek to control the x -variable according to the desired equation

$$\dot{x} = D(x, y).$$

In order to do this, we need to determine a control strategy u by solving $f(x, y, u) = D(x, y)$ for u . As before this leads to a continuous solution $u = U(x, y)$ whenever the Jacobian matrix $D_u f$ is nonsingular and $D(x, y) \in f(x, y, \Omega)$. The y -variables are not controllable directly by this strategy. Instead $y = y(t)$ must be a solution of the equation

$$\dot{y} = g(x, y, U(x, y)).$$

By combining this we see that (3) takes on the form

$$(4) \quad \dot{x} = D(x, y), \quad \dot{y} = g(x, y, U(x, y)).$$

This process of solving for u is referred to as *dynamic inversion*.

The dynamical properties of uncontrollable variables y are determined by (4). It is these properties which will decide whether a given control strategy is desirable, and we expect that the same properties will oftentimes determine the flying qualities of an aircraft and a collection of flight maneuvers. We will illustrate this in a moment, after we define the Equilibrium Manifold for (1).

2. The Equilibrium Manifold. In order to simplify our treatment a bit, we will assume a special form of (1) which is given by

$$(5) \quad \dot{w} = F(w) + G(w)H(w, u),$$

where the functions F, G and H are smooth functions with

$$F: R^{n+m} \rightarrow R^{n+m}$$

$$G: R^{n+m} \rightarrow L(R^n, R^{n+m})$$

$$H: R^{n+m} \times R^n \rightarrow R^n$$

¹ More generally one could introduce local coordinates $w = (x, y)^T$ and restrict x to lie on some given manifold M in R^{n+m} . The function D is then a desired vector field on M , and y denotes the normal coordinates to M .

and $L(R^n, R^{n+m})$ denotes the space of linear mappings from R^n into R^{n+m} . In other words, for each $w \in R^{n+m}$ and $u \in R^n$, $F(w)$ is a $(n+m) \times 1$ column vector, $H(w, u)$ is a $n \times 1$ column vector, and $G(w)$ is a $(n+m) \times n$ matrix.²

Let Ω denote the subset of R^{n+m} where the rank of the Jacobian matrix $D_w G(w)$ is n , and assume that Ω is a nonempty open set R^n . This permits one to introduce local coordinates $w = (x, y)^T$ so that (5) takes on the equivalent form

$$(6) \quad \begin{cases} x' = f_1(x, y) + g_1(x, y)H(x, y, u) \\ y' = f_2(x, y) + g_2(x, y)H(x, y, u). \end{cases}$$

where g_1 is an $n \times n$ matrix, and g_2 is an $2 \times n$ matrix. We assume that the local coordinates have been chosen so that g_1 is invertible.³ Here x denotes the controllable variables and y the uncontrollable variables. Next we define a manifold M_0 for (6) as

$$M_0 = \{(x, y) \in R^{n+m} : f_1(x, y) + g_1(x, y)H(x, y, u) = 0\}.$$

The manifold M_0 is invariant for (6), and on M_0 one has

$$(7) \quad H(x, y, u) = -g_1^{-1}(x, y)f_1(x, y).$$

By inserting (7) into (6) we obtain

$$(8) \quad y' = K(x, y)$$

where

$$K(x, y) = f_2(x, y) - g_2(x, y)g_1^{-1}(x, y)f_1(x, y)$$

and $x = \text{constant}$. On the invariant manifold M_0 equation (6) reduces to

$$(9) \quad \begin{cases} x' = 0 \\ y' = K(x, y) = f_2(x, y) - g_2(x, y)g_1^{-1}(x, y)f_1(x, y). \end{cases}$$

By fixing H so that (7) holds, the controllable variable x is held constant. The function H may change with time, but this only reflects the adjustment in H caused by the time variation of the uncontrollable variable y , which is a solution of (8).

The *Equilibrium Set* for (6) is defined as the set

$$E = \{(x, y) \in M_0 : f_2(x, y) + g_2(x, y)H = 0\},$$

²We will concentrate our attention on the special model equation (5). The general dynamical theory we describe here is not dependent on the fact that the control in (5) enters as a linear factor H . The only role that the special form (5) plays in this report is to simplify some of the algebraic considerations which arise below.

³This is possible because of the rank condition on the Jacobian matrix $D_w G$.

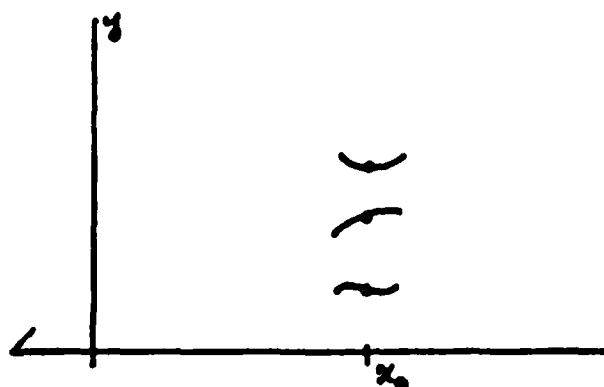


Figure 1. The Equilibrium Manifold near a point x_0 .

where H is given by (7). Notice that $(x, y) \in E$ if and only if $(x, y) \in M_0$ and

$$(10) \quad K(x, y) = f_2(x, y) - g_2(x, y)g_1^{-1}(x, y)f_1(x, y) = 0.$$

If the Jacobian matrix $D_y K$ is nonsingular, then one can solve (10) locally for $y = c(x)$ where $c(x)$ is continuous in x .⁴ It is possible that for a given x , equation (10) may have several solutions $y = c(x)$, see Figure 1.

The Equilibrium Manifold is a subset of the equilibrium set and is defined by

$$M = \{(x, y) \in E : D_y K(x, y) \text{ is nonsingular}\}.$$

For each $(x_0, y_0) \in M$ there is a neighborhood U of x_0 and a C^1 -function $c : U \rightarrow R^m$ such that $(x, c(x)) \in M$ for $x \in U$ and $c(x_0) = y_0$. This means that in the vicinity of every point on the equilibrium manifold M , the equilibrium set E agrees with M , and E is locally a smooth manifold. The behavior of E near points $(x, y) \in E$ where $D_y K(x, y)$ is singular, can be very complicated. These singular points, which can be bifurcation points, will not be analyzed in this report.

Since the equilibrium points for (6) are generally not isolated, it is not possible for them to be asymptotically stable in the full dynamics (6). However it is possible that equilibrium points of the y -equation (8) are asymptotically stable. Because of the importance of this fact, we introduce the following stability concept: We shall say that at point (x_0, y_0) is strongly stable if (x_0, y_0) is an equilibrium point for (6), and y_0 is asymptotically stable for equation (8).

Assume for the moment that for each $x \in R^n$, equation (8) has an isolated equilibrium point $c(x)$ and that $c(x)$ varies continuously in x . Assume further that over some interval of time I the controller $u(t)$ is chosen so as to maintain a given value for x and that $y = c(x)$ for $t \in I$. (Since x and y are constant on I , it follows from (7) that H is constant as well.)

⁴An argument for showing the existence of a solution $c(x)$ is given below as a part of the proof of the Stable Manuever Theorem.

Next we ask, what would happen if a small disturbance is introduced into this system? Clearly this will be strongly influenced by the stability properties of the equilibrium point $e(x)$. If the linearization of the vector field at $e(x)$ gives rise to an eigenvalue with positive real part, then one can expect an abrupt change in the response. One would like (9) to have strong stability properties and to be free of destabilizing bifurcations. We shall look into this further in Section 5.

For equation (6) it is convenient to separate the problem of controllability into two parts. Since u enters this problem through the function H only, one can think of H itself as a controller. For example, the aircraft pilot may select a specific value H_0 for H at a given time t , then the onboard computer would solve the equation

$$(11) \quad H(x, y, u) = H_0$$

for u to drive the rudder, thrust, etc. The solvability of the last equation for u depends, of course, on the Implicit Function Theorem, and usually requires the Jacobian matrix $D_u H$ to be nonsingular. We emphasize that the dynamical properties we are studying here are independent of whether or not (11) is solvable for u .

So far we have been tacitly assuming that any point in the (x, y) -space is attainable via a flight maneuver. This is by no means the case. Furthermore, the coordinates for the problem need not be Euclidean coordinates. Angular variables are natural in many cases. What this means is that one should consider the original problem, either (1) or (5), to be given on a prescribed subset A of some manifold M . We shall refer to A as the *attainable set*.⁵

In applications developed by others on this project, one has $n = 4$, $m = 2$, and consequently (8) represents an ordinary differential equation in the plane R^2 . The equilibrium manifold M in this case has dimension 4.

3. Flight Maneuvers. We define a flight maneuver to be the response of an aircraft to a time-varying controller on some time interval I . For the model equation

$$(12) \quad \begin{cases} x' = f_1(x, y) + g_1(x, y)H \\ y' = f_2(x, y) + g_2(x, y)H \end{cases}$$

where $H = H(t) = H(x, y, u, t)$ is now a time-varying input, a flight maneuver is a solution $(x(t), y(t))$ of (12), for $t \in I = (a, b)$. The function H is referred to as the maneuver input. We will assume that the inputs $H(t)$ are piece-wise continuous functions of t on I . Furthermore, we restrict our attention to inputs $H(t)$ for which the response $(x(t), y(t))$ remains in the attainable set A .

⁵Even though we shall continue to write our equations in terms of Euclidean coordinates, this is really not essential for our theory.

There are two maneuvers which are of special interest for flight control. The first of these is a basic maneuver on an interval I . This maneuver occurs when there exists x_a, y_a such that

$$H(t) = -g_1^{-1}(x_a, y(t))f_1(x_a, y(t)) \quad t \in I,$$

where $y(t)$ is the solution of (8) with $y(a) = y_a$. In a basic maneuver the quantity x_a is referred to as the base state of the aircraft. For a basic maneuver the system (12) reduces to the system (9). These maneuvers are quite common for aircraft motion. They occur, for example, when the aircraft is ascending (or descending) with a fixed angle of attack, or when the aircraft is turning with the controls held fixed.

The second maneuver, which we call an advanced maneuver, occurs when $H(t)$ is continuous at $t = a, b$ and one has

$$H(t) = -g_1^{-1}(x(t), y(t))f_1(x(t), y(t)) \quad t = a, b,$$

where $(x(t), y(t))$ is a solution of (12) on I . Advanced maneuvers occur, for example, during a barrel roll, or when the pilot is changing the thrust vector. Any aircraft trip, from takeoff to landing, is a sequence of basic maneuvers interspersed with advanced maneuvers.

There is a convenient way to distinguish between basic and (non-basic) maneuvers. Assume that the maneuver input H satisfies

$$(13) \quad H(t) = -g_1^{-1}(x(t), y(t))f_1(x(t), y(t)), \quad t \in I.$$

It then follows that the x -equation reduces to $x' = 0$, or $x(t) = x_a$, a constant, for $t \in I$. In other words a maneuver is a basic maneuver if and only if (13) is satisfied. The extent to which $H(t)$ deviates from satisfying (13) is a measure of the strength of a maneuver. We can quantify this by defining the norm, or strength, of a maneuver $N(H)$ by

$$N(H) = \sup \{ |H(t) + g_1^{-1}(x(t), y(t))f_1(x(t), y(t))| : t \in I \}.$$

Notice that one has $N(H) = 0$ if and only if H is the input for a basic maneuver. In the Stable Maneuver Theorem, which we give below, we show that if a maneuver begins near a strongly stable equilibrium point on the equilibrium manifold M and if $N(H)$ is small, then the aircraft remains near the strongly stable equilibrium points on M throughout the entire maneuver.

An advanced maneuver can be viewed as trajectory which changes the base state of an aircraft from x_a to x_b . The point to emphasize is that the full equations (12) are needed to describe the dynamical behavior of an aircraft during an advanced maneuver. However at time $t = a, b$ these equations reduce to (9). Since an advanced maneuver ends with (9) being satisfied at $t = b$, it follows that the equations (12) are asymptotically autonomous. We shall present next a brief review of limiting equations and asymptotically autonomous equations in the next section.

4. Limiting Equations. We begin with a nonlinear time-varying differential equation $x' = f(x, t)$, where $f \in C(R^N \times R, R^N)$ and $C(R^N \times R, R^N)$ denotes the space of continuous functions from $R^N \times R$ to R^N . In order to simplify the discussion we will assume that all functions $f(x, t)$ considered in this section are Lipschitz continuous in x , and that every solution of $x' = f(x, t)$ is defined for all $t \in R$.⁶

For $f \in C(R^N \times R, R^N)$ we define the translation f_τ by $f_\tau(x, t) = f(x, t + \tau)$. The mapping

$$\sigma(f, \tau) = f_\tau$$

defines a flow on $C(R^N \times R, R^N)$. If we let $\phi(x, f, t)$ denote the solution of $x' = f(x, t)$ satisfying $\phi(x, f, 0) = x$, then

$$\pi(x, f, \tau) = (\phi(x, f, \tau), f_\tau)$$

is a (skew-product) flow on $R^N \times C(R^N \times R, R^N)$.

In the flow σ on $C(R^N \times R, R^N)$ we define the hull⁷ of f by

$$H(f) = \text{Cl} \{f_\tau : \tau \in R\}$$

and the positive hull by

$$H^+(f) = \text{Cl} \{f_\tau : \tau \geq 0\}.$$

The ω -limit set of a function $f \in C(R^N \times R, R^N)$ is given by

$$\Omega(f) = \bigcap_{\tau \geq 0} H^+(f_\tau).$$

The limiting equations for $f \in C(R^N \times R, R^N)$ is defined as the collection of all equations $x' = g(x, t)$ with $g \in \Omega(f)$. The following theorem gives a useful sufficient condition for the collection of limiting equations to be nonempty and compact. The proof of this theorem is given in Sell (1967ab) and is based on the Ascoli-Arzelà Theorem.

LIMITING EQUATION THEOREM. Let $f \in C(R^N \times R, R^N)$ be such that for every compact set $K \subset R^N$ there is a constant $k \geq 0$ and a function $\delta = \delta(\epsilon)$ with the following two properties:

- (1) $f(x, t)$ is Lipschitz continuous in x , uniformly in t , i.e. $|f(x, t) - f(y, t)| \leq k|x - y|$ for all $x, y \in K, t \in R$.
- (2) $f(x, t)$ is uniformly continuous on $K \times R$, i.e. $|f(x, s) - f(y, t)| \leq \epsilon$ for all $x, y \in K, s, t \in R$ with $|x - y| \leq \delta(\epsilon)$ and $|t - s| \leq \delta(\epsilon)$.

⁶The assumptions on the Lipschitz continuity of f and the global existence of solutions of $x' = f(x, t)$ can be dropped. See Sell (1967ab, 1973), Miller and Sell (1970) and Sacker and Sell (1977) for details.

⁷The closure operation Cl used here is the closure in the topology of uniform convergence on compact subsets of $R^N \times R$.

Then $\Omega(f)$ is a nonempty, compact, connected subset of $C(R^N \times R, R^N)$. Furthermore every $g \in \Omega(f)$ satisfies the Lipschitz condition (1) above.

The main advantage of the limiting equations is that one can use the standard theory of ω -limit sets to describe the behavior of solutions of the original differential equation $x' = f(x, t)$ as $t \rightarrow \infty$. In particular, let $f \in C(R^N \times R, R^N)$ and let $\phi(x, f, t)$ be a solution of $x' = f(x, t)$ that stays in a given compact set $K \subset R^N$ for $t \geq 0$. Assume further that f satisfies the hypotheses of the Limiting Equation Theorem. Then the motion $\pi(x, f, \tau)$ remains in compact set in $R^N \times C(R^N \times R, R^N)$. Furthermore for every sequence $\tau_n \rightarrow \infty$ there is a subsequence, which we denote again by τ_n , and a point $(y, g) \in R^N \times C(R^N \times R, R^N)$ such that

$$\begin{aligned}\phi(x, f, \tau_n) &\rightarrow y \\ f_{\tau_n} &\rightarrow g \\ \phi(x, f, t + \tau_n) &\rightarrow \phi(y, g, t)\end{aligned}$$

where the last limit is uniform on compact subsets of R .

There are two special situations concerning limiting equations, which arise in the theory of flight maneuvers. We say that a function $f \in C(R^N \times R, R^N)$ is asymptotically autonomous if f satisfies the hypotheses of the Limiting Equation Theorem and if the ω -limit set of f consists of one point, say $\Omega(f) = \{g\}$. Since the ω -limit set is invariant under the flow σ on $C(R^N \times R, R^N)$, it follows that $g_\tau = g$ for all $\tau \in R$, i.e. g is autonomous (independent of time). Similarly a function $f \in C(R^N \times R, R^N)$ is asymptotically periodic if f satisfies the hypotheses of the Limiting Equation Theorem and if $\Omega(f)$ consists of a single periodic orbit. In this case $g \in \Omega(f)$ is periodic in t .

Let $x' = f(x, t)$ be an asymptotically autonomous differential equation with limiting equation $x' = g(x)$. Let x_0 be an asymptotically stable equilibrium point for $x' = g(x)$. Then one can show that there is a neighborhood U of x_0 such that for all $x_1 \in U$ the solution $\phi(x_1, f, t)$ of $x' = f(x, t)$ satisfies $\phi(x_1, f, t) \rightarrow x_0$ as $t \rightarrow \infty$, see Markus (1956). In other words, the solutions of $x' = f(x, t)$ beginning in U are stable, as a matter of fact, they are asymptotically stable. The stability properties of asymptotically periodic equations are similar, see LaSalle (1962) and Sell (1966).

In this report we shall restrict our study to flight maneuvers which are asymptotically autonomous. Eventhough it may appear that all flight maneuvers are asymptotically autonomous, this need not be the case. For example, if one wishes to study the effects of small random disturbances (i.e. noise) on the aircraft, then one may need the full theory of limiting equations. The references cited below offer a good introduction to this theory.

For applications to the study of the dynamical properties of flight maneuvers, one should note that the limiting behavior of a function f may be assumed in finite time. In particular if $f \in C(R^N \times R, R^N)$ has the property that there is an autonomous function $g \in C(R^N \times R, R^N)$ and a time T such that $f(x, t) = g(x)$ for all $t > T$, then f is

asymptotically autonomous and $\Omega(f) = \{g\}$. Similarly if $f \in C(R^N \times R, R^N)$ has the property that there is a time-periodic function $g \in C(R^N \times R, R^N)$ and a time T such that $f(x, t) = g(x, t)$ for all $t > T$, then f is asymptotically periodic and

$$\Omega(f) = \{g_\tau : 0 \leq \tau \leq P\}$$

where P is a time-period of g , see Sell (1967ab).

5. Applications to Flight Maneuvers. During an advanced maneuver on an interval $I = (a, b)$ the equations of motion are given by

$$(12) \quad \begin{cases} x' = f_1(x, y) + g_1(x, y)H \\ y' = f_2(x, y) + g_2(x, y)H. \end{cases}$$

The motion begins at (x_a, y_a) at time $t = a$ and ends at (x_b, y_b) at time $t = b$. Equation (12) is an asymptotically autonomous system with the limiting equation given by

$$(9) \quad \begin{cases} x' = 0 \\ y' = K(x_b, y) = f_2(x_b, y) - g_2(x_b, y)g_1^{-1}(x_b, y)f_1(x_b, y). \end{cases}$$

As a matter of fact (12) reduces to (9) for $t \geq b$. Clearly the location of y_b , the value of y at time $t = b$, can play a significant role on the dynamics of the maneuver. Let us look at a few examples.

Example 1: Assume that y_b lies in the basin of attraction of an asymptotically stable equilibrium point $e(x_b)$ of $y' = K(x_b, y)$. In this case, $y(t)$ is attracted towards $e(x_b)$ for $t > b$. If y_b is close enough to $e(x_b)$, then the transient behavior will be short-lived, and for all practical purposes, one would have $y(t) \sim e(x_b)$ after some short time interval. (This situation is quite common and very likely is the outcome of most flight maneuvers.) On the other hand, if y_b is far away from $e(x_b)$, then the transient behavior will persist for a long time, and the aircraft could be under the influence of the transient part of $y(t)$ when the next advanced maneuver commences. For example, if y_b is close to the boundary of the basin of attraction, then one would expect that the dynamical behavior of the boundary set will have greater influence on the aircraft than that of the equilibrium point $e(x_b)$.

Example 2: Assume that y_b does not lie in the basin of attraction of any asymptotically stable equilibrium point. For instance, y_b may lie on a periodic orbit, or in an unstable or chaotic portion of the y -space. This could have very serious consequences for the aircraft. One would not want to implement such a maneuver without detailed knowledge of the underlying dynamical properties of (9).

Because of the considerations raised in the last two paragraphs, one of the goals in the study of the dynamics of flight maneuvers is to understand the dynamical properties of $y' = K(x_b, y)$ in every fiber $A(x_b)$, where $A(x)$ is defined to be those y for which

$(x, y) \in A$. The set $A(x)$ is simply the fiber of the attainable set A over the point x . Because of our assumption that every input $H(t)$ yield an attainable response, one must have $y(t) \in A(x(t))$, for all $t \in I$. One would like to show that $A(x_b)$ has additional dynamical properties. For example, one may want to show that if an advanced maneuver ends in a position (x_b, y_b) , then the trajectory $y(t)$ of $y' = K(x_b, y)$ with $y(b) = y_b$ remains in $A(x_b)$ for all $t \geq b$.

While the overall dynamical properties of flight maneuvers can be very complicated, there is one practical situation which is amenable to analysis. In this case we consider an advanced maneuver which begins at a point (x_a, y_a) which is close to the equilibrium manifold M . This means that y_a is close to some equilibrium state $e(x_a)$ of $y' = K(x_a, y)$. We assume that $e(x_a)$ is asymptotically stable and that the maneuver input $H(t)$ is close to the nominal value $-g_1^{-1}(x(t), y(t))f_1(x(t), y(t))$, i.e. the norm $N(H)$ is small. We will show that the terminal value (x_b, y_b) is close to the equilibrium manifold M and that y_b is close to an asymptotically stable equilibrium point $e(x_b)$ of $y' = K(x_b, y)$. More precisely we will prove the following

STABLE MANUEVER THEOREM. *Let $(x_a, e(x_a))$ be a strongly stable equilibrium point on the equilibrium manifold M , i.e. $e(x_a)$ is an asymptotically stable equilibrium point for $y' = K(x_a, y)$. Then there exists positive constants κ, c_1, c_2, c_3 and ϵ_0 such that for any $\epsilon, 0 < \epsilon < \epsilon_0$, the following holds: Let $H(t)$ be the input for any maneuver on any interval $I = (a, b)$ where the following conditions are satisfied:*

- (1) *The maneuver begins at (x_a, y_a) where $|y_a - e(x_a)| \leq c_1 \epsilon$.*
- (2) *One has $|x(t) - x_a| \leq c_2 \epsilon$ for $a \leq t \leq b$.*
- (3) *One has $|H(t) + g_1^{-1}(x(t), y(t))f_1(x(t), y(t))| \leq N(H) \leq c_3 \epsilon$ for $a \leq t \leq b$.*

Then for each $\tau \in I$ there exists a strongly stable equilibrium point $(x(\tau), e(x(\tau)))$ of (12) such that $|y(\tau) - e(x(\tau))| \leq \kappa \epsilon$ for all $\tau \in I$.

Before proving this result one should note that we do not assume anything concerning the length of the time interval $I = (a, b)$. The interval length can be large. The constants κ, c_1, c_2, c_3 and ϵ_0 are independent of the interval I . As a result, this theorem does apply to any sequences of basic and advanced maneuvers which satisfy (2) and (3).

Proof of Stable Maneuver Theorem. There is no loss in generality in assuming that $(x_a, e(x_a)) = (0, 0)$. (Indeed if this were not the case, then the change of variables

$$\begin{aligned} x &\rightarrow x + x_a \\ y &\rightarrow y + e(x_a) \end{aligned}$$

would result in a new system of differential equations with the desired property.) As a result one has $K(0, 0) = 0$ and the matrix $A = D_y K(0, 0)$ is stable. The latter means that there exist $K_1 > 0$ and $\lambda > 0$ such that

$$(14) \quad |e^{At}| \leq K_1 e^{-\lambda t}, \quad t \geq 0$$

Next define

$$\Delta(t) = H(t) + g_1^{-1}(x(t), y(t))f_1(x(t), y(t)), \quad t \in I.$$

Then (12) reduces to

$$\begin{cases} x'(t) = g_1(x(t), y(t))\Delta(t), \\ y'(t) = K(x(t), y(t)) + g_2(x(t), y(t))\Delta(t). \end{cases}$$

Furthermore, for $t \in I$ one has $|\Delta(t)| \leq N(H)$, the norm of the maneuver.

Our first step is to show that there exists a continuous solution $y = e(x(t))$ of the equation

$$K(x(t), y) = 0, \quad t \in I.$$

This is, in fact, a consequence of the Implicit Function Theorem. Since we also need an estimate of the size of $e(x(t))$ we will present the details here. Define $B(x, y)$ by

$$B(x, y) = y - A^{-1}K(x, y).$$

Then $D_y B(0, 0) = 0$. Next fix $a_0 > 0$ and $b_0 > 0$ so that

$$(15) \quad |D_y B(x, y)| \leq \frac{1}{2}, \quad |x| \leq a_0, |y| \leq b_0.$$

Let M_1, M_2, M_3, M_4 be constants so that

$$(16) \quad \begin{cases} |B(x, 0) - B(0, 0)| \leq M_1|x|, \\ |D_y K^{-1}(x, y)D_x K(x, y)| \leq M_2, \\ |g_1(x, y)| \leq M_3, \\ |g_2(x, y)| \leq M_4, \end{cases}$$

for $|x| \leq a_0, |y| \leq b_0$. By making a_0 smaller, if necessary, we can assume that $2M_1a_0 \leq b_0$. Because of (15) the mapping $y \rightarrow B(x, y)$ is a strict contraction, and consequently the equation $y = B(x, y)$ has a fixed point $y = e(x)$ for $|x| \leq a_0$. Furthermore $y = e(x)$ is also a solution of $K(x, y) = 0$, and $e(x)$ is a C^1 -function of x which satisfies the following estimates: With $y = e(x) = B(x, y)$ and $0 = B(0, 0)$ one has

$$\begin{aligned} |e(x)| &= |B(x, y) - B(0, 0) + B(x, 0) - B(x, 0)| \\ &\leq |B(x, y) - B(x, 0)| + |B(x, 0) - B(0, 0)| \\ &\leq \frac{1}{2}|e(x)| + M_1|x|. \end{aligned}$$

Hence $|e(x)| \leq 2M_1|x| \leq 2M_1a_0 \leq b_0$. Consequently for $x = x(t)$ one has

$$|e(x(t))| \leq 2M_1|x(t)| \leq 2M_1c_2\epsilon$$

provided $\epsilon \leq \epsilon_0 \leq \frac{2a}{c_2}$. Furthermore one has

$$\begin{aligned}\frac{d}{dt}e(x(t)) &= D_x e(x(t))x'(t) \\ &= D_x e(x(t))g_1(x(t), y(t))\Delta(t).\end{aligned}$$

If one differentiates $e(x) = e(x) - A^{-1}K(x, e(x))$ with respect to x , one obtains

$$D_y K(x, e(x))D_x e(x) = -D_x K(x, e(x))$$

and consequently from (16)

$$|D_x e(x)| \leq |D_y K^{-1}(x, e(x))D_x K(x, e(x))| \leq M_2.$$

Next we define $z(t) = y(t) - e(x(t))$, and for the remainder of the proof we let $z = z(t)$, $x = x(t)$, $y = y(t)$ and $e = e(x(t))$. Then

$$(17) \quad z' = Az - L(x, z),$$

where L is given by

$$\begin{aligned}L(x, z) &= K(x, y) - Az + g_2(x, y)\Delta - e' \\ &= K(x, y) - Az + g_2(x, y)\Delta - D_x e(x(t))g_1(x, y)\Delta.\end{aligned}$$

Now fix η so that

$$(18) \quad K_1 \lambda^{-1} \eta \leq \frac{1}{2},$$

where K_1 and λ are given by (14). Next choose $a_1, b_1, 0 < a_1 \leq a_0, 0 < b_1 \leq b_0$ so that

$$(19) \quad |D_y K(x, y) - D_y K(0, 0)| \leq \eta$$

for $|x| \leq a_1, |y| \leq b_1$. Since $K(x, e(x)) = K(0, 0) = 0$ we obtain the following from the Taylor expansion:

$$\begin{aligned}K(x, y) - Az &= K(x, y) - K(x, e(x)) - Az \\ &= K(0, 0) + \left(\int_0^1 D_y K(x, e + \theta z) d\theta \right) z - Az \\ &= \left(\int_0^1 [D_y K(x, e + \theta z) - D_y K(0, 0)] d\theta \right) z.\end{aligned}$$

Assume that ϵ_0 satisfies

$$\epsilon_0 \leq \min \left(\frac{a_0}{c_2}, \frac{b_1}{4M_1} \right).$$

If $|x| \leq \epsilon_0$ we have $|c| \leq 2M_1\epsilon_0$, and therefore if $|z| \leq \frac{b_1}{2}$ we have $|c + \theta z| \leq b_1$. From (19) we get

$$(20) \quad |K(x, y) - Ax| \leq \eta|x|$$

for $|x| \leq \epsilon_0, |y| \leq b_1$. From (16) we obtain

$$(21) \quad \begin{aligned} |g_2(x, y)\Delta| &\leq M_3N(H) \leq M_3c_3\epsilon \\ |D_x c(x)g_1(x, y)\Delta| &\leq M_2M_4N(H) \leq M_2M_4c_3\epsilon. \end{aligned}$$

Now (20) and (21) imply that

$$(22) \quad |L(x, z)| \leq \eta|z| + M_5\epsilon$$

for $|x| \leq \epsilon \leq \epsilon_0, |z| \leq \frac{b_1}{2}$, where $M_5 = M_3c_3 + M_2M_4c_3$. By the Variation of Constants Formula, the solution of (17) is given by

$$z(t) = e^{A(t-a)}z_a + \int_a^t e^{A(t-s)}L(x(s), z(s))ds.$$

This means that $z(t)$ is a fixed point of the operator

$$F(z)(t) = e^{A(t-a)}z_a + \int_a^t e^{A(t-s)}L(x(s), z(s))ds.$$

Assume that $|z(s)| \leq \frac{b_1}{2}$ for $s \in I$. Then by using (14) and (22) we have

$$\begin{aligned} |F(z)(t)| &\leq K_1e^{-\lambda(t-a)}|z_a| + \int_a^t e^{-\lambda(t-s)}(M_5\epsilon + \eta|z(s)|)ds \\ &\leq K_1e^{-\lambda(t-a)}|z_a| + K_1M_5\lambda^{-1}\epsilon(1 - e^{-\lambda(t-a)}) + K_1\eta \int_a^t e^{-\lambda(t-s)}|z(s)|ds. \end{aligned}$$

Since $|z_a| = |y_a - c(x_a)| \leq c_1\epsilon \leq c_1\epsilon_0$ we get

$$(23) \quad \begin{aligned} |F(z)(t)| &\leq M_6\epsilon + K_1\eta \int_a^t e^{-\lambda(t-s)}|z(s)|ds \\ &\leq M_6\epsilon + K_1\eta\lambda^{-1}\|z\| \end{aligned}$$

where $M_6 = K_1c_1 + K_1M_5\lambda^{-1}$ and $\|z\| = \sup \{|z(s)| : s \in I\}$. Since $\|z\| \leq \frac{b_1}{2}$ it follows from (18) that $|F(z)(t)| \leq M_6\epsilon_0 + \frac{b_1}{4}$. In order to assure that $|F(z)(t)| \leq \frac{b_1}{2}$ we require ϵ_0 to satisfy

$$\epsilon_0 \leq \min \left(\frac{a_0}{c_2}, \frac{b_1}{4M_1}, \frac{b_1}{4M_6}, \frac{b_1}{2c_1} \right).$$

Since $z(t) = F(z)(t)$ it follows from (18) and (23) that $|z(t)| \leq 2M_6\epsilon$ whenever $\epsilon \leq \epsilon_0$, which completes the proof.

6. Open Problems. There are a number of unresolved mathematical questions which deserve study in the future. These are the following:

- (1) Describe the dynamical properties of flight maneuvers in the vicinity of bifurcation points on the equilibrium set E .
- (2) Analyze the effect of small random disturbances on the dynamics of flight maneuvers.
- (3) Determine what effect control saturation has on the dynamics of aircraft motion.
- (4) Describe the dynamical behavior of specific flight maneuvers with inputs H with large norm $N(H)$.

REFERENCES

- [1] J. P. LASALLE (1962), *Asymptotic stability criteria*, "Proc. Symposium Appl. Math.," Amer. Math. Soc., pp. 299-307.
- [2] L. MARKUS (1956), *Asymptotically autonomous differential systems*, "Contributions to Nonlinear Oscillations," Princeton University Press.
- [3] R. K. MILLER (1965), *Almost periodic differential equations as dynamical systems with applications to the existence of a.p. solutions*, J. Differential Equations, 1, 337-345.
- [4] R. K. MILLER AND G. R. SELL (1970), *Volterra integral equations and topological dynamics*, Memoirs Amer. Math. Soc., 102.
- [5] R. J. SACKER AND G. R. SELL (1977), *Lifting properties in skew-product flows with applications to differential equations*, Memoirs Amer. Math. Soc., 190.
- [6] G. R. SELL (1966), *Periodic solutions and asymptotic stability*, J. Differential Equations, 2, 143-157.
- [7] G. R. SELL (1967A), *Nonautonomous differential equations and topological dynamics I. The basic theory*, Trans. Amer. Math. Soc., 127, 241-262.
- [8] G. R. SELL (1967B), *Nonautonomous differential equations and topological dynamics II. Limiting equations*, Trans. Amer. Math. Soc., 127, 263-283.
- [9] G. R. SELL (1973), *Differential equations without uniqueness and classical topological dynamics*, J. Differential Equations, 14, 42-56.

END

DATE

FILMED

5-88
DTIC